



Institut für Chemie und Dynamik der Geosphäre
Institut IV: Agrosphäre

***Pesticide Volatilization from Soil and
Plant Surfaces: Measurements at
Different Scales versus Model Predictions***

André Wolters

***Pesticide Volatilization from Soil and
Plant Surfaces: Measurements at
Different Scales versus Model Predictions***

André Wolters

Berichte des Forschungszentrums Jülich ; 4073

ISSN 0944-2952

Institut für Chemie und Dynamik der Geosphäre

Institut IV: Agrosphäre Jül-4073

D82 (Diss., Aachen, RWTH, 2003)

Zu beziehen durch: Forschungszentrum Jülich GmbH · Zentralbibliothek

D-52425 Jülich · Bundesrepublik Deutschland

☎ 02461/61-5220 · Telefax: 02461/61-6103 · e-mail: zb-publikation@fz-juelich.de

1	INTRODUCTION	1
1.1	Pesticides in the Atmosphere.....	2
1.1.1	Sources: Application and Post-application Processes	2
1.1.2	Distribution: Transport Processes.....	3
1.1.3	Removal: Deposition and Photochemical Reactions.....	3
1.2	Key Process: Volatilization	4
1.2.1	Overview: Experimental Determination	5
1.2.2	Registration: German and European Guidelines	7
1.3	Aims and Scope	10
2	THEORETICAL CONSIDERATIONS AND MODEL APPROACHES	11
2.1	Pesticide Volatilization from Bare Soil.....	11
2.1.1	Factors Governing Volatilization from Soil.....	12
2.1.2	Model Approaches: Volatilization from Soil	14
2.1.2.1	Empirical Approaches: Volatilization from Soil	15
2.1.2.1.1	Estimation Method: Smit et al. (1997)	15
2.1.2.1.2	Estimation Method: Woodrow & Seiber (1997).....	15
2.1.2.2	Screening Approach: Behavior Assessment Model	16
2.1.2.3	Sophisticated Approaches: Improvement of PEC Models.....	17
2.1.2.3.1	PEARL: Description of Volatilization from Soil.....	18
2.1.2.3.2	PELMO: Description of Volatilization from Soil.....	19
2.2	Pesticide Volatilization from Plant Surfaces	20
2.2.1	Factors Governing Volatilization from Plants	21
2.2.2	Model Approaches: Volatilization from Plants.....	22
2.2.2.1	Empirical Approach: SMIT et al. (1998)	22
2.2.2.2	Model Approach on the Basis of a Boundary-layer Concept.....	23
3	EXPERIMENTAL METHODS AND INSTRUMENTATION	27
3.1	Volatilization Measurements at Different Scales	27
3.1.1	Laboratory Studies: Photovolatility Chamber	27
3.1.1.1	Main Features of the Photovolatility Chamber	28
3.1.1.2	Characterization of the Aerodynamic Conditions and Water Content	30
3.1.1.3	Air sampling: Adsorption Capacity of the PUF plugs	30
3.1.1.4	Performance of Studies on Volatilization: Application Process	31
3.1.1.5	Performance of Studies on Volatilization: Analysis.....	31
3.1.1.6	Process Studies on the Influence of Soil Moisture and Temperature	32
3.1.2	Semi-field Scale: Wind Tunnel	33
3.1.2.1	Characteristics of the Wind Tunnel and Measuring Technique	33
3.1.2.2	Application Device: Semi-automatic Sprayer	34
3.1.2.3	Air Sampling Unit: High-volume Sampler and Medium-volume Sampler	34
3.1.2.4	Study on Volatilization from Soil Surfaces.....	36
3.1.2.5	Study on Volatilization from Plant Surfaces.....	37
3.1.3	Field Study: Micrometeorological Methods	38

3.1.3.1	Field Site and Application	38
3.1.3.2	Meteorological Measurements	39
3.1.3.3	Plant and Soil Sampling	40
3.1.3.4	Pesticide Concentrations in Air	40
3.1.3.5	Micrometeorological Methods for Determining Volatilization Fluxes	41
3.2	Phase Partitioning Studies	42
3.2.1	Measurement of Soil-Air Partitioning Coefficients	42
3.2.1.1	A Novel Chamber for Partitioning Studies: Main Features	42
3.2.1.2	Air Supply and Air Sampling Unit	43
3.2.1.3	Studies on Soil-Air Partitioning	44
3.2.2	Measurement of Soil-Water Partitioning Coefficients	44
3.2.2.1	Studies on Soil-Water Partitioning: Experimental Set-up	44
3.2.2.2	Calculation of Sorption Coefficients for Pesticides	45
3.3	Analytics	45
3.3.1	Sample Preparation	45
3.3.2	Radioactivity Measurements	47
3.3.3	Quantification of Pesticides and Metabolites	47
3.3.3.1	Thin-layer Chromatography (TLC)	47
3.3.3.2	Gas Chromatography / Mass Selective Detector (GC-MSD)	48
3.3.3.3	High Pressure Liquid Chromatography (HPLC)	49
3.3.3.4	Thermodesorption System (TDS)	49
3.4	Test Compounds	50
3.4.1	Parathion-methyl	51
3.4.2	Fenpropimorph	51
3.4.3	Terbuthylazine	51
3.4.4	Chlorpyrifos	52
3.4.5	Quinoxifen	52
3.5	Experimental Soil	52
3.5.1	Gleyic Cambisol	52
3.5.2	Orthic Luvisol	53
4	RESULTS AND DISCUSSION	54
4.1	Volatilization from Bare Soil	54
4.1.1	Laboratory Studies on Volatilization of Parathion-methyl	54
4.1.1.1	Measurements of Air Velocity and Pressure Differential	54
4.1.1.2	Validation of the Total-volume Sampler (TVS)	55
4.1.1.3	Water Content in the Soil Container	56
4.1.1.4	Validation of Uniform Spray Distribution Pattern	57
4.1.1.5	Influence of Soil Moisture on Cumulative Volatilization and Kinetics	58
4.1.1.5.1	Radioactivity and Mass Balance	58
4.1.1.5.2	Metabolization and Mineralization	59
4.1.1.5.3	Cumulative Volatilization and Kinetics	60
4.1.1.6	Influence of Soil Temperature on Volatilization	61
4.1.2	Wind-tunnel Study: Pesticide Application to Bare Soil	63
4.1.2.1	Wind-tunnel Study on Soil: Environmental Conditions	63
4.1.2.2	Overview: Application and Mass Balances	65

4.1.2.3	Soil Residues and Mineralization of ^{14}C -labeled Compounds	66
4.1.2.4	Cumulative Volatilization and Kinetics	67
4.1.2.5	Comparison between Studies at Different Scales: Parathion-methyl	70
4.1.3	Model Approaches: Volatilization from Soil	71
4.1.3.1	Empirical Approaches and Screening Model for Volatilization from Soil.....	71
4.1.3.2	PELMO: Evaluation and Improvement of the Volatilization Description.....	72
4.1.3.3	PEARL: Evaluation of the Volatilization Description and Outlook	75
4.2	Volatilization from Plant Surfaces.....	78
4.2.1	Wind-tunnel Study: Pesticide Application to Winter Wheat	78
4.2.1.1	Wind-tunnel Study on Winter Wheat: Environmental Conditions.....	78
4.2.1.2	Overview: Radioactivity and Mass Balances	80
4.2.1.3	Mineralization of ^{14}C -labeled Parathion-methyl	81
4.2.1.4	Soil and Plant Residues.....	82
4.2.1.5	Cumulative Volatilization and Kinetics	85
4.2.1.6	Comparison between Volatilization from Soil and Plants: Parathion-methyl	86
4.2.2	Field Study: Pesticide Application to Winter Wheat.....	87
4.2.2.1	Meteorological Data.....	87
4.2.2.2	Plant Residues and Rinsability	90
4.2.2.3	Determination of Volatilization Fluxes: Micrometeorological Methods.....	91
4.2.3	Model Approach: Volatilization from Plants	92
4.2.3.1	Calibration of Rate Coefficients and Boundary-layer Thickness	93
4.2.3.2	Advanced Testing: Wind-tunnel Study on Winter Wheat	94
4.2.3.3	Implementation of the Boundary-layer Concept in PELMO	100
4.3	Phase Partitioning Studies	101
4.3.1	Soil-Air Partitioning: Development of a Novel Chamber	101
4.3.1.1	Validation and Preliminary Studies	101
4.3.1.2	Temperature Dependence of Soil-Air Partitioning of Fenpropimorph.....	103
4.3.2	Temperature Dependence of Soil-Water Partitioning	104
4.3.2.1	Adsorption Isotherms of Parathion-methyl	104
4.3.2.2	Adsorption Isotherms of Terbutylazine	106
5	CONCLUSIONS AND SUGGESTIONS FOR FURTHER WORK.....	108
6	REFERENCES	111
	Annex 1: Field Study: Data for Calculation of Pesticide Volatilization Fluxes.....	122
	Annex 2: Phase Partitioning Chamber: Main Elements.....	124

Fig. 1.1	Major processes involved in the environmental fate of pesticides.....	1
Fig. 1.2	Basic principle of small-scale volatility chambers.....	5
Fig. 1.3	Investigations on the behavior of plant protection product active ingredients in the air-examination.....	8
Fig. 2.1	Scheme of diffusion steps involved in soil-atmosphere exchange.....	11
Fig. 2.2	Approaches for the description of volatilization from soil.....	14
Fig. 2.3	Standard scenario used for BAM simulations.....	17
Fig. 3.1	Experimental devices for volatilization measurement at different scales	27
Fig. 3.2	Schematic of the photovolatility chamber	28
Fig. 3.3	Center of the photovolatility chamber	29
Fig. 3.4	Schematic of the water replenishing system.....	30
Fig. 3.5	Total-volume sampler for sampling organic air constituents	31
Fig. 3.6	Schematic of the wind tunnel for measuring volatilization of pesticides.....	33
Fig. 3.7	Semi-automatic application unit for pesticides	34
Fig. 3.8	High-volume sampler/adsorption unit for sampling of ^{14}C -labeled air constituents	35
Fig. 3.9	Schematic diagram of the medium-volume sampler	35
Fig. 3.10	Location of the field site and the treated area	38
Fig. 3.11	Construction and operation of the soil-water-air-partitioning chamber	43
Fig. 3.12	Air supply and air sampling unit used in the phase partitioning chamber.....	43
Fig. 4.1	Aerodynamic conditions in the glass dome of the photovolatility chamber.....	55
Fig. 4.2	Soil moisture profiles of gleyic cambisol in the soil container	57
Fig. 4.3	Spray distribution pattern of ^{14}C -labeled parathion-methyl	58
Fig. 4.4	Cumulative volatilized radioactivity of ^{14}C -parathion-methyl	60
Fig. 4.5	Volatilization rates of ^{14}C -parathion-methyl after soil surface application.....	61
Fig. 4.6	Volatilization of ^{14}C -parathion-methyl after increasing soil surface temperature.....	63
Fig. 4.7	Climatic conditions over the course of the wind-tunnel study	64
Fig. 4.8	Cumulative volatilization of ^{14}C -labeled pesticides	67
Fig. 4.9	Volatilization fluxes after soil surface application of chlorpyrifos	68
Fig. 4.10	Wind-tunnel experiment: measured volatilization rates of ^{14}C -labeled compounds	69
Fig. 4.11	Measured and predicted (PELMO) volatilization fluxes.....	72
Fig. 4.12	Modifications included in the improved PELMO version	74
Fig. 4.13	Calculations using the improved PELMO version.....	75
Fig. 4.14	Measured and predicted (PEARL) volatilization fluxes.....	76
Fig. 4.15	Model approach: Volatilization fluxes and soil moisture calculated by PEARL	77
Fig. 4.16	Climatic conditions during the wind-tunnel experiment	79

Fig. 4.17	Mineralization rates of ^{14}C -parathion-methyl after application to winter wheat	81
Fig. 4.18	Determination of ^{14}C -labeled plant residues	83
Fig. 4.19	Volatilization of parathion-methyl, quinoxifen, and fenpropimorph.....	86
Fig. 4.20	Climatic conditions over the course of the field study on winter wheat.....	88
Fig. 4.21	Wind speed at 0.7 and 1.5 m above the soil surface during the field study.....	89
Fig. 4.22	Plant residues of quinoxifen and fenpropimorph.....	91
Fig. 4.23	Predicted cumulative volatilization of ^{14}C -fenpropimorph (radish plants).....	93
Fig. 4.24	Predicted (well-exposed scenario) cumulative volatilization of ^{14}C -parathion-methyl	95
Fig. 4.25	Predicted (poorly-exposed scenario) cumulative volatilization of ^{14}C -parathion-methyl	96
Fig. 4.26	Predicted cumulative volatilization of fenpropimorph (winter wheat).....	97
Fig. 4.27	Predicted cumulative volatilization of quinoxifen (winter wheat)	98
Fig. 4.28	Influence of varying vapor pressure on predicted cumulative volatilization of pesticides.....	99
Fig. 4.29	PELMO calculation for application of ^{14}C -labeled fenpropimorph	100
Fig. 4.30	Adsorption isotherms of parathion-methyl	105
Fig. 4.31	Adsorption isotherms of terbuthylazine	107

Table 1.1	Benefits and disadvantages of semi-field and field experiments	6
Table 1.2	Demanding list of requirements for experiments on volatilization.....	9
Table 2.1	Main parameters involved in the volatilization process from soil	12
Table 2.2	Data required in model approach for predicting volatilization from plants	26
Table 3.1	Application parameters and conditions of photovolatility chamber studies.....	32
Table 3.2	Wind-tunnel study on volatilization from bare soil: application details	36
Table 3.3	Wind-tunnel study on volatilization from winter wheat: application details....	37
Table 3.4	Field study on volatilization from winter wheat: application details	39
Table 3.5	Chromatographic conditions for TLC quantification	48
Table 3.6	Selected ion monitoring (SIM) and retention times for pesticides.....	48
Table 3.7	Chromatographic conditions for HPLC quantification	49
Table 3.8	Physicochemical active ingredient data of the investigated compounds.....	50
Table 3.9	Soil properties and soil profile of gleyic cambisol.....	53
Table 3.10	Soil properties of orthic luvisol.....	53
Table 4.1	¹⁴ C-recovery in the total-volume sampler.....	56
Table 4.2	¹⁴ C-recoveries from experiments on soil moisture dependence.....	58
Table 4.3	Characterization of ¹⁴ C-labeled compounds in the methanol extracts	59
Table 4.4	Results of a 3-day photovolatility chamber experiment	62
Table 4.5	Wind-tunnel study on bare soil: Recoveries of ¹⁴ C-labeled compounds.....	65
Table 4.6	Wind-tunnel study on winter wheat: radioactivity balance	80
Table 4.7	Characterization of ¹⁴ C-labeled compounds in the methanol extracts	82
Table 4.8	Soil and plant residues of quinoxifen and fenpropimorph.....	84
Table 4.9	Rainfall at the experimental plot during the field study	89
Table 4.10	Solvent rinsability of pesticide residues deposited on winter wheat leaves	90
Table 4.11	Volatilization fluxes of fenpropimorph determined with aerodynamic and Bowen ratio methods after application to winter wheat	91
Table 4.12	Soil-air partitioning chamber: pesticide recoveries for orthic luvisol.....	102
Table 4.13	Soil-air partitioning chamber: measured and calculated fraction of fenpropimorph in the gas phase	103
Table 4.14	Freundlich coefficients and coefficients of determination for adsorption isotherms of parathion-methyl	105
Table 4.15	Freundlich coefficients and coefficients of determination for adsorption isotherms of terbuthylazine.....	106

AD	Aerodynamic method
A.I.	Active ingredient
APECOP	Effective Approaches for Predicting the Environmental Fate of Pesticides
AR	Applied Radioactivity
BAM	Behavior Assessment Model
BBA	<i>Biologische Bundesanstalt für Land- und Forstwirtschaft</i> German Federal Biological Research Centre for Agriculture and Forestry
BR	Bowen ratio method
C _{ORG}	Organic carbon content
DCM	Dichloromethane
EC	Emulsifiable concentrate
EVA	Exposure Via Air
FAO	Food and Agriculture Organization of the United Nations
FOCUS	Forum for the Coordination of Pesticide Fate Models and their Use
GC-MSD	Gas chromatography / mass selective detector
I.D.	Inner diameter
ISO	International Organization for Standardization
HPLC	High-pressure liquid chromatography
HVS	High-volume sampler
K _F	Freundlich coefficient
K _H	Henry's law constant
K _{OC}	Organic carbon partitioning coefficient
K _{OM}	Organic matter partitioning coefficient
K _{OW}	Octanol-water partitioning coefficient
K _{SA}	Soil-air partitioning coefficient
LSC	Liquid scintillation counting
MWC	Maximum water holding capacity
MVD	Mean droplet diameter
MVS	Medium-volume sampler
O.D.	Outer diameter
OECD	Organization for Economic Co-operation and Development
PEARL	Pesticide Emission Assessment at Regional and Local Scales
PEC	Predicted Environmental Concentrations
PELMO	Pesticide Leaching Model
PESTLA	Pesticide Leaching and Accumulation Model
PRZM	Pesticide Root Zone Model
PSL	Photostimulated luminescence
PUF	Polyurethane foam
PTFE	Polytetrafluoroethylene

SPE	Solid-phase extraction
TDR	Time-domain reflectometry
TDS	Thermodesorption system
TLC	Thin-layer chromatography
TVS	Total-volume sampler
USEPA	United States Environmental Protection Agency
VOC	Volatile organic compound
WHO	World Health Organization
WP	Wettable powder

Pesticide Volatilization from Soil and Plant Surfaces

Simulation of pesticide volatilization from plant and soil surfaces as an integral component of pesticide fate models is of utmost importance, especially as part of the PEC (Predicted Environmental Concentrations) models used in the registration procedures for pesticides. Experimentally determined volatilization rates at different scales were compared to model predictions to improve recent approaches included in European registration models.

To assess the influence of crucial factors affecting volatilization under well-defined conditions, a laboratory chamber was set-up and validated. Aerodynamic conditions were adjusted to fulfill the requirements of the German guideline on assessing pesticide volatilization for registration purposes. Determination of soil moisture profiles of the upper soil layer illustrated that a defined water content in the soil up to a depth of 4 cm could be achieved by water-saturation of the air. Cumulative volatilization of ^{14}C -parathion-methyl ranged from 2.4% under dry conditions to 32.9% under moist conditions revealing a clear dependence of volatilization on the water content in the top layer.

At the semi-field scale, volatilization rates were determined in a wind-tunnel study after soil surface application of pesticides to gleyic cambisol. The following descending order of cumulative volatilization was observed: chlorpyrifos > parathion-methyl > terbutylazine > fenpropimorph.

Parameterization of the models PEARL (Pesticide Emission Assessment at Regional and Local Scales) and PELMO (Pesticide Leaching Model) was performed to mirror the experimental boundary conditions. Model predictions deviated markedly from measured volatilization fluxes and showed limitations of current volatilization models, such as the uppermost compartment thickness having an enormous influence on predicted volatilization losses. Moreover, the impact of soil moisture on volatilization from soil was not reflected by the model calculations. Improvements of PELMO, including the temperature-dependence of water-air partitioning, the reduction of the compartment size of the top layer and the introduction of a moisture-dependent sorption coefficient, contributed to a more realistic reflection of experimental findings, especially at the initial stage of the studies.

Studies on volatilization from plants included a field study and a wind-tunnel study after simultaneous application of parathion-methyl, fenpropimorph and quinoxifen to winter wheat. Parathion-methyl was shown to have the highest volatilization during the wind-tunnel study of 10 days (29.2%). Volatilization of quinoxifen was about 15.0%, indicating a higher volatilization tendency in comparison with fenpropimorph (6.0%), which may be attributed to enhanced penetration of fenpropimorph counteracting the volatilization process.

A mechanistic approach using a laminar air-boundary layer concept for the consideration of volatilization from plant surfaces was adjusted and calibrated on the basis of a series of wind-tunnel studies. Calibration of the thickness of the air-boundary layer and the rate coefficients of phototransformation and penetration into the leaves allowed the implementation of this description in PELMO and enabled the simultaneous estimation of volatilization from plants and soil.

The need to determine critical factors affecting volatilization, especially phase partitioning coefficients, resulted in the development and validation of a novel chamber system for measurements of the temperature dependence of the soil-air partitioning of fenpropimorph. Additional batch studies allowed for the quantification of the general tendency of pesticides towards enhanced soil sorption after lowering the temperature.

1 INTRODUCTION

The benefits of agriculture have been immense. Global cereal production has doubled in the past 40 years, mainly from the increased yields resulting from greater inputs of fertilizer, water and pesticides, new crop strains and other technologies of the green revolution (FAO, 2001).

A doubling in global food demand projected for the next 50 years poses huge challenges for the sustainability both of food production of terrestrial and aquatic ecosystems and the services they provide to society. Further increases in agricultural output are essential for global political and social stability and equity (Tilman et al., 2002).

Agricultural practices determine the level of food production and, to a great extent, the state of the global environment. The main environmental impacts of agriculture come from the conversion of natural ecosystems to agriculture, from agricultural nutrients that pollute aquatic and terrestrial habitats, and from pesticides, especially bioaccumulating or persistent organic agricultural pollutants. Despite intensive research, it is only partially understood how chemical pollutants move between soil, water and atmosphere and what transformation they undergo during transport. The fate of a pesticide and the potential for its movement from the site of application are affected by chemical and physical properties of the pesticide, site characteristics such as soil, geology, and vegetation, climate and local weather conditions, and the handling practice of the pesticide user. Pesticides may be transformed by degradation processes or transported from the site of application by several processes including runoff, movement through the soil to ground water, volatilization, transport on soil particles, and wind erosion (**Fig. 1.1**). Individual pesticides vary widely in their response to environmental processes. Each factor has to be considered when determining the likelihood of pesticide movement and off-target effects.

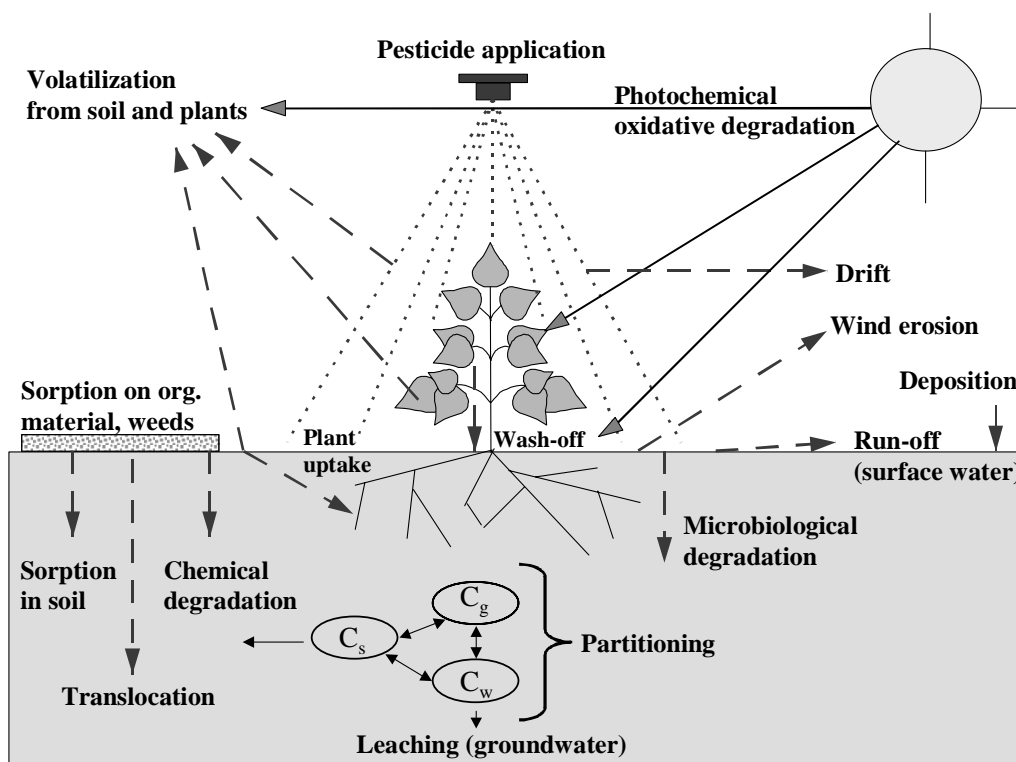


Figure 1.1 Major processes involved in the environmental fate of pesticides after their application to soil or plants. C_g , C_w , and C_s represent the pesticide concentrations in gaseous, aqueous, and solid phases, respectively (adapted from Führ et al., 1998).

1.1 Pesticides in the Atmosphere

Until the 1960's, atmospheric pesticide contamination was generally thought of as a „local“ problem caused by spray drift. The detection of DDT and other organochlorine compounds in fish and mammals in the Antarctic (George & Frear, 1966) and Arctic (Addison & Smith, 1974) changed this notion. These organochlorine residues could not exclusively be attributed to movement in surface water and distribution through the food chain, so the idea of atmospheric depositions as a main source of contamination in remote areas gained significance. Currently the atmosphere is recognized as the major transport pathway depositing pesticides and other organic and inorganic compounds in areas far away from their sources (Majewski & Capel, 1995).

1.1.1 Sources: Application and Post-application Processes

The most important source of pesticide contamination in the atmosphere is agricultural use. About 75% of the pesticides are used annually on agricultural crops (Aspelin, 1994), which involves large acreage, large quantities and most major types of pesticides. Other sources of pesticide contamination include manufacturing processes and waste effluents, urban and industrial weed control, turf management of golf courses etc. (Majewski & Capel, 1995). Agricultural sources of pesticide contamination fall into two main categories: application and post-application processes.

Off-target drift during pesticide application occurs to varying degrees, ranging from 1 to 75% of the applied spray dose (e.g. Glotfelty et al., 1990; Symons, 1977) and is mainly affected by application methods, formulation, and spray-cloud processes (Majewski & Capel, 1995). To date, measurements of pesticide emission during application are concentrating on spray drift of droplets or particles. In Germany, data on spray drift to adjacent watercourses for various techniques and crops were collected by Ganzelmeier et al. (1995) and threshold rates of spray drift for evaluation and registration purposes were determined (Anonymous, 2000). Based on these data, the estimation model EVA 1.1 (Exposure Via Air) for the prediction of aerially derived input of pesticides and metabolites, including drift and volatilization, on terrestrial and aquatic non-target areas was developed (BBA, 2002). A draft protocol for drift measurement is being discussed by the International Organization for Standardization (ISO, 1999), which would enable a comparison of drift data from various sources obtained by different methods. In most cases drift measurements have been limited to the determination of the mass of pesticide deposited on the surface adjacent to the treated field and to measurements of droplets in the air close to the ground leaving the target area. Little is known about the total fraction of the dosage, which does not reach the target area. A portion of the pesticide that does not reach the target area consists of gas-phase pesticide and small droplet or particles (aerosols), which are or have become so small that they cannot be captured effectively by drift collectors. For this fraction, measurement may be possible, but would require some form of isokinetic sampling (Van den Berg et al., 1999).

Once on the surface, the pesticide residue can volatilize or be transported into the atmosphere attached to dust particles (Glotfelty & Schomburg, 1989). Volatilization occurs continuously over a much longer time period than off-target drift and the resulting losses of the application rate can be a significant source of pesticide input into the lower atmosphere.

1.1.2 Distribution: Transport Processes

After volatilization, pesticides or related compounds enter the boundary layer. During daytime, this boundary layer is usually unstably stratified, generally well mixed by mechanical and thermal turbulence, and typically extending several kilometers above the surface (Wyngaard, 1990). Any compound released into the atmosphere under these conditions becomes well mixed and dispersed throughout the surface boundary layer. At night, because of surface cooling, the boundary layer depth typically decreases to between a few tens to several hundred meters and is usually only slightly turbulent, quiescent, or very stable (Smith & Hunt, 1978). Chemicals released into a stably-stratified atmosphere can be transported horizontally for long distances and generally undergo little mixing or dilution. Local transport of pollutants (on the range of tens of kilometers) is confined to the environmental surrounding of the application area if they remain in the surface boundary layer (the lower troposphere).

If pesticides are rapidly transported to the mid- and upper troposphere (5-16 km), their residence times increase with range. The transport time of an air parcel during large-scale vertical perturbations from the surface to a height of 10 km is in the order of hours (Dickerson et al., 1987). In the upper atmosphere, the global wind circulation pattern controls long-range transport of airborne pollutants. The general global longitudinal circulation is a form of thermal convection driven by the difference in solar heating between the equatorial and polar regions. In the Northern Hemisphere, the most intense atmospheric circulation occurs during the winter months when the temperature and pressure gradients are the steepest over the western perimeter of the North Atlantic Ocean. Airborne pollutants from mid-latitude Eurasia and North America also are transported northward during the winter months (Barrie, 1986). This northward transport together with the lower ambient temperatures combine to increase the deposition rates (cf. 1.1.3) of airborne pesticides into the Arctic and produce a warm-to-cold distillation effect (Cotham & Bidleman, 1991). Atmospheric transport of synthetic organic compounds might be the major input pathway to most oceans (Kurtz & Atlas, 1990).

1.1.3 Removal: Deposition and Photochemical Reactions

The residence time of a pesticide in the atmosphere depends on how rapidly it is removed by deposition or chemical transformation. Atmospheric depositional processes can be classified into two categories, those involving precipitation, called wet deposition, and those not involving precipitation, called dry deposition (Bidleman, 1988).

The effectiveness of the various removal processes depends on the physical and chemical characteristics of the particular compound, along with meteorological factors, and the underlying depositional surface characteristics. Model experiments showed that the contribution of the emission from the field to the wet deposition is usually less important compared to the contribution from dry deposition (Asman, 2001).

Dry deposition of pesticides associated with particles includes gravitational settling, and turbulent transfer to a surface followed by interception, or diffusion onto surfaces such as vegetation, soil, and water. Although larger particles usually tend to settle out faster, most of the sorbed pesticide may be concentrated on smaller particles because of their higher surface area-to-volume ratio (Bidleman & Christensen, 1979). Wet deposition includes the deposition by rainout and washout. Rainout is a process where cloud droplets acquire

contaminants within the cloud. Clouds form by condensation of water vapor around nuclei such as particles or aerosols, both of which may contain organic contaminants. Washout is a process by which atmospheric contaminants are removed by rain below the clouds by scavenging of particles and by partitioning of organic vapors into the rain droplets or snowflakes as they fall to the ground.

Dry/wet deposition at distances 20 m less from the application site can be of the same order as deposition caused by spray drift due to sedimentation, whereas dry/wet deposition dominates at larger distances. Both dry and wet deposition of gaseous pesticides, increase with pesticide solubility in water, so in general atmospheric lifetime is related to their solubility (Asman, 2001).

Other factors, especially atmospheric chemical reactions, also influence the lifetime of pesticides. Photochemical reactions are the most important reaction type for airborne pesticides because these residues are totally exposed to sunlight. Airborne pesticides can undergo photochemical degradation by directly adsorbing sunlight or by indirectly reacting with photochemically generated oxidants such as ozone or hydroxyl radicals. The atmospheric photoreaction half-lives of certain classes of pesticides, such as organophosphates, range from a few minutes to several hours (Woodrow et al., 1977). Most oxidative reaction products are more polar than the parent compound, suggesting increased water solubility and more readily removal by wet-depositional processes or by air-water exchange. Details on the photodegradation of pesticides, with particular reference to the studies describing the mechanisms of processes involved, the nature of reactive intermediates and final products, can be taken from a recently published review (Burrows et al., 2002).

1.2 Key Process: Volatilization

For most pesticides, volatilization is just as important as chemical and microbiological degradation in causing the dissipation of pesticides from soil and plants. Subsequent deposition is even the major source of pesticide contamination in some environments (Eisenreich et al., 1981). Volatilization decreases the amount of a pesticide available for control of pests and the potential for ground water contamination but increases the potential for contaminating the atmosphere and surface water. Since many pesticides are considered to be toxic or carcinogenic (Doull, 1989), volatilization may increase the risk of illness to persons living down-wind from treated fields (Yates, 1993). Growing concerns regarding the risks from exposure to airborne pesticides accelerated the development of numerous laboratory and field methods to characterize the most important factors affecting volatilization in recent years (Taylor & Spencer, 1990; Burkhard & Guth, 1981; Stork et al., 1994). Laboratory experiments have confirmed that the environmental behavior of pesticides after application is controlled by physical and chemical properties, but still more information is needed on the behavior of volatile organics under typical atmospheric conditions. Particularly, methods for accurate and efficient measurement of volatilization rates from soil and plant surfaces are needed, as well as further improvements in model approaches describing transport and fate of these compounds.

1.2.1 Overview: Experimental Determination

Preliminary studies to elucidate the processes governing the volatilization of pesticides were performed in small laboratory volatilization chambers whereby investigations were limited to soil-surface applied compounds (Sanders & Seiber, 1983; Burkhard & Guth, 1981; Farmer et al., 1972). Volatility chambers are the most common test system to perform studies on volatilization at the laboratory scale (**Fig. 1.2**). Preconditioned air is led over a surface treated with the test compound. Volatilized compounds are adsorbed by suitable sorbent material and these compounds may be quantitated by analytical standard methods. Enhanced chamber systems allow for studies on volatilization from plants (e.g. Orchard et al., 2000) and enable simultaneous determination of photodegradation from soil and plant surfaces (Kromer et al., 1999; Kromer, 2001). Even with further development of facilities inside the chamber (e.g. Cherif & Wortham, 1997), the volatilization chamber method still has a number of limitations. Substantial differences may occur between the atmospheric conditions in the field and the simulated weather conditions in the volatilization chamber. Air turbulence and wind profile in the chamber are likely to be different from those in the field. Moreover, the transferability to outdoor conditions is limited by low wind speed and air exchange rates. Further, the flow of air through the chamber may result in a light vacuum in the volatilization chamber, which may cause an advective transport component and result in measurement error (Van den Berg et al., 1999).

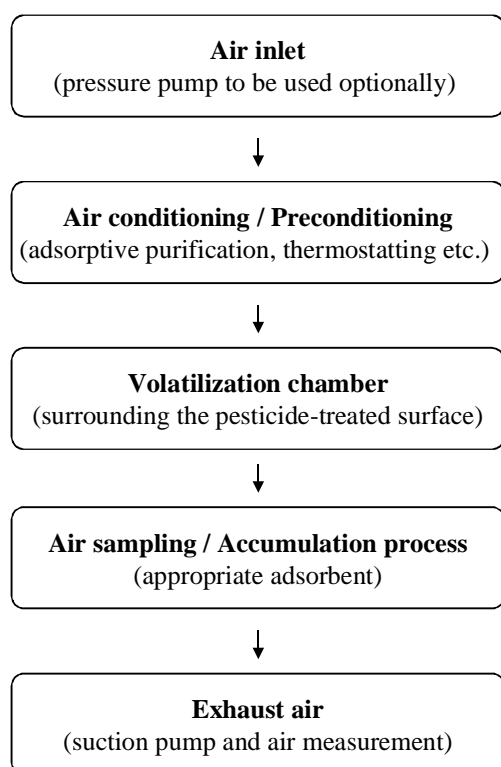


Figure 1.2 Basic principle of small-scale volatility chambers for direct measurement of volatilization rates.

Dynamic flux chambers have been extensively used in the field to measure emissions from surfaces to the atmosphere (e.g. Reichman & Rolston, 2002). This method involves placing an open-bottom chamber over a small area of soil surface and measuring the gaseous emissions into the chamber. Various assumptions are applied to these chamber methods, and models based on these assumptions were developed and used to calculate fluxes from

the data obtained (e.g. Livingston & Hutchinson, 1995). The flux chamber method is probably one of the simplest tools for measuring volatilization, yet it has several disadvantages compared to micrometeorological-based measurements (Yates et al., 1997). First, when the chamber sampling area is a small fraction of total area for emission, the measured flux could be highly variable due to soil spatial heterogeneity. Second, the presence of the chamber will change the environmental properties (such as soil and air temperature and wind profile near the soil surface) of the sampled area compared to the rest of the surface area. Furthermore, chambers cannot measure small-scale spatial variability of volatilization either associated with soil surface conditions or soil variability (Allaire et al., 2002).

Alternatively, wind-tunnel systems have been developed to approximate field conditions as closely as possible (Kubiak et al., 1993; Rüdel & Wayman, 1992; Stork et al., 1994; Stork, 1995). The wind tunnel used within this thesis allows for direct measurement of volatilization and biomineralization under field-like conditions, in combination with the advantages of laboratory facilities, e.g. use of radioisotopes. Both, continuous air sampling, which quantifies volatile organic compounds and $^{14}\text{CO}_2$ separately, and the detection of surface-located residues allow for a complete radioactivity and mass balance. In this system, weather variables such as wind speed, air humidity, and solar radiation can be controlled, thus field conditions can be approximated by simulating the weather conditions as closely as possible.

Table 1.1 Benefits and disadvantages of semi-field (wind tunnel and volatilization chamber) and field experiments for determining pesticide volatilization.

Semi-field studies	Field studies
± climatic conditions partially (wind tunnel) and completely (chamber) under control	± variable and non-predictable climatic conditions
– experimental conditions can deviate significantly from realistic conditions	+ most realistic conditions
+ systematic studies on single factors are possible (in the volatilization chamber)	– unique, non-repeatable scenario
+ use of radio-labeled compounds allows for complete mass balances	– no mass balance possible
+ good reproducibility	– error margin is comparatively high
– transferability of results to field situation depends on accurate simulation	

Direct determination of pesticide volatilization in the field can be achieved by using micrometeorological methods (Taylor & Spencer, 1990; Woodrow et al., 1990), such as the aerodynamic-gradient and the Bowen-ratio methods (cf. 3.1.3.5). Beside various climatic parameters, the concentration of active ingredients in the air must be measured at different heights above the field. Substance flux in the atmosphere can be calculated using various mathematical models (Majewski, 1999). Micrometeorological measurements in the field are very sophisticated and therefore not suitable for routine investigations and, like any field experiment, the error margin is comparatively high. Because the use of radio-labeled compounds is prohibited in the field, a complete detection of metabolites or non-

extractable residues is impossible for most non-labeled compounds. The complexities of field measurements have made it virtually impossible to obtain a complete mass balance and to determine quantitatively the amount transferred to the atmosphere under field conditions (Plimmer, 1992). Basic benefits and disadvantages of field studies and semi-field experiments are given in **Table 1.1**.

When simulating field application in a semi-field system, significant differences between the conditions in this system and those prevailing in the field can occur which make the evaluation of results very difficult. These differences can be due to differences in the initial penetration of the pesticide, differences in the soil surface temperature (caused by shielding of the soil surface from solar radiation in the semi-field system), and by soil puddling and compaction due to higher intensity of the sprinkling events in the semi-field system than that of rainfall in the field (Van den Berg et al., 1999). For example, Stork et al. (1998) measured a difference between the volatilization rates in the field and those in the wind tunnel of up to about factor 10.

1.2.2 Registration: German and European Guidelines

Registration of pesticides requires, among other things, details on risks to the balance of nature that might be caused by the substance in question. The assessment of the volatilization potential was adopted by the German authority for registration of pesticides (Federal Biological Research Center for Agriculture and Forestry, BBA) in their registration procedure (BBA, 1990). The guideline was intended to prevent pesticides from being registered that would volatilize in considerable amounts and thus be widely distributed. The guideline prescribes a graduated three-step plan for experiments assessing the fate of pesticides in air (**Fig. 1.3**). If a trigger value for the hydrolysis or photolysis half-life of the pesticide (4 days) is exceeded, then the cumulative volatilization of the pesticide is to be determined for a 24-hour period after application. If a trigger value of 20% loss is exceeded, then further assessment, involving the subsequent stability of the pesticide in air, has to be made. For the conditions mentioned in the guideline, the error in measurements of cumulative volatilization was estimated to be $\pm 5\%$.

Volatilization studies according to step 2 of the assessment scheme ought to fulfill a number of requirements and preconditions (**Table 1.2**). Generally, experiments should be performed under field-like conditions and the use of formulated compounds is prescribed. The applicant is allowed to perform field studies or chamber studies optionally. Concerning the chamber studies, details on the test system or special devices are not prescribed. Limitations and applicability of the guideline are discussed in detail by Stork (1995). With regard to the chamber experiments, some crucial points are listed as follows: The guideline does not include a specification of the height above soil or plant surfaces where the minimum air velocity should be achieved. In meteorological research applications the indication of a wind velocity without specification of height is useless. Considering the registration purpose of the guideline, the choice to determine the height of measurement of air velocity enables the experimentalist to influence the results of the volatilization measurement for his own benefit.

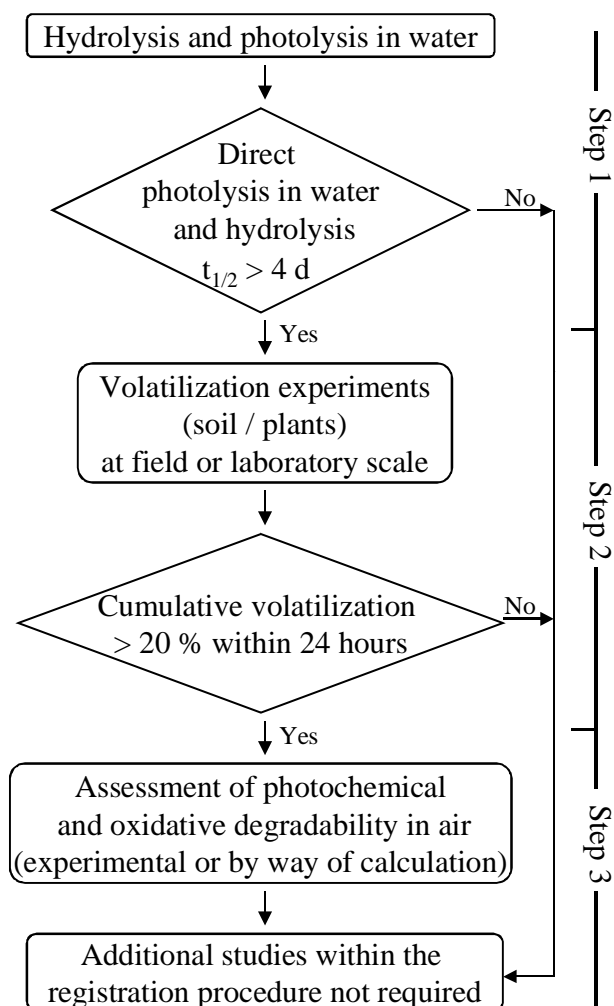


Figure 1.3 Investigations on the behavior of plant protection product active ingredients in the air-examination according to BBA Guideline Part IV, 6-1 (BBA, 1990).

Furthermore, the climatic scenario prescribed for the chamber experiments appears quite unrealistically. It is characterized by an almost desert-like relative air humidity (35% at 20 °C) and the soil moisture shall be kept at 60% MWC during the experiment. Obviously, these conditions were supposed to allow for maximum evaporation rates of soil water and subsequently should cause maximum volatilization rates. Though, high evaporation rates complicate the maintenance of the required soil moisture, even when using a water replenishing system for moistening. Consequently, drying of the soil top layer may lead to other experimental scenarios than originally intended and may finally cause a strong decrease in volatilization (cf. 2.1.1).

In addition, the water loss is accompanied by evaporative cold and entails decreasing soil temperature (approx. 4-5 °C under the corresponding air temperature; Waymann, 1994), suggesting that the required air temperature (20 °C) is hard to maintain.

Some shortcomings of the guideline may be due to the fact that no standard method of assessing volatilization was at hand when the guideline was developed. It was therefore decided to design an instruction with only a few specific demands to be met by the method applied (Walter, 1998). On the other hand, after several years of experience, an evaluation of the methods in use should be possible and it should be decided whether a more detailed guideline should be issued.

Table 1.2 Demanding list of requirement for experiments on the volatilization behavior of pesticides according to step 2 of the BBA-Guideline Part IV, 6-1 (BBA, 1990).

Volatility chamber studies
<ul style="list-style-type: none"> • simulation of plant stand (standard crop: French bean) • experimental soil: min. 70% sand and max. 1.5% organic carbon • wind speed (index value): $> 1 \text{ m s}^{-1}$ (measured immediately above the soil or vegetative stand) • gas exchange in the chamber: min. 60 times h^{-1} • soil moisture: 60% MWC • soil temperature: approx. 20 °C • relative air humidity: approx. 35% • field-like application and use of formulated compounds • volatilization measurement: use of direct (^{14}C-labeled compounds preferred) or indirect methods
Field studies
<ul style="list-style-type: none"> • field-like application and use of formulated compounds • volatilization measurement: indirect method (determination of soil residues) • data on air temperature, humidity, wind speed, precipitation, irradiation (duration and intensity), and on the general weather situation must be supplied • amount of volatilization should be assessed 1, 3, 6, 12, and 24 hours after application • no application under calm conditions

A concise overview of authorization procedures for pesticides within the European Union was presented by Gilbert (1999). Within the European Union approval of pesticides carried out under the terms of the Authorizations Directive (Council Directive 91/414/EEC, 1991) calls on regulatory authorities of member states to consider the fate and behavior of pesticides in air. The directive envisages, to implement uniform principles for assessing the risk associated with the use of plant protections products, and thus to support a harmonized registration at the EU level. Predicting the environmental concentrations of pesticides by means of mathematical models is a core action in risk assessment. For improving the effectiveness of risk assessment, modeling tools and methods need to be continuously updated and evaluated. Quality assurance of mathematical modeling implies validation, documentation and maintenance of the environmental fate modeling codes and scenarios. The “Forum for the Coordination of pesticide fate models and their Use” (FOCUS), created in 1993 by the European Commission, is the current platform where common modeling methodologies are designed and subjected for approval to the European authorities. Yet, the FOCUS groundwater scenarios working group identified a range of uncertainties related to the validity of the present state leaching models and scenarios. To mitigate some of these problems, the EU R&D project APECOP (Effective Approaches for Assessing the Predicted Environmental Concentrations of Pesticides) was designed. A main focus of the APECOP project is to reduce the uncertainties in the predictions of the actual models, by improving the description of preferential flow of plant protection products in soils and volatilization of these substances to air (Vanclooster et al., 2003).

1.3 Aims and Scope

Currently the understanding of processes, factors and relationships that control pesticide transport from soil, water, and plants into the atmosphere is limited. This information is required to develop and refine mechanisms and process descriptions for use in model approaches to predict environmental pesticide concentrations and to improve guidelines for pesticide registration. Improved models will protect the atmosphere and sensitive non-targeted ecosystems from pesticide contamination, benefiting the environment of urban and agricultural areas.

The main objectives of this thesis were to perform experimental volatilization studies at different scales, to provide physical-based descriptions of volatilization processes on plant and soil surfaces on the basis of these experimental findings and to incorporate volatilization modules in European registration models.

In a first part of the work, theoretical considerations on the processes affecting volatilization were presented, including testing and validation of currently available model approaches.

In the second part, a detailed experimental program based on this evaluation was conducted to improve recent knowledge on basic processes.

Finally, the advanced knowledge was used to develop and optimize volatilization modules to be included in PEC models.

As follows, the main goals are summarized in detail:

- Quantification of the influence of crucial factors, e.g. soil moisture and temperature, on pesticide volatilization from bare soil at the laboratory scale
- Up-scaling of the laboratory findings and generating suitable data sets on volatilization from soil for model purposes at the semi-field scale
- Evaluation and improvement of recent soil volatilization modules included in PELMO and PEARL
- Generating data sets on volatilization from plant surfaces under semi-field and field conditions
- Application and optimization of a novel model approach based on a boundary-layer concept for the consideration of volatilization from plants
- Calculation of pesticide volatilization from soil and plants after implementation of the novel boundary-layer approach in the PEC model PELMO
- Determination of the temperature dependence of soil-water partitioning coefficients of pesticides
- Set-up and validation of a novel chamber system for measurements of soil-air and water-air partitioning of low volatile pesticides

2 THEORETICAL CONSIDERATIONS AND MODEL APPROACHES

Models are a key concept in science, and specifically so in environmental sciences, where the applicability of experimental determination is limited by the open and non-replicable character of environmental systems. They refer to a simplified representation of what is thought to be an underlying more complex reality. However, the seemingly simple technical term “model” covers a wide range of different conceptualizations and images of the real world, ranging from drastic reductions and simplifications to maximum complexity. A numerical model is a computer code, generally based on a set of dynamical equations that are supposed to represent “the physics of the system”. Within the framework of this thesis, main focus is on the use of numerical models for predicting the environmental behavior of pesticides.

The precise simulation of volatilization behavior as an integral component of a complete pesticide transport model is of utmost importance. Attention should be paid to the fact that many models used for pesticide registration, including those used by USEPA, do not take volatilization losses into account when evaluating surface water and groundwater contamination risks (Vanclooster et al., 2000; USEPA, 2001).

2.1 Pesticide Volatilization from Bare Soil

Pesticides in the soil will partition between the soil solids, the interstitial soil solution and the gas filled soil pores (Cousins et al., 1999). For a sorbed chemical to volatilize from the surface of the soil, it must first desorb from the soil solids into the soil interstitial solution, from where it can partition into the soil air. Once in the soil air at the surface, there is the potential for transportation across the boundary layer and into the bulk atmosphere (Fig. 2.1).

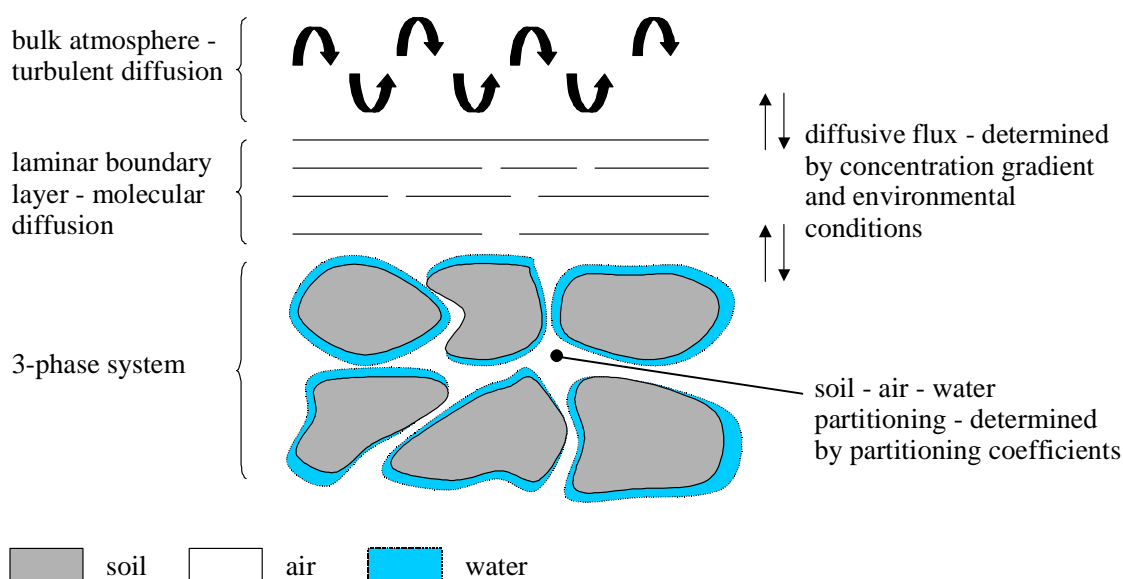


Figure 2.1 Schematic overview of the diffusion steps involved in the exchange of pesticides between soil and atmosphere.

Transfer across this boundary layer is via diffusion. The magnitude of the diffusive flux will be determined by the concentration gradient between the atmospheric and the soil air compartments. It will also be affected by environmental variables such as temperature, surface roughness and soil characteristics. The situation is made more complex in that some of these variables are interlinked. For example, temperature will affect the effective diffusion coefficient in soil by its influence on the free air diffusion coefficient and also the soil moisture content which will affect the partitioning of the pesticides between the soil solids and the air phase. In the following chapter, a summary of the most important factors affecting volatilization from soil is given.

2.1.1 Factors Governing Volatilization from Soil

Volatilization from soil is a complex system, requiring the balancing of several processes. The main factors controlling pesticide volatilization from soil, as summarized in **Table 2.1**, include: the intrinsic properties of the pesticide (e.g. vapor pressure, water solubility), followed by the method of application (soil surface versus incorporation), and soil physical factors (e.g. moisture distribution, soil organic matter content, soil temperature, and transport properties of the soil).

Table 2.1 Main parameters involved in the volatilization process from soil.

Influence field	Supply parameter
Pesticide properties	<ul style="list-style-type: none"> vapor pressure water solubility and liposolubility (hydrophobic properties) phase partitioning coefficients: soil-water partitioning (K_F or K_{OC}), soil-air partitioning (K_{SA}), and Henry's law constant (K_H) diffusion coefficients (gaseous and liquid phase) degradability (degradation rate $t_{1/2}$) and reactivity
	<ul style="list-style-type: none"> application dose application method (incorporation or surface application, droplet size etc.) formulation (suspension, emulsion etc.)
Soil physical properties	<ul style="list-style-type: none"> soil water content and its distribution bulk density and pore volume, soil texture soil pH soil water evaporation rate organic matter and clay content soil temperature, surface roughness
	<ul style="list-style-type: none"> air temperature and air humidity incident solar radiation wind velocity and turbulent flow (eddy diffusion coefficient) precipitation
Meteorological conditions	

The most significant physical property regarding pesticide losses to the air is its vapor pressure. In experiments studying the environmental fate of several pesticides, a correlation of the initial volatilization rate after surface application and the vapor pressure was detected (Farmer et al., 1972; Glotfelty et al., 1984). Though, the vapor pressure solely does not allow for a prediction of the volatilization rates because a large number of factors, especially phase partitioning and adsorption effects, affect the long-term volatilization tendency. In practical situations, the “effective” vapor pressure is likely to be lower than the “pure” vapor pressure because there may be interactions of the pesticide with the soil surface. For instance, increasing soil adsorption under dry conditions may cause a reduction of the vapor pressure and may lead to lower volatilization rates (Taylor & Spencer, 1990).

Organic matter content, soil texture or clay content, and soil pH exert their influence over volatilization through adsorption effects on reducing the solution concentration and vapor density in the soil. For weakly polar or nonionic chemicals, the amount of soil organic matter is related to increasing adsorption and, consequently, to decreasing vapor density or potential volatility. With more polar or ionic molecules, clay minerals play an increasingly important role in adsorption and volatility. Bulk density or porosity is important because of its influence on vapor and nonvapor phase movement of the chemical and also because of its influence on water evaporation rates (Spencer et al., 1995).

In the field, the effect of soil moisture distribution upon pesticide volatilization outweighs all other factors such as soil organic matter content and temperature (Glotfelty et al., 1984). As mentioned above, pesticides vaporize much more rapidly from wet than from dry soils. Measurements of vapor pressure in soil at various water contents conclusively demonstrated that the greater volatilization from wet than from dry soils is due mainly to an increased vapor pressure resulting from displacement of the pesticide from soil surfaces by water (Spencer & Cliath, 1974). Under field-conditions, many soils rapidly form a dry surface layer that greatly suppresses pesticide volatilization. The effect of soil drying is largely reversible, however, and when the soil is remoistened, volatilization resumes. Thus, any climatic condition or tillage practice that affects the soil moisture distribution will have a profound effect on the amount of volatilization.

Temperature influences volatilization rates mainly through its effect on vapor pressure and through its effect on the movement of the chemical to the surface by diffusion or mass flow in evaporating water. For these effects, increases in temperature are usually associated with increases in volatilization rate. However, this may not always be the case, since an increase in temperature is also associated with an increase in the drying rate of the soil surface, thereby possibly decreasing vapor density and resulting in less volatilization than at the lower temperature.

Air humidity is important because of its effect on the water evaporation rate and the water content of the surface layer of soil. Wind speed and insolation also affect the water evaporation rate, as well as the pesticide movement from the soil surface. All other things being equal, volatilization rate will increase with increasing wind speed or increasing insolation. Rainfall, of course, greatly affects the water status of the soil and usually moves pesticides downward away from the soil surface.

Generally, the interdependence of factors governing soil volatilization as indicated above renders predictions of the time course of volatilization more difficult. Of course, the intrinsic properties of individual pesticides are important, but experimental data suggest that the volatilization rate of a specific pesticide in soil is controlled mainly by soil

conditions. Meteorological variables are important insofar as they control the soil conditions, but soil conditions, and particularly soil moisture levels, are critical in controlling the supply of available pesticide at the surface, which in turn controls the volatilization rate.

Correlation between physicochemical characteristics and the fluxes is also limited by the fact that the pesticides applied are commercial formulations, whereas vapor pressure, aqueous solubility and adsorption coefficient are properties of the active ingredient (Bedos et al., 2002). The major effects of formulations are probably most evident during application due to drift and volatilization from droplets, but the formulation can also influence the penetration of the applied pesticide into the soil.

Pesticides can diffuse through the soil in both the vapor and nonvapor phases (Spencer, 1970). Gas-phase diffusion is approximately 10^4 times greater than liquid-phase diffusion. Though, vapor-phase diffusion is of comparable magnitude to nonvapor diffusion because only a small fraction of the pesticide exists in the gas phase. As an additional transport process, water evaporation from the surface induces an upward flow of soil solution, which carries with it salt, organic matter, pesticide, and other solutes. The mass flux of pesticides depends upon the evaporation rate and the concentration in the soil solution. Obviously, convective flow will be more important when the soil is wet than when it is dry. The balance between convective flow and diffusion also depends upon the intrinsic properties of the pesticide. Low solubility and high vapor pressure favors diffusive flux of a compound like trifluralin (Harper et al., 1976). On the other hand, loss of the more soluble lindane was shown to be five-times greater with water evaporation than by diffusion alone (Spencer & Cliath, 1973). In addition, volatilization rapidly becomes dependent upon relatively slow diffusion and convective flow processes, when the pesticide is incorporated. Shallow soil incorporation at the time of application is, therefore, an effective management technique in preventing pesticide volatilization.

2.1.2 Model Approaches: Volatilization from Soil

Existing approaches and estimations for the consideration of soil volatilization reflect crucial soil processes, e.g. transformation, diffusion and convection, with a varying degree of accuracy, covering a broad range from empirical and screening models to atmospheric dispersion models (Fig. 2.2).

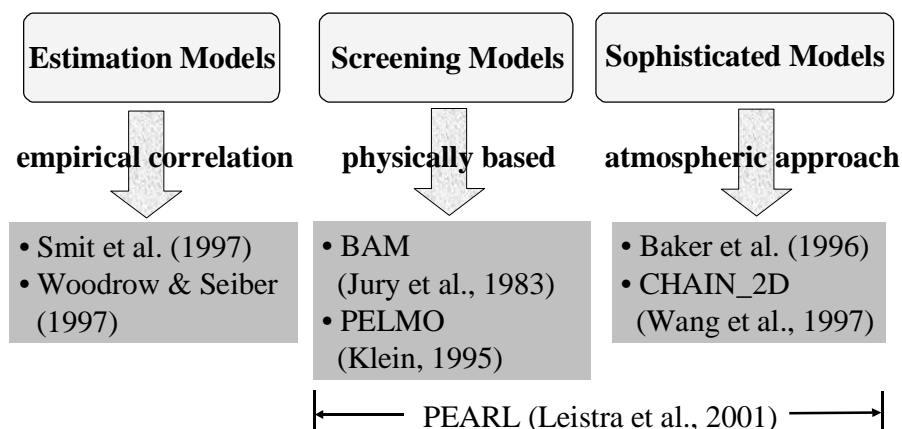


Figure 2.2 Approaches for the description of volatilization from soil: Main groups and examples of the different types currently in use.

2.1.2.1 Empirical Approaches: Volatilization from Soil

Generally, empirical approaches allow for prediction of the volatilization behavior of pesticides by correlating physicochemical properties of the compounds to experimental findings. The uncertainty in the calculated pesticide flux and that in the cumulative loss depends on the quality of the underlying data used in the respective correlation. These correlations were intended as a simpler and less costly and time-consuming alternative to measuring emissions.

2.1.2.1.1 Estimation Method: Smit et al. (1997)

For surface applied pesticides, the estimation method of Smit et al. (1997) correlates cumulative volatilization reported in the literature to the calculated fraction of the pesticide in the gas phase.

After spraying, the pesticide is distributed over the gas, liquid, and solid phases of the topsoil layer. This method requires values for vapor pressure, water solubility, and sorption coefficient as input parameters for the calculation of the fractions of the pesticide in the different phases (cf. 2.1.2.3.1: PEARL). Corrections were made for the effect of temperature on the vapor pressure and water solubility using the Clausius-Clapeyron equation (Klotz & Rosenberg, 1974).

By correlating the calculated fraction of the pesticide in the gas phase to the cumulative volatilization, regression equations were derived for various field and greenhouse conditions. The empirical relation for normal to moist field conditions at 21 days after application is:

$$CV = 71.9 + 11.6 \cdot \log(100 \cdot FP_{gas}) \quad [1]$$

where CV = cumulative volatilization [% of dosage active ingredient], and FP_{gas} = fraction of pesticide in the gas phase.

2.1.2.1.2 Estimation Method: Woodrow & Seiber (1997)

Another empirical approach for estimating the volatilization behavior was developed by relating the physicochemical properties of pesticides and other organics to their published volatilization fluxes determined immediately after soil treatment (within 12 - 24 h) (Woodrow & Seiber, 1997). The volatilization flux ($Flux$) is plotted against the ratio (R_{surf})

$$R_{surf} = \frac{VP}{K_{OC} \cdot S_W} \quad [2]$$

where VP = vapor pressure [Pa], K_{OC} = organic carbon partition coefficient [mL g⁻¹], and S_W = soil water solubility [mg L⁻¹], on a double-logarithmic diagram for each compound, resulting in a small scatter about the regression line

$$\ln(Flux) = 28.355 + 1.6158 \cdot \ln(R_{surf}) \quad [3]$$

Assuming that the volatilization flux should be directly related to the application rate (AR), a further term was added to the above ratio to give

$$R = \frac{VP \cdot AR}{K_{OC} \cdot S_w}, \quad [4]$$

resulting in the following correlation:

$$\ln(Flux) = 19.35 + 1.0533 \cdot \ln(R). \quad [5]$$

2.1.2.2 Screening Approach: Behavior Assessment Model

For a more accurate calculation of the volatilization flux, a model is used which describes a pesticide's fate in the soil and the exchange with the lower part of the atmospheric boundary layer. A description of volatilization from soil in terms of properties of the compound, soil, and evaporation of water was developed by Jury et al. (1983, 1984A,B,C). The model considers pesticide transport in the soil by diffusion in the liquid and vapor phases and convective transport by water movement. It assumes linear, equilibrium partitioning between vapor, liquid and adsorbed chemical phases, net first-order degradation, and chemical movement to the atmosphere by volatilization loss through a stagnant boundary layer at the soil surface (**Fig. 2.3**). The compound is considered to be placed at uniform initial concentration in a soil layer of a thickness L at $t = 0$. Water flow J_w is steady and either upward, downward, or zero. The pesticide vapor obeys Fick's law [eq. 6] and the dissolved chemical obeys convection-dispersion flux equation [eq. 7]. From this description and the assumption of steady-state upward or downward flow, an analytical solution can be derived for the volatilization flux.

$$J_g = -\xi_g(a) \cdot D_g^{air} \cdot \frac{\partial C_g}{\partial z} = -D_g^{soil} \cdot \frac{\partial C_g}{\partial z} \quad [6]$$

$$J_l = -D_e \cdot \frac{\partial C_l}{\partial z} + C_l \cdot J_w \quad [7]$$

where J_g = gaseous diffusion mass flux [$\mu\text{g cm}^2 \text{d}^{-1}$], $\xi_g(a)$ = gas phase tortuosity factor, C_l , C_g = phase concentrations (liquid, gaseous) [$\mu\text{g cm}^{-3}$], D_g^{air} , D_g^{soil} = gaseous diffusion coefficients in air and soil [$\text{cm}^2 \text{d}^{-1}$], J_l = flux of dissolved solute [$\mu\text{g cm}^2 \text{d}^{-1}$], D_e = effective diffusion and dispersion coefficient [$\text{cm}^2 \text{d}^{-1}$], and z = soil depth [cm].

This model, which was intended to screen organic compounds for their relative susceptibility to different loss pathways (volatilization, leaching, degradation) in soil and air, requires knowledge of the environmental conditions and physicochemical properties of the compounds. According to Jury et al. (1983), the duration, intensity and time course of the volatilization process from moist soil depends mostly on the Henry's law constant (K_H). On this basis, pesticides were divided into three classes, depending on whether their soil-to-air transfer was dominated by resistance in the soil layer (category I), the air layer (category III) or both (category II). Category I comprises highly volatile pesticides with a non-dimensional $K_H \gg 2.65 \cdot 10^{-5}$; category II moderately volatile pesticides with intermediate values of K_H and category III slightly volatile pesticides with $K_H \ll 2.65 \cdot 10^{-5}$. For category I compounds, e.g. methyl bromide and some organophosphates, the volatilization rate is highest immediately after application, and then decreases at a rate dependent on

whether soil water is evaporating or not. Pesticides belonging to category III, e.g. atrazine, tend to accumulate on the soil surface as water evaporates from soil, so that volatilization increases with time, or slowly declines if water evaporation does not occur.

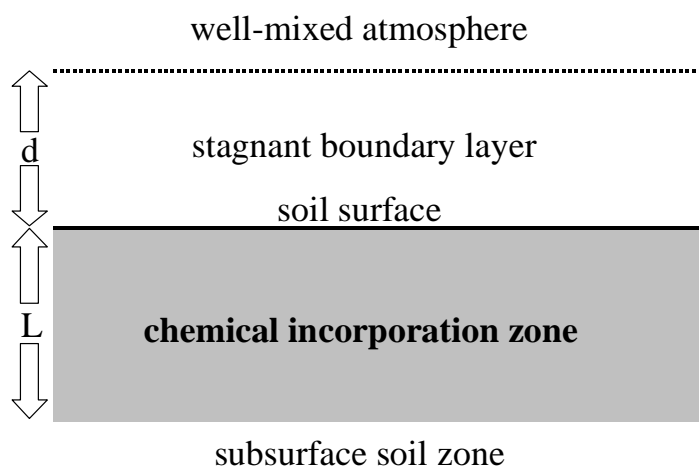


Figure 2.3 Standard scenario used for BAM (Behavior Assessment Model) simulations.

It is important to point out that this description is not a simulation model because the implied conditions are far too idealized to represent a field simulation, e.g. pesticide properties may not remain constant over time or with different soil conditions. The model assumes a constant soil moisture content and constant soil moisture advection. The lack of soil moisture movement in the model implies that chemical movement through the soil occurs solely via molecular diffusion. Additionally, there are influences on volatilization that are not taken into account in the model: When the soil surface layer dries out sufficiently, adsorption of chemicals to the mineral or organic surfaces increases significantly and volatilization rates decrease. A detailed discussion of the limitations is given by Jury (1993).

The applicability of BAM is limited to situations where the above-ground concentration of the volatile compound is zero above a boundary layer because the surface boundary condition in BAM is homogeneous. Important situations of the accumulation of the volatile compound below buildings, in vegetation or below material stored on the ground are thereby excluded from consideration. An extension of BAM has been proposed by Anderssen et al. (1997). An analytic solution for the non-homogeneous surface boundary condition extension of BAM was derived which allows its exploratory potential to be extended to the more realistic scenarios mentioned above. This analytical solution contains the BAM solution as a special case.

2.1.2.3 Sophisticated Approaches: Improvement of PEC Models

As an alternative to the screening models presented above, Baker et al. (1996) proposed that volatilization occurs as a process of unsteady diffusion; that is, diffusion from the soil to the atmosphere interrupted at random intervals by dispersive events that represent eddies of the smallest scale. Thus, small parcels of air brought into contact with the soil surface remain there for a period before being ejected or swept away by local-scale turbulence. This approach has been used to describe mathematically evaporation of water from rough and smooth surfaces (Brutsaert, 1975). Baker et al. (1996) applied this concept to sur-

face/atmosphere exchange of pesticides, linking it with a convective/dispersive model of soil chemical transport and algorithms for heat and water flow driven by solution of the surface energy balance.

This model matches measurements well during the first day following chemical application, but subsequently tends to overpredict volatile losses. Water flow, heat flow, and surface/atmosphere exchange processes are obviously important, but the uncertainties attendant to their simulation are probably less important than those associated with adsorption/desorption, and gas/liquid partitioning. Examination of these questions will require the development of new methodologies for characterizing chemical behavior under dynamic conditions in unsaturated soil.

An example for “sophisticated models” which combines several elements of different volatilization models has been given by Wang et al. (1997). He used CHAIN_2D (Simunek & Van Genuchten, 1994) for characterizing the volatilization of methyl bromide. CHAIN_2D is a model for simulating two-dimensional variably saturated water flow, heat transport, and the movement of solutes involved in sequential first-order decay reactions. The program numerically solves the Richards’ equation for saturated-unsaturated water flow and the convection-dispersion equation for solute and heat transport. A volatilization boundary condition according to Jury et al. (1983) is implemented. A resistance analogue similar to Baker et al. (1996) was used to determine the transfer coefficient between surface and atmosphere. Wang et al. (1997) emphasized that his model may be improved by including atmospheric barometric pressure variations, early time pressure-driven advective flow and density-driving flow.

The main focus of this thesis was to evaluate and improve the volatilization approaches used in the currently available PEC models for registration purposes in the European Union, especially the Dutch model PEARL (cf. 2.1.2) and the German model PELMO (cf. 2.1.2). As follows, the basic assumptions of these sophisticated approaches, which were used for the calculations (cf. 4.1.3), are summarized.

2.1.2.3.1 PEARL: Description of Volatilization from Soil

Modifications and further development of the Behavior Assessment Model (cf. 2.1.2.2) have become part of other approaches such as the Pesticide Leaching and Accumulation Model (PESTLA; Van den Berg et al., 1999) and the subsequent model PEARL (Leistra et al., 2001; Tiktak et al., 2000).

The PEC model PEARL (Pesticide Emission Assessment at Regional and Local Scales) was developed to evaluate the leaching of pesticides to the groundwater in support of the European and Dutch pesticide registration procedures (Leistra et al., 2001; Tiktak et al., 2000; Van Dam et al., 1997). It is a one-dimensional, dynamic, multi-layer model describing the fate of a pesticide and relevant transformation products in the soil-plant system and includes a module for estimation of pesticide volatilization from soil.

In the current version of the PEARL model, the volatilization of the pesticide from soil is described assuming a boundary air layer through which the pesticide has to diffuse before it can escape into the atmosphere (Leistra et al., 2001). The volatilization flux depends on the concentration gradient of the pesticide across the boundary air layer and is also dependent on the concentration gradient of the pesticide in the top compartment of the soil profile.

The following equation is used for determining the volatilization flux:

$$J = -\frac{c_{g,l}}{r_a + r_s} \quad [8]$$

where J = volatilization flux through the boundary air layer [$\text{kg m}^{-2} \text{d}^{-1}$], $c_{g,l}$ = concentration in the gas phase at the center of the upper computation layer in soil [kg m^{-3}], r_a = resistance for transport through the boundary air layer [d m^{-1}], and r_s = resistance for diffusion through the top boundary soil layer [d m^{-1}].

Resistances can be described as:

$$r_a = \frac{d_a}{D_a} \quad [9]$$

$$r_s = \frac{0.5 \cdot z_1}{D_{dif,g}} \quad [10]$$

where d_a = thickness of boundary air layer [m], D_a = pesticide diffusion coefficient in air [$\text{m}^2 \text{d}^{-1}$], z_1 = thickness of upper computation layer in soil [m], and $D_{dif,g}$ = coefficient for pesticide diffusion in the gas phase [$\text{m}^2 \text{d}^{-1}$].

The concentration of the pesticide in the gas phase is calculated using the equations describing the partitioning of pesticides between the soil phases. The partitioning between the solid and the liquid phases is described with a Freundlich-type equation. Partitioning between the gas and liquid phases is expressed as:

$$K_H = \frac{c_G}{c_L} \quad [11]$$

where K_H = non-dimensional Henry's law constant, c_G = pesticide concentration in the gas phase [kg m^{-3}], and c_L = pesticide concentration in the liquid phase [kg m^{-3}].

The potential evapotranspiration was calculated by the Penman-Monteith method (Monteith, 1965). PEARL needs input from a model simulating water flow and heat transport in soil. For this purpose, PEARL is coupled to the hydrological model SWAP (Soil Water Atmosphere Plant Model; Van Dam et al., 1997). The upper boundary condition for the soil heat conduction model is the daily-average temperature, at the lower boundary of the soil system, the temperature is set at the long-term average temperature of 283 K. Soil horizons were distinguished and a common input file was designed for SWAP and PEARL containing soil properties per horizon of the lysimeter. In addition, initial pressure heads were calculated from the measured volumetric water content at the beginning of the experiment. PEARL does not allow for direct input of measured soil moisture over the course of the experiment and uses the pressure heads for calculating the time-dependent volumetric water content. For details on the combined computation of SWAP and PEARL refer to Leistra et al. (2001).

2.1.2.3.2 PELMO: Description of Volatilization from Soil

The PEC model PELMO (Pesticide Leaching Model) was developed to estimate the leaching potential of pesticides through distinct soil horizons. It is a bucket model based on the PRZM-1 code of the USEPA (Carsel et al., 1984), but was improved with regard to the

requirements of the German authorities responsible for the registration of pesticides (Klein, 1995). Processes include estimation of soil temperatures, pesticide degradation, sorption, volatilization, and actual evapotranspiration.

The official version of PELMO used for registration purposes (FOCUS PELMO 1.1.1) estimates volatilization from soil using a simple volatilization module based on Fick's and Henry's law (Klein, 1995). It is assumed that the concentration of the pesticide in the air above the soil is neglectably low. PELMO considers volatilization from soil water and does not include a description of soil-air partitioning. Volatilization rates are calculated according to the following equation:

$$J = -D \frac{H' c_{sol}}{d} \quad [12]$$

where J = volatilization rate [$\text{g cm}^{-2} \text{d}^{-1}$], D = diffusion coefficient in air [$\text{cm}^2 \text{d}^{-1}$], H' is the non-dimensional Henry's law constant, d is the air boundary layer [cm], and c_{sol} is the pesticide concentration in the soil water [g cm^{-3}].

The standard scenario for PELMO simulations implies default values for soil layer thickness (5 cm) and volatilization depth (1 mm; thickness of the soil layer actively involved in the volatilization process). PELMO allows input of the volumetric water content of the soil layers measured at several depths at the beginning of the experiment.

Within the framework of the APECOP project, the official PELMO version was enhanced and the following improvements of the volatilization module were implemented:

- Based on Henry's law constants measured or estimated at two temperatures, exponential approaches were included for calculating the temperature-dependence of water-air partitioning over the relevant temperature range, enabling PELMO to assess Henry's law constants over the course of the study for actual soil temperatures.
- The compartment size of the top soil layer was reduced from 5 cm to 1 mm for a more realistic simulation of the pesticide volatilization immediately after soil surface application.
- The moisture dependence of the soil adsorption coefficients at low water content was taken into consideration. For moistures ranging from above air dry conditions to below wilting point, an increase of the soil sorption coefficient was assumed to occur in the top millimeter of the soil. The sorption coefficient at air dry soil, whose water content was estimated to be 10% of the water content at the wilting point, was increased by a factor of 100. In the range between air-dry soil and wilting point, an exponential approach was used for calculating the moisture-dependent adsorption coefficient. Above the wilting point, the sorption coefficient remained unchanged.
- Optionally, the improved version enabled volatilization fluxes to be calculated in an hourly resolution, subject to the condition that environmental data were also provided on hourly basis.

2.2 Pesticide Volatilization from Plant Surfaces

Although volatilization from plant surfaces is one of the main pathways of pesticide emission to the environment and mostly exceeds soil volatilization, the knowledge of the rate-determining processes is not yet sufficient for model purposes. The physical principles

of the processes and the main factors affecting plant volatilization, as summarized below, lead to the currently available approaches for modeling and indicate how experimental procedures should be conducted to enhance their usefulness for model development.

2.2.1 Factors Governing Volatilization from Plants

The dominant factors that influence the volatilization of pesticides from crops are the physicochemical properties (**Table 2.1**), the persistence on the plant surface and the environmental conditions (atmospheric stability, wind, temperature, and air humidity).

In accordance with soil volatilization, vapor pressure is also expected to be a key parameter governing plant volatilization. In several studies, the relationship between volatilization flux during the first hours after application and vapor pressure was found to have the highest correlation coefficient (Woodrow et al., 1997; Smit et al., 1998). Though, emission into the air is counteracted by molecular interaction forces in the deposit, which may vary from weak (volatile liquids) to very strong (low-volatile crystalline solids). The sink process of adsorption by plant foliage, e.g. the cuticle on leaf surface, is described by octanol-water partitioning coefficients (K_{ow}). The adsorption of the pesticide to the leaf surface is expected to increase with time, mostly under moist conditions. This process is influenced by water solubility and Henry's law constant, which also govern plant volatilization under moist conditions. Thus, the competing processes affected by chemical properties indicate the difficulties to predict volatilization behavior.

The persistence on the leaf surface depends on the various dissipation processes, such as photodegradation, wash-off by rainfall or irrigation, and uptake of the pesticide by the plant leaves. As mentioned above, the extent of penetration into the leaves is highly dependent on the physicochemical properties of the compound. For non-charged compounds, especially molecular size and polarity are important characteristics (Bentson, 1990). Various weak acid and weak basic pesticides show good penetration into plants, followed by transport to the action sites. The fate processes on the leaf surface that affect the pesticide are not well understood. Some important factors include the nature of the plant, the stage of development of the plant, e.g. seedling versus fully mature, the characteristics of the leaf surface, e.g. waxy cuticle type, and the density and the height of the canopy. Under rainy conditions, parts of the pesticide deposit may be washed-off from the leaves, resulting in a drastic reduction in its volatilization rate. The extent of this process depends on pesticide properties, properties of the formulation, e.g. sticking agents, and the time elapsed after application. Pesticides deposited on leaf surfaces may be subject to transformation, especially to photochemical transformation. For effective plant-applied pesticides, photodegradation is not very fast as this would impede their usefulness. However, several pesticides exhibit some extent of phototransformation on leaf surfaces. Photodegradation may lead to products that also show volatilization, e.g. the photo-oxidation of parathion to paraoxon.

Furthermore, little is known on the effect of the formulation type on the waxy layer. Some spray formulations can disrupt the epicuticular wax layer, e.g. the penetration of atrazine into weed leaves was enhanced by adding crop oil concentrate to the spray liquid (McCall et al., 1986).

The influence of environmental conditions on plant volatilization is similar to the effects concerning soil volatilization (cf. 2.1.1). Obviously, a higher temperature tends to favor

volatilization from plants, because the vapor pressure of the compound is exponentially temperature-dependent and additionally the adsorption to the leaf surface decreases with increasing temperature. Due to its effect on air temperature and leaf-surface temperature, solar irradiance also enhances volatilization.

One of the most important differences between soil and plant processes deals with the aerodynamic scenario. Recent simulations showed that under still and convective conditions the vapors emitted by a source point rapidly form stationary envelopes around the leaves. Vapor concentrations within these unstirred layers depend on the vapor pressure of the compound in question and on its affinity to the lipoid surface layers on the leaf (Riederer et al., 2002).

The resistance in air to the volatilization of substances is often described in terms of an equivalent thickness of the air boundary layer (Majewski et al., 1990). The pesticide has to pass this layer, which provides laminar air flow, by diffusion from the deposit surface to the turbulent air where fast removal of substances occurs. The thickness of the air boundary layer is influenced by parameters like wind speed, atmospheric turbulence and surface roughness. Generally, increasing wind speed and more turbulent climatic conditions are expected to decrease the air boundary layer. Compared to bare soil the air flow through a plant canopy is rather complex, e.g. complicated by moving leaves, so there may be no single equivalent value of the thickness of the air boundary layer for all heights in the canopy, suggesting that model descriptions are rendered more difficult.

2.2.2 Model Approaches: Volatilization from Plants

Currently, no models are available for reliable, physical based estimation of volatilization fluxes of pesticides from plant surfaces. A screening-level estimate of the initial volatilization rate after spraying of the crop was performed using the vapor pressure of the pesticide (Woodrow & Seiber, 1997). A good correlation between the logarithm of the volatilization rate and the logarithm of the vapor pressure was observed. For the cumulative loss from plant surfaces an estimation method was developed by Smit et al. (1998).

In the present version of the PEARL model (Leistra et al., 2001), the pesticide processes in the plant canopy are characterized in a simplified way. Volatilization is described as a first-order process, for which a rate coefficient can be introduced. To describe volatilization in a more mechanistic way, accounting for the factors influencing the process, a simplified model on the basis of a series of well-defined experiments using the fungicide fenpropimorph was developed (Leistra, unpublished) and applied to the data generated within the wind-tunnel experiment on winter wheat (cf. 4.2.3).

2.2.2.1 Empirical Approach: SMIT et al. (1998)

Smit et al. (1998) found the following statistical relation for the accumulated emission of pesticides during 7 days after application to crops that fully cover the soil in the field and in climate chambers:

$$\log(CV) = 1.528 + 0.466 \log(VP) \quad \text{for } VP \leq 10.3 \text{ mPa} \quad [13]$$

where CV = accumulated emission during 7 days after application [% of dosage], and VP = vapor pressure [mPa].

This method is expected to overestimate the cumulative volatilization for compounds subject to fast transformation, e.g. due to hydrolysis or phototransformation, or for compounds which act systemically in the plant leaves. Data available on these pesticide properties are limited and often show wide ranges, which impedes their inclusion in the approach.

2.2.2.2 Model Approach on the Basis of a Boundary-layer Concept

Within the framework of the APECOP project, a basic approach for predicting plant volatilization was developed (Leistra, unpublished). The model simulates the environmental fate of pesticides after application on plant surfaces on an hourly basis, including volatilization from the leaves, penetration into the leaves, wash-off and phototransformation. The well-known processes, e.g. the calculation of volatilization fluxes by determining vapor diffusion through the laminar air boundary layer, were described in a mechanistic way. Other processes and factors, especially photochemical transformation and penetration into the leaves, did not allow for a quantitative description yet, so an empirical description was chosen to take these processes into consideration. This empirical estimation includes the thickness of the air boundary layer and the rate coefficients for penetration, phototransformation and wash-off to be calibrated on the basis of measurements.

The net applied amount of the pesticide and the fraction of the dosage intercepted by the crops were introduced in the model. Within simulations referring to studies where standard field sprayers were used, the factor for the effect of spray distribution in the crop canopy on volatilization (f_{dis}) is considered to be 1.0 (standard distribution). The factor for the effect of the formulation on volatilization (f_{for}) is assumed to be 1.0 for spraying standard formulations, e.g. emulsifiable concentrates and wettable powders.

The vapor pressure of the pesticide at the prevailing temperature is calculated by the following form of the Clausius-Clapeyron equation (Tinsley, 1979; Grain, 1982).

$$P_{act} = P_{ref} \exp \left[\left(\frac{-H_v}{R} \right) \left(\frac{1}{T} - \frac{1}{T_{ref}} \right) \right] \quad [14]$$

where P_{act} = actual vapor pressure of the pesticide [Pa], P_{ref} = saturated vapor pressure of the pesticide at reference temperature [Pa], H_v = molar enthalpy of vaporization [J mole⁻¹], R = molar gas constant [8.314 J mole⁻¹ K⁻¹], T = temperature [K], T_{ref} = reference temperature [K]. The reference temperature for all temperature-dependent quantities is taken to be 20 °C.

The concentration of the pesticide in the air at the deposit surface on the leaves is calculated by using the general gas law:

$$C_{a,s} = \left(\frac{M P_{act}}{RT} \right) \quad [15]$$

where $C_{a,s}$ = concentration of the pesticide in the air at the surface [kg m^{-3}], M = molar mass [kg mole^{-1}].

The coefficient D_a for pesticide diffusion in air at the prevailing temperature is calculated according to Tucker & Nelken (1982):

$$D_a = D_{a,ref} \left(\frac{T}{T_{ref}} \right)^{1.75} \quad [16]$$

where D_a = diffusion coefficient of pesticide in air [$\text{m}^2 \text{d}^{-1}$], and $D_{a,ref}$ = diffusion coefficient in air at reference temperature [$\text{m}^2 \text{d}^{-1}$].

Volatilization of pesticide from the deposit surface on the leaves is determined by vapor diffusion through the laminar air boundary layer. The potential rate of volatilization of pesticide from the deposit/leaf surface is calculated as follows:

$$J_{vol,pot} = D_a \frac{(C_{a,s} - C_{a,t})}{d_{lam}} \quad [17]$$

where $J_{vol,pot}$ = potential flux of volatilization from the surface [$\text{kg m}^{-2} \text{d}^{-1}$], $C_{a,t}$ = concentration in the turbulent air just outside the laminar air layer [kg m^{-3}], d_{lam} = equivalent thickness of the laminar air boundary layer [m]. The pesticide concentration in the turbulent air layer outside the laminar boundary layer ($C_{a,t}$) is taken to be zero.

The actual rate of pesticide volatilization is described by taking the mass of pesticide deposited on the plants, the distribution in the canopy and the formulation of the pesticide into account:

$$J_{vol,act} = f_{mas} f_{dis} f_{for} J_{vol,pot} \quad [18]$$

where $J_{vol,act}$ = actual rate of pesticide volatilization [$\text{kg m}^{-2} \text{d}^{-1}$], f_{mas} = factor for the effect of pesticide mass on the plants [-], f_{dis} = factor for the effect of pesticide distribution in the canopy [-], f_{for} = factor for the effect of formulation [-].

The pesticide is assumed to be deposited on the leaves in spots with variable thickness. The thinner the deposit at a certain place is, the earlier that place will be depleted by volatilization. The concept bases on the assumption that the volatilizing surface decreases in proportion to the decrease in mass of pesticide in the deposit. So, the factor f_{mas} is calculated from the ratio $A_p/A_{p,ref}$, where A_p = areic mass of pesticide on plants [kg m^{-2}], $A_{p,ref}$ = reference areic mass of pesticide on plants [10^{-4}kg m^{-2}] ($= 1 \text{kg ha}^{-1}$).

The rate of pesticide penetration into the leaves is calculated by:

$$R_{pen} = k_{pen} A_p \quad [19]$$

where R_{pen} = rate of pesticide penetration into the leaves [$\text{kg m}^{-2} \text{d}^{-1}$], k_{pen} = rate coefficient of penetration [d^{-1}].

The rate of pesticide wash-off from the leaves by rainfall is set dependent on rainfall intensity and wash-off coefficient:

$$R_w = k_w W_r A_p \quad [20]$$

where R_w = rate of pesticide wash-off from the leaves [$\text{kg m}^{-2} \text{d}^{-1}$], k_w = coefficient for pesticide wash-off [mm^{-1}], W_r = rainfall intensity [mm d^{-1}].

The rate of pesticide transformation by solar irradiation is described by first-order kinetics:

$$R_{ph} = k_{ph} A_p \quad [21]$$

where R_{ph} = rate of phototransformation on the leaves [$\text{kg m}^{-2} \text{d}^{-1}$], k_{ph} = rate coefficient of phototransformation [d^{-1}].

The rate coefficient k_{ph} is set dependent on sunlight irradiation intensity:

$$k_{ph} = \left(\frac{I_{act}}{I_{ref}} \right) k_{ph,ref} \quad [22]$$

where I_{act} = actual solar irradiation intensity [W m^{-2}], I_{ref} = reference solar irradiation intensity [500 W m^{-2}], $k_{ph,ref}$ = rate coefficient of phototransformation at reference irradiation intensity [d^{-1}].

The equation for the conservation of mass of pesticide on the plants reads as follows:

$$\frac{dA_p}{dt} = -J_{vol,act} - R_{pen} - R_w - R_{ph} \quad [23]$$

In various volatilization experiments, an initial period with fast volatilization of the pesticide was observed, followed by an extended period with comparatively low volatilization rates. It may be impossible to describe the course of volatilization with time by assuming a single deposit class. The model provides the option to distinguish two deposit classes: a well-exposed and a poorly-exposed class. The deposit in the latter class may be enclosed by plant parts (e.g. in leaf axils), it might be located on the lee side of the air flow, or it is assumed to be located deeper in the canopy. To trace the effect of two deposit classes on the course of volatilization, the fraction of poorly-exposed deposit was set at 20% of the applied dose. Furthermore, the rate of the decrease processes for the poorly-exposed deposit was set at 20% of the rates of the corresponding process for the well-exposed deposit. The definition of two deposit classes requires the use of two mass conservation equations, one for the well-exposed and one for the poorly-exposed deposit.

A summary of the input parameters and the coefficients to be calibrated is given in **Table 2.2**.

Table 2.2 Data required in the boundary-layer approach for predicting volatilization from plant surfaces.

Pesticide properties	Environmental data	Parameters to be calibrated
M = molar mass [g mole ⁻¹]	T = air temperature [°C]	d_{lam} = thickness of laminar air boundary layer [m]
P_{ref} = saturated vapor pressure at reference temperature [hPa]	I_{act} = irradiation [W m ⁻²]	k_{pen} = rate coefficient of penetration [d ⁻¹]
$D_{a,ref}$ = diffusion coefficient in air at reference temperature [m ² d ⁻¹]	W_r = irrigation [mm d ⁻¹]	$k_{ph,ref}$ = rate coefficient of phototransformation at reference irradiation intensity [d ⁻¹]
H_v = heat of vaporization [kJ mole ⁻¹]		k_w = wash-off coefficient [mm ⁻¹]

3 EXPERIMENTAL METHODS AND INSTRUMENTATION

3.1 Volatilization Measurements at Different Scales

Experiments on the volatilization behavior of pesticides were performed at different spatial scales, ranging from laboratory studies, via semi-field experiments to field studies (Fig. 3.1). The experimental volatilization studies were particularly dependent on comprehensive, high-resolution measuring systems and data acquisition systems. Thus, the existing instrumentation, e.g. the measuring device of the photovolatility chamber and the wind tunnel, was optimized to fulfill the requirements of volatilization studies in support of model purposes.

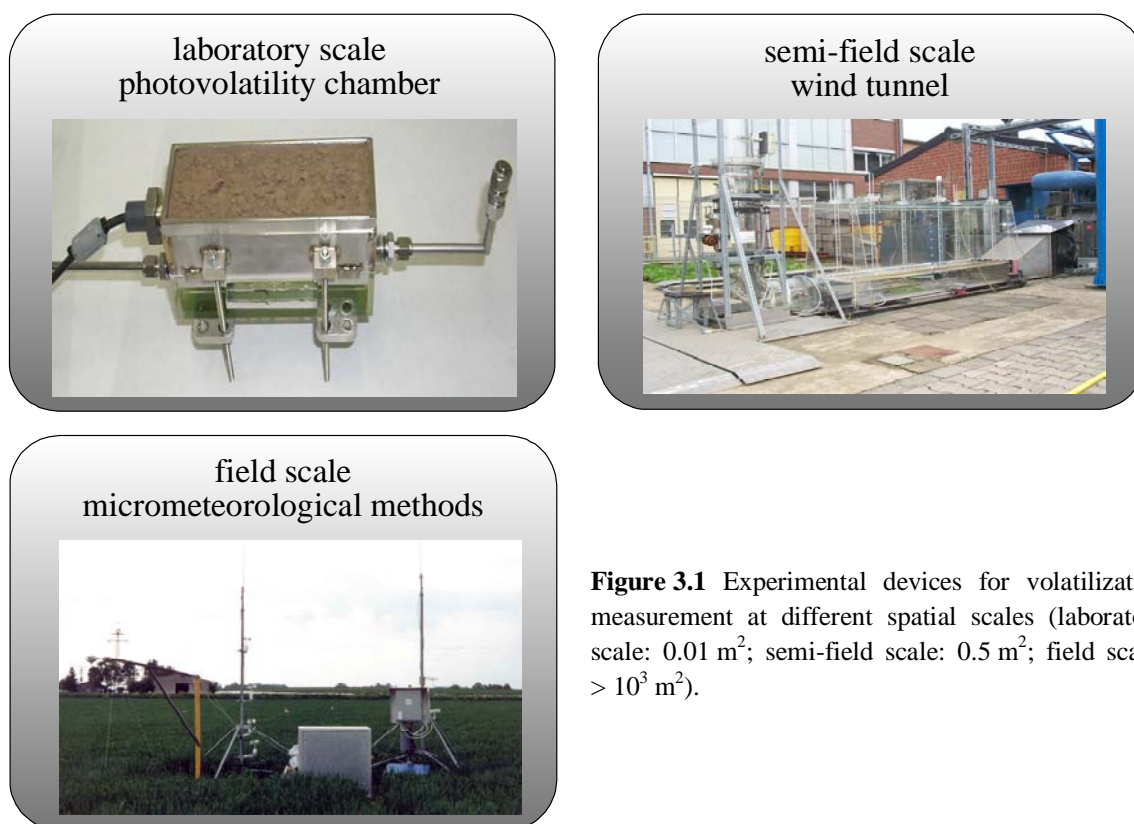


Figure 3.1 Experimental devices for volatilization measurement at different spatial scales (laboratory scale: 0.01 m^2 ; semi-field scale: 0.5 m^2 ; field scale: $> 10^3 \text{ m}^2$).

3.1.1 Laboratory Studies: Photovolatility Chamber

The laboratory photovolatility chamber allows for simultaneous measurement of volatilization and photodegradation of ^{14}C -labeled pesticides under controlled constant, but variable climatic conditions (Kromer et al., 2003; Kromer, 2001). The apparatus had been previously established for detailed studies of direct and indirect photodegradation processes of pesticides on surfaces but had to be modified to suit the particular needs of process studies on volatilization. The set-up of the chamber was improved to characterize the influence of soil moisture, soil temperature, and evaporation on volatilization behavior from soil. Experimental features of the chamber (e.g. instruments, data logging system, air conditioning, and water replenishing system) and the application process were optimized to allow the adjustment of scenarios to field-like conditions.

3.1.1.1 Main Features of the Photovolatility Chamber

The photovolatility chamber and the air conditioning unit are installed in an environmental chamber to obtain constant preconditioned climatic parameters (**Fig. 3.2**).

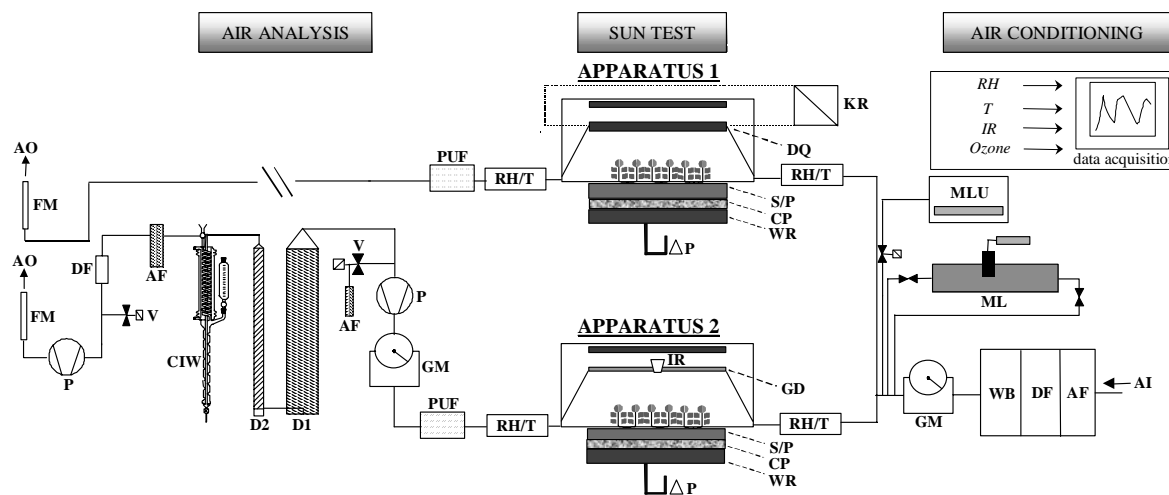


Figure 3.2 Schematic of the photovolatility chamber (air conditioning unit and sun test apparatus are installed in a climate chamber). AF = activated charcoal filter, AI = air inlet, AO = air outlet, CIW = cooled intensive wash bottle, CP = ceramic plate, D1 = first drying stage (silica gel), D2 = second drying stage (phosphorus pentoxide), DF = dust filter, FM = flow meter, DQ = double-walled quartz vessel with water jacket, GD = glass dome, GM = gas meter, IR = infrared sensor, KR = cryostat, ML = mercury lamp for ozone generation, MLU = ozone analyzer, P = metal bellows pump, ΔP = moisture tension, PUF = polyurethane foam plugs, RH/T = control of relative humidity and air temperature, S/P = soil/plant container, V = control valve, WB = wash bottle, WR = water reservoir.

The air passing through the chamber is purified via a filter system consisting of activated charcoal and dust filters to ensure defined and reproducible conditions while reducing photochemical effects caused by trace gases and particulate contamination in the sample air. To achieve water-saturated air and to prevent drying of the soil surface, the air stream passes through two wash bottles (cf. 4.1.1.3). In order to study the influence on photodegradation of environmental chemicals at the interface to the atmosphere, ozone can be selectively added using a by-pass system containing a low-pressure mercury lamp (Penray; Schultz et al., 1995). During the experiments, a metal bellows pump (Ansyco GmbH, Karlsruhe, Germany) provides constant air flow rates up to 12 L min^{-1} passing through the chamber. Significant climatic parameters, including ozone concentration, air humidity, air temperature, and soil temperature, are monitored continuously using various sensors (**Fig. 3.2**).

The center of the chamber consists of two major modules to be used optionally (**Fig. 3.3**): Apparatus 1 consists of a water-cooled, UV-permeable quartz dome mounted inside an irradiation device (Sun Test apparatus CPS⁺, Atlas Material Testing Solutions, Hanau, Germany) on a specially integrated base plate. The set-up guarantees adjustable air temperatures in the chamber (Kromer et al., 1999; Misra et al., 1997). The irradiation device is composed of an adjustable xenon burner and a 290 nm cut-off filter in order to simulate natural sunlight as closely as possible. Natural variations of the spectral photon intensity due to daytime, latitude and variation with season can be simulated by a stepwise programming of the irradiation device.

Apparatus 2 was developed for process studies on volatilization in the dark without using an irradiation device. An additional infrared sensor for measuring the temperature of the soil surface was installed at the center of the glass dome. Analogous to apparatus 1 the glass dome is mounted on a base plate to allow the use of containers with different surfaces, e.g. glass, teflon, soil dust, soil layers and soil/plant systems. Containers of adjustable height can be used for soil bodies of different thickness and provide a surface area of approx. 0.01 m^2 ($18.0 \text{ cm} \times 5.6 \text{ cm}$). Together with the semi-cylinder of the domes (maximum height 31 mm, width 62 mm) the surface area creates a chamber volume of approx. 0.34 L. Air temperature as well as relative humidity of the air fed into the photovolatility chamber can be adjusted to the required conditions. The volatilization studies on the influence of soil moisture and temperature were solely performed using apparatus 2 (cf. 3.1.1.6).

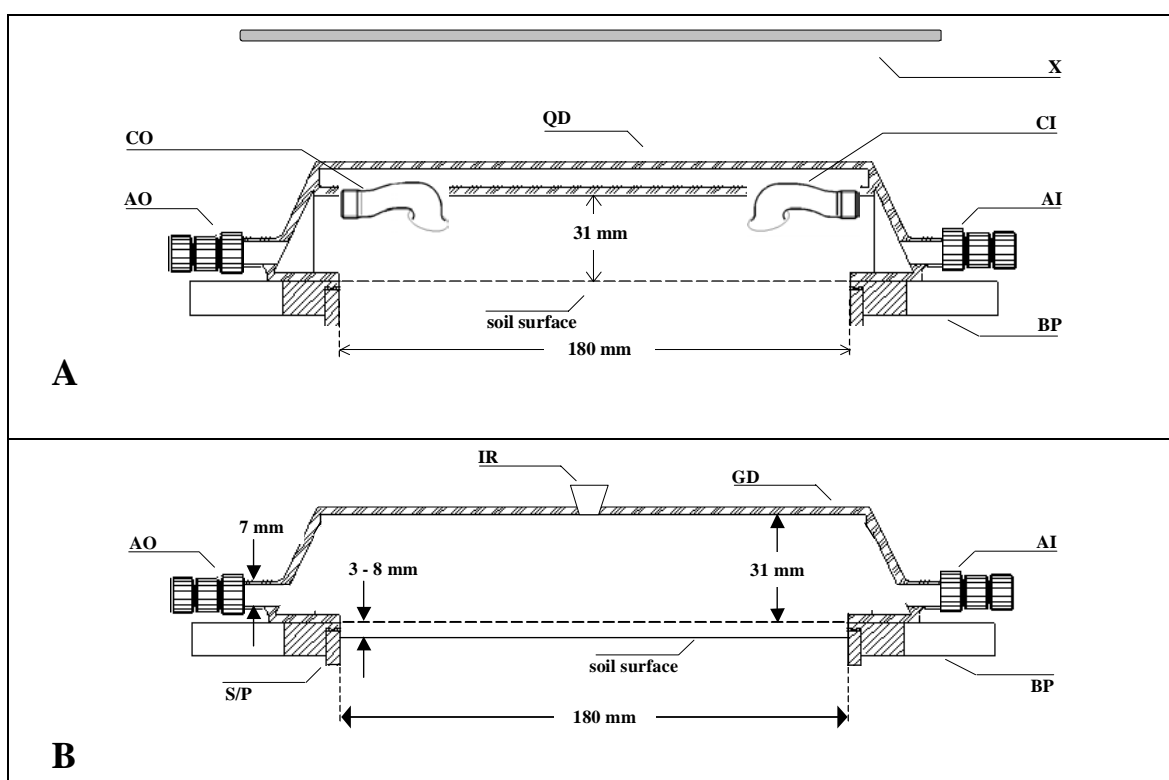


Figure 3.3 Center of the photovolatility chamber. **A:** quartz dome (apparatus 1). **B:** glass dome (apparatus 2). AI = air inlet, AO = air outlet, BP = base plate, CI = cooling inlet, CO = cooling outlet, GD = glass dome, IR = infrared sensor, QD = double-walled water cooled quartz dome, S/P = soil/plant container, X = xenon burner.

An air analysis system (cf. 3.1.1.3) was connected to record gaseous losses. This system is based on the set-up originally designed for wind-tunnel experiments (Stork, 1995; Stork et al., 1994). ^{14}C -labeled organic compounds in the sample air are collected in the total-volume sampler (**Fig. 3.5**) consisting of a glass cartridge filled with three precleaned polyurethane foam plugs (PUF, 30 mm o.d., $3 \times 50 \text{ mm}$). In addition, $^{14}\text{CO}_2$ arising from the complete mineralization of the test compound is measured by a medium-volume sampler (cf. 3.1.2.3) to gain complete radioactivity and mass balances (Stork et al., 1997).

3.1.1.2 Characterization of the Aerodynamic Conditions and Water Content

Measurement of flow profile and pressure differential

For measurements of the air velocity at the soil surface, the infrared sensor installed at the center of the glass dome (**Fig. 3.3B**) was replaced with a thermal anemometer (Airflow Developments Ltd., High Wycombe, UK). The velocity-sensitive thermistor was fixed at several heights (intervals of 3-5 mm). A number of readings of each height were used to calculate the average velocity. The pressure within the chamber was measured using a pressure transducer (Leybold Vakuum GmbH, Cologne, Germany).

Determination of soil moisture: TDR equipment and gravimetric analysis

A water replenishing system shown in **Fig. 3.4** allowed for adjustment of a defined water tension, correlating with the volumetric water content measured by time domain reflectometry (TDR) equipment at a depth of 2.5 cm, during the process studies on volatilization. After finishing the experiments, the soil was removed in layers (thickness: 5 mm) and the soil moisture of the layers was measured by gravimetric analysis: The water mass was determined by drying a weighed soil sample of 5-10 g at 105 °C to constant weight and calculating the moisture content in dry weight basis as the ratio of the mass of water present to the dry weight of the soil sample.

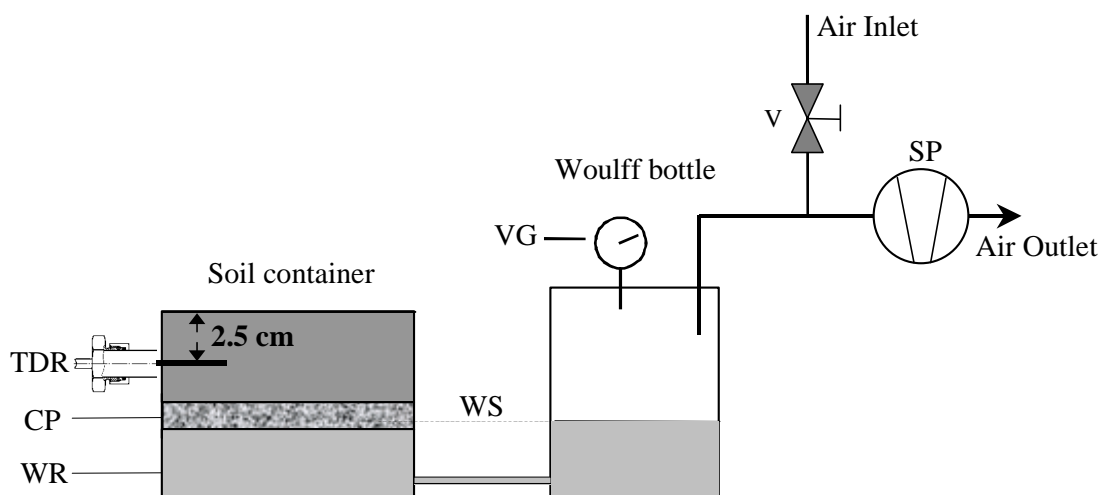


Figure 3.4 Schematic of the water replenishing system. CP = ceramic plate, SP = suction pump, TDR = time domain reflectometry, V = needle valve, VG = vacuum gauge, WR = water reservoir, WS = water surface.

3.1.1.3 Air sampling: Adsorption Capacity of the PUF plugs

Prior to experimental use of the photovolatility chamber in studies on the influence of soil moisture and temperature on volatilization (cf. 3.1.1.6), preliminary tests were carried out to verify the adsorption capacity of the PUF plugs in the total-volume sampler (TVS, **Fig. 3.5**) and to prevent pesticide losses because of increased air exchange rates up to 12 L min⁻¹ after extension of the chamber. Validation studies were performed using a special vaporization apparatus (Stork, 1995). Defined amounts of [phenyl-UL-¹⁴C]-parathion-methyl (approx. 100 mg) were heated, completely vaporized and passed through the air sampling system at exchange rates up to 16 L min⁻¹. Vaporization temperatures of

up to 65 °C were used. After 24 h the plugs were manually squeezed (four times in 35-45 mL methanol, respectively) and all contaminated components were washed with acetone. Radioactivity of extracts was determined by LSC (cf. 3.3.2).

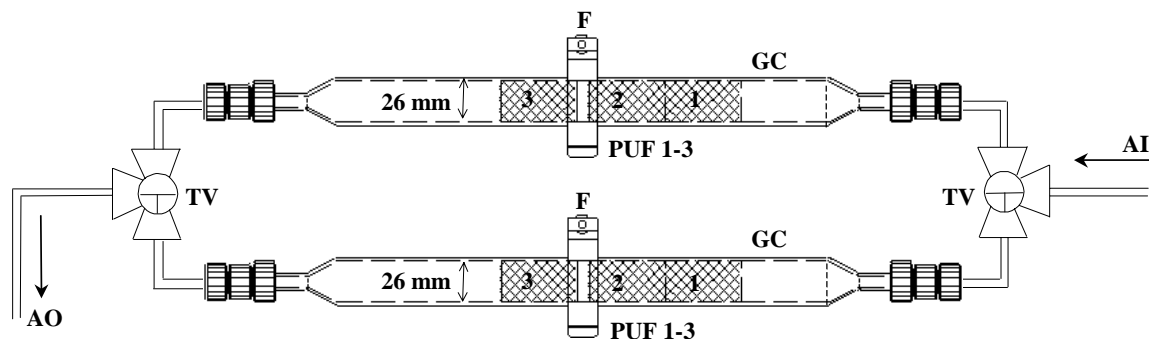


Figure 3.5 Total-volume sampler (TVS) for sampling organic air constituents. AI = air inlet, AO = air outlet going to $^{14}\text{CO}_2$ detection (MVS), F = flange, GC = glass cartridges (26 mm i.d.), PUF 1-3 = polyurethane foam plugs (30 mm o.d. x 50 mm), TV = 3-way valves (PTFE).

3.1.1.4 Performance of Studies on Volatilization: Application Process

For the experiments, the A_p horizon (plow layer) of gleyic cambisol (cf. 3.5.1) was air-dried and sieved with mesh size 2 mm. Subsequently, the soil was mixed with water, the slurry was transferred into the soil container and the water content was adjusted according to the procedure mentioned above (cf. 3.1.1.2). EC-formulated ^{14}C -parathion-methyl was applied using an airbrush (spray pressure: 0.8 bar) with a mean droplet diameter (MVD) of 200 μm and an application volume of 400-500 μL 0.01 m^{-2} , corresponding to 400-500 L ha^{-1} . During the spray application, a contamination shield lined with aluminum foil was attached to the soil container. Afterwards, the soil container (depth 5 cm) was mounted onto the base plate of apparatus 2 of the photovolatility chamber (**Fig. 3.2**). Fittings and connections used in the test system were sealed, subsequently the metal bellows pump was switched on and air sampling started (cf. 3.1.1.5). Decontamination of the air brush and the application shield with acetone allowed for the quantification of application losses.

Preliminary experiments were performed for studying the uniformity of the longitudinal and transversal distribution pattern of the applied compounds on the target surface. Thus, TLC plates were applied with ^{14}C -labeled parathion-methyl according to the above mentioned procedure and evaluated using a Bio-Imaging Analyzer (cf. 3.3.3.1).

3.1.1.5 Performance of Studies on Volatilization: Analysis

Air samples were taken at intervals of up to 24 h. PUF plugs were manually squeezed (four times in 35-45 mL methanol). At the end of the experiments, all contaminated parts of the set-up were rinsed with acetone to obtain a complete radioactivity balance. Radioactivity of extracts was determined by LSC (cf. 3.3.2). Aliquots of the upper soil layers were extracted with methanol in a Soxhlet apparatus for 16 h (cf. 3.3.1). Non-extractable radioactivity in soil material was measured by combustion (cf. 3.3.2). The active ingredient of air and soil samples was characterized for parathion-methyl and its metabolites by radio-TLC (cf. 3.3.3.1) and radio-HPLC (cf. 3.3.3.3).

3.1.1.6 Process Studies on the Influence of Soil Moisture and Temperature

Volatilization rates of ^{14}C -parathion-methyl applied to gleyic cambisol were determined in photovolatility chamber experiments of 3-6 days each. Details on the experimental procedure, including rates of application and environmental scenarios, are compiled in **Table 3.1**. To characterize the influence of soil moisture on volatilization, three process studies were performed under various moisture conditions at the soil top layer, ranging from 1.18 to 8.67%_{weight} (cf. 3.1.1.2). The ambient conditions, especially soil surface temperature (19.0-19.7 °C) and air exchange rate (10-12 L min⁻¹), were maintained nearly constant to ensure comparability of the experiments.

An additional study was performed after elevating the soil surface temperature to 30 °C (**Table 3.1**). With the exception of air temperature and soil temperature, the environmental conditions during this experiment were similar to those during the 1st soil moisture study, especially the water content of the soil top layer. Thus, the comparison of these experiments enables the quantification of the temperature dependence of volatilization of parathion-methyl.

Table 3.1 Application parameters and experimental conditions of photovolatility chamber studies with ^{14}C -parathion-methyl on gleyic cambisol.

Process study	1 st soil moisture study (dry)	2 nd soil moisture study (medium)	3 rd soil moisture study (moist)	soil surface temperature (30 °C)
Formulation	----- Emulsion concentrate † (40% a.i.) -----			
Duration [d]	4	3	6	3
Applied radioactivity [kBq]	167.1	166.5	140.8	182.4
Applied a.i. [μg 0.01 m ⁻²]	86.1	85.8	72.6	94.0
Climatic parameters				
Air humidity [%] ‡	43.1 ± 5.1	91.9 ± 1.8 §	89.6 ± 1.0 §	84.4 ± 7.0 §
Air temperature [°C]	19.4 ± 0.2	19.2 ± 0.1	19.3 ± 0.1	30.2 ± 0.2
Soil surface temperat. [°C]	19.7 ± 0.2	19.0 ± 0.2	19.4 ± 0.1	30.0 ± 0.6
Air exchange rate [L min ⁻¹]	12.1 ± 0.1	9.9 ± 0.3	10.9 ± 0.7	11.2 ± 0.7
Evaporation [mm d ⁻¹]	1.1 ± 0.3	-1.8 ± 0.7	1.0 ± 0.1	1.0 ± 0.9
Soil moisture (top layer, 0-7 mm) [% _{weight}]	1.18	3.41	8.67	1.61
Soil moisture (TDR, depth 2.5 cm) [% _{vol}]	15.7 ± 0.2	14.1 ± 0.6	20.3 ± 0.2	13.7 ± 0.9

† specific radioactivity: 1.94 MBq mg⁻¹ a.i., radiochemical purity: > 99.0%

‡ before passing through the glass dome

§ use of wash bottles for water saturation of air

¶ calculated from differences between relative humidity of air stream before and after passing through the glass dome

3.1.2 Semi-field Scale: Wind Tunnel

Wind-tunnel experiments allow for direct measurement of pesticide volatilization and biomineralization under field-like conditions, combining the advantages of laboratory facilities, e.g. use of radioisotopes, and field studies. In the following, the experimental set-up and the adjustment with regard to the semi-field studies on volatilization within this thesis is presented.

3.1.2.1 Characteristics of the Wind Tunnel and Measuring Technique

As an extension of the lysimeter concept (Führ et al., 1998), a glass wind tunnel was set up above a lysimeter with a soil surface area of 0.5 m² to measure the gaseous emissions of the applied pesticide mixture (**Fig. 3.6**). A detailed description of the system was given by Stork (1995) and Linnemann (2002).

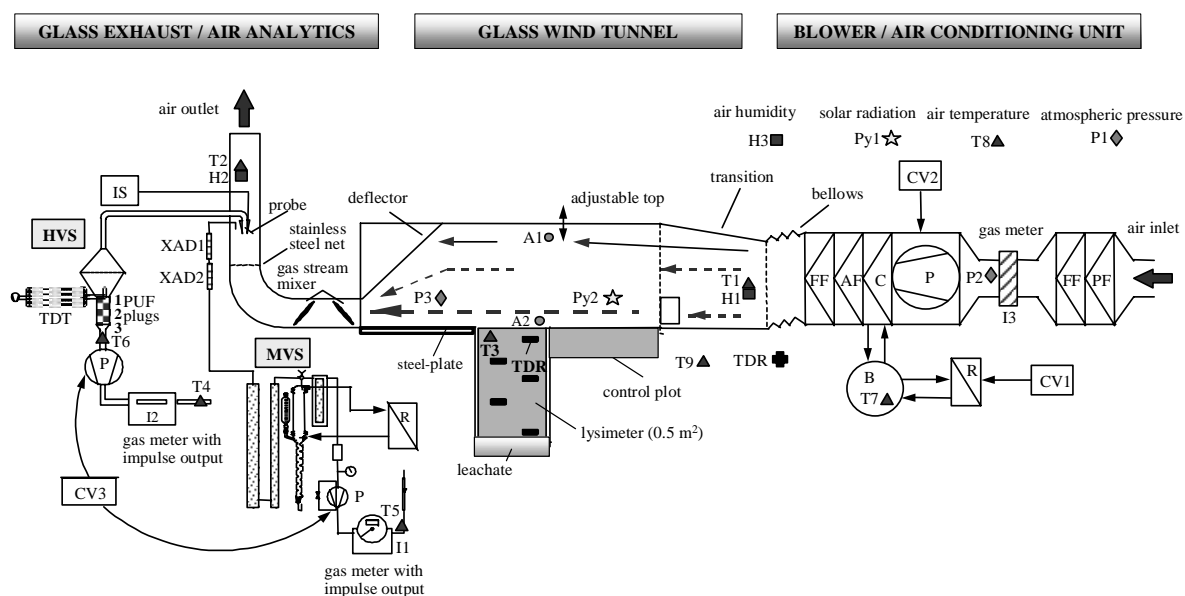


Figure 3.6 Schematic of the wind tunnel for measuring volatilization of pesticides from the soil surface under field-like conditions. A1-2 = anemometer, AF = activated charcoal filter, B = brine tank, C = cooler, CV1-3 = converter, FF = fine filter, H1-3 = hygrometer, I1-3 = gas volume (sensors), IS = isokinetic sensor, P = pump/blower, P1-3 = pressure (sensors), PF = prefilter, PY1-2 = pyranometer, R = refrigeration, PUF = polyurethane foam, T1-9 = thermo sensors, TDR = time domain reflectometry, TDT = thermal desorption tubes, XAD = adsorbing resin (Amberlite XAD-7).

The glass wind tunnel is 1.1 m high, 0.7 m wide and 2.7 m long. Its design (**Fig. 3.1**) ensures that the glass structure can withstand weather influences (wind pressure, temperature changes, rain etc.) A single blower presses air into the wind tunnel after intensive cleaning in various filter stages (max. 1500 m³ h⁻¹). Air filters and subsequent sieves ensure a uniform air stream through the glass tunnel. The top of the wind tunnel can be adjusted in height and thus be adapted to the level of growing plants. Therefore, constant wind velocities from 0.3 to 3.5 m s⁻¹ can be achieved with a minimum air volume. Realistic conditions are simulated inside this wind tunnel by a continuous, automatic adjustment of the air temperature to the outdoor situation. Due to the glass design, sufficient light intensity is ensured so that experiments with plants can be performed. The

use of UV-transparent glass (side walls) and UV-transparent acrylic glass (lid) as construction materials guarantees for sufficient irradiation and light quality. During the experiments significant climatic parameters were monitored using various sensors, including the determination of volumetric water content in the soil by TDR measurement in several depths (**Fig. 3.6**). Precipitation events can be simulated by irrigation nozzles in the lid of the wind tunnel.

3.1.2.2 Application Device: Semi-automatic Sprayer

Application of radioactive spray mixtures is performed using a semiautomatic sprayer driven by a single-axe linear unit (**Fig. 3.7**). The pressure tank of the spray mixture is flow-optimized to guarantee bubble-free and homogeneous spraying of the fluid. The sprayer permits an application volume of 100-800 L ha⁻¹, according to good agricultural practice at a velocity of 6 km h⁻¹. For application, the sprayer is placed above the wind tunnel. A contamination shield lined with aluminum foil is provided inside. All application losses are detected by decontamination to determine the net applied radioactivity.

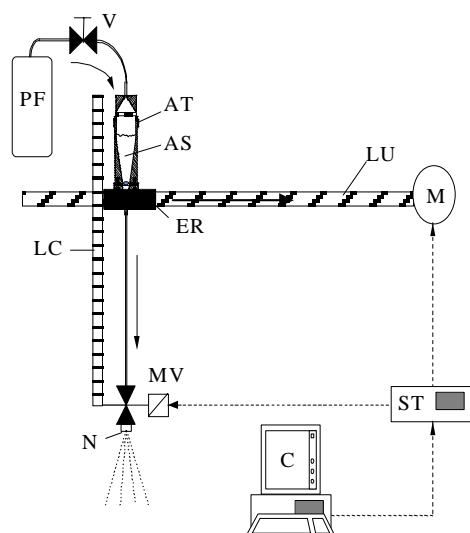


Figure 3.7 Semi-automatic application unit for pesticides. AS = application solution, AT = application tank, C = personal computer, ER = electronic stirrer, LC = lifting cylinder, LU = linear unit, M = motor, MV = magnetic valve, N = nozzle, PF = pressure flask, ST = steering, V = valve.

Immediately after application, the wind tunnel is closed by replacing the glass lid, using a special suction lifting device (Stork, 1995). At the same time, all units of the wind tunnel are started. The time interval between end of application and beginning of experiment is about 15 minutes.

3.1.2.3 Air Sampling Unit: High-volume Sampler and Medium-volume Sampler

The organic ¹⁴C-labeled air constituents were sampled using a high-volume sampler (HVS; **Fig. 3.8**) equipped with an adhesive-free glass fiber filter (185 mm o.d.) to trap particulate matter followed by three polyurethane foam plugs (100 mm o.d. x 150 mm) held within a glass sleeve. Aliquots were taken isokinetically based on industrial guidelines for the sampling of stack air (VDI, 1981). The maximum sampling rate was 50 m³ h⁻¹, corresponding to 3-10% of the total airflow through the wind tunnel. Sampling period of the high-volume sampler (HVS) was between 1 h to max. 24 h.

Foam plugs were extracted separately with methanol (approx. 200-300 mL) using a special squeezing apparatus (Niehaus et al., 1990). Extracts were reduced to 5-10 mL using a rotary evaporator and further concentrated using a nitrogen gas blowdown. Glass fiber filters were extracted with methanol (70 mL) in a Soxhlet apparatus for 16 h. Radioactivity of extracts was determined using LSC (cf. 3.3.2). Active ingredients were characterized by radio-TLC (cf. 3.3.3.1) and radio-HPLC (cf. 3.3.3.3). Non-labeled compounds were quantified using a gas chromatograph equipped with a mass-selective detector (cf. 3.3.3.2).

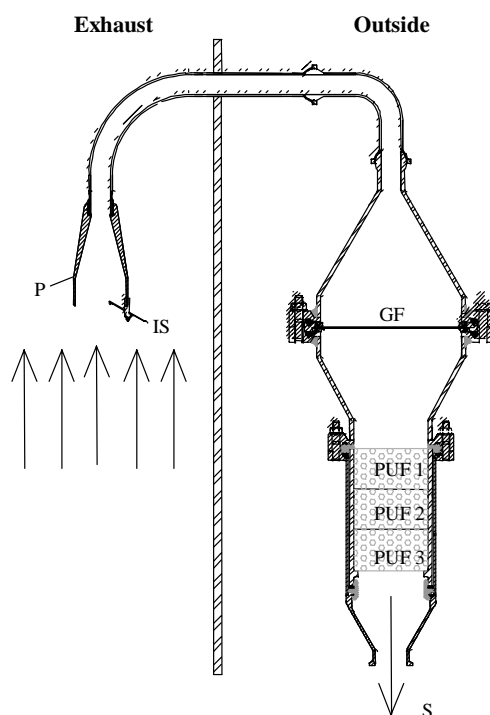


Figure 3.8 High-volume sampler: adsorption unit for sampling ^{14}C -labeled organic air constituents. GF = adhesive-free glass fiber filter, IS = isokinetic sensor (consisting of two Pt-100-sensors), P = isokinetic probe (stainless steel), PUF 1-3 = polyurethane foam plugs, S = suction by vacuum pump.

A medium-volume sampler (MVS, **Fig 3.9**) was used for measuring $^{14}\text{CO}_2$ arising as the end product of biomineralization of ^{14}C -labeled compounds in wind tunnel and photovolatility chamber experiments (Stork et al., 1997).

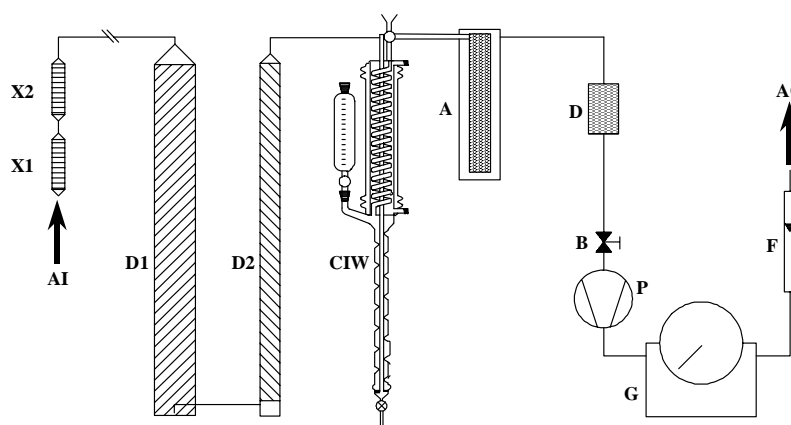


Figure 3.9 Schematic diagram of the medium-volume sampler (MVS) for measurement of $^{14}\text{CO}_2$. A = activated charcoal filter, AI = air inlet, AO = air outlet, B = bypass with control valve, CIW = cooled intensive wash bottle with 2-methoxypropylamine, D = dust filter, D1 = drying stage 1 (silica gel), D2 = drying stage 2 (phosphorus pentoxide), F = flow meter, G = gas meter, P = metal bellows pump, X1/2 = XAD cartridges.

Air samples of max. 3.5 L min^{-1} were taken from the wind-tunnel exhaust air, corresponding to a sampling rate of 10 m^3 in 48 h. The absorption capacity was limited to

about 10 m³ by the natural CO₂ content of the intake air (approx. 370 ppmv). In order to ensure a sampling of ¹⁴CO₂ only, volatile organic compounds were trapped with two cartridges (25 mm i.d., 168 mm high) filled with about 55 mL XAD-7. The adsorption of organic constituents was considered to be quantitative as long as no significant radioactivity was analyzed in the second cartridge. Prior to CO₂ absorption, the air sample was dried intensively using silica gel and phosphorus pentoxide. Both CO₂ and ¹⁴CO₂ were quantitatively absorbed in a special cooled intensive wash bottle in 60 mL of 2-methoxy-propylamine (Carbosorb E⁺, Canberra Packard, Frankfurt, Germany). Losses of highly volatile 2-methoxy-propylamine were minimized by intensive reflux cooling (-40 °C). For determination of ¹⁴CO₂, 10 mL aliquots of the absorption fluid were measured using LSC (cf. 3.3.2).

3.1.2.4 Study on Volatilization from Soil Surfaces

Volatilization rates of four pesticides (¹⁴C-labeled parathion-methyl, fenpropimorph, terbuthylazine and non-labeled chlorpyrifos; cf. 3.4) were determined in a wind-tunnel experiment of 13 days after simultaneous soil surface application to gleyic cambisol (cf. 3.5.1). In accordance with agricultural practice, realistic application conditions, including application rate, volume of water and droplet spectrum of the spray emulsion, were obtained by using the semiautomatic sprayer (cf. 3.1.2.2). Application details are shown in **Table 3.2**.

Table 3.2 Wind-tunnel study on volatilization from bare soil: Application details.

Pesticide	Parathion-methyl	Fenpropimorph	Terbuthylazine	Chlorpyrifos
¹⁴ C-labeling	phenyl-UL- ¹⁴ C	morpholine-2(6)- ¹⁴ C	triazine-U- ¹⁴ C	none
Specific radioactivity	1.94 MBq mg ⁻¹ a.i., radiochemical purity: > 99.0%	6.89 MBq mg ⁻¹ a.i., radiochemical purity: > 99.0%	3.17 MBq mg ⁻¹ a.i., radiochemical purity: 98.9%	-
Formulation	emulsified concentrate, 40% a.i.	emulsified concentrate, 80% a.i.	suspension concentrate, 50% a.i.	emulsified concentrate, 480 g a.i. L ⁻¹
Net applied radioactivity	12.06 MBq	7.91 MBq	102.55 MBq	-
Net applied a.i.	124.30 g ha ⁻¹ †	651.80 g ha ⁻¹ , (¹⁴ C-labeled: 3.66%)	647.00 g ha ⁻¹ †	696.53 g ha ⁻¹
Applied water	----- 720 L ha ⁻¹ -----			

† applied compound was quantitatively ¹⁴C-labeled

The lid of the wind tunnel was adjusted to a height of 30 cm and the wind velocity was kept constant at 1 m s⁻¹ in a height of 20 cm. Irrigation (8 mm) was given on Day 8 after application. At the end of the experiment, soil layers up to 10 cm were completely

removed and soil cores of deeper layers were taken, leachate was also pumped off. Subsequently, sample preparation (cf. 3.3.1) and analysis of water samples and soil samples (cf. 3.3.3) were performed. Soil moisture of the top layers was determined by gravimetric analysis (cf. 3.1.1.2).

3.1.2.5 Study on Volatilization from Plant Surfaces

Volatilization rates of three pesticides (^{14}C -labeled parathion-methyl, non-labeled fenpropimorph and quinoxifen; cf. 3.4) were determined in a wind-tunnel experiment of 10 days after simultaneous spray application to winter wheat sowed on orthic luvisol (cf. 3.5.2). Application conditions, including application rate and volume of water using the semiautomatic sprayer (cf. 3.1.2.2), and data on plant development are summarized in **Table 3.3**. The top of the wind tunnel was adjusted to a height of 70 cm (approx. 20 cm above the level of the plants). Wind velocity was kept constant at 1 m s^{-1} in a height of 10 cm above the plants. Irrigation was given on Day 7 (8 mm) and Day 8 (8 mm). At the end of the experiment, plants on lysimeter and control plot were completely harvested and pesticide residues were determined (cf. 3.3.1). Soil sampling was performed according to the above described method (cf. 3.1.2.4). Sample preparation, analytical procedure and gravimetric determination of soil moisture are summarized in 3.3.1, 3.3.3 and 3.1.1.2.

Table 3.3 Wind-tunnel study on volatilization from winter wheat: Application details.

Pesticide	Parathion-methyl	Fenpropimorph	Quinoxifen
^{14}C -labeling	phenyl-UL- ^{14}C	none	none
Specific radioactivity	1.94 MBq mg^{-1} a.i., radiochemical purity: > 99.0%	-	-
Formulation	emulsified concentrate, 40% a.i.	suspension concentrate † 250 g a.i. L^{-1}	66.7 g a.i. L^{-1}
Net applied radioactivity	15.56 MBq	-	-
Net applied a.i.	480.27 g ha^{-1} , (^{14}C - labeled: 33.40%)	247.87 g ha^{-1}	65.38 g ha^{-1}
Plant age	----- mid-tillering stage of crop growth (BBCH 31 ‡) -----		
Soil coverage	----- 80 % at application time (estimate) -----		
Applied water	----- 720 L ha^{-1} -----		

† commercial product FORTRESS TOP (Dow AgroSciences)

‡ according to Zadoks et al. (1974)

3.1.3 Field Study: Micrometeorological Methods

A field study of 7 days was performed in cooperation with *Alterra Green World Research* (Wageningen, NL) to determine the environmental behavior of parathion-methyl, fenpropimorph, and quinoxifen after application to winter wheat. The Dutch partners were responsible for air sampling, meteorological measurements and for the calculation of volatilization fluxes (cf. 3.1.3.5).

3.1.3.1 Field Site and Application

The experiment was performed on a rectangular field of about 6 ha near Jülich-Merzenhausen (**Fig. 3.10**). The landscape around the field was rather open, with only a few obstacles in the north (“Haus Brühl”, with trees). These were supposed to disturb the dispersion pattern of the pesticide vapor above and around the treated field when the wind comes from north to north-east. Due to the fact that the main wind direction observed in this area was between west and south-west, the field fulfilled the requirements set by the aerodynamic methods used for measurement of the flux densities.

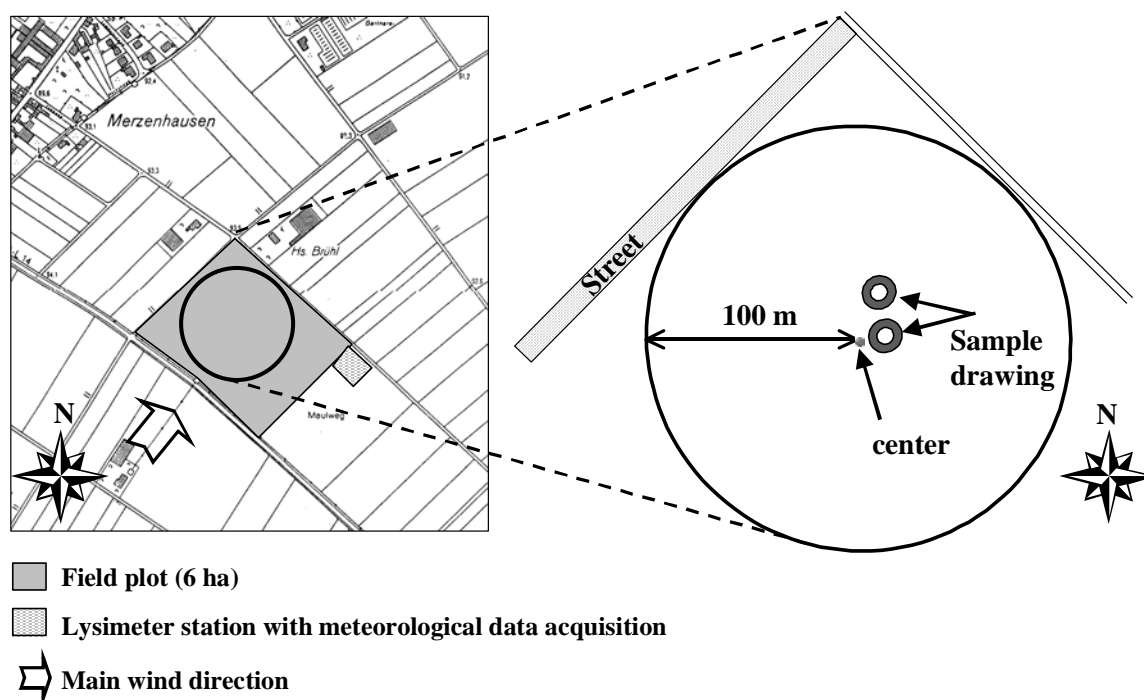


Figure 3.10 Location of the field site and the treated area.

The average height of the winter wheat was measured around the air sampling location (**Fig. 3.10**) through a hole in the center of a polystyrene disc (diameter: 0.8 m) which was placed on the plants. At the first day after application, the height ranged between 0.52 and 0.55 m and increased to an average height of 0.68 m by the end of the study.

A computer-assisted Dubex field sprayer was used for the pesticide application. The boom (width: 27 m in total; divided in 9 sections of 3 m) was equipped with 54 nozzles (Turbo drop TD 025, Dubex). In previous studies, the rate of water release by the nozzles of the field sprayer at the relevant pressure to achieve the volume rate at a normal driving speed was checked. During pesticide application the driving speed was measured and appeared to

be 8.1 km h^{-1} at a spray pressure of about 6 bar, corresponding to an areic spray volume of 198 L ha^{-1} . The concentration of each pesticide in the spraying solution was measured by taking samples from the tank and from the liquid released by the outermost nozzle during spraying. Subsamples of 2.5 mL were taken and added immediately to glass flasks filled with 50 mL methanol. The flasks were shaken manually for a few minutes and further shaken on a mechanical shaker for 30 min and stored cool until analysis.

Application conditions, including the composition of the applied pesticide mixture, are summarized in **Table 3.4**.

Table 3.4 Field study on volatilization from winter wheat: Application details.

Pesticide	Parathion-methyl	Fenpropimorph	Quinoxifen
Formulation	wettable powder (40% a.i.) †	suspension concentrate ‡ $250 \text{ g a.i. L}^{-1}$	$6.7 \text{ g a.i. L}^{-1}$
Nominal applied a.i. §	164 g ha^{-1}	343 g ha^{-1}	91 g ha^{-1}
Net applied a.i. ¶	114 g ha^{-1}	241 g ha^{-1}	61 g ha^{-1}
Plant age	----- mid-tillering stage of crop growth (BBCH 31 #) -----		
Soil coverage	----- 70-80% at application time (estimate) -----		
Leaf area index	$3.3 \text{ m}^2 \text{ m}^{-2}$	$3.3 \text{ m}^2 \text{ m}^{-2}$	$3.3 \text{ m}^2 \text{ m}^{-2}$
Applied water	----- 198 L ha^{-1} (total volume: 1188 L applied on field plot) -----		

† commercial product ME 605 (Bayer AG)

‡ commercial product FORTRESS TOP (Dow AgroSciences)

§ calculated values related to the applied amount (2.7 kg ME 605 and 9 L FORTRESS TOP mixed with 1300 L water)

¶ determined after taking samples from the spray mixture (before, half-way and at the end of the application)

according to Zadoks et al. (1974)

3.1.3.2 Meteorological Measurements

A tripod with cup anemometers (Vector Instruments, type A100R) and a wind vane were placed in the center of the treated area (**Fig. 3.10**). The wind speed was measured at four heights: 0.7, 1.0, 1.5 and 2.2 m above the soil surface. The wind direction was determined at a height of 2.5 m. The dew point of the air was measured at 1.0 and 1.5 m above the ground with a chilled mirror hygrometer. The air temperature was measured at the same heights with thermocouples. The soil temperature was measured at depths of 0.02 and 0.06 m with integrated sensors (PT type). The soil heat flux was determined at 0.08 m depth with two heat flux plates. Net radiation and albedo were measured at a height of 1.5 and 2.0 m, respectively. A sensor for measuring the wetness of the leaf surface was placed 10 cm below the maximum crop height. The course with time of all these meteorological variables was registered with a battery-powered Campbell Scientific 21X micrologger. Wind speed and wind direction were measured in 10 s intervals and used for the calculation of 10 min averages. For the BR measurements (cf. 3.1.3.5), 20 min averages were calculated.

Rainfall was measured with an electronic tipping-bucket rain gauge (resolution: 0.25 mm) within the test field. The data were recorded with a Tattle datalogger. The collected water was also periodically transferred into a measuring flask, which enabled the calibration of

the layer of rain water corresponding to one pulse recorded with the datalogger. This method made it possible to record also rainfall of less than 0.25 mm.

3.1.3.3 Plant and Soil Sampling

The rate of decline of the pesticides on the crops was measured by taking leaf samples at several times after application. The treated area was divided into four sections of identical size. In each section, four samples were collected at each sampling time. Each leaf sample consisted of 50 randomly collected leaves, which were put into glass bottles with airtight screw caps. Details on the analytical procedure, including the determination of the rinsability of the pesticide residues, are summarized in 3.3.1.

Total efficiency by the storage and extraction method was determined by extracting leaves which were placed horizontally on four polystyrene plates (1.0 m x 0.1 m) at crop height in each quadrant of the field during spraying. Within 10 min after application, the sprayed leaves were pooled per plate and extracted as described above. The results were compared with the calculated dosage to estimate the efficiency of the sampling procedure for the pesticide formulations sprayed on the field.

The recovery of the extraction procedure and analysis of the pesticides of leaf samples was checked in a preliminary experiment with young winter wheat leaves. Defined amounts of the applied compounds were added to 40 punches of the leaves. After extraction, quantification was performed as described in 3.3.3 and recoveries were determined.

Soil cores were drawn simultaneously with plant sampling using short core samplers (surface: 78.5 cm²; volume: 100 cm³; thickness: up to 5 cm). On each quadrant, up to 16 soil cores were taken per sampling date, subsequently combined and homogenized for analysis. Additional soil samples were taken for determining bulk density and soil moisture by gravimetry.

3.1.3.4 Pesticide Concentrations in Air

The pesticide vapors were trapped on polystyrene XAD-4 adsorbent, held in sampling probes. The sampling probes were constructed from glass tubes (inner diameter: 35 mm) with screw thread on both sides. Inside the glass tube, a stainless steel gauze (mesh width: 0.1 mm) was placed. This tube was provided with 10 g XAD-4 adsorbent. The tube with adsorbent was fixed vertically on a coupling unit which was connected to a gas meter. Another glass tube with the same diameter was screwed on top of the tube to prevent the adsorbent being blown out by the wind. The glass tubes were linked together with SVL 42 coupling units provided with PTFE-wrapped rubber rings to ensure gas-tight connections between the glass tubes.

Downwind sampling heights were 1.0, 1.2 and 1.5 m above the soil surface. The sampling rates were around 3 m³ h⁻¹. Upwind samples were taken at 1.5 m height at a flow rate of about 4 m³ h⁻¹ in a distance of 15-26 m upwind from the treated area. On the day of application, two series of one-hour air samples were taken, starting about 90 minutes after spraying the last track. Extraction procedure and sample preparation are summarized in 3.3.1.

The recovery and retention of the applied pesticide mixture by XAD-4 granules were checked in preliminary experiments. A special apparatus (Stork, 1995), as described in

3.1.1.3, was used for heating and vaporization of defined pesticide amounts (280 μL methanolic stock solution containing parathion-methyl, fenpropimorph and quinoxifen, each at a concentration of $33.3 \mu\text{g mL}^{-1}$). The vaporized pesticides were drawn through a sampling head filled with 10 g XAD-4 adsorbent for 2 h at an air temperature of 55°C (air exchange rate: $3.2 \text{ m}^3 \text{ h}^{-1}$). A second sampling head filled with 10 g XAD-4 was placed in series with the first head for checking breakthrough. Subsequently, XAD-4 granules of each sampling head were shaken separately with 130 mL hexane/ethylacetate (1:1) for 90 min (cf. 3.3.1); extracted pesticides were quantitated by GC-MSD (cf. 3.3.3.2) and recovery was calculated.

In parallel, 10 g XAD-4 adsorbent were filled in a flask and spiked with 300 μL methanolic stock solution. After 2 h, the XAD-4 granules were extracted according to the above described procedure and the average recovery from the XAD-4 was determined for each pesticide.

3.1.3.5 Micrometeorological Methods for Determining Volatilization Fluxes

Two sampling systems were used, one for air sampling upwind of the treated field and the other for measuring the concentration gradient in the air downwind the treated area. Both systems consisted of a vacuum pump with a buffer vessel and a pressure regulator valve.

Two micrometeorological methods (aerodynamic and Bowen ratio methods) were used to determine the volatilization rates of the applied pesticides after application. The aerodynamic (AD) method is based on the Thornthwaite-Holzman equation. Volatilization fluxes are proportional to the difference in the concentration of pesticides in air over a certain height interval and the difference in wind speed over the same interval. Further, the calculated rate is corrected for the stability of the surface air layer. For the calculation of the correction factor, empirical relations have been derived (Majewski et al., 1990). Using the AD method, an upwind fetch, e.g. the length of treated area upwind, is required of at least 100 times the greatest height above the soil surface at which an air sample is taken to measure the concentration of pesticide in the air. More detailed information on the AD method is given by Majewski et al. (1989, 1990). In this study, the concentration of each pesticide in air was measured at three heights (1.0, 1.2 and 1.5 m above the soil surface; cf. 3.1.3.4). Two heights were the same as used for measuring the wind speed gradient.

The Bowen ratio (BR) method is based on the assumption that the coefficient for the dispersion of sensible heat is the same as that of the pesticide. The flux density of sensible heat is calculated from measurements on the energy balance at the earth's surface. The Bowen ratio coefficient, e.g. the ratio between the latent and sensible heat flux densities, is calculated by dividing the temperature gradient by the water vapor pressure gradient and multiplying it by the psychrometer constant. From the Bowen ratio coefficient and the measured soil heat and net radiation flux densities, the sensible heat flux density is calculated. The coefficient for the dispersion of sensible heat is calculated by multiplying the sensible heat flux density with the vertical air temperature gradient measured. The rate of volatilization of pesticide is calculated from this coefficient and the measured vertical pesticide concentration gradient in air. More detailed information on the BR method can be taken from Majewski et al. (1990). In the present study, net and global radiation was measured at a height of 1.2 m above the top of the plants. As the soil heat flux density is measured at a depth of 0.08 m, a correction needs to be made to take into account the heat

stored or released in the top 0.08 m layer, thus enabling the calculation of the soil heat flux density at the soil surface. In this calculation procedure, the data given in Annex 1 including soil bulk densities, average soil moisture contents and aerodynamic conditions were used.

3.2 Phase Partitioning Studies

Studies on phase partitioning of pesticides included the development and application of a new set-up for measurement of soil-air and water-air partitioning (cf. 3.2.1) and experiments on the temperature-dependence of soil-water partitioning performed in accordance with a standard protocol for “batch” studies (cf. 3.2.2).

3.2.1 Measurement of Soil-Air Partitioning Coefficients

The experimental device developed within this thesis allows for direct measurement of the partitioning of pesticides between soil and air. The main objective in the first stage of the study was the optimization and adjustment of the features to ensure the reliability of the measurement procedures and to obtain reproducible results. In the second stage, experiments on the temperature dependence of the soil-air partitioning of fenpropimorph were performed.

3.2.1.1 A Novel Chamber for Partitioning Studies: Main Features

Set-up and operation of a novel chamber system for measurement of soil-air partitioning coefficients is illustrated in **Fig. 3.11**. The basic element of the phase partitioning chamber is a double-walled glass tube (1.00 m in length, internal diameter of 0.15 m) equipped with several sampling ports situated at regular intervals along the chamber body and glass threads used for connecting the chamber with a cooling system and for fixing measuring instruments (Annex 2A). To minimize sorption artifacts the whole chamber was constructed out of glass. The use of sealing rings and quick-release caps (Annex 2B) on both sides of the glass tube enables gas-tight sealing. The glass axis is provided with propellers for mixing air and adjusted in the chamber by ball-and-socket joints installed in both caps (Annex 2C). On one side of the apparatus the axis is connected to a stirrer. The air sampling unit (cf. 3.2.1.2) is attached to the chamber by an additional sampling port in the cap.

The chamber can be run using the cooling-heating system between 5 and 35 °C. The chamber body and end caps were insulated using Armaflex insulating tape. To minimize photodegradation of susceptible compounds the chamber is provided with a reflecting foil layer under the insulating material to block out light.

For experiments, a metal tray filled with a very thin soil layer (layer thickness: approx. 5 mm), which was adjusted to a defined water content and a defined pesticide concentration, was put into the glass tube (Annex 2D). Purified air was led into the glass chamber. The problem of gas tight fittings at each end seizing up with running the chamber over prolonged periods was resolved by the application of silicone grease to the fittings.

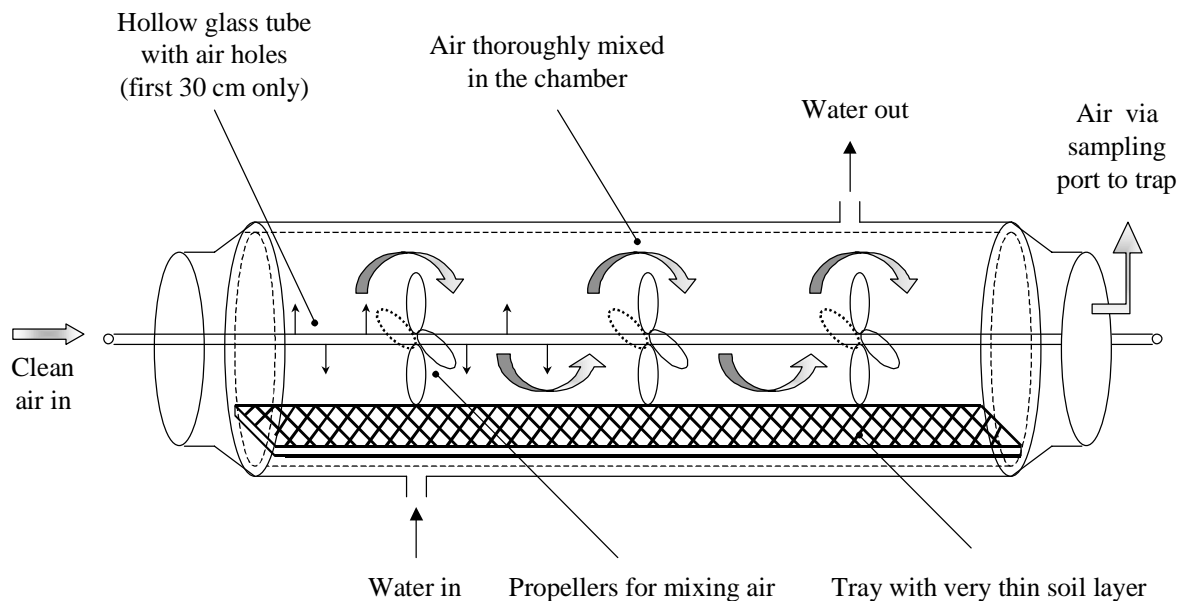


Figure 3.11 Construction and operation of the soil-water-air-partitioning chamber. 9 sealable sampling ports are available for air sampling, temperature and humidity sensors (not shown, 3 in each cap and 3 along the length of the chamber). For air sampling, air is drawn using a programmable pump through thermal desorption tubes filled with a solid adsorbent (tenax). Analysis is performed by thermal desorption GC-MSD (cf. 3.3.3.4).

3.2.1.2 Air Supply and Air Sampling Unit

A schematic of the chamber including the air conditioning unit and the air sampling device is given in **Fig. 3.12**. A suction pump (GS 301, Desaga GmbH, Wiesloch, Germany) allowed for the adjustment of defined air exchange rates ranging from 0.1 to 1.5 L min⁻¹. The incoming air was purified by activated charcoal and passed through two wash bottles filled with water to bring the air humidity of the incoming air up to near saturation. The temperature gradient along the entire chamber body was less than 1 °C.

After leaving the chamber, the pesticides contained in the exhaust air were trapped on tenax tubes and quantified by subsequent thermal desorption (cf. 3.3.3.4).

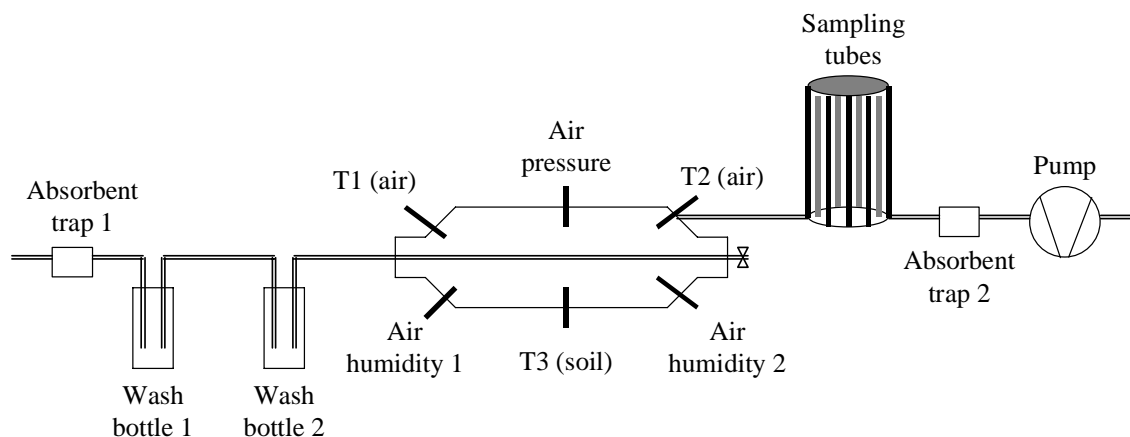


Figure 3.12 Air supply and air sampling unit used in the phase partitioning chamber. T1-3 = thermo sensors.

3.2.1.3 Studies on Soil-Air Partitioning

For each experiment, 500 g air dried and 2 mm sieved gleyic cambisol were used. A 50 g sub-sample was taken and added to a mortar. 1 mL of a methanolic spike solution of fenpropimorph at a concentration of $1 \mu\text{g mL}^{-1}$ was added to the surface of the soil taking care not to contaminate the sides of the mortar. The soil was allowed to become air dry and subsequently homogenized. The soil inoculum was added to the remaining 450 g of soil to a solvent rinsed jar, resulting in a soil concentration of $2 \mu\text{g kg}^{-1}$. The jar was sealed and well mixed on a rotary shaker for at least 2 hours. As a final stage the spiked soil was to be adjusted to the required soil moisture (40% MWC) by adding the corresponding volume of distilled water. Half of the water volume was added to the metal tray (**Fig. 3.11**), the soil was transferred to the tray and finally the remaining water was sprayed on the soil surface. The tray was introduced into the chamber and the system was sealed. Air was drawn continuously at a flow rate of 0.2 L min^{-1} through the chamber and the downstream tenax tubes. A sampling duration of 5 h per tenax tube was chosen and about 10 tenax tubes were sampled per experiment.

For the determination of soil concentrations, a cleanup method for the spiked soil used in the chamber was developed. 20 g of soil were weighed into cellulose thimbles and Soxhlet-extracted for 12 h using 100 mL acetone. The Soxhlet-extract was filled in a separating funnel and 400 mL water, 50 mL saturated sodium chloride solution and 50 mL dichloromethane (DCM) were added. The mixture was shaken for 2 min, allowed to separate and the bottom DCM layer was collected in a solvent cleaned round bottomed flask. Another 50 mL DCM were added and the mixture was shaken for a further 2 min. The DCM layer was collected with the above fraction, rotary evaporated to dryness and taken up in 500 μL hexane. The sample was added on a silica column and eluted with hexane, hexane-DCM (1:1) and DCM. An injection standard (20 μg 1-methylnaphthalene) was added to the various fractions which were then all rotary evaporated down to about 500 μL final volume and quantitated by GC-MSD (cf. 3.3.3.2).

In preliminary studies, the losses during the cleanup procedure of soil were quantified by comparing the levels in spiked and unspiked soil samples. 3 replicates each of 20 g orthic luvisol were spiked with the following levels of pesticides: terbuthylazine, parathion-methyl and chlorpyrifos (10 μg) and fenpropimorph (2 μg). In addition, 3 soil samples remained unspiked. The replicates were Soxhlet-extracted and cleaned up as described above. Recoveries were calculated by subtracting the blank levels from the levels found in the spiked samples.

3.2.2 Measurement of Soil-Water Partitioning Coefficients

For the determination of the temperature-dependence of the soil-water partition coefficients, “batch” studies were performed according to the OECD Guideline on adsorption/desorption, first adopted in 1981 and revised since (OECD, 2000).

3.2.2.1 Studies on Soil-Water Partitioning: Experimental Set-up

The two soil types studied were the A_p horizons of gleyic cambisol and orthic luvisol (cf. 3.5). The soils were air dried and passed through a 2 mm sieve.

^{14}C -terbuthylazine (suspension concentrate, 50% a.i.) and ^{14}C -parathion-methyl (emulsified concentrate, 40% a.i.) were studied separately to avoid any possible competition. Terbuthylazine studies were performed with ^{14}C -labeled compound of a purity higher than 99%. Parathion-methyl studies were carried out with a mixture of non-labeled and ^{14}C -labeled compound (approx. 1% ^{14}C -labeled). Solutions were prepared in aqueous 0.01 M CaCl_2 . Due to the different water solubility of the applied compounds (**Table 3.8**), concentrations ranging from 1 to 1000 $\mu\text{g L}^{-1}$ (terbuthylazine) and from 0.1 to 12 mg L^{-1} (parathion-methyl) were used to determine adsorption isotherms.

Studies were performed in 100-mL glass centrifuge tubes in a thermostatted shaker. 10 g of soil were pre-equilibrated for 24 h in 50 mL of 0.01 M CaCl_2 in order to minimize soil mineral balance disruption. After centrifugation, the supernatant was rejected and pesticide solutions were added to the slurry to give initial concentrations within the above mentioned range (up to 5 different concentrations tested). All solids were studied in triplicate and blanks were run for each experimental condition. The test tubes were then shaken for the same duration as the equilibration time (24 hours), centrifuged, and the pesticide concentration in solution was measured by LSC (cf. 3.3.2). In preliminary studies, the soil phase was analyzed by Soxhlet extraction and combustion (cf. 3.3.1) to confirm mass balance.

3.2.2.2 Calculation of Sorption Coefficients for Pesticides

The amount of pesticide sorbed was calculated from the difference between the initial solution concentration and the equilibrium concentration. The sorption isotherm was obtained by fitting the measured values with the Freundlich adsorption equation:

$$C_S = K_F \cdot C_E^{1/n} \quad [24]$$

or in the linear form:

$$\log(C_S) = \log(K_F) + \frac{1}{n} \log(C_E) \quad [25]$$

where C_S = concentration of pesticide sorbed to the soil [$\mu\text{g g}^{-1}$], K_F = Freundlich adsorption coefficient [$\mu\text{g}^{1-1/n} \text{g}^{-1} \text{mL}^{1/n}$], $1/n$ = constant [-], and C_E = equilibrium solution pesticide concentration [$\mu\text{g mL}^{-1}$].

3.3 Analytics

The general analytical techniques, including sample preparation and procedures for quantification, are summarized as follows. Mention of brand names is for information only and does not imply endorsement or exclusion of other products that might also be suitable. All solvents used were analytical grade.

3.3.1 Sample Preparation

Air

During the wind-tunnel studies and the photovolatility chamber experiments, sampling of the air for pesticide residues was accomplished by drawing known volumes of air through

preconditioned (separate squeezing with hexane, toluene and methanol) polyurethane foam (PUF) plugs. Details on the sampling technique and the extraction procedure can be taken from 3.1.1.5 and 3.1.2.3. The applied compounds were determined without further clean-up.

During the field study, the pesticides were trapped on XAD-4, as described in 3.1.3.4. Prior to use, XAD-4 adsorbent was precleaned by Soxhlet extraction with hexane and ethylacetate for 16 hours, respectively. After sampling, XAD-4 was transferred into glass flasks and shaken with 100 mL hexane-ethylacetate for 90 min. The total volume of the extract was recorded, subsequently the extracts were reduced by rotovap and stored at -20°C in tight glass flasks until GC-MSD analysis. For HPLC analysis, subsamples of the extract were resolved in methanol. The extract volumes were reduced by rotovap and solvent exchanged to hexane. TDS tubes were spiked with 10 μL of the internal standard, methylpyrene, prior to analysis.

Soil

Soil samples were stored at -20°C until extraction. Pesticides were recovered from the soil in triplicate by using a Soxhlet extractor (Pyrex No. 3910). 20 g of soil were extracted for 16 h with 100 mL methanol. For ^{14}C -labeled compounds, radioactivity of extracts was determined by LSC. After air-drying of the Soxhlet-extracted samples and combustion of subsamples (3 x 0.5 g), non-extractable radioactivity in the soil was quantified after combustion by LSC (cf. 3.3.2).

In previous extractions of gleyic cambisol, which was spiked with defined amounts of ^{14}C -labeled parathion-methyl and fenpropimorph, the Soxhlet extraction was shown to recover an overall average fraction $> 90\%$. In general, the variance within a pesticide and between pesticides was low.

Extract volumes were reduced by rotovap before analysis by GC-MSD, HPLC and TLC.

Water

Radioactivity of water samples was determined by LSC (cf. 3.3.2). Solid-phase extraction (SPE) was used for the purification and extraction of non-labeled pesticides from water samples. To pre-condition the monomerically bonded C18 silica sorbent (Discovery DSC-18Lt, Supelco), the SPE tube packing was successively rinsed with 6 mL methanol and 6 mL water. The water sample was transferred to the tube using a vacuum manifold, which increases the solvent flow rate through the cartridge. After washing the packing with 10 mL water, the cartridge was vacuum dried for approx. 5 minutes to remove any excess water from the sorbent. Subsequently, the packing was rinsed with acetonitrile (3 x 2 mL, dropwise flow rates) to elute the pesticides. The eluate was collected and further prepared, e.g. solvent exchanged to hexane, for quantification using GC-MSD or HPLC.

Plants

After finishing the wind-tunnel study on winter wheat, the plants were completely harvested and rinsed with solvents of decreasing polarity (2-3 L of water, methanol and chloroform, respectively). Subsamples of organic solvents were analyzed by GC-MSD, aqueous solutions were solid-phase extracted. Subsequently, the leaves were lyophilized and homogenized by grinding. After combustion of subsamples (3 x 0.5 g), the non-washable radioactivity was quantitated by LSC (cf. 3.3.2).

During the field study, the rinsability of the pesticide residues was determined in the same way, except combustion was omitted due to the application of non-labeled compounds. Additionally, leaf samples were taken to determine the rate of decline of the pesticides over the course of the study (cf. 3.1.3.3). About 50 leaf punches were collected in glass flasks with screw caps, methanol (100 mL) was added and the flasks were shaken for one hour. The supernatant was transferred into a glass flask with screw-cap and stored at about -20°C until analysis.

3.3.2 Radioactivity Measurements

Liquid samples

Radioactivity of liquid samples was measured directly by liquid scintillation counting (LSC; TRI-CARB 2500, Canberra Packard, Frankfurt, Germany), using a multi-purpose scintillation counter. Depending on sample size and expected activity, 5-10 mL of the samples were mixed with corresponding volumes of scintillation cocktail. Samples were counted for 15 min or until a 2-sigma-value of 2 was reached. All measurements were carried out in triplicate.

Solid samples

Solid samples were combusted in an Oxidizer (TRI-CARB Sample Oxidizer 306, Canberra Packard, Frankfurt, Germany). Combustion times depended on sample material and size. CO_2 formed during the combustion process was trapped in scintillation vials filled with scintillation cocktail.

3.3.3 Quantification of Pesticides and Metabolites

3.3.3.1 Thin-layer Chromatography (TLC)

Radio-thin-layer chromatography (radio-TLC) was used for quantification of ^{14}C -labeled parathion-methyl, terbuthylazine, fenpropimorph, and their metabolites.

A sealable developing chamber was filled to a depth of approx. 3 mm with the solvent system used as mobile phase (**Table 3.5**). A piece of filter paper cut to appropriate size was placed inside the chamber. The chamber was closed to ensure saturation of the atmosphere in the chamber. A solution of the sample was prepared in a volatile solvent such as methanol or chloroform. The solution was placed onto a TLC plate with an automatic applicator (Linomat IV, Camag, Berlin, Germany), approx. 1.0 cm from the bottom. Standard solutions of active ingredients and some of their degradation products were applied to the same plates. Standard solutions were not radio-labeled. The solvent was allowed to evaporate and the plate was transferred into the developing chamber. The mobile phase was allowed to climb to about 1 cm from the top of the plate. Subsequently, the plate was removed and the solvent front was marked. The positions of the separated spots of the non-labeled standards on the fluorescent plates were detected under ultraviolet light. Details on the chromatographic conditions are given in **Table 3.5**. Analytes were quantitated using a Bio-Imaging analyzer (Fujix BAS 100, Fuji, Tokyo, Japan).

Table 3.5 Chromatographic conditions for TLC quantification of ^{14}C -labeled parathion-methyl, terbuthylazine and fenpropimorph.

Active ingredient	Parathion-methyl	Fenpropimorph	Terbuthylazine
stationary phase	silicagel 60, F254, 0.25 mm, 20 cm x 20 cm glass plates (Merck, Darmstadt, Germany)		
mobile phase	----- toluene:methanol (9:1) -----		
Degradation products analyzed	4-nitrophenol paraoxon-methyl RIB 12023, 12025, 12080	fenpropimorph acid	-

3.3.3.2 Gas Chromatography / Mass Selective Detector (GC-MSD)

Sample analysis was conducted with a Hewlett-Packard 6890-5973 GC-MSD (Hewlett-Packard, Ratingen, Germany) equipped with a 30-m fused silica DB-1 capillary column with a 0.25-mm i.d. and a 0.25- μm film thickness. The MSD source (held at 230 °C) was operated in positive electron ionization mode, while the mass filter quadrupole (held at 150 °C) was operated in selective ion monitoring (SIM) mode. Selected ions for each pesticide are summarized in **Table 3.6**. The injector and GC-MSD transfer line were operated at 240 and 270 °C, respectively. An HP 6890 series autoinjector was used to inject 1 μL of sample in splitless mode. The oven temperature started at 90 °C (3-min hold) and was then programmed at 8 °C/min to 270 °C and held for 1 min, which made the total run time 26.50 min. Throughout the run the carrier gas (helium) was maintained at 1.0 mL min^{-1} . Pesticide concentrations were calculated by comparing the ratio of peak area response of the analyte over the internal standard (1-methylpyrene) in samples to those of calibration standards.

Table 3.6 Selected ion monitoring (SIM) and retention times for pesticides.

Pesticide	MS fragments (m/z)
parathion-methyl	263 (M^+ , 100%), 109 (112%), 125 (98.2%)
fenpropimorph	128 (100%), 173 (3.2%), 303 (M^+ , 4.3%)
terbuthylazine	173 (34%), 214 (100%), 229 (M^+ , 28%)
quinoxifen	237 (100%), 272 (36.4%), 307 (M^+ , 27.6%)
chlorpyrifos	197 (67.2%), 199 (80.4%), 314 (67.2%)

3.3.3.3 High Pressure Liquid Chromatography (HPLC)

(Radio-)high pressure liquid chromatography was used for separation and quantification of ^{14}C -labeled parathion-methyl and non-labeled pesticides (parathion-methyl, fenpropimorph and quinoxifen) in organic and aqueous solutions (**Table 3.7**).

Table 3.7 Chromatographic conditions for HPLC quantification.

column	CS, LiChrospher 60 RP-select B (5 μm), 250-3.	
guard column	Merck, LiChrospher 60 RP-select B (5 μm), 4-4.	
detection	UV detection (Typ UVD 160, Gynkotec): 274 nm (parathion-methyl), 200 nm (fenpropimorph), 239 nm (quinoxifen)	
flow / temperature	0.7 mL min ⁻¹ / 25 °C	
radioactivity detector	Berthold HPLC Radioactivity Monitor LB506C equipped with an yttrium silica flow cell (type YG-150 S4)	
	^{14}C -parathion-methyl	non-labeled compounds (simultaneous detection)
mobile phase components	A: acetonitrile B: water (+ 2 mL H ₃ PO ₄ (85%) per liter) 0 – 10 min: 10% A, 90% B 10 – 15 min: 32% A, 68% B 15 – 17 min: 36% A, 64% B 17 – 21 min: 43% A, 57% B	A: acetonitrile B: water (+ 250 μL NH ₃ per liter) 0 – 10 min: 30% A, 70% B 10 – 15 min: 32% A, 68% B 15 – 17 min: 36% A, 64% B 17 – 21 min: 43% A, 57% B
gradient shape	21 – 23 min: 48% A, 52% B 23 – 29 min: 75% A, 25% B 29 – 40 min: 90% A, 10% B 40 – 50 min: 10% A, 90% B	21 – 23 min: 48% A, 52% B 23 – 29 min: 75% A, 25% B 29 – 35 min: 90% A, 10% B 35 – 40 min: 70% A, 30% B 40 – 50 min: 30% A, 70% B
injection volume	3 x 10-150 μL	3 x 10-150 μL

3.3.3.4 Thermodesorption System (TDS)

A combination of adsorption and subsequent thermal desorption was used, wherein the components trapped on a preferably selective adsorbent (tenax tubes) were thermally desorbed after achievement of the required enrichment, and subsequently transferred onto a GC column. The system consists of a thermodesorption system (TDS-2, Gerstel GmbH, Mülheim a.d. Ruhr, Germany), a temperature programmable cooled injection system (CIS-4), a gaschromatograph (cf. 3.3.3.2) equipped with a 25-m fused silica DB-5 capillary column with a 0.25-mm i.d. and a 0.32- μm film thickness, and a mass-selective detector.

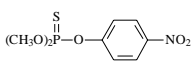
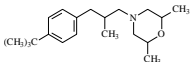
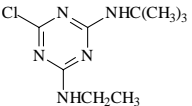
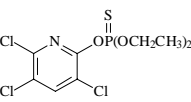
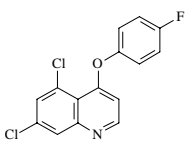
TDS tubes were spiked with 10 μL of the internal standard, 1-methylpyrene, prior to analysis. The adsorbed compounds were thermally desorbed (TDS-2), cryofocussed in the CIS-4 (solvent vent mode; initial temperature: -50 °C, programmed at 12 °C/min to

260 °C, 1-min hold) and transferred onto the column. The oven temperature started at 90 °C, 3-min hold, then programmed at 8 °C/min to 220 °C, held for 3 min, then programmed at 20 °C/min to 280 °C, and held for 1 min. The GC-MSD transfer line was operated at 290 °C. Helium was used as carrier gas at a constant flow rate of 1.0 mL min⁻¹. Pesticides were quantitated according to 3.3.3.2.

3.4 Test Compounds

The physicochemical properties of the pesticides used for the investigations within this thesis are summarized in **Table 3.8**. Details on the use of radiolabeled compounds, application doses, and formulation of the pesticides are given in the corresponding chapters. As follows, the main features, including applicability in agricultural practice of the pesticides, are presented.

Table 3.8 Physicochemical active ingredient data of the investigated compounds (Tomlin, 2000).

Common name	Parathion-methyl	Fenpropimorph	Terbuthylazine	Chlorpyrifos	Quinoxifen
Type	Insecticide	Fungicide	Herbicide	Insecticide	Fungicide
Chemical class	organo-phosphorus	morpholine derivative	triazine	organo-phosphorus	phenoxy-quinoline
Molecular formula	C ₈ H ₁₀ NO ₃ PS	C ₂₀ H ₃₃ NO	C ₉ H ₁₆ ClN ₅	C ₉ H ₁₁ Cl ₃ NO ₃ PS	C ₁₅ H ₈ Cl ₂ FNO
Structural formula					
Molecular weight	263.2 g mole ⁻¹	303.5 g mole ⁻¹	229.7 g mole ⁻¹	350.6 g mole ⁻¹	308.1 g mole ⁻¹
Water solubility	60.0 mg L ⁻¹ (25 °C) †	4.3 mg L ⁻¹ (20 °C)	8.5 mg L ⁻¹ (20 °C)	1.4 mg L ⁻¹ (25 °C)	116 µg L ⁻¹ (20 °C)
Henry's law constant ‡	5.2 · 10 ⁻⁷ (25 °C)	7.0 · 10 ⁻⁵ (20 °C)	1.2 · 10 ⁻⁶ (25 °C)	1.6 · 10 ⁻⁴ (20 °C)	2.1 · 10 ⁻⁵ (25 °C)
K _{om}	141 L kg ⁻¹	2075 L kg ⁻¹	180 L kg ⁻¹	3469 L kg ⁻¹	12460 L kg ⁻¹
Vapor pressure	0.2 · 10 ⁻⁵ hPa (20 °C) §	2.3 · 10 ⁻⁵ hPa (20 °C)	0.15 · 10 ⁻⁵ hPa (25 °C)	2.7 · 10 ⁻⁵ hPa (25 °C)	1.2 · 10 ⁻⁷ hPa (20 °C)
DT ₅₀ (soil)	68 d (25 °C, pH 5)	67 d	86 d (20 °C, pH 5)	94 d	75 d (pH 4)

† Hornsby et al. (1996)

‡ dimensionless values (calculated)

§ Tomlin (1994)

3.4.1 Parathion-methyl

Parathion-methyl [*O,O*-dimethyl *O*-(4-nitrophenyl) phosphorothioate] is a non-systemic insecticide belonging to a class of insecticides referred to as organophosphates. Parathion-methyl is available in dust, emulsion concentrate, microencapsules and wettable powder formulations. For experiments, ^{14}C -labeled parathion-methyl was used as emulsion concentrate (40% a.i.; specific radioactivity: 1.94 MBq mg^{-1} ; radiochemical purity > 99.0%) obtained from Sigma Aldrich GmbH, Deisenhofen, Germany. Non-labeled parathion-methyl was used as the commercial product ME 605 (wettable powder; 40% a.i.) obtained from Bayer CropScience AG, Monheim, Germany.

3.4.2 Fenpropimorph

Fenpropimorph [cis-4-[3-[4-(1,1-dimethylethyl)phenyl]-2-methylpropyl]-2,6-dimethylmorpholine] is a systemic fungicide which is formulated in 49 fungicidal products, mostly in mixtures with other fungicides, although the emulsion concentrate (EC) is the most commonly used. ^{14}C -fenpropimorph (80% a.i.; specific radioactivity: 6.89 MBq mg^{-1} ; radiochemical purity > 99.0%) and the non-labeled EC formulation Corbel were supplied by BASF AG, Limburgerhof, Germany. The suspension concentrate FORTRESS TOP, containing both fenpropimorph ($250 \text{ g a.i. L}^{-1}$) and quinoxifen ($66.7 \text{ g a.i. L}^{-1}$), was obtained from Dow AgroSciences GmbH, Munich, Germany.

Oxidation is the first stage of metabolism in plants, followed by degradation of the morpholine ring. Over 60% of the residue on the day of application was on the leaf surface and was mainly unchanged fenpropimorph. After three weeks about 30% of the applied radioactivity was absorbed into the leaf and only about 7% of that was unchanged fenpropimorph. Under neutral conditions fenpropimorph is stable in water. Under field conditions degradation in soil proceeds by oxidation and opening of the morpholine ring to give fenpropimorph acid.

3.4.3 Terbutylazine

Terbutylazine [6-chloro-N-(1,1-dimethylethyl)-N'-ethyl-1,3,5-triazine-2,4-diamine], the replacement product for atrazine, which was banned in Germany in 1992, is a broad-spectrum pre- or post-emergence herbicide. Terbutylazine is mostly used as an aqueous suspension concentrate. ^{14}C -labeled terbutylazine was used as suspension concentrate (50% a.i.; specific radioactivity: 3.17 MBq mg^{-1} ; radiochemical purity: 98.9%) obtained from Syngenta AG, Basel, Switzerland.

In soil, metabolism studies using ^{14}C -labeled terbutylazine showed mineralization with formation of nitrogen-containing derivatives and carbon dioxide. Decomposition by means of photolysis was also observed on the surface of the soil. Degradation of terbutylazine occurs under a variety of environmental conditions. The rate of decomposition is strongly influenced by temperature, moisture levels, microbial activity, pH, and aeration. Soil mobility studies showed an adsorption of terbutylazine onto soil particles within 2 hours; adsorption increased with humus content of the soil. The mobility of terbutylazine is lower than that of atrazine but highly dependent upon soil type (WHO, 1998).

3.4.4 Chlorpyrifos

Chlorpyrifos [*O,O*-diethyl *O*-(3,5,6-trichloro-2-pyridinyl) phosphorothioate] is a broad-spectrum organophosphorous pesticide. Chlorpyrifos is formulated in a number of different commercial products. The most commonly available formulations include emulsifiable concentrates, granulars, and wettable powders. For experiments, non-labeled chlorpyrifos was used as commercial product Dursban 4E (emulsion concentrate; 480 g a.i. L⁻¹) obtained from Dow AgroSciences, Indianapolis, USA.

Chlorpyrifos is a degradable compound, and both abiotic and biotic transformations processes effect its degradation within environmental compartments. In all cases, the major pathway of transformation involves cleavage of the phosphate ester bond to form 3,5,6-trichloro-2-pyridinol. Chlorpyrifos is susceptible to photolytic transformation, with the greatest photolysis observed for thin films present on exposed, inert surfaces, for which half-lives up to 13.7 days have been demonstrated. Photolysis in aqueous systems proceeds at a slower rate (Racke, 1993).

3.4.5 Quinoxifen

Quinoxifen [5,7-dichloro-4-quinolyl 4-fluorophenyl ether] is a surface-mobile fungicide from the chemical class of phenoxyquinolines which is used for the control of wheat powdery mildew (Longhursts et al., 1996). Quinoxifen is used in sequence in alternation or in tank-mix with fungicides of different modes of action. Non-labeled quinoxifen was applied as suspension concentrate in combination with fenpropimorph (FORTRESS TOP; cf. 3.4.2).

Quinoxifen is only slightly metabolized in wheat, with low residues found in the crop. The main metabolite in the soil was formed by hydroxylation at the 3-position of the quinoline ring, a minor metabolite formed by cleavage of the ether bridge was observed, especially in acidic soil (Tomlin, 2000).

3.5 Experimental Soil

The experimental soil for studies at the laboratory scale was prepared as mentioned before (cf. 3.1.1.4 & 3.2.2.1). For the lysimeter studies, undisturbed soil monoliths with a profile depth of 1.10 m were removed from the field plots with the aid of stainless steel cylinders and inserted in stainless steel containers firmly embedded in the soil (Führ et al., 1998). Fertilization and complementary plant protection measures of the field plot and the lysimeters were closely coordinated with agricultural practice. The main properties of the used soil types are summarized as follows.

3.5.1 Gleyic Cambisol

According to the Food and Agriculture Organization of the United Nations (FAO, 1990) the experimental soil used for the laboratory studies and for the wind-tunnel experiment on bare soil was classified as a gleyic cambisol. Soil properties, including physical properties required for PEARL calculations (cf. 2.2.2.3.1), are listed in **Table 3.9**.

Table 3.9 Soil properties and soil profile of gleyic cambisol.

Basic soil properties					
Horizon [m]	Sand [%]	Silt [%]	Clay [%]	C _{org} [%]	pH
0.00 – 0.05	73.3	23.1	3.6	0.99	5.35
0.05 – 0.30	73.3	23.1	3.6	0.99	5.35
0.30 – 0.62	81.3	15.7	3.0	0.29	5.49
0.62 – 0.80	76.9	20.6	2.5	0.17	5.76
0.80 – 1.15	92.5	6.1	1.4	0.06	5.96
Soil physical properties					
Horizon [m]	Saturated volume fraction of water in the soil system θ_s [m ³ m ⁻³]	Residual volume fraction of water in the soil system θ_{res} [m ³ m ⁻³]	Parameter in Van Genuchten hydraulic relationship α [cm ⁻¹]	Empirical parameter in Van Genuchten equation n [-]	Saturated hydraulic conductivity K _s [m d ⁻¹]
0.00 – 0.05	0.452	0.045	0.0162	1.957	1.000
0.05 – 0.30	0.452	0.045	0.0162	1.957	0.200
0.30 – 0.62	0.392	0.038	0.0254	1.643	0.001
0.62 – 0.80	0.459	0.032	0.0405	1.636	0.001
0.80 – 1.15	0.433	0.021	0.0496	1.813	0.001

3.5.2 Orthic Luvisol

The soil at the field plot in Jülich-Merzenhausen was classified as an orthic luvisol (FAO, 1990). Basic soil properties are summarized in **Table 3.10**.

Table 3.10 Soil properties of orthic luvisol.

Horizon [m]	Sand [%]	Silt [%]	Clay [%]	C _{org} [%]	pH
0.00 – 0.39	6.4	78.2	15.4	1.1	7.2
0.39 – 0.55	1.0	77.1	21.9	0.4	6.9
0.55 – 0.77	0.1	73.4	26.5	0.3	6.8
0.77 – 0.98	0.8	74.1	25.1	0.3	6.7
0.98 – 1.19	0.7	72.7	26.6	0.3	6.5

4 RESULTS AND DISCUSSION

4.1 Volatilization from Bare Soil

Result and discussion on volatilization from soil are organized along four key areas:

- Development and optimization of an accurate set-up for process studies on volatilization at the laboratory scale under field-like conditions (cf. 4.1.1)
- Gathering of new experimental data sets by performing semi-field experiments (wind tunnel) with the aim of up-scaling the results of the laboratory studies (cf. 4.1.2)
- Evaluation of screening models and estimation tools for volatilization from soil to define precisely several limitations and shortcomings of the currently available model approaches (cf. 4.1.3.1)
- Integration of modified or new modules for the consideration of volatilization into the existing PEC models (PEARL, PELMO) and revaluation (cf. 4.1.3.2 & 4.1.3.3)

4.1.1 Laboratory Studies on Volatilization of Parathion-methyl

Due to increased flow rates passing through the chamber the air sampling system had to be validated to ensure quantitative adsorption of pesticides. Measurements included the compilation of soil moisture profiles of the upper soil layer and the determination of the aerodynamic conditions in the glass dome of the chamber. After validation of the new device, studies on the environmental fate of ^{14}C -parathion-methyl after soil surface application to gleyic cambisol were performed and the influence of soil moisture and soil temperature on volatilization was characterized.

4.1.1.1 Measurements of Air Velocity and Pressure Differential

Exchange rates in the photovolatility chamber were increased using a powerful suction pump generating a flow profile as shown in **Fig 4.1A**. The flow rate of 10 L min^{-1} changed the atmosphere in the glass dome of the chamber $30 \text{ times min}^{-1}$ and minimized the potential build-up of volatilized contaminants, as evidenced by low contaminant concentrations on the surface of the glass dome and the air sampler (approx. 0.2% of net applied radioactivity) after experiments with parathion-methyl (**Table 4.2**). The wind velocity rose with increasing distance from the soil surface reaching a maximum at 3.3 cm (0.3 m s^{-1}) and decreased higher up due to frictional resistance caused by the glass dome. For registration purposes, the German guideline on assessing pesticide volatilization implies a wind velocity above the surface of 1 m s^{-1} (BBA, 1990). Assuming logarithmic flow profiles according to Prandtl's law (Prandtl, 1990), wind-tunnel experiments performed with a defined wind velocity of 1 m s^{-1} at 20 cm height (cf. 3.1.2.4) required a wind velocity of $0.15\text{-}0.20 \text{ m s}^{-1}$ at 1-2 cm above the soil surface. Using the photovolatility chamber, this corresponded to an air exchange rate of $10\text{-}12 \text{ L min}^{-1}$. Experimental results, including diminished air velocity near to soil surface, are in good accordance with the above deviated values and confirm that suitable aerodynamic conditions to perform process studies on volatilization and to meet the requirements for studies for registration purposes are obtained in the extended photovolatility chamber.

Additional measurements of the pressure differential as a function of flow rates within the chamber revealed that the system is under slight negative pressure when the flow rate exceeds 9 L min^{-1} (**Fig 4.1B**), e.g. a flow rate of 9.5 L min^{-1} corresponds to an air pressure of 987 mbar (atmospheric pressure: 1018 mbar, air temperature: 20°C). This value is not very far from a meteorological low-pressure area. The pressure inside the chamber reached atmospheric conditions at a flow rate of 8.6 L min^{-1} (**Fig. 4.1B**). The use of an additional pump at the air inlet pressing air into the photovolatility chamber in support of the suction pump enabled studies under slight excessive pressure. Slowing down the suction pump while maintaining the pumping power at the air inlet caused an increase in pressure exceeding the atmospheric pressure outside the chamber underneath an air exchange rate of 8.6 L min^{-1} .

In comparison with other laboratory systems currently in use for determining the fate of volatile organic compounds (Orchard et al., 2000), the pressure differential appears acceptable.

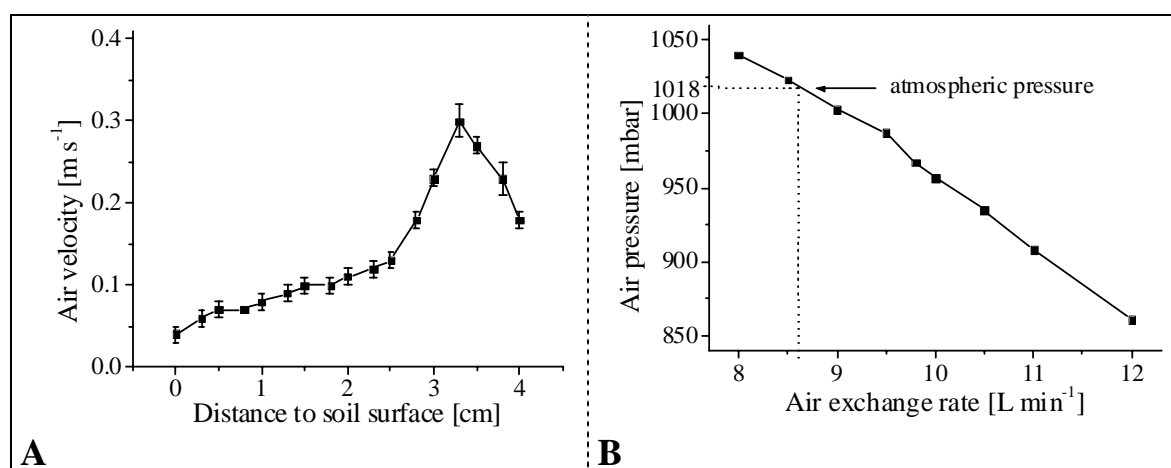


Figure 4.1 Aerodynamic conditions in the glass dome of the photovolatility chamber. **A:** Measurement of the air velocity using a thermal anemometer at an air exchange rate of 10 L min^{-1} and an air temperature of 20°C above the center of the soil surface. Data are presented as means \pm standard deviation, each after 10 min recording of air velocity. **B:** Measurement of the pressure differential in the glass dome as a function of air exchange rates using a pressure transducer at an air temperature of 20°C .

4.1.1.2 Validation of the Total-volume Sampler (TVS)

In earlier vaporization studies it was shown that the air sampling system of the photovolatility chamber (TVS) ensured quantitative adsorption of ^{14}C -parathion-methyl and its metabolites on the PUF plugs using flow rates of about 3 L min^{-1} (Kromer, 2001). The results of preliminary experiments to verify the effectiveness of the TVS using increased air exchange rates are summarized in **Table 4.1**. It could be shown that the vaporized compound had been completely adsorbed onto the first plug, the following plugs remaining pesticide-free. Dimensions of sampling efficiency and recovery rate agree with validation studies regarding wind-tunnel experiments with parathion-methyl (Stork et al., 1994). Taking into account that the applied concentrations and flow rates in the validation experiments were much higher than used in photovolatility chamber experiments, the sampling unit is suitable even for high flow rates.

Table 4.1 ^{14}C -recovery in the total-volume sampler after vaporization of ^{14}C -parathion-methyl.

duration [h]	24	Σ PUF † plugs [kBq]	11.54 ± 0.08
vaporization temperature [$^{\circ}\text{C}$]	65	PUF † sampling efficiency [%]	101.5 ± 0.7
average air flow rate [L min^{-1}]	13.4 ± 0.8	system losses (contamin.) [%]	1.8 ± 0.3
applied radioactivity [kBq]	11.37	average ^{14}C -recovery [%]	103.3 ± 0.4
applied substance [mg]	103.3		

† PUF: polyurethane foam

4.1.1.3 Water Content in the Soil Container

A basic requirement for process studies under defined environmental conditions is to ensure constant soil moisture at the soil surface. The water replenishing system (**Fig. 3.4**) allows the adjustment of a defined water tension, which correlates with the volumetric water content measured by TDR equipment. Although the soil moisture remains constant at a defined depth a gradient is built up within the soil container, e.g. the airflow causes a fast drying of the surface layer. This gradient is essential for adsorption and volatilization, especially in the top layer (Boesten, 2000). To measure soil moisture profiles after finishing the experiments soil layers were removed and water content was determined by gravimetric analysis. Without remoistening of the soil surface (**Table 3.1**: 1st soil moisture study, air humidity: 40-50%) an almost complete drying of the top layer was observed and the moisture profile reached a maximum near to the ceramic plate (**Fig. 4.2**). When the surface layer (a few millimeters) dries out totally, adsorption of chemicals to the soil surface increases significantly and volatilization rates decrease (Spencer et al., 1973). To characterize the influence of soil moisture on volatilization it is therefore essential to prevent drying and to ensure defined soil moisture in the top layer.

The use of wash bottles to achieve water-saturated air (**Table 3.1**: 2nd soil moisture study, air humidity about 90%) under constant environmental conditions increased soil moisture at the surface and soil moisture values remained nearly constant down to a depth of 4 cm (**Fig. 4.2**). This effect of relative humidity on surface moisture is in good accordance with previous studies (Spencer et al., 1973). Experiments on volatilization of parathion-methyl from glass surfaces showed that increased air humidity did not affect volatilization rates (Spencer et al., 1979). Water-saturated air influences volatilization mainly through its effect on soil moisture and does not directly influence volatilization of pesticides. Thus, water saturation by wash bottles is appropriate for use in experiments on the influence of soil moisture on volatilization.

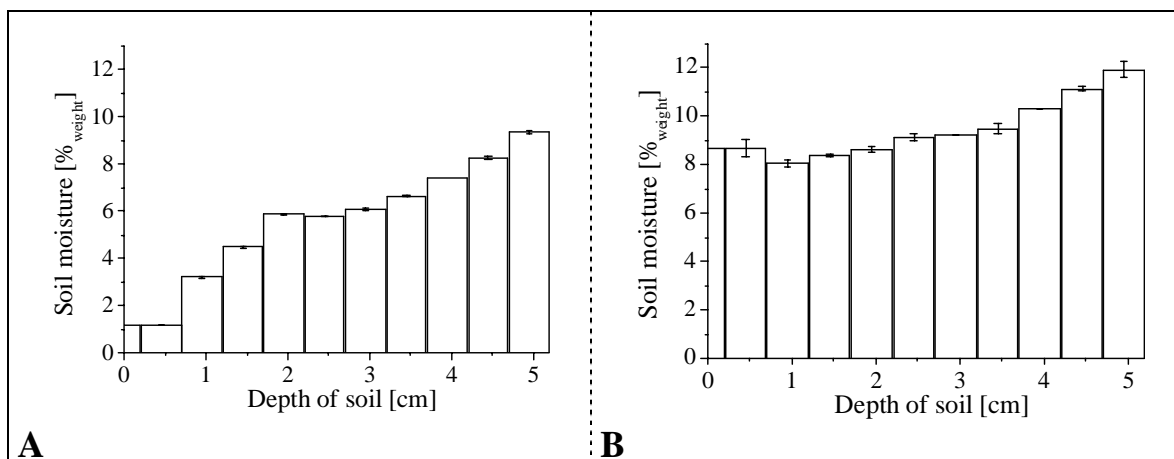


Figure 4.2 Soil moisture profiles of gleyic cambisol in the soil container after photovolatility chamber experiments of 4 to 6 days. **A:** Dry conditions (Table 3.1: air humidity: $43.1 \pm 5.1\%$, soil moisture at 2.5 cm depth: $15.7 \pm 0.2\%$ vol). **B:** Moist conditions (use of wash bottles; air humidity: $89.6 \pm 1.0\%$, soil moisture at 2.5 cm depth: $20.3 \pm 0.2\%$ vol). With the exception of soil moisture, both experiments were performed under constant environmental conditions (Table 3.1: air temperature: 19.4 ± 0.2 °C, evaporation: 1.1 ± 0.3 mm d⁻¹). Water content of soil layers was determined as percentage of dry weight gravimetrically at the end of the experiments. Data are presented as mean values of three replicates \pm standard deviation.

4.1.1.4 Validation of Uniform Spray Distribution Pattern

A uniform distribution is the main goal for most pesticide applications. To ensure a homogenous distribution of the application solution, the spray distribution pattern and the application losses were recorded after application of ¹⁴C-labeled parathion-methyl on TLC plates. Previous studies revealed a spray pressure of 0.8 bar and a mean droplet diameter (MVD) of 200 μ m being suitable to achieve field-like conditions. Application losses amounted to an approximately constant value of 50% of the application volume and enabled the calculation and use of field-like spray volumes within the process studies on volatilization. Determination of an averaged pattern after three manual air brush applications revealed an almost uniform distribution of ¹⁴C-labeled parathion-methyl (**Fig. 4.3**). Accidental intensity differences, mainly occurring at the periphery of the TLC plate, were caused by irregularity of the manual application. Considering spray application under field conditions also showing slight variation in pesticide concentration, e.g. caused by the roughness of the soil surface (Kromer, 2001), the distribution after manual application corresponds quite well with the field applications.

Regarding plant volatilization, droplet size governs the competition between absorption by plant surfaces and volatilization; small droplets tend to evaporate more quickly than larger ones, and larger ones tend to be absorbed faster (Breeze et al., 1992). For that reason, droplet size, spray volume and distribution pattern of the applied pesticide mixture should be related as closely as possible to the agricultural practice to meet the requirements of field-like studies.

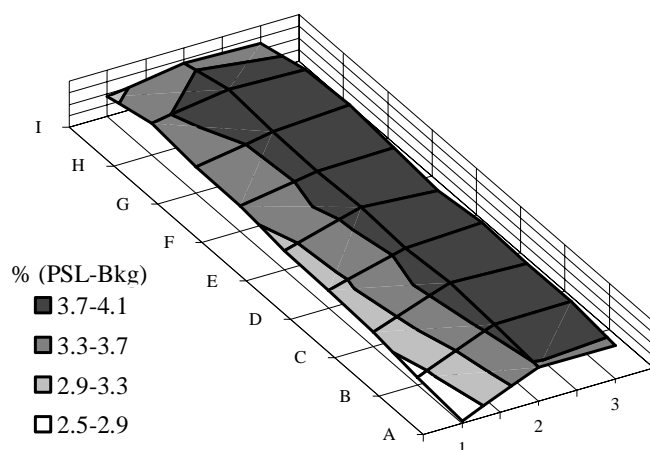


Figure 4.3 Spray distribution pattern of ^{14}C -labeled parathion-methyl after manual application (air brush, MVD: 200 μm) on a TLC plate. Results were evaluated using the Bio-Imaging Analyzer (cf. 3.3.3.1); mean values of three separate applications are shown. PSL: photostimulated luminescence. Bkg: background. A-I, 1-3: system of co-ordinates used for the computer-assisted evaluation of intensity differences.

4.1.1.5 Influence of Soil Moisture on Cumulative Volatilization and Kinetics

The main goal of the process studies using the photovolatility chamber was to quantify the influence of soil moisture on volatilization of ^{14}C -parathion-methyl while maintaining constant environmental conditions.

4.1.1.5.1 Radioactivity and Mass Balance

The functionality of the photovolatility chamber and the air sampling unit is documented by total ^{14}C -recoveries ranging from 94.8 to 99.9% of the applied radioactivity (**Table 4.2**).

Table 4.2 ^{14}C -recoveries determined in experiments on soil moisture dependence of the volatilization of ^{14}C -parathion-methyl (data in % of net applied radioactivity).

Process study	1 st soil moisture study (dry conditions) †	2 nd soil moisture study (medium conditions) ‡	3 rd soil moisture study (moist conditions) †
Contamination §	0.2	0.5	0.3
Soil (0–0.7 cm)	91.7	83.5	61.3
Soil (0.7–1.2 cm)	0.4	0.4	0.1
Soil (1.2–5.2 cm)	0.1	ND ¶	0.1
Leachate	ND ¶	ND ¶	ND ¶
Volatilization	2.4	12.8	32.9
Mineralization to $^{14}\text{CO}_2$	ND ¶	0.2	5.2
Σ ^{14}C	94.8	97.4	99.9

† Fig. 4.2

‡ Table 3.1

§ contamination of the glass dome and the air sampler by volatilization

¶ ND = not detectable

System contamination was very low ($\leq 0.5\%$ of net applied radioactivity), which can be attributed to the use of glass and polytetrafluoroethylene as the main construction materials and high air exchange rates (Ophoff et al., 1996). The percentage distribution of the detected radioactivity in soil, water and air (including volatilization and mineralization) within the three studies on the influence of soil moisture is given in **Table 4.2** and is discussed in the following sections.

4.1.1.5.2 Metabolization and Mineralization

Gleyic cambisol was identified as a major sink for the applied compound, 61.5 to 92.2% of the applied radioactivity was recovered (**Table 4.2**). In accordance with the strong adsorption of parathion-methyl (cf. 4.1.1.5.3), the compound predominately remained in the top layer of the soil (0-7 mm), only traces were detected in the underlying layers.

The moderately acid experimental soil (pH 5.35; **Table 3.9**) is known to favor a stepwise degradation of parathion-methyl leading to the end product 4-nitrophenol (Roberts & Hutson, 1999). Thus, enhanced amounts of ^{14}C -4-nitrophenol and unidentified less polar compounds were detected in the soil samples, especially under moist conditions (**Table 4.3**). As parathion-methyl is classified as moderately degradable in soil and water (Domsch, 1992; Adamson & Inch, 1973), $^{14}\text{CO}_2$ as the final degradation product of mineralization was detected within the 2nd experiment (0.2%) and to a higher degree in the 3rd experiment (5.2%), suggesting an increasing mineralization of parathion-methyl with increasing soil moisture.

Experiments were performed in the dark and ozone-free air was used to reduce the influence of photodegradation. Thus, only minor amounts of metabolites were found in the air samples and up to 97.1% AR of the extracted radioactivity was characterized as unchanged ^{14}C -parathion-methyl (**Table 4.3**).

Table 4.3 Characterization of ^{14}C -labeled compounds in the methanol extracts of soil and PUF plugs (data in % of extracted radioactivity). Values of the soil moisture adjusted in the studies are given in Fig. 4.2 and Table 3.1.

Sample	Soil layer (0–7 mm)			PUF plugs ‡		
	1 st study (dry)	2 nd study (medium)	3 rd study (moist)	1 st study (dry)	2 nd study (medium)	3 rd study (moist)
Parathion-methyl	82.2	76.9	72.7	97.1	96.7	96.9
4-nitrophenol	5.6	6.4	12.0	1.1	0.7	0.8
Paraoxon-methyl	ND †	ND †	ND †	0.1	ND †	ND †
Unknown polar products	12.2	16.7	15.3	1.8	2.6	2.4

† ND = not detectable

‡ PUF: polyurethane foam; values averaged within the experimental duration

4.1.1.5.3 Cumulative Volatilization and Kinetics

An unambiguous dependence of volatilization on the water content in the top layer of the soil was established within the three soil moisture studies (**Fig. 4.4**), exemplified by a cumulative volatilization of 12.8% under medium conditions (2nd study) and 32.9% under moist conditions after 6 days in the 3rd experiment (**Table 4.2**). Only a slight volatilization of 2.4% AR in the 1st experiment performed under dry conditions was detected after 4 days. The pronounced enhancement of volatilization, e.g. changing from dry to moist conditions led to an increase by a factor of approx. 14, allowed for a pure quantification of the influence of soil moisture, without being affected by varying environmental conditions. Thus, the constant environmental scenario during the laboratory studies (**Table 3.1**), especially soil moisture and soil temperature, enabled the definite correlation between volatilization and water content.

In contrast to the 1st and 3rd experiment, which were characterized by evaporation rates of approx. 1.0 mm d^{-1} , an infiltration of water was measured (**Table 3.1**: $-1.8 \pm 0.7 \text{ mm d}^{-1}$) during the 2nd soil moisture study. Obviously, the adjustment of a higher water tension in the 2nd study caused a lower water content in the soil container and entailed a stronger moistening of the soil by the water-saturated air, finally resulting in an infiltration of water (cf. 3.1.1.2). Considering the clear correlation between soil moisture and cumulative volatilization measured in the process studies (**Fig. 4.4**), evaporation of water does not have a significant influence on the volatilization behavior. Even though water transfer contributes to pesticide transport inside the soil matrix, its influence on the volatilization of surface applied compound seems to be negligible. Observations of volatilization rates apparently following the diurnal pattern of soil water evaporation as described by Stork et al. (1998), can be attributed to the influence of soil temperature which follows the same diurnal course in most cases.

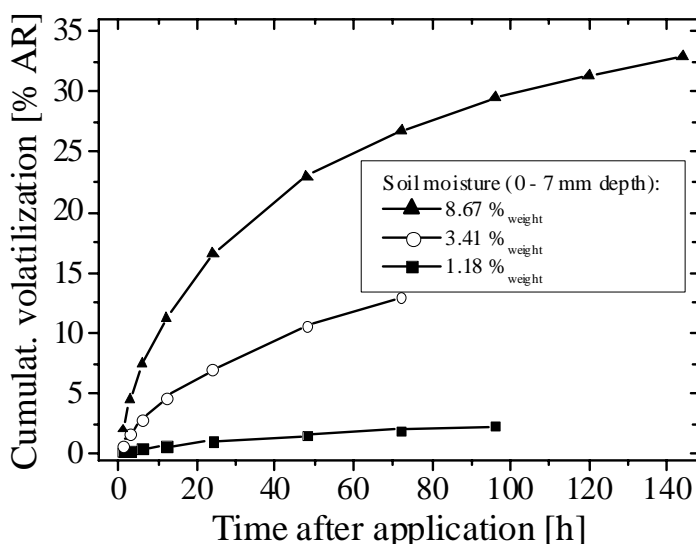


Figure 4.4 Cumulative volatilized radioactivity after soil surface application of ^{14}C -parathion-methyl to gleyic cambisol determined in PUF plugs. Net applied radioactivity (AR) = 100%.

Highest volatilization rates were measured directly after application (**Fig. 4.5**). During the following days, volatilization rates decreased and finally reached extremely low constant daily rates. The strong decrease of volatilization rates after the first hours of the experiment corresponds to the kinetics as observed in an interlaboratory comparison of volatilization

assessment methods (Walter et al., 1996) and reveals a “phasing out” of volatilization between the second and third day after application.

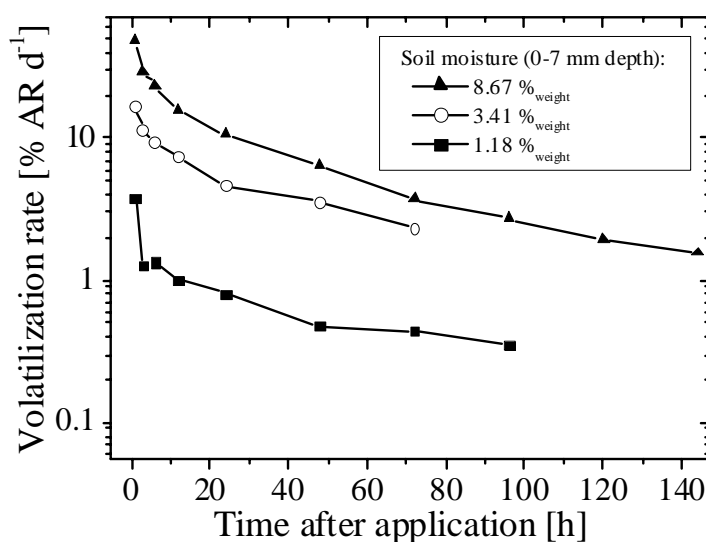


Figure 4.5 Volatilization rates of ^{14}C -parathion-methyl after soil surface application to gleyic cambisol (semi-logarithmic plot). Net applied radioactivity (AR) = 100%.

These volatilization rates illustrate a major problem concerning experimental procedures. Because of the crucial importance of the first 24 hours for volatilization, seemingly minor differences in application or micro-climatic conditions during these hours may therefore have substantial influence on the results observed. This effect is even more essential in field experiments, where climatic conditions are outside the experimenter's control. Even though the soil moisture content effectively controls the adsorption of pesticide residues, the factors controlling changes in moisture content in surface layers of soil are not well understood (Spencer et al., 1995). The ability to understand and predict drying and rewetting in surface soils of various textures under a range of management practices will be an essential step in improving the prediction of pesticide volatilization rates.

4.1.1.6 Influence of Soil Temperature on Volatilization

The environmental conditions in the study on the influence of soil temperature were chosen comparable to those in the 2nd soil moisture study (Table 3.1), with the exception of the soil surface temperature, which was increased from 20 to 30 °C. Although the adjustment of the same water tension inside the water replenishing system resulted in an almost identical volumetric water content measured by TDR at a depth of 2.5 cm, the gravimetric soil moisture at the top layer (1.61%_{weight}) was considerably lower than after the 2nd soil moisture study performed at 20 °C (3.41%_{weight}). Obviously, the air humidity of approx. 84% could not compensate for the water loss (evaporation: 1.0 ± 0.9) caused by temperature raising. Experimental conditions, especially the water content at the top layer were rather comparable to the 1st soil moisture study under dry conditions (1.18%_{weight}). To take into account the temperature effect on the soil moisture of the top layer, future studies on temperature dependence of volatilization ought to be performed under moister conditions, e.g. the adjustment of lower water tension in the soil container or the use of additional wash-bottles might be considered.

Just as the studies on soil moisture dependence (cf. 4.1.1.5.1), ^{14}C -recoveries of parathion-methyl and merely slight contamination losses illustrate the functionality of the set-up (**Table 4.4**). In comparison with the studies on the influence of soil moisture, which were performed at a soil temperature of 20 °C, enhanced amounts of metabolites, especially 4-nitrophenol, were detected after temperature raising to 30 °C. In addition, the increase of mineralization to $^{14}\text{CO}_2$ compared to the 1st soil moisture study illustrates the tendency towards enhanced degradation rates in soil after increasing the temperature (Domsch, 1992). Remarkably, the formation of $^{14}\text{CO}_2$ (5.2%) was much lower than measured in the 3rd soil moisture study, which was performed at 20 °C but under moister conditions (**Table 4.2**). With regard to mineralization, the effect of increasing soil moisture leading to an enhancement of microbial degradation (Hurle, 1982) seems to exceed the effect of decreasing temperature.

Table 4.4 Results of a 3-day photovolatility chamber experiment after soil surface application to gleyic cambisol (soil surface temperature: 30 °C). **A:** ^{14}C -recoveries (data in % of net applied radioactivity). **B:** Characterization of ^{14}C -labeled compounds in the methanol extracts of soil and PUF plugs (data in % of extracted radioactivity).

A: ^{14}C-recoveries		B: Metabolization		
		Sample	Soil layer (0 – 0.7 cm)	PUF plugs †
Contamination ‡	0.8	Parathion-methyl	65.0	95.9
Soil (0 – 0.7 cm)	56.2	4-nitrophenol	19.4	1.3
Soil (0.7 – 1.2 cm)	0.1	Paraoxon-methyl	ND §	ND §
Soil (1.2 – 5.2 cm)	0.1	Unknown polar products	15.5	2.8
Leachate	ND §			
Volatilization	32.7			
Mineralization to $^{14}\text{CO}_2$	0.9			
Σ ^{14}C	90.8			

† PUF: polyurethane foam plugs; values averaged within the experimental duration

‡ contamination of the glass dome and the air sampler by volatilization

§ ND = not detectable

In accordance with the studies on soil moisture influence, highest volatilization rates were measured directly after application (**Fig. 4.6B**). Subsequently, the volatilization rates decreased and finally resulted in a cumulative volatilization of 32.7% AR after 3 days (**Fig. 4.6A**). A comparison with the cumulative volatilization measured in the 1st soil moisture study after 3 days (2.0% AR, **Fig. 4.4**) under almost identical moisture conditions reveals that an increase of 10 °C in soil temperature enhanced the volatilization of parathion-methyl from gleyic cambisol by a factor of approx. 16. This enhancement clearly illustrates that temperature effects on volatilization may exceed the influence on vapor pressure which was shown to cause a three- to four-fold increase in vapor pressure for most pesticides after a 10 °C increase (Spencer & Cliath, 1990). Obviously, the measured

temperature dependence of volatilization is not simply parallel to the temperature dependence of vapor pressure. This suggests that the determination of the temperature dependence of vapor pressure does not allow a prediction of the volatilization behavior of pesticides. Instead, to get a realistic impression of actual processes influencing volatilization behavior the effect of soil-drying on volatilization should be taken into consideration. As mentioned above, temperature raising under field conditions is mostly accompanied by soil drying, which tends to promote the adsorption of pesticides on the soil matrix (cf. 4.1.1.5). The availability of surface-applied compounds and thus the volatilization tendency is limited by soil dryness and causes comparatively low enhancement of volatilization rates after temperature raising under field conditions, e.g. it was reported that an increase of 10 °C in soil temperature increased the volatilization of halogenated pesticides applied to moist soil by a factor of 1.8 (Nash & Gish, 1989). Therefore, the use of wash-bottles to prevent soil drying (cf. 4.1.1.3) allows for an undisturbed quantification of the temperature effect on volatilization unaffected by varying soil moisture.

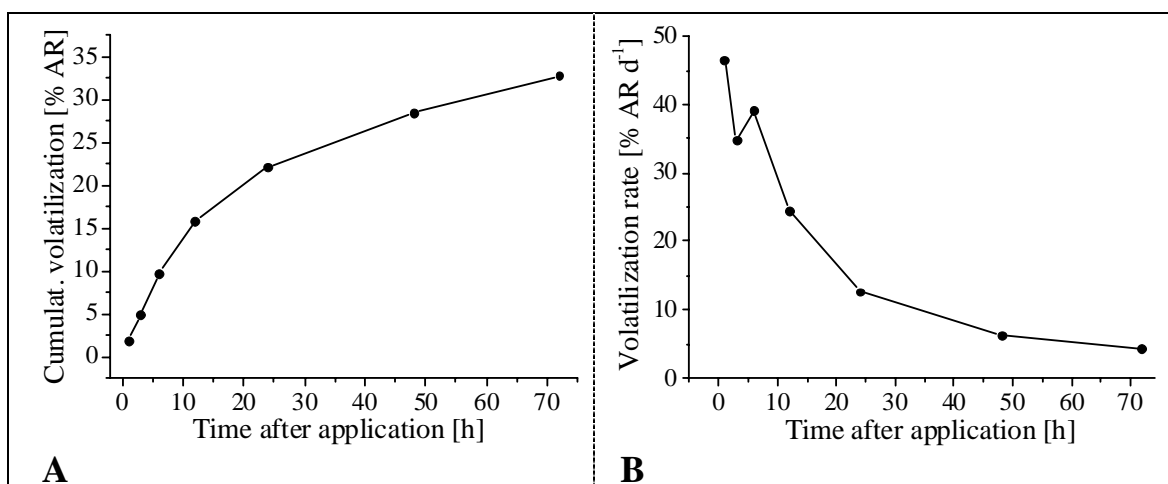


Figure 4.6 Volatilization of ^{14}C -parathion-methyl after increasing the soil surface temperature from 20 to 30 °C. **A:** Cumulative volatilized radioactivity. **B:** Volatilization rates. Net applied radioactivity (AR) = 100%.

4.1.2 Wind-tunnel Study: Pesticide Application to Bare Soil

Measurements of the volatilization behavior of four pesticides include the quantification of ^{14}C -organic compounds and $^{14}\text{CO}_2$ separately and the detection of soil residues of the ^{14}C -labeled pesticides (parathion-methyl, fenpropimorph, terbuthylazine), just as determination of volatile losses of non-labeled chlorpyrifos (cf. 3.1.2.4). Well-defined conditions over the course of the experiment were illustrated by continuous recording of the most important environmental parameters.

4.1.2.1 Wind-tunnel Study on Soil: Environmental Conditions

The measuring device installed in the wind tunnel (**Fig. 3.6**) allowed for continuous monitoring of soil moisture, soil temperature, air temperature, air humidity, and radiation over the course of the experiment (**Fig. 4.7**).

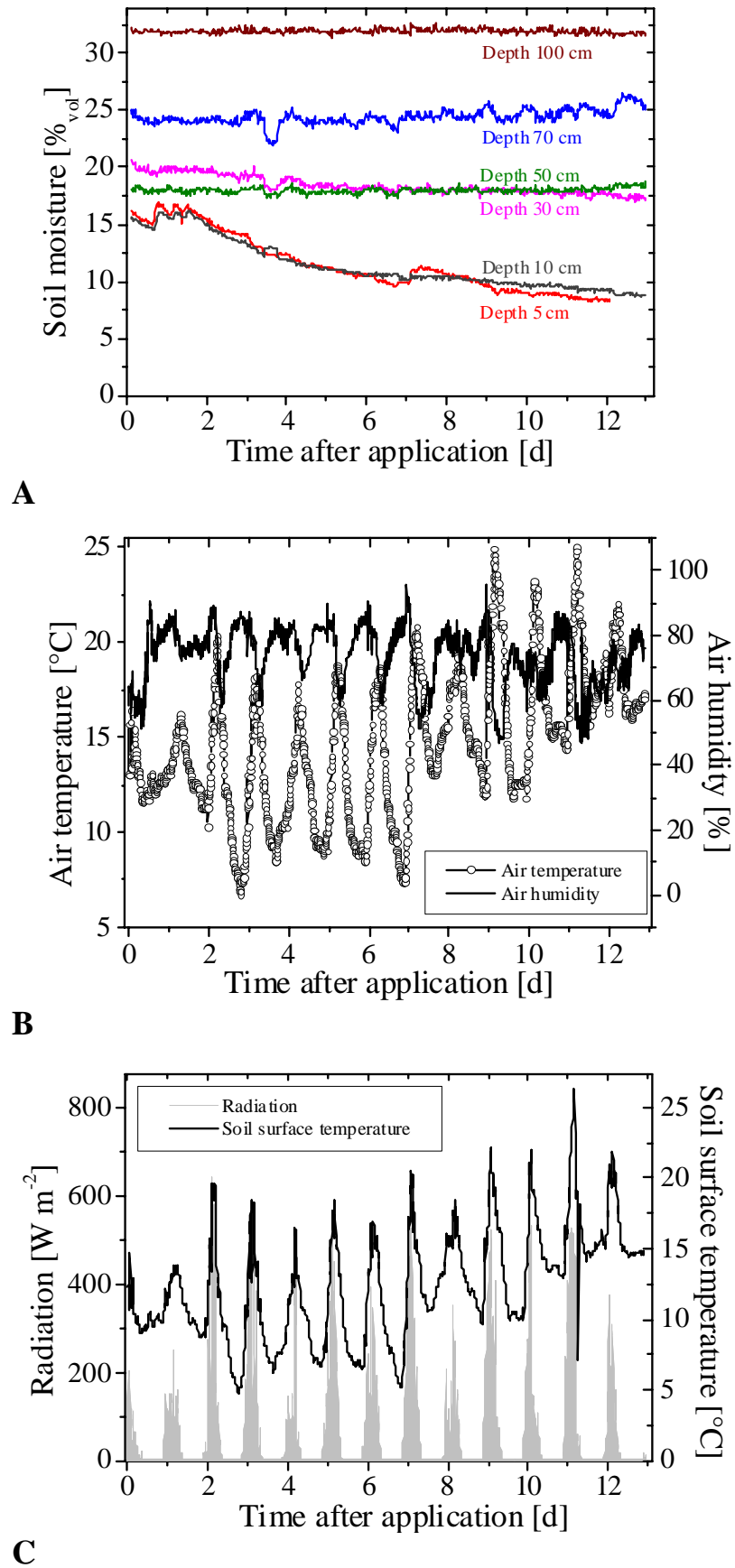


Figure 4.7 Climatic conditions over the course of the wind-tunnel study after soil surface application to gleyic cambisol. **A:** Volumetric water content measured by TDR equipment in several depths. **B:** Air temperature and air humidity. **C:** Irradiation and soil surface temperature.

The uniform airflow passing over the lysimeter surface (cf. 3.1.2.4) caused drying of the top soil, illustrated by decreasing volumetric water content of the top layers (depth 5 cm and 10 cm) during the first week of the experiment (**Fig. 4.7A**), whereas water content of deeper soil layers (depth ≥ 30 cm) remained almost constant in time. Irrigation given on Day 8 resulted in a significant increase of soil moisture in the top centimeters of the soil (depth 5 cm) and did not affect the underneath layers.

Monitoring of air temperature (**Fig. 4.7B**) revealed, besides the expected diurnal fluctuations, a marked increase of the average temperature between Day 9 and Day 11. Generally, the time course of the soil surface temperature was similar to the course of the air temperature (**Fig. 4.7C**). Obviously, the raising of air temperature and soil surface temperature at the end of the study was due to an increase in solar radiation within the same period.

4.1.2.2 Overview: Application and Mass Balances

Recoveries of the ^{14}C -labeled compounds ranging from 94.4 to 103.5% allowed for almost complete radioactivity and mass balances (**Table 4.5**).

Table 4.5 Wind-tunnel study on bare soil: Recoveries of ^{14}C -labeled compounds (data in % of net applied radioactivity).

	Pesticide	Parathion-methyl	Fenpropimorph	Terbuthylazine
	Contamination †	0.2	0.2	0.2
Soil:	Extractable	67.8	80.4	74.7
	Non-extractable	8.6	8.2	7.5
	Leachate	ND ‡	ND ‡	ND ‡
Volatilization:	Parent compound	26.0	4.3	8.8
	Metabolites	ND ‡	2.1 §	0.7 ¶
	Mineralization to $^{14}\text{CO}_2$	0.9 #	0.9 #	0.9 #
	Glass fiber filter (particulate matter)	0.4	5.4	1.6
	$\Sigma \text{ }^{14}\text{C}$	103.9	101.5	94.4

† contamination of the wind tunnel and the high-volume sampler

‡ ND = not detectable

§ fenpropimorph acid

¶ desethyl-terbuthylazine

mean value: distinction between contribution of the three ^{14}C -labeled test compounds is not possible

System contaminations were very low (0.2% AR), which can be attributed to the use of glass as the main construction material and high air exchange rates (cf. 4.1.1.5.1; Ophoff et al., 1996). After finishing the experiment, no radioactivity was detected in the leachate. In previous studies it was shown that parathion-methyl (Gerstl & Helling, 1984), fenpropimorph (Ebing et al., 1995) and terbuthylazine (Gerstl et al., 1997) exhibited only slight tendencies towards soil leaching. Thus, the comparatively short experimental period of the wind-tunnel study (13 days) did not allow for the displacement of the applied compounds in soil.

The percentage distribution of the recovered radioactivity, as summarized in **Table 4.5**, is discussed in the following sections.

4.1.2.3 Soil Residues and Mineralization of ^{14}C -labeled Compounds

Soil analysis (cf. 3.3.1) at the end of the experiment revealed that in total 81.6% of the net applied radioactivity was located in the top layer of the lysimeter soil (0-5 cm), less than 0.2% of the applied radioactivity was found in deeper layers. Approximately 7% of the extractable soil residues was characterized as desethyl-terbuthylazine, illustrating a slight metabolization of terbuthylazine over the course of the experiment, whereas no metabolites of fenpropimorph and parathion-methyl were detected. Considerable amounts of unidentified highly polar compounds were detected in the soil samples (11% of the extractable residues) suggesting that metabolic processes, possibly due to photolysis on the soil surface, strongly influence the dissipation of pesticides.

Approximately 10% of the soil-located radioactivity was not extractable and only determinable by combustion, thus a distinction between contributions of the compounds was not possible. For short-cut calculation, the amount of the non-extractable fraction of each pesticide was estimated from the measurements of the proportionate radioactivity in the extractable fraction (**Table 4.5**), assuming uniform compositions of extractable and non-extractable fractions. Due to the short duration of the experiment the different tendencies of the compounds to form bound residues were neglected.

The formation of $^{14}\text{CO}_2$ was determined as a sum parameter including the mineralization of the ^{14}C -labeled compounds during the experiment. After 13 days a cumulative mineralization of 0.9% of the applied radioactivity was observed (**Table 4.5**). Due to the simultaneous application of three ^{14}C -labeled compounds it was not possible to relate the formation of $^{14}\text{CO}_2$ to a single pesticide.

Previous studies revealed that mineralization of ^{14}C -terbuthylazine is very small throughout most experiments (Gerstl et al., 1997), e.g. Langenbach et al. (2001) reported $^{14}\text{CO}_2$ production from ^{14}C -labeled terbuthylazine ranging between 0.08 and 0.10% over a 2-month period. In contrast, mineralization of fenpropimorph and parathion-methyl may occur, especially in moist soils. 3.3 and 1.1% of initially applied fenpropimorph were mineralized within 4 days after soil surface application on sandy loam and loamy clay, respectively (Müller et al., 1998). Within the photovolatility chamber experiments (cf. 4.1.1.5.1), mineralization of parathion-methyl up to 5.2% after 6 days was detected.

The different tendencies of the applied compounds towards mineralization suggest that mineralization of terbuthylazine probably did not occur during the wind-tunnel experiment and that the main amount of $^{14}\text{CO}_2$ arises from the degradation of parathion-methyl and fenpropimorph.

4.1.2.4 Cumulative Volatilization and Kinetics

Cumulative volatilization of 4.3% AR (fenpropimorph) and 2.1% AR (fenpropimorph acid) within 13 days was observed during the wind-tunnel study (**Fig. 4.8**). Volatilization rates reached a maximum at 24 hours after application under moist conditions. During this time the loss kinetics were primarily dictated by volatilization of the pesticide from the liquid phase. The constant airflow caused drying out of the soil surface between 2nd and 7th day and volatilization rates decreased markedly. Investigations on the volatility of fenpropimorph from the surface of a loamy sand by Müller et al. (1998) revealed a volatilization of 11.4% AR after 4 days, probably caused by the adjustment of soil moisture to 50% of the maximum water-holding capacity by using an irrigation system integrated in the topsoil of a laboratory chamber. The general tendency of pesticides towards enhanced volatilization under moist conditions (Spencer et al., 1973) may account for the reported volatilization rates in the chamber. The observed volatilization kinetics of fenpropimorph in the wind-tunnel experiment (**Fig. 4.10C**) confirmed a clear correlation between volatilization rates and soil moisture content in the top layer. Under dry conditions, the high K_{om} value of fenpropimorph (**Table 3.8**) results basically in a strong adsorption by soil, lowering the vapor pressure and leading to a decrease of volatilization rates. Consequently, irrigation at Day 8 caused a slight increase of volatilization followed by an almost uniform decrease during the last days of the experiment. Finally volatilization rates reached extremely low daily rates, revealing a “phasing out” after 12 days.

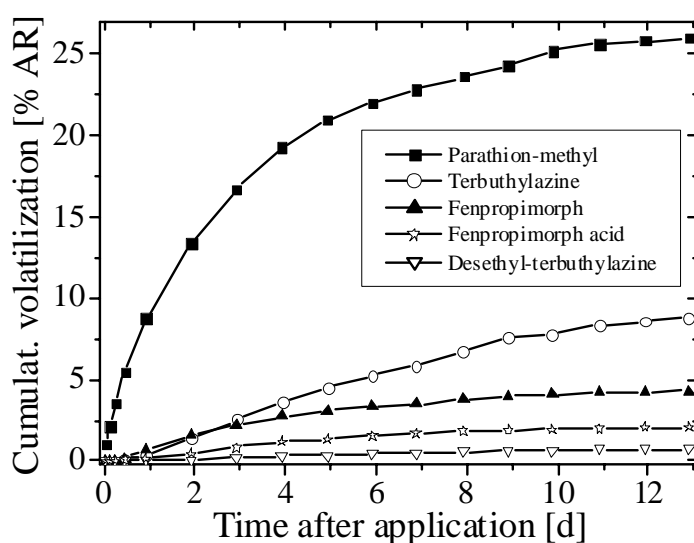


Figure 4.8 Cumulative volatilization of ^{14}C -labeled pesticides (parathion-methyl, terbutylazine, fenpropimorph) and metabolites (fenpropimorph acid, desethyl-terbutylazine) after soil surface application to gleyic cambisol determined in polyurethane foam (PUF) plugs. Net applied radioactivity (AR) = 100%.

Similar to the behavior of fenpropimorph, the highest volatilization fluxes of chlorpyrifos were measured directly after application under moist conditions (**Fig. 4.9**), during the following days the fluxes declined. A slight increase of fluxes was observed when irrigation was given (Day 8). Summing up the amounts of chlorpyrifos collected in the polyurethane foam traps led to a cumulative volatilization of 44.4% after 13 days. In the present study, only the parent molecule, chlorpyrifos, was analyzed. The oxon form of chlorpyrifos is known to be formed rapidly and may have contributed significantly to total residue levels, if it had been included in the analysis (Seiber et al., 1993; Rawn & Muir, 1999).

The environmental fate and effects of chlorpyrifos have been extensively investigated (Racke, 1993). Volatilization of chlorpyrifos, when applied to a no-till agricultural setting for 4 days, was estimated at 23% (Whang et al., 1993). Despite its organic matter partitioning coefficient of $3469 \text{ dm}^3 \text{ kg}^{-1}$ which would seem to favor adsorption to soil, the high volatilization may be attributed to its air water partition coefficient (Henry's law constant = $1.6 \cdot 10^{-4}$; McConnell et al., 1997). Majewski et al. (1989) measured the volatilization of chlorpyrifos from fallow soil under field conditions and observed the highest fluxes in the early morning hours when heavy dew was present on the field surface. These results suggest that Henry's law constant is the driving factor in volatilization of chlorpyrifos from moist soils.

Within the course of the experiment 26.0% of the applied parathion-methyl volatilized whereas no metabolites were detected in the air samples (Table 4.5). The highest volatilization rates of parathion-methyl were measured directly after application (Fig. 4.10A). During the following days volatilization rates decreased and finally reached extremely low constant daily rates. These results correspond to the volatilization kinetics observed in an interlaboratory comparison of volatilization assessment methods (Walter, 1998) and were also measured in the photovolatility chamber experiments under moist conditions (cf. 4.1.1.5.3). However, the environmental conditions fail to explain the observed volatilization kinetics, e.g. a clear correlation between volatilization rates and soil moisture was not measured (Fig. 4.10A). Although volatilization rates followed the pattern of soil moisture from Day 2 up to Day 7 volatilization did not increase with remoistening of soil after irrigation was given. Within a previous study it was shown that terbuthylazine was influenced by increasing soil moisture in nearly the same way (Stork et al., 1998). As an explanation it was discussed that both pesticides have Henry's law constants $< 10^{-5}$ (Table 3.8) and are thus category III chemicals (non-volatile) according to the classification by Jury et al. (1983).

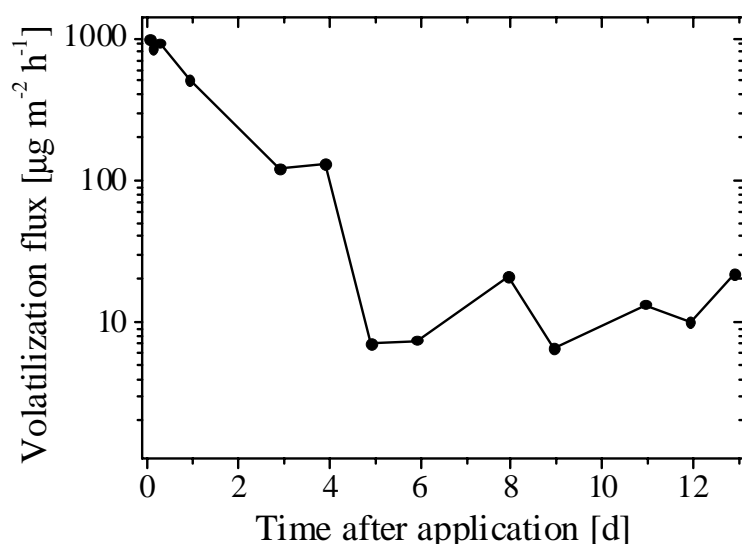


Figure 4.9 Volatilization fluxes after soil surface application of chlorpyrifos to gleyic cambisol (semi-logarithmic plot).

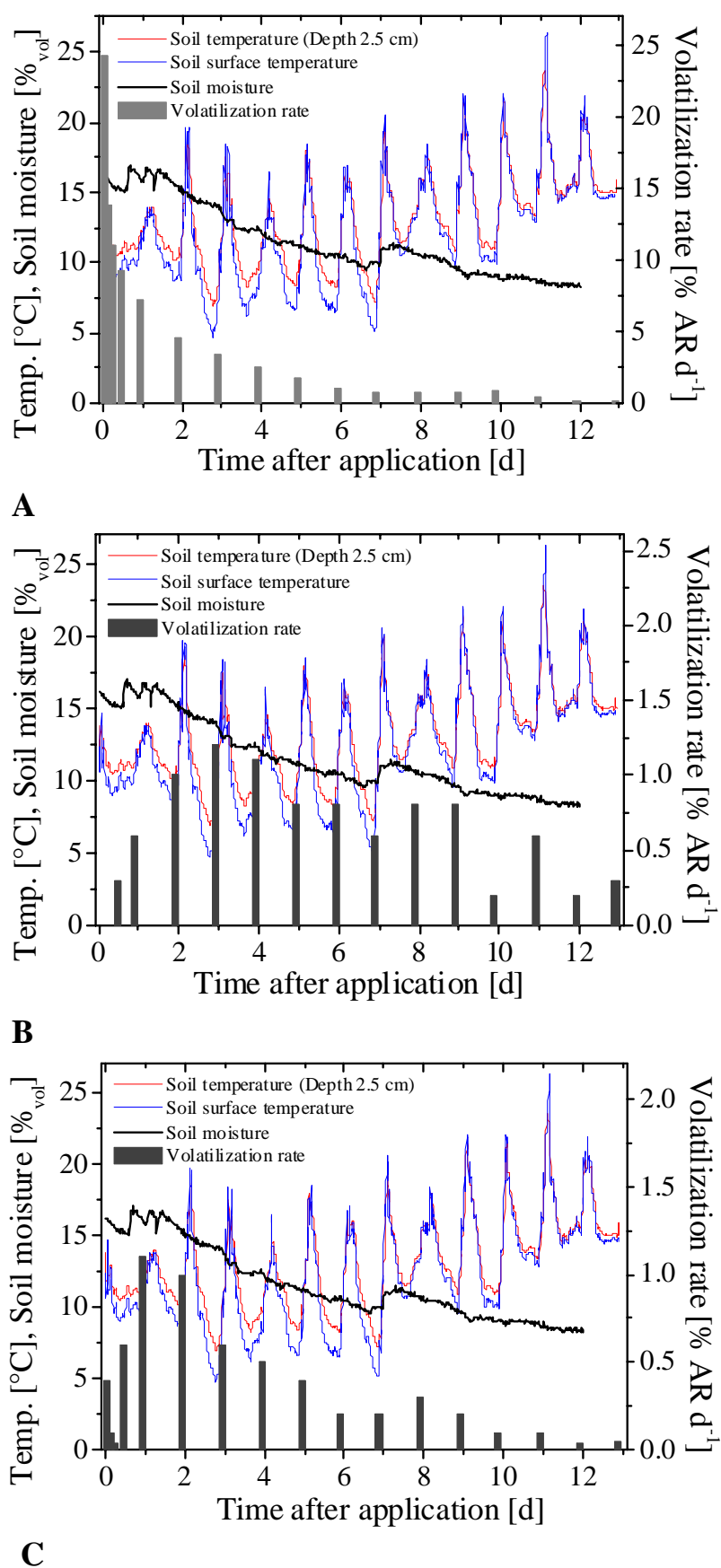


Figure 4.10 Wind-tunnel study: measured volatilization rates of ^{14}C -labeled compounds after soil surface application to gleyic cambisol. Irrigation (8 mm) was given on Day 8 after application. Net applied radioactivity (AR) = 100%. **A:** Parathion-methyl. **B:** Terbutylazine. **C:** Fenpropimorph.

Volatilization kinetics of terbuthylazine exhibited an initial increase of volatilization rates during the first 3 days followed by a slight decrease and an increase shortly after irrigation was given (**Fig. 4.10B**). At the end of the study, in total, 8.8% of the applied terbuthylazine had volatilized (**Table 4.5**). Volatilization rates of terbuthylazine cover a broad range of measurement and are strongly dependent on evaporation of soil water. Water movement downwards caused by high irrigation resulted in a rapid displacement of the pesticide from the evaporating surface to deeper layers (Schroll et al., 1999; Lembrich et al., 1999; Langenbach et al., 2001). In accordance with previous studies using test microcosms (Gerstl et al., 1997), cumulative volatilization of terbuthylazine and its main metabolite desethyl-terbuthylazine shown in **Fig. 4.8** revealed that over 90% of the volatilized material was parent compound.

The reasons for the differing behavior of parathion-methyl and terbuthylazine remain speculative and reveal a general problem concerning volatilization studies. Data on pesticide volatilization are extremely heterogeneous and sometimes even contradictory, e.g. discrepancies in results even from partially standardized laboratory volatilization experiments were reported (Walter, 1998). The comparison of experiments on volatilization is generally associated with uncertainty due to the strong influence of micro-climatic conditions and soil conditions.

4.1.2.5 Comparison between Studies at Different Scales: Parathion-methyl

The cumulative volatilization of parathion-methyl after application to gleyic cambisol measured in the wind tunnel (26.0% AR within 13 days; **Table 4.5**) and in the photovolatility chamber (ranging from 12.8 to 32.9% AR under comparable soil moisture conditions; **Table 4.2**) reveals that the different methods used yielded results of the same order of magnitude, indicating that both methods can be used successfully at their own specific scale. Due to the complete radioactivity balances, it can be assumed that both test systems measured correct volatilization rates within the respective system.

The comparison of the wind-tunnel results with the laboratory studies, which were performed under defined constant conditions, is limited by the variability of the environmental conditions during the wind-tunnel study (**Fig. 4.7**). The recommended method to scale up is not the averaging of fluxes measured at different sites, but to establish the relation between the volatilization fluxes and the processes controlling them, and the environmental conditions. This knowledge can then be combined with information on the spatial and temporal variations in the controlling factors, allowing to estimate the flux at a larger scale (Asman et al., 1999; Matson et al., 1989). The use of the photovolatility chamber had focused on the question which soil parameters and physicochemical pesticide properties regulate volatilization fluxes. The experimental design therefore captured the range of physical and chemical variability which may enable incorporation in subsequent models. In general, a main goal of such small-scale studies is to use a set of readily obtained environmental variables to simulate long-term volatilization fluxes from soil to provide the basis for extrapolation to field scale emission estimates, and to validate these findings against direct measurements (Fowler, 1999).

It was shown that the photovolatility chamber (cf. 4.1.1) and the wind tunnel (Stork, 1995) reflect field-like conditions as closely as possible. However, the aerodynamic conditions inside the chamber and the wind tunnel are still different from field conditions, e.g. there is

no turbulence inside the chamber (or a different turbulence, if fans are used). This is usually not critical for soils where the flux is controlled by soil processes and diffusion in the soil and not by air turbulence. The conditions are more critical when there is a canopy (grass, agricultural crops) for which the exchange is a function of turbulence (Asman et al., 1999).

4.1.3 Model Approaches: Volatilization from Soil

Within this thesis, main focus was laid on the evaluation and improvement of the volatilization modules included in the European registration models PEARL and PELMO. An overview of the variety of model approaches for the prediction of volatilization from soil is given in 2.1.2.

To allow for identification of limitations and shortcomings, simple empirical approaches and screening tools were used for rough estimation of volatilization in the beginning of the project (**Fig. 2.2**), especially due to the fact that PEC models have been developed starting from BAM (Behavior Assessment Model; cf. 2.1.2.2) as the basis model. The main findings of these preliminary model approaches are summarized below.

4.1.3.1 Empirical Approaches and Screening Model for Volatilization from Soil

The volatilization rates of ^{14}C -fluoranthene and ^{14}C -diflufenican as determined in previous wind-tunnel studies (Ophoff et al., 1996; Stork, 1995), were compared with the output of BAM (Jury et al., 1983) and estimation models by Smit et al. (1997) and Woodrow & Seiber (1997).

The estimation method by Smit et al. (1997) was used to calculate the cumulative volatilization during a period of 21 days, applying concentrations in the gas phase as input variables (cf. 2.1.2.1.1). In this approach environmental conditions and properties of the applied compound are assumed to remain constant during the experimental period. A similar correlation (cf. 2.1.2.1.2; eq. 2 & 3) was derived by Woodrow & Seiber (1997). The findings of both screening-level estimations were rather similar, reflecting the related assumptions and equations. Simulations of fluoranthene volatilization were in reasonably good accordance with the experimental results, but volatilization rates for diflufenican were overestimated.

Essentially, application of BAM revealed differences between measured and calculated values during the initial phase after application, suggesting that this model is not able to reflect non-equilibrium conditions at the initial stage of the experiment. Moreover, the applied input parameters entail other problems. It was not considered in the calculations that the physicochemical properties of pesticides may change during the experiment, e.g. due to different soil conditions. Average values for infiltration rate and soil moisture used for calculating the cumulative volatilization hardly reflected experimental conditions characterized by irrigation during the experiment.

A main limitation of these approaches is that environmental conditions just as properties of compounds are assumed to remain constant during experiments. A detailed description of the calculations, including parameterization and scenarios, can be taken from Wolters et al. (2002).

4.1.3.2 PELMO: Evaluation and Improvement of the Volatilization Description

For evaluation of the volatilization description included in PELMO, volatilization fluxes determined in a wind-tunnel study after simultaneous application of parathion-methyl, fenpropimorph, terbuthylazine, and chlorpyrifos to gleyic cambisol (cf. 4.1.2) were compared to predictions of the previous and improved versions of PELMO (**Fig. 4.11**).

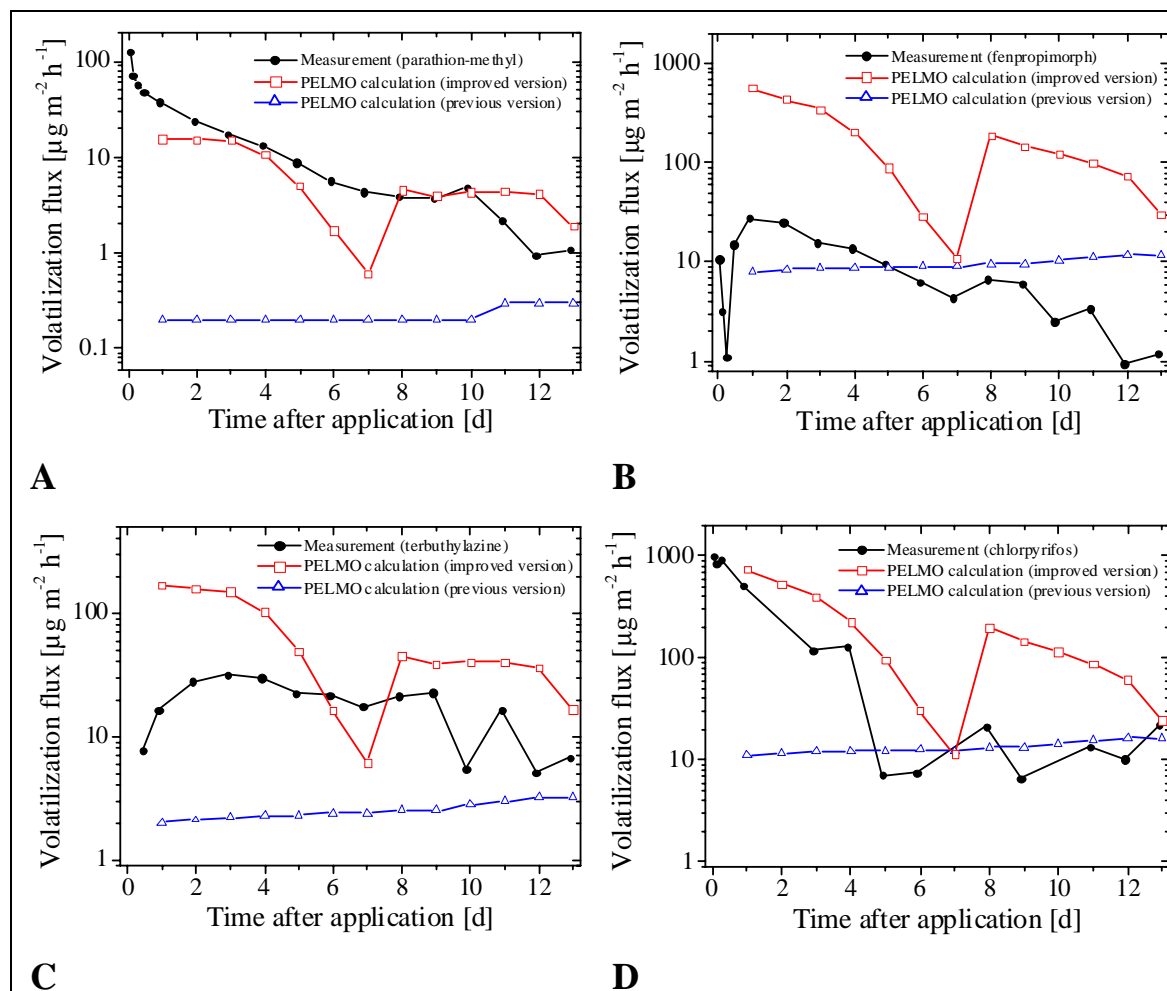


Figure 4.11 Measured (wind-tunnel study) and predicted (PELMO) volatilization fluxes after soil surface application to gleyic cambisol (semi-logarithmic plots). Differences between previous and improved PELMO versions used for calculations are summarized in 2.1.2.3.2. Details on the experimental findings can be taken from 4.1.2. **A:** Parathion-methyl. **B:** Fenpropimorph. **C:** Terbuthylazine. **D:** Chlorpyrifos.

The “previous version” is based on the official FOCUS PELMO 1.1.1 version used for registration proposes in Germany. An exponential approach was already included for calculating the temperature-dependence of Henry’s law constants (cf. 2.1.2.3.2).

Immediately after application, the previous version of PELMO underestimated volatilization rates of the applied compounds markedly (**Fig. 4.11**), e.g. measured fluxes of chlorpyrifos exceeded the PELMO predictions by approximately 2 orders of magnitude. During the following days a subsequent rapid decline in volatilization rates was not reflected by PELMO estimating an almost linear increase of volatilization over the course of the study. This discrepancy to experimental findings was due to the quite simple volatilization module included in the previous PELMO version according to 2.1.2.3.2 (eq. 12).

Due to the reasonably-well agreement between calculations and experimental volatilization rates of chlorpyrifos after Day 5 (**Fig. 4.11D**), one might conclude that the previous PELMO version generally allows for proper predictions in advanced stages of the studies. Taking into consideration the large differences between the sharp decline of measured volatilization rates and the almost linear increase of predicted values of fenpropimorph and terbuthylazine from Day 5 until the end of the experiment, this conclusion appears not appropriate. The agreement between predictions and actual volatilization rates of chlorpyrifos after Day 5 is obviously accidental and may not be attributed to PELMO's apparent ability to predict volatilization rates correctly.

A similar disagreement between calculations and measurements was determined in simulations using the Behavior Assessment Model (Jury et al., 1983), which did not reflect correctly the volatilization rates immediately after application (cf. 4.1.3.1). Obviously, the description of pesticide volatilization is subject to considerable uncertainty, particularly for surface-applied pesticides whose initial volatilization rates are hardly limited by the soil boundary layer. Considering the main route for pesticide volatilization from the soil surface, relevant processes occurring immediately after spray application, e.g. phase distribution of the pesticide and drying-out of the top soil, have to be taken into account. A thin water layer moistens only a fraction of the top millimeters of the soil surface and evaporates rapidly, resulting in an elevated pesticide concentration at the soil surface (Boesten, 2000). In contrast, PELMO assumed the applied pesticides being homogeneously incorporated in a top soil compartment size of 5 cm, an assumption which required revision.

To study the impact of intermediate soil moisture variation, irrigation was given on Day 8 resulting in increased volatilization rates on the subsequent day, especially for chlorpyrifos (**Fig. 4.11D**). This observation is in accordance with studies on soil moisture dependence of volatilization (Spencer et al., 1973). The previous PELMO version did not allow for correct estimation of soil moisture dependence on volatilization, illustrating a general limitation of currently available volatilization approaches: the previous PELMO version implicitly assumes partition coefficients being independent of water content and consequently calculates lower pesticide vapor pressures at the surface after irrigation (Baker et al., 1996).

As a result of the comparison between predictions of the previous PELMO version and experimental findings, the "improved version" of PELMO uses a more realistic compartment size of the top soil layer (1 mm instead of 5 cm; cf. 2.1.2.3.2) and reflects the moisture dependence of soil adsorption coefficients. For water contents ranging from above air dry conditions to below wilting point (gleyic cambisol: 4.5%_{vol}), the soil sorption coefficients of the pesticides are increased by the correction factors shown in **Fig. 4.12B**.

Volatilization rates predicted by the improved PELMO model are markedly higher than those calculated by the previous version; for fenpropimorph and terbuthylazine the computed values even exceeded the measured values at the initial stage of the study by a factor of 20. Chlorpyrifos revealed the best agreement between measured and calculated values on the first day (**Fig. 4.11**). Calculated fluxes of all compounds decreased by Day 8 and increased enormously when irrigation was given, indicating that PELMO obviously mirrors the tendency of pesticides towards enhanced volatilization under moist conditions. However, the increase of volatilization predicted by PELMO was much higher than experimentally determined and during the following days predictions exceeded measurements by up to an order of magnitude.

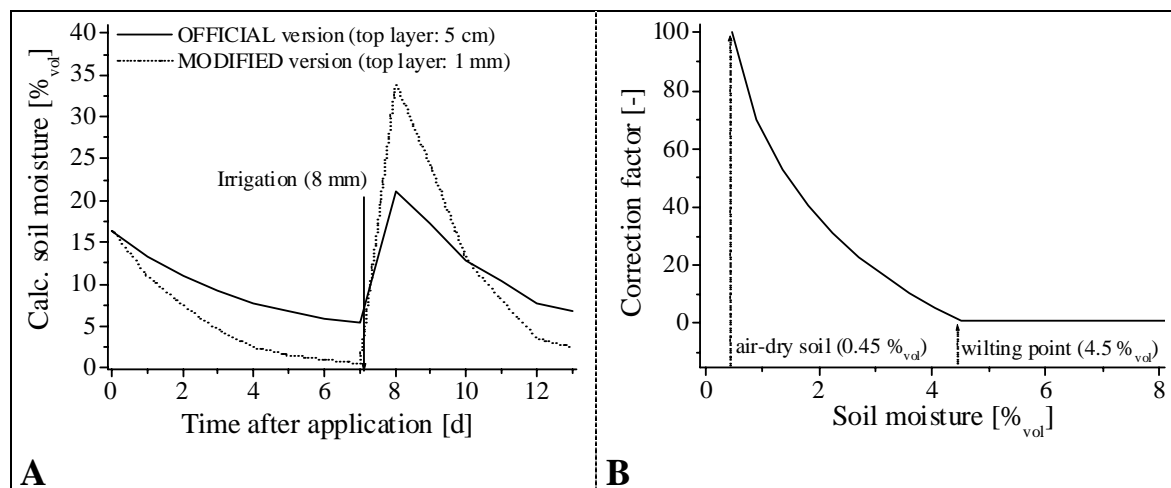


Figure 4.12 Modifications included in the improved PELMO version. **A:** Calculated soil moisture profiles over the course of the wind-tunnel study on gleyic cambisol (cf. 4.1.2) using the official PELMO version (FOCUS PELMO 1.1.1, top compartment thickness: 5 cm) and the modified version (top compartment thickness: 1 mm). **B:** Correction factor for soil adsorption coefficients. For moistures in the top millimeter of the soil ranging from above air dry conditions to below wilting point, the sorption coefficients were increased by the given correction factors.

The strong increase of volatilization fluxes in comparison to the calculations of the previous PELMO version is attributed to the reduction of the top compartment size from 5 cm to 1 mm leading to the calculation of higher pesticide concentrations at the soil surface and subsequently causing higher volatilization predictions, as can be taken from eq. 12 (cf. 2.1.2.3.2). As an additional effect, the lower top compartment size results in changing soil moisture of the top millimeter over the course of the study (**Fig. 4.12A**). Drying out and remoistening of the top soil layer were calculated to occur much faster after reducing the compartment size, e.g. leading to a large rise in calculated soil moisture from 0.5 to 34%_{vol} within 24 hours after irrigation was given. In combination with the correction factor included for describing the increase of soil moisture at low water contents (**Fig. 4.12B**), this effect enhances the impact on predicted volatilization rates, consequently resulting in an overestimation of volatilization increase caused by irrigation. To prevent overestimation of the soil moisture effect, the correction factor for soil sorption may be reduced.

For a reliable estimation of the correction factor contributing to the development of new model concepts, further progress might be achieved considering experimentally determined soil-water partitioning coefficients under low-water-content conditions. Instead of using an exponential approach resulting in a uniform correction factor for all applied compounds to estimate the effect of decreasing water content (**Fig. 4.12B**), experimental values would allow for a more detailed reflection of different sorption tendencies of pesticides. For this purpose, a completely new experimental set-up to determine soil-air-water-partitioning and its dependence on temperature and soil moisture was constructed (cf. 4.3.1).

The ability of the improved PELMO version to reflect correctly the tendency of the soil moisture effect on pesticides is a huge advantage in comparison to the previous model. As a future improvement, calibration of the model predictions by using experimental results is required for adjusting predictions to experimental findings as closely as possible.

In addition to the requirement of an improved physical-based description, the reliability of model predictions generally depends on the quality of the underlying data. Due to the volatilization rates being calculated on the basis of Henry's law (eq. 12), the soil-water partitioning coefficient (Henry's law constant K_H) is the most important pesticide property affecting PELMO's predictions. The significant effect of K_H including the variation of default values within the range of literature values on calculated volatilization rates of parathion-methyl (K_H between $5.2 \cdot 10^{-7}$ and $3.4 \cdot 10^{-6}$) and chlorpyrifos (K_H between $1.6 \cdot 10^{-4}$ and $2.7 \cdot 10^{-4}$) is shown in **Fig. 4.13**. For both compounds, a marked increase in volatilization was calculated and a disproportionate effect of irrigation on volatilization rates was predicted after K_H was enhanced. With regard to chlorpyrifos, an apparently slight increase of K_H from $1.6 \cdot 10^{-4}$ to $2.7 \cdot 10^{-4}$ resulted in an enormous increase of predicted volatilization, especially under moist conditions at the early stage of the simulation and after irrigation was given (Day 8). Taking into consideration that surface-applied compounds generally show the highest volatilization rates during the first hours after application (cf. 4.1.2), this increase obviously affects significantly the predicted cumulative volatilization, which is usually the basis value for risk assessment. Thus, uncertainty in experimental determination of K_H is a crucial factor influencing predicted volatilization rates, indicating that reliable experimental procedures for measurement of key factors, e.g. K_H , are as important as accurate model approaches for certain calculations.

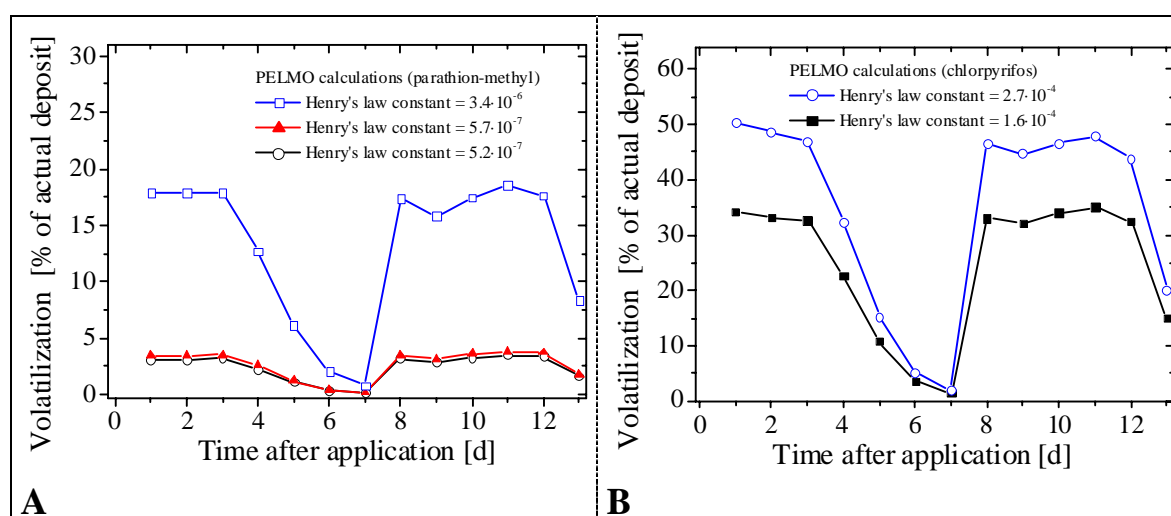


Figure 4.13 Calculations using the improved PELMO version (cf. 2.1.2.3.2), including variation of Henry's law constants (dimensionless values, calculated at 25 °C). **A:** Parathion-methyl. **B:** Chlorpyrifos.

4.1.3.3 PEARL: Evaluation of the Volatilization Description and Outlook

The ability of the PEARL model (FOCUS PEARL 1.1.1) to predict volatilization rates of pesticides applied under defined environmental conditions was investigated by comparing experimental findings determined in a wind-tunnel study after soil surface application (cf 4.1.3.2) to model calculations.

In accordance with the evaluation of the volatilization module implemented in PELMO (cf 4.1.3.2), the soil compartment thickness of the top layer was also found to be the most important parameter governing the extent of predicted volatilization losses after surface application calculated by the PEARL model. The sensitivity of volatilization to the

thickness of the top compartment is exemplified by a strong increase of volatilization fluxes of chlorpyrifos and fenpropimorph after reducing the top compartment thickness from 1 cm to 1 mm, e.g. the calculated volatilization fluxes of fenpropimorph ranged from 2.5 to 5.0 $\mu\text{g m}^{-2} \text{h}^{-1}$ for a compartment thickness of 1 cm and from 40.9 to 96.0 $\mu\text{g m}^{-2} \text{h}^{-1}$ for a compartment thickness of 1 mm (**Fig. 4.14B**). Corresponding values of chlorpyrifos revealed the same tendency towards enhanced volatilization with decreasing compartment thickness, illustrated by fluxes ranging from 4.0 to 8.2 $\mu\text{g m}^{-2} \text{h}^{-1}$ and from 51.5 to 148.4 $\mu\text{g m}^{-2} \text{h}^{-1}$ for compartment thickness of 1 mm and 1 cm, respectively (**Fig. 4.14A**).

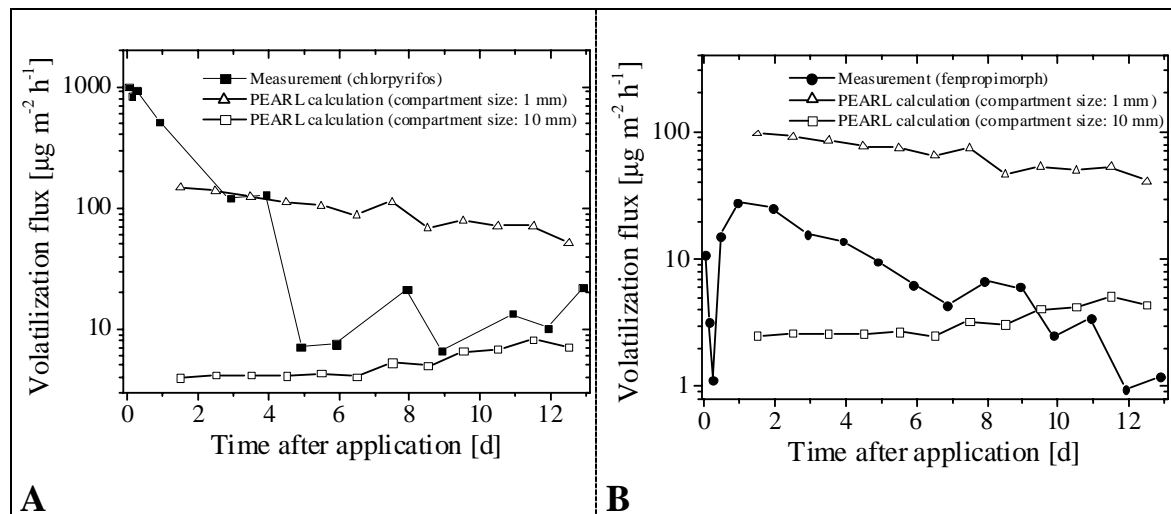


Figure 4.14 Measured (wind-tunnel study) and predicted (PEARL) volatilization fluxes after soil surface application to gleyic cambisol (semi-logarithmic plot). Details on experimental findings can be taken from 4.1.2. **A:** Chlorpyrifos **B:** Fenpropimorph. For each compound, calculations were performed using top compartment sizes of 1 mm and 10 mm, respectively.

Equation 10 (cf. 2.1.2.3.1) illustrates that decreasing top compartments lead to smaller soil resistances, i.e. thickness of the top compartment of 1 cm results in a soil resistance $r_s = 0.071 \text{ d m}^{-1}$ and decreasing thickness leads to a linear rise in volatilization fluxes. The thickness of the boundary air layer used in the parameterization is rather high (1 cm), thus resulting in transport resistance $r_a = 0.023 \text{ d m}^{-1}$ according to equation 9. Decreasing the boundary air layer by a factor of 10 does not increase volatilization fluxes to the same degree, because the increasing soil resistance dominates the rise in transport resistance. Because the size of the time step is controlled within the PEARL software (Leistra et al., 2001), the user is left with the responsibility for choosing an appropriate compartment thickness to obtain a realistic scenario. Depending on soil and pesticide properties, restrictions of compartment thickness and time steps arising from a numerical solution procedure may cause miscalculations and keep PEARL from finishing the simulation correctly (Leistra et al., 2001). Therefore, the set of conditions used for calculation of the behavior of parathion-methyl and terbuthylazine goes wrong for a system with 1 mm compartments and requires default values for compartment thickness of at least 5 mm. Applicability of the model is severely limited by this restriction, especially with regard to spray applications where the assumption of top compartments exceeding a few millimeters appears quite unrealistic. A new version of PEARL will include an improved procedure to

calculate the time steps and will probably be able to handle 1 mm compartments in the parathion-methyl and terbuthylazine runs (Van den Berg, personal communication, 2003).

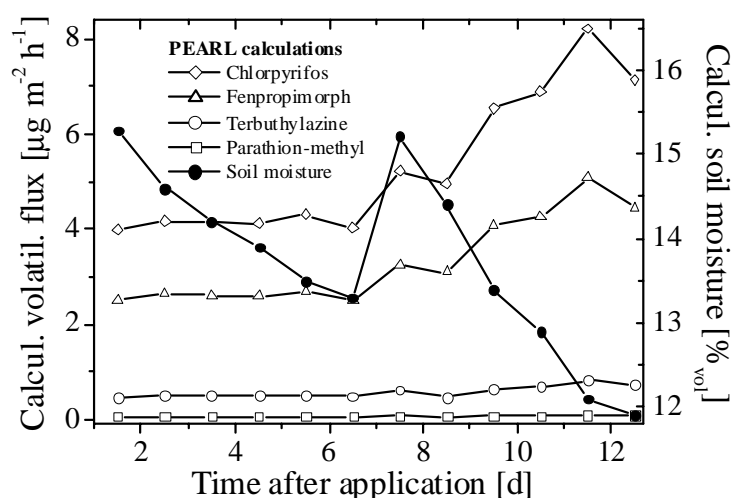


Figure 4.15 Pure model approach: Volatilization fluxes and soil moisture calculated by PEARL (compartment thickness: 1 cm). Environmental conditions can be taken from 4.1.2.1.

Due to the noticeable increase in calculated volatilization fluxes after irrigation, PEARL gives the impression to have the ability to reflect correctly the influence of soil moisture on volatilization. However, a direct correlation of calculated volatilization fluxes with calculated water content in the top layer (**Fig. 4.15**) revealed a suppression of volatilization due to irrigation on Day 8. During the following days PEARL calculates increasing fluxes for all pesticides observed, even though the soil dries out. The reason for this calculated increase in volatilization after Day 8 is a strong rise in average soil surface temperature (**Fig. 4.10B**) resulting in higher concentrations of pesticides in the gas phase of the soil and therefore in higher volatilization fluxes. Neither PEARL nor the previous PELMO version (cf. 4.1.3.2) allow for correct estimation of soil moisture dependence on volatilization, illustrating a general limitation of the used volatilization approaches: Similar to the previous PELMO version, PEARL assumes partition coefficients being independent of soil moisture, resulting in a wrong estimation of increasing volatilization with decreasing water content. A future PEARL version will take into consideration the moisture-dependence of soil sorption. Moreover, the current concept of a air boundary layer of constant thickness will probably be supplemented with a more dynamic concept of aerodynamic resistances governing the transport through the air layers above the soil surface. The improvement of the concept will require the inclusion of additional input parameters in the calculations (e.g., roughness length and stability conditions of the atmosphere).

The development of an approach based on transport resistances necessitates a detailed understanding of the complex behavior of localized micrometeorological processes. This realization is very difficult to achieve, even when simple parameters such as temperature are measured. Due to analytical problems in obtaining adequate material for quantitative determinations of volatile fluxes of pesticides, sample collection times are typically > 30 min, which may be long enough for the microclimate over the field to undergo changes, e.g. intermittent cloud cover is supposed to cause very rapid fluctuations in temperature. Therefore, it may become very difficult to verify and refine any model predictions that do not account for short time intervals (Rice et al., 2002).

Due to slight differences between atmospheric conditions in the wind tunnel and field conditions, the application of an improved model to the volatilization rates obtained in the wind tunnel would require an additional parameterization. Boundary conditions coupling soil and atmospheric processes were found to provide an accurate and credible simulation of the instantaneous volatilization rates after soil fumigation of methyl bromide compared to a stagnant boundary-layer condition (Yates et al., 2002). Though, in the same study it was shown that for some information such as cumulative emissions, the simulations for each boundary condition provided similar results, indicating that simplified methods may be appropriate for obtaining certain information that is integrated over relatively long periods.

4.2 Volatilization from Plant Surfaces

Uncertainties and shortcomings in the understanding of volatilization from crops may be attributed to a lack of knowledge concerning the processes occurring on plant surfaces (cf. 2.3). A deeper comprehension of plant volatilization requires detailed studies under defined environmental scenarios reflecting the microclimatic situation under field-conditions as closely as possible. Within this thesis, a contribution to experimental and theoretical determination of volatilization after application to plants included the following work steps:

- Gathering of high-resolution data sets on volatilization under field-like conditions after pesticide application to winter wheat using a wind-tunnel (cf. 4.2.1)
- Performance of a field study under conditions comparable to those prevailing in the wind-tunnel study with the aim of up-scaling and evaluating the results of field-like studies (cf. 4.2.2)
- Use of the experimental findings for development and validation of a simplified model approach for the prediction of plant volatilization (cf. 4.2.3)

4.2.1 Wind-tunnel Study: Pesticide Application to Winter Wheat

The determination of volatilization behavior of three pesticides after application to winter wheat includes the measurement of volatile organic compounds and $^{14}\text{CO}_2$ arising from mineralization of ^{14}C -labeled parathion-methyl. Volatile losses of the non-labeled parent compounds fenprophimorph and quinoxifen were quantitated separately, just as measurements of soil and plant residues of the applied pesticides. Due to the simultaneous application of the pesticide cocktail under a defined environmental scenario, suitable data sets for validating the model approach under comparable conditions were achieved (cf. 4.2.3).

4.2.1.1 Wind-tunnel Study on Winter Wheat: Environmental Conditions

Continuous monitoring of soil moisture revealed a drying of the top layers (5-10 cm) during the first week of the wind-tunnel study (**Fig. 4.16A**).

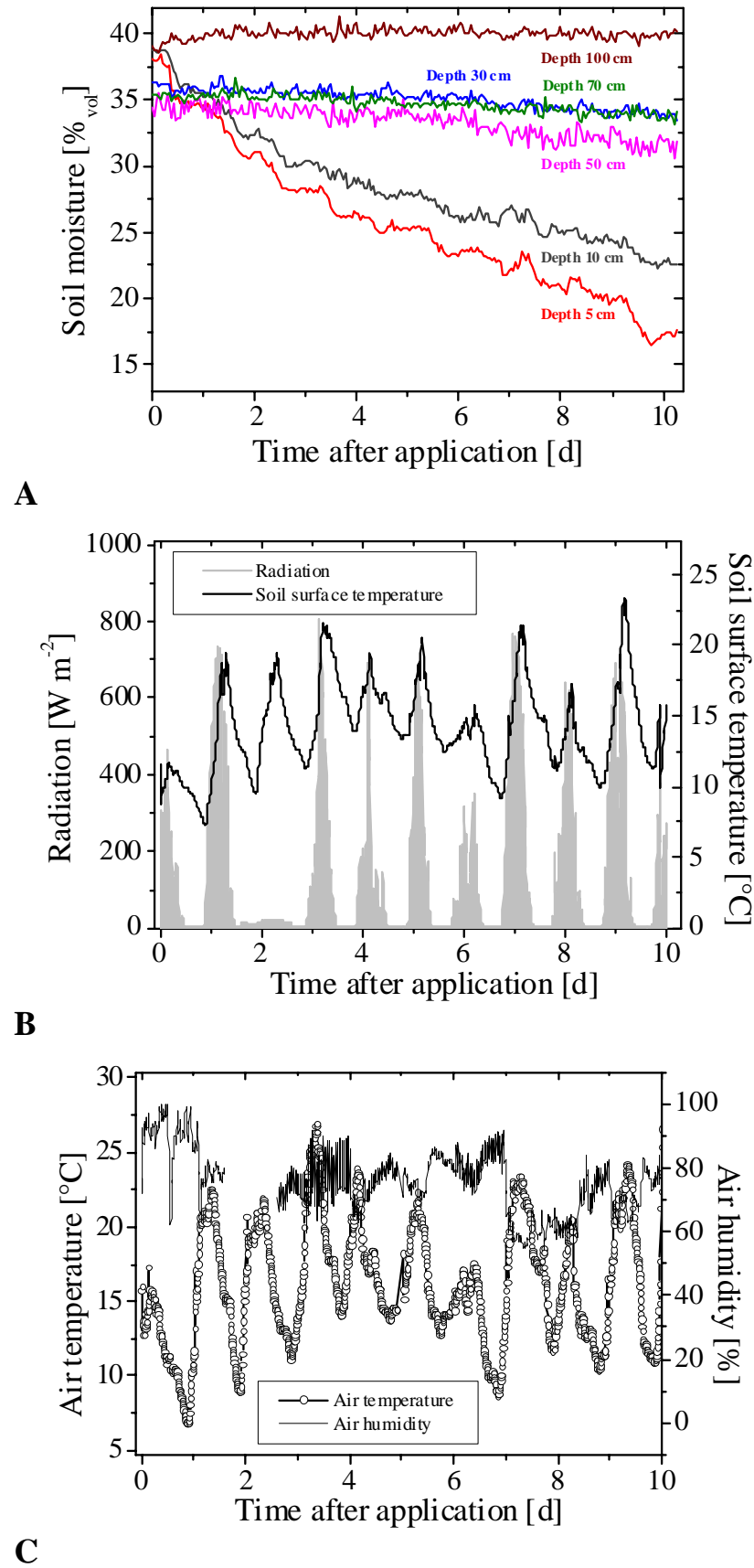


Figure 4.16 Climatic conditions over the course of the wind-tunnel experiment after simultaneous soil surface application to winter wheat. **A:** Volumetric water content measured by TDR equipment at several depth. **B:** Radiation and soil surface temperature. **C:** Air temperature and air humidity (malfunction of measuring device between Day 2 and Day 4).

A slight increase was observed after irrigation was given on Day 7 and Day 8 (cf. 3.1.2.5), followed by a subsequent decrease during the final day of the experiment. Deeper soil layers (depth ≥ 30 cm) were not influenced by irrigation and showed only marginally decreasing water content over the course of the study. Obviously, the increase in soil-drying in comparison with the measurements during the wind-tunnel study on bare soil (cf. 4.1.2.1) is due to the higher evapotranspiration caused by the crops on the lysimeter. Measurements of air temperature and soil surface temperature corresponded well during the experiment. Diurnal fluctuations and a nonuniform time course of the average temperature with a maximum at Day 9 (approx. 23 °C) were observed. A lack of values for radiation and air humidity between Day 2 and Day 4 was caused by malfunction of the measuring device (**Fig. 4.16B+C**).

4.2.1.2 Overview: Radioactivity and Mass Balances

Recovery of ^{14}C -labeled parathion-methyl was about 87.2% AR (**Table 4.6**), thus proximating the guideline values for registration purposes ranging from 90 to 110% of the applied amount.

Table 4.6 Wind-tunnel study on winter wheat: radioactivity balance of ^{14}C -labeled parathion-methyl. Net applied radioactivity (AR) = 100%.

Sample		Radioactivity [% AR]
Contamination †		ND ‡
Soil	Extractable	4.4 §
	Non-extractable	13.6 ¶
	Leachate	ND ‡
Control plot		0.1
Plants	Leaves	21.5
	Roots	0.5
Parent compounds		29.2
Volatilization		
Metabolites		3.3
Mineralization to $^{14}\text{CO}_2$		6.4
Glass fiber filter (particulate matter)		8.2
Σ ^{14}C		87.2

† contamination of the wind tunnel and the high-volume sampler

‡ ND = not detectable

§ soil layer (0-2.5 cm): 4.1% AR; soil layer (2.5-5.0 cm): 0.3% AR

¶ soil layer (0-2.5 cm): 13.0% AR; soil layer (2.5-5.0 cm): 0.6% AR

Both, radioactivity of the leachate and system contaminations were below detection limits. After finishing the experiment, the major part of the remaining radioactivity was detected on the plants, including extractable and non-extractable fraction of leaves and roots

(approx. 22% AR). In comparison with the wind-tunnel study on bare soil (approx. 76% AR characterized as soil residues) only slight amounts of soil residues were detected (18% AR). These findings may be attributed to the lysimeter being abundantly covered with vegetation during application. In agreement with the wind-tunnel study on bare soil, a displacement of radioactivity in deeper layers (> 5 cm) did not occur (cf. 4.1.2.3). A good deal of the radioactivity remaining in the soil was not extractable (13.6% AR), indicating increasing sorption of parathion-methyl on the soil during the experiment.

In previous studies, the glass fiber filter was shown to have a retention of > 99.9% for particles > 10 nm (detection limit) on a filter test apparatus (Stork et al., 1994). It may thus be assumed that all particulate residues in air are quantitatively retained (8.4% AR). However, it is to be considered that adsorption of gaseous residues on the glass fiber filters over the course of the experiment cannot be excluded since many pesticide vapors possess high adsorptive properties (Winberry et al., 1990). Therefore a clear distinction between gaseous and particulate residues adsorbed on the filters is not possible.

Due to the use of non-labeled compounds, no complete mass balances were obtained for fenpropimorph and quinoxifen, especially the amount of mineralization to $^{14}\text{CO}_2$ was not quantitated. A summary of non-labeled soil and plant residues is given below (cf. 4.2.1.4).

4.2.1.3 Mineralization of ^{14}C -labeled Parathion-methyl

Rates of the formation of $^{14}\text{CO}_2$, arising as the end product of mineralization of ^{14}C -labeled parathion-methyl, are summarized in **Fig. 4.17**. During the first two days of the study the mineralization rates increased to reach a maximum after 48 hours (approx. 1.6% AR d⁻¹). Decreasing rates in the further course of the experiment finally resulted in a cumulative mineralization of 6.4% AR within 10 days (**Table 4.6**).

A comparison with mineralization rates measured in the photovolatility chamber after soil-surface application of parathion-methyl to bare soil in the dark (**Fig. 4.17**) allows for an estimation of the different contributions of soil degradation and plant surface processes to cumulative mineralization.

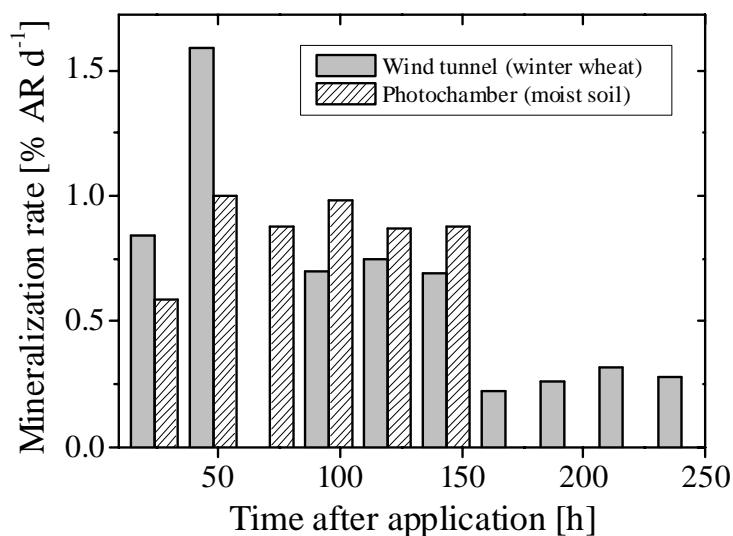


Figure 4.17 Mineralization rates of ^{14}C -parathion-methyl after application to winter wheat (wind-tunnel study) and after soil surface application to gleyic cambisol (cf. 4.1.1.5.1: 3rd soil moisture photochamber study).

During the first days, mineralization rates determined in the photovolatility chamber were lower than the rates measured in the wind-tunnel study, reaching a maximum after 2 days and, in contrast to the wind-tunnel study, remained on a high level by the end of the experiment. After 6 days, 5.2% AR were mineralized (**Table 4.2**). Taking into consideration that only a slight fraction of ^{14}C -labeled parathion-methyl was applied on the soil in the wind-tunnel study (**Table 3.3**), the high mineralization rates suggest that photo-mineralization on plant or soil surfaces was a main degradation pathway leading to complete mineralization, especially immediately after application. These findings were affirmed by studies revealing that $^{14}\text{CO}_2$ was accumulated after application of parathion-methyl on soybeans under sterile conditions (Abo El-Seoud & Frost, 1994). In addition, the chemically similar compound parathion is known to be completely degraded by crops to CO_2 with 4-nitrophenol arising as an intermediate. For parathion-methyl, similar degradation pathways may be assumed, especially with regard to the high amounts of 4-nitrophenol and unknown polar metabolites detected in the plant samples after finishing the wind-tunnel experiment (cf. 4.2.1.4).

Fenpropimorph and quinoxifen were not ^{14}C -labeled, thus, definitive statements about biodegradation and mineralization will not be made.

4.2.1.4 Soil and Plant Residues

Besides unchanged parathion-methyl, 17.4% of the radioactivity detected in methanol extracts of the PUF plugs was characterized as metabolites, suggesting that metabolic transformation on the plant surfaces might have contributed to the formation of volatile metabolites which were subsequently trapped on the PUF plugs (**Table 4.7**).

Table 4.7 Characterization of ^{14}C -labeled compounds in the methanol extracts of soil samples, PUF plugs, and glass fiber filters (data in % of extracted radioactivity).

Sample	Soil layer (0–2.5 cm)	PUF plugs †	Glass fiber filter
Parathion-methyl	28.5	82.6	17.0
4-nitrophenol	34.1	4.1	42.5
Paraoxon-methyl	ND ‡	4.1	6.8
RIB 12080 (BAYER AG) §	ND ‡	0.8	ND ‡
Unknown polar products	37.4	8.4	33.7

† PUF: polyurethane foam; values averaged within the experimental duration

‡ ND = not detectable

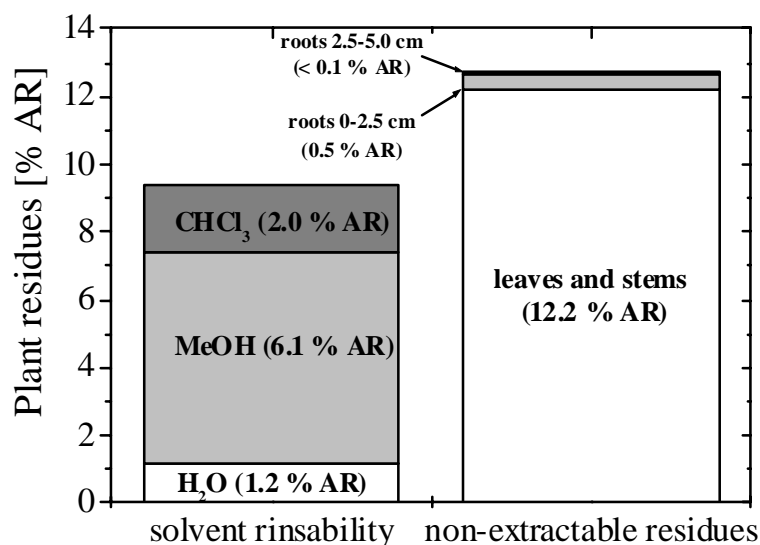
§ parathion-methyl-S-nitrophenylester

These findings are in full agreement with the above mentioned general tendency of parathion-methyl towards photomineralization on plant surfaces leading to increased formation of $^{14}\text{CO}_2$ (cf. 4.2.1.3). A high quantity of metabolites (83% of extracted radioactivity) was detected in the methanol extracts of the glass fiber filters used for the

retention of particulate residues in air. The magnitude of metabolization exceeds the corresponding amount of metabolites detected in the soil samples (71.5% of extracted radioactivity). Metabolization of parathion-methyl on the PUF plugs or glass fiber filters during sampling, as suggested by Stork et al. (1994), is considered as additional degradative pathway which might have caused the higher amounts of metabolites in air samples compared to soil samples.

Immediately after finishing the experiment, plants were harvested and successively rinsed with solvents of decreasing polarity (cf. 3.1.3.3). Analysis of the solvents allows for the quantification of pesticides adsorbed on the plant surface and those adsorbed in deeper cuticular layers. Besides the measurement of solvent rinsability, the use of ^{14}C -labeled parathion-methyl enables the determination of non-extractable residues by combustion. In total, 22% of the net applied radioactivity were characterized as plant residues. Only 9.3% AR were washable with water, methanol and chloroform (**Fig. 4.18**), whereas 12.7% AR remained as non-extractable residues. In previous studies it was shown that parathion-methyl and parathion tend to build bound residues after application to soil surfaces (cf. 4.1.2.3) or crops (Gerstl & Helling, 1984). The high amount of non-extractable residues indicates uptake and incorporation of the parent compound or its metabolites into the plant matrix. The distribution of the radioactivity in the different solvents reveals the greatest amounts of soluble radioactivity being present in methanol (6.1% AR) and the chloroform (2.0% AR) phases. Due to a decomposing effect on the cuticula, these non-polar solvents mainly extract residues penetrated into the plant material, suggesting a displacement of parathion-methyl into the leaves during the experiment.

Figure 4.18 Determination of ^{14}C -labeled plant residues after wind-tunnel study on winter wheat. For measurement of solvent rinsability, plants were successively submersed for 30 sec in water, methanol and chloroform. Non-rinsable residues were determined by combustion. Radioactivity measurements were performed by LSC (cf. 3.3.2).



In total, less than 10% of the radioactivity detected in the wash solutions was identified as unchanged parathion-methyl, the rest of the rinsable fraction was characterized as 4-nitrophenol and as unknown polar metabolites (data not shown). Thus, in comparison with the soil extracts (**Table 4.7**), a much higher magnitude of metabolization was detected in the plant samples. Corresponding results were obtained after application of parathion-methyl to bush beans (Ophoff, 1999), indicating that higher degradation rates in plants compared to soil samples are not dependent on the investigated plant species but represent a general tendency. As a reason for the lower degradation rates in soil, different

degradation kinetics in soil and plants are discussed. Plant cells allow for enzymatic degradative pathways, whereas degradation performance in the “unorganized” soil is governed by the rather accidental occurrence of metabolic processes (Führ, 1987). In addition, penetration and metabolization of pesticides depends on the morphology and surface texture of the cuticula, e.g. aging of the wax layer causes decreasing wettability of the leaf surface and is supposed to promote penetration into the leaves. A detailed discussion of the textural properties of leaves and their influence on the environmental fate of pesticides is beyond the scope of this thesis and can be taken from Schönherr & Baur (1994). However, due to the antagonizing effect on volatilization from leaf surfaces, a deeper process understanding of penetration and transformation is required for future development of model approaches for prediction of environmental concentrations after plant applications.

Distribution of both fenpropimorph and quinoxyfen in the different solvents after rinsing the plants showed the highest amounts of the pesticides in the methanol and chloroform samples, whereas only slight amounts of quinoxyfen and no fenpropimorph were identified in the aqueous solutions (**Table 4.8**). Due to its mode of action as systemic pesticides, fenpropimorph obviously penetrates into the leaves enabling a long-term protective effect. Quinoxyfen is known to be extensively photodegraded on the wheat leaf surface, giving multiple polar degradation products, whereas it is only slightly metabolized in wheat, with low residues found in crops (Tomlin, 2000). Therefore, the slight amount of quinoxyfen in the aqueous solution and the comparable high recovery of quinoxyfen in the methanol and chloroform phases may be attributed to the photodegradation mainly occurring at the plant surface.

Table 4.8 Soil and plant residues of quinoxyfen and fenpropimorph after finishing a wind-tunnel study on winter wheat (data in % of net applied amount).

Pesticide		Fenpropimorph	Quinoxyfen
Soil residues		2.0	5.4
Water		ND †	0.9
Plant residues	Methanol	0.7	4.9
	Chloroform	0.9	5.1

† ND = not detectable

Metabolites of fenpropimorph and quinoxyfen were not targeted in this study. Soil and plant residues revealed higher amounts of quinoxyfen in comparison with fenpropimorph, indicating a lower metabolization of quinoxyfen over the course of the experiment. These findings were in agreement with the minimal photolysis of quinoxyfen on soil surfaces ($DT_{50} > 1$ year, Southern England) ascertained in previous studies (Tomlin, 2000). Enhanced metabolization was observed in acidic soil, indicating that the soil used in the wind-tunnel study on winter wheat (orthic luvisol: pH 7.2) did not provide the most favorable terms for metabolization of quinoxyfen. Fenpropimorph was shown to form large amounts of non-extractable residues and metabolites, e.g. fenpropimorph acid (Stockmaier,

1996). So, the small amount of detectable residues is probably due to considerable metabolism of fenpropimorph. In support of this assumption a comparatively low cumulative volatilization of fenpropimorph indicates that high amounts of metabolites might be volatilized during the experiment (cf. 4.2.1.5).

4.2.1.5 Cumulative Volatilization and Kinetics

In total, 32.5% AR were volatilized by the end of the wind-tunnel study, corresponding to 29.2% parathion-methyl and 3.3% of metabolites (**Table 4.6**). About 25% AR already volatilized within the first 24 h, followed by a sharp decrease (**Fig. 4.19A**), indicating other processes like foliar uptake counteracting the volatilization process. The major part of volatilization took place immediately after application due to a weak adsorption/bonding of the pesticide on the leaf surface. Decreasing volatilization rates were observed following the first 24 h, illustrating the long-term release of protected or adsorbed pesticide residues. Increasing air temperatures and irrigation caused only temporary increases of volatilization rates. Due to a maximum air temperature on Day 4 (approx. 27.5 °C; **Fig. 4.16C**), the volatilization rate of parathion-methyl increased on Day 4, but decreased subsequently parallel to the decrease of air temperature. A sharp rise of volatilization was observed on Day 7 and Day 8 which may be attributed to the simultaneously given irrigation. Irrigation generally increases volatilization from soil and plant surfaces (cf. 2.1.1 & 2.2.1) and this effect was enhanced by an additional increase of temperature on Day 7.

In total, 6.0% of the applied fenpropimorph volatilized in the wind tunnel (**Fig. 4.19A**). Only about 9.6% of the applied amount of fenpropimorph, including soil and plant residues and the volatilized fraction, was recovered after 10 days. One possible explanation is a rapid decomposition of fenpropimorph under semi-field conditions due to the UV transparency of the side walls of the tunnel facilitating photochemical degradation. Indirect methods (disappearance, measurement of residues) showed 70% of the applied fenpropimorph or its metabolites had been lost undetected via the atmosphere, as determined in a lysimeter study on winter wheat (Ebing et al., 1995), while measurements of volatilization including the detection of metabolites revealed cumulative volatilization up to 60% of the applied radioactivity from summer barley (Staimer et al., 1996). Taking into consideration that metabolites were not analyzed within the presented wind-tunnel study on winter wheat, the results imply that a major portion of the applied fenpropimorph might have volatilized as metabolites. As an additional process counteracting volatilization, penetration into the leaves has to be considered. The results of soil and plant analysis (cf. 4.2.1.4) revealed that major parts of the applied amount of fenpropimorph had penetrated into the crops over the course of the study, indicating that both penetration and metabolism had contributed to the low volatilization of the parent compound.

Besides negligible deviations on Day 1, the volatilization kinetics of fenpropimorph followed rather the same course as parathion-methyl (**Fig. 4.19B**), yet the decrease of the volatilization rate showed a marked decrease on Day 9. This finding may be attributed to the disappearance of fenpropimorph from the plant surfaces, illustrated by a non-detectable fenpropimorph amount in the aqueous wash solution (**Table 4.8**).

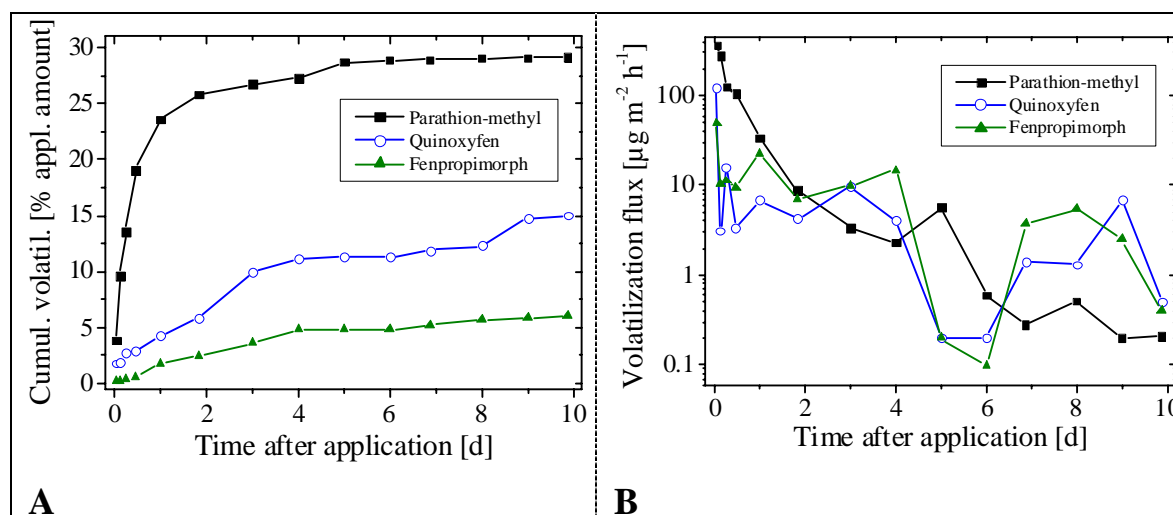


Figure 4.19 Volatilization of parathion-methyl, quinoxifen, and fenpropimorph after application to winter wheat. **A:** Cumulative volatilized amount. Net applied active ingredients = 100%. **B:** Volatilization fluxes. ^{14}C -labeled parathion-methyl was quantitated by LSC (cf. 3.3.2), non-labeled quinoxifen and fenpropimorph were determined by GC-MSD (cf. 3.3.3.2).

Cumulative volatilization of quinoxifen over the course of the experiment was about 15.0% of the net applied amount (**Fig. 4.19B**), apparently indicating a higher volatilization tendency of quinoxifen in comparison with fenpropimorph. However, due to the lower metabolism of quinoxifen, which is documented by a recovery rate of approx. 31.0%, the lower cumulative volatilization of the parent compound fenpropimorph may be attributed to its higher degradability, to the occurrence of non-detectable metabolites and to its systemic activity. The low application dose of quinoxifen (65.38 g ha^{-1} ; **Table 3.3**) in comparison with fenpropimorph (247.87 g ha^{-1}) accounts for the volatilization rates of quinoxifen falling below the corresponding values of fenpropimorph during the wind-tunnel study (**Fig. 4.19B**). However, a clear dependence of volatilization of quinoxifen on air temperature and irrigation, illustrated by increasing rates on Day 4 and Day 7, was established.

4.2.1.6 Comparison between Volatilization from Soil and Plants: Parathion-methyl

Volatilization of ^{14}C -parathion-methyl after soil surface application was slightly lower as compared to plant application, as documented by 32.5% AR (including 29.2% parent compound and 3.3% metabolites; **Table 4.6**) volatilizing within 10 days from its application to winter wheat, whereas 26% AR (no metabolites) volatilized within 13 days after application on bare soil. This effect has been described for many pesticides, since soil adsorption reduces effectively the volatilization potential of a pesticide (Spencer et al., 1979). In contrast to soil, plant surfaces are not subject to strong adsorption of pesticides. Instead, drying of the application solution on the plant surface causes high vapor pressure of the applied compound, almost reaching the corresponding value of the pure compound (Taylor & Spencer, 1990). However, the differences between the cumulative volatilization of parathion-methyl from soil and plants were not as great as detected in previous studies (Stork et al., 1998). These findings may be attributed to the different soils used in the wind-tunnel studies. Gleyic cambisol used for the study on fallow soil is known to allow for higher volatilization rates than orthic luvisol which was used for the experiment on

plant application. The use of orthic luvisol enabled a comparison with the results achieved in the field study (cf. 4.2.2). Due to different water conditions and lower organic carbon content of gleyic cambisol (**Table 3.9 & 3.10**), its ability to adsorb pesticides on the soil surface is reduced and volatilization increases. Thus, the stronger adsorption of the pesticide fraction applied to orthic luvisol during the study on winter wheat reduces the overall volatilization rate, including soil and plant volatilization.

Furthermore, the comparability of semi-field and field studies after plant and soil application is generally limited by uncertainty of the calculations of volatile losses arising from the fraction of soil-applied compound after plant application. Even though an estimation of the applied dose on the soil surface may be achieved via analysis of the soil residues, a clear distinction of the contributions of soil-applied and plant-applied compound to the overall volatilization over the course of the study is impossible. Under laboratory conditions losses to the soil may be prevented, e.g. by lining the soil surface with filter paper during the application and subsequent calculation of the net applied dose on the plant surface, but under field-like conditions a clear distinction of the different sources of volatile losses cannot be drawn.

4.2.2 Field Study: Pesticide Application to Winter Wheat

Within a field study of 7 days, parathion-methyl, fenpropimorph, and quinoxifen were applied as non-labeled compounds to winter wheat (cf. 3.1.3.1). For the quantification of the applied compounds, soil and plant samples were taken at four different times over the course of the study (cf. 3.1.3.3). Air sampling at different heights allowed for the determination of pesticide concentrations in the air and was used for the calculation of volatile losses by means of micrometeorological methods (cf. 3.1.3.5).

Analysis exhibited an inhomogeneous distribution pattern and plant and soil deposits of parathion-methyl covering a broad range of values, which may be due to the nozzles of the field sprayer being obstructed by undissolved parathion-methyl at the beginning of application. Furthermore, analysis of air samples indicated degradation of parathion-methyl on the adsorbents (XAD-4). Due to the results on parathion-methyl being afflicted with a high degree of uncertainty, these findings are not discussed within this thesis.

4.2.2.1 Meteorological Data

Measurements of the climatic conditions over the course of the study are summarized in **Fig. 4.20**. Average values of the essential parameters for calculation of the volatilization rates during air sampling with the micrometeorological methods are presented in Annex 1. The course of the net radiation roughly corresponds to that for the soil temperature (**Fig. 4.20A**). Immediately after application, the net radiation was relatively low with values around 300 W m^{-2} , which resulted in low soil temperatures ($\approx 14^\circ\text{C}$) and air temperatures ($\approx 16^\circ\text{C}$). The great differences between soil and air temperature in comparison with the low differences observed during the study on bare soil (**Fig. 4.7**) may be attributed to the plant coverage acting as shadow shield. On Day 2 and 3 the net radiation reached a maximum with values up to 590 W m^{-2} , followed by a decrease between Day 4 and 6 ($< 500 \text{ W m}^{-2}$) and a strong increase at the end of the study (600 W m^{-2}). The air temperature followed the same pattern and reached a maximum value

of 25 °C on Day 3 and decreased during the following days. As expected, the time course of both net radiation and temperature showed diurnal rhythm.

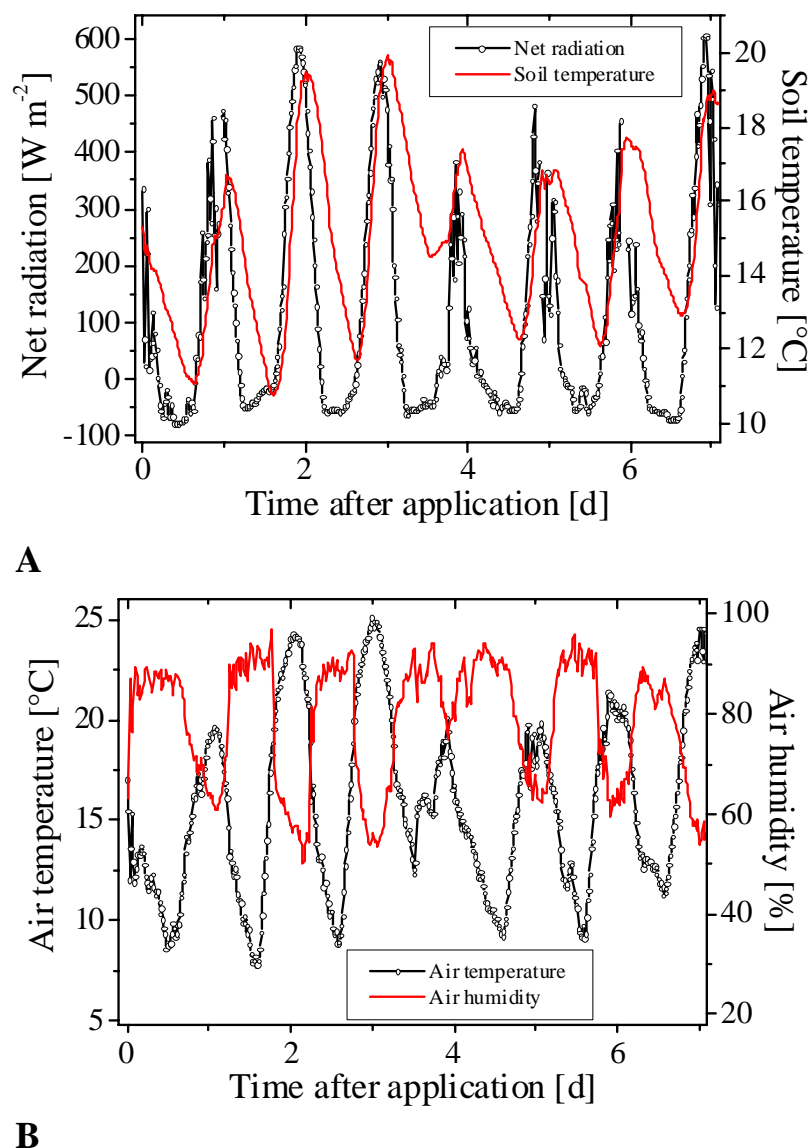


Figure 4.20 Climatic conditions over the course of the field study on winter wheat. **A:** Net radiation measured at 1.5 m above the soil surface and measurement of soil temperature averaged from the values for the thermocouples at 0.02 and 0.06 m depth. **B:** Average air temperature and air humidity measured at 1.0 m above the soil surface. Data are presented as mean values averaged over intervals of 20 minutes.

Data on the rainfall during the experimental period are presented in **Table 4.9**. A few minutes after the end of the application (5/14/02 4:00 PM) it rained for 10 minutes, followed by an additional flurry of rain occurring an hour later. In agricultural practice pesticides are generally applied under dry conditions to prevent wash-off from the leaf surface. As a rule of thumb, a rainless period of at least 3-6 hours after application is assumed to be sufficient for drying of the pesticide mixture on the leaves. Thus, rainfall immediately after application as observed in this study is expected to have a significant effect on the results. Rainfall may cause wash-off and subsequently reduce the pesticide concentration on the crops and lead to an increase of the soil concentrations. As an

additional effect, the distribution of the remaining plant residues may be disturbed, resulting in displacement of the pesticides to parts of the crops which are not well-exposed and therefore do not allow for volatilization, e.g. the axils.

Table 4.9 Rainfall at the experimental plot near Merzenhausen during the field study (5/14/02 – 5/21/02).

Date	Time	Time after application [d] †	Rainfall [mm]
5/14/02	4:07 – 4:17 PM	0.019	1.0
	5:28 – 5:36 PM	0.075	0.5
5/18/02	7:55 – 9.33 AM	3.677	1.3
	3:14 – 6:49 PM	3.982	3.4

† application time: 5/14/02 3:40 PM; start of rain period taken as reference

The time course of the wind speed, which was recorded at four heights (cf. 3.1.3.2), is illustrated by the average values measured at 0.7 and 1.5 m above the soil surface (**Fig. 4.21**). During the first hour after application, the above mentioned rainfall was accompanied by windy conditions, exemplified by the maximum wind speed measured over the course of the study (6.5 m s^{-1} at 1.5 m). With the exception of an increase after 1.5 days (3.8 m s^{-1}), the wind speed measured at 1.5 m during the following days was rather low, but fairly constant. Generally, the wind speed measured at a height of 0.7 m was lower, but followed the same pattern. During the 3rd and the 5th day of the study the wind speed at 0.7 m dropped below the lowest measurable value (0.25 m s^{-1}). At the 6th and the 7th day, a slight increase was observed, illustrated by a wind speed of 2.8 m s^{-1} at 1.5 m.

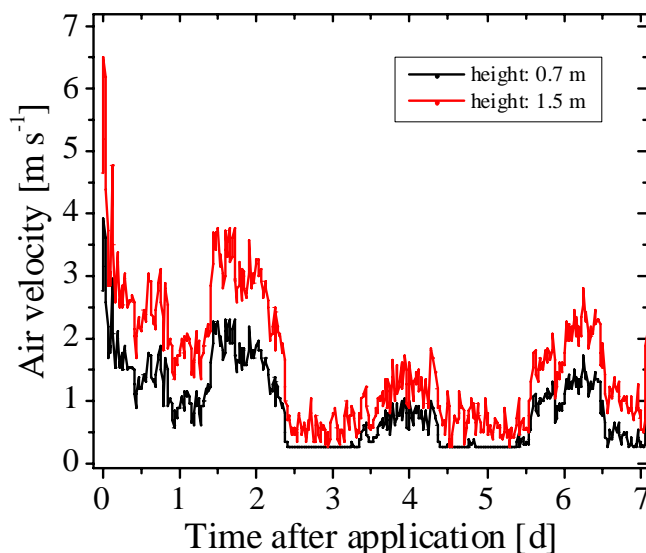


Figure 4.21 Wind speed at 0.7 and 1.5 m above the soil surface during the field study on winter wheat. Data are presented as means, each after 10 min recording of air velocity. Constant wind speed (offset value: 0.25 m s^{-1}) was recorded for wind speed $\leq 0.25 \text{ m s}^{-1}$, thus including calm periods.

4.2.2.2 Plant Residues and Rinsability

The results of rinsing the leaves with solvents of decreasing polarity (water, methanol and chloroform) are summarized in **Table 4.10**. About 18 hours after spraying, the greatest fraction of the residue of fenpropimorph (64.32%) was removed with water, indicating that fenpropimorph had not much penetrated into the wax layer of the leaves. Six days later, the residue was mainly rinsable with methanol and chloroform, whereas only slight amounts of fenpropimorph (7.12%) were rinsed with water.

These findings indicate a high penetration of fenpropimorph into the leaf surfaces over the course of the study, which is in good agreement with the plant residues determined after the wind-tunnel study on winter wheat (**Table 4.8**).

In contrast to fenpropimorph, the plant sampling at 18 hours after application revealed only slight amounts of the applied quinoxifen rinsable with water (13.19%) and about 72.49% detectable in the chloroform phase. This distribution, which apparently indicates a displacement of quinoxifen into deeper layers during the first day of the study, is in contradiction to the classification of quinoxifen as a surface-mobile fungicide (cf. 3.4.5). As a possible explanation, the low amount of quinoxifen detected in the aqueous solution may be attributed to a wash-off caused by the rainfall immediately after application. This explanation would imply that the wash-off effect leading to decreasing plant deposits of quinoxifen exceeds the simultaneously occurring wash-off of fenpropimorph. A lower wash-off of fenpropimorph would require a higher tendency of fenpropimorph towards adherence on the leaves, which may be attributed to its systemic activity.

Table 4.10 Solvent rinsability of pesticide residues deposited on winter wheat leaves.

Date	Time after application [d] †	Solvent	Mass of rinsed pesticide [µg]	
			Fenpropimorph	Quinoxifen
5/15/02	0.7708	Water	41.61 (64.32%)	2.28 (13.19%)
		Methanol	0.61 (0.94%)	2.47 (14.32%)
		Chloroform	22.47 (34.74%)	12.51 (72.49%)
5/17/02	2.7917	Water	24.49 (30.96%)	1.71 (3.66%)
		Methanol	34.88 (44.09%)	32.41 (69.21%)
		Chloroform	19.74 (24.96%)	12.71 (27.14%)
5/21/02	6.7639	Water	4.12 (7.12%)	1.53 (2.29%)
		Methanol	34.75 (60.12%)	52.13 (77.85%)
		Chloroform	18.94 (32.76%)	13.30 (19.86%)

† application time (5/14/02 3:40 PM) taken as reference

The rate of decline of the pesticide amount on the leaves for fenpropimorph and quinoxifen is given in **Fig. 4.22**. About 2 hours after application, on average 83% and 28% of the calculated dosages were recovered for quinoxifen and fenpropimorph, respectively. The low recovery of fenpropimorph may partly be attributed to the comparatively weak extraction method (shaking for 30 min at room temperature), which was apparently not sufficient for a complete extraction of fenpropimorph from the crops. In addition,

metabolization and incorporation into the plant material might have contributed to low recoveries of fenpropimorph during the experiment (cf. 4.2.1.4), due to the fact that metabolites were not targeted within this study.

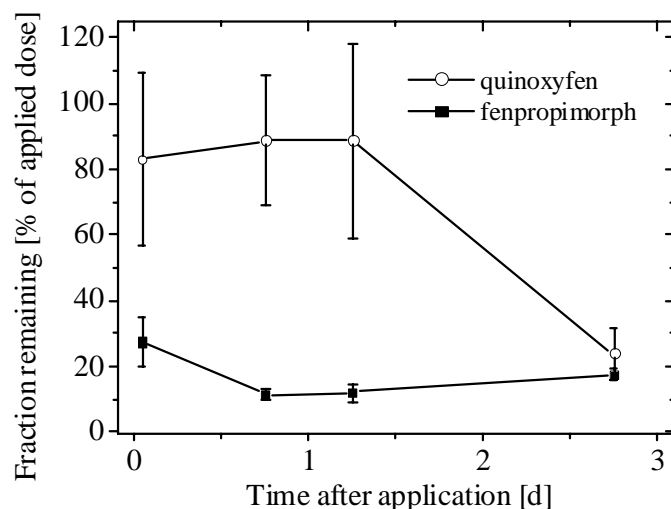


Figure 4.22 Plant residues of quinoxyfen and fenpropimorph after application to winter wheat. Plant sampling and extraction are summarized in 3.3.1.

Quinoxyfen is known as a surface-mobile fungicide. The high recovery of 83% during the first 2 days of the study probably is a consequence of a low degree of penetration and therefore easy extractability. The sharp decrease of the recovery at Day 3 might be caused by photodegradation on the wheat leaf surface (cf. 4.2.1.5).

4.2.2.3 Determination of Volatilization Fluxes: Micrometeorological Methods

Pesticide concentrations in the air at three sampling heights and in the upwind samples were measured for calculation of volatilization rates using micrometeorological methods, (cf. 3.1.3.4 & 3.1.3.5). Quinoxyfen concentrations detected in the upwind samples were as high as the concentrations measured in the field and in some cases even higher. These findings point to quinoxyfen having been applied to the surrounding field plots (**Fig. 3.10**) during or immediately before the beginning of the field study, e.g. by farmers tilling their farmland. Due to this high background concentration, a correlation between measured concentrations in the air and the volatilization from the field plot treated with a defined dose of quinoxyfen was impossible.

Table 4.11 Volatilization fluxes of fenpropimorph determined with aerodynamic (AD) and Bowen ratio (BR) methods during the first day (5/14/02) after application to winter wheat.

Sampling period	Average time after application [d]	Volatilization flux			
		AD method		BR method	
		$[\mu\text{g m}^{-2} \text{h}^{-1}]$	[%] †	$[\mu\text{g m}^{-2} \text{h}^{-1}]$	[%] †
5:55 – 6:55 PM	0.1146	986	2.7	1637	4.4
7:04 – 8:09 PM	0.1667	117	0.32	356	0.96

† percentage of initial dosage per hour

For fenpropimorph, a vertical concentration gradient was established for the first two sampling series, enabling the calculation of volatilization fluxes using the AD and BR methods for the first day after application (**Table 4.11**). This linear relationship between the pesticide concentrations in air and the logarithm of the sampling heights, resulting from the naturally logarithmic wind profile, was expected (Smelt et al., 1997). Differences in concentration between the lowest (1.0 m) and highest sampling height (1.5 m) were used for the calculation of the volatilization rates by micrometeorological methods (cf. 3.1.3.4). In agreement with the findings of the wind-tunnel study (cf. 4.2.1.5), the volatilization was highest immediately after application and decreased on the first day of the study.

The initial volatilization rates ranging between 2.7 and 4.4% of the applied dosage were higher than the rates determined in the wind-tunnel study (approx. 0.3% within 3 hours after application; **Fig. 4.19A**), even though the air temperature measured in both studies was within the same range (**Fig. 4.16 & 4.20**). As a reason for the significant differences between wind-tunnel and field studies, the rainfall occurring immediately after application is assumed to have contributed to fast volatilization of fenpropimorph from the aqueous phase (cf. 4.2.2.1).

The volatilization rates determined with the AD method were lower than those determined with the BR method. The differences in volatilization rates as measured with these two methods probably are related to differences in atmospheric conditions (Van den Berg et al., 1995). For example, some of the volatilization rates determined by Majewski et al. (1990), which were highest for the AD method, were determined during periods with fairly high wind speed, i.e. greater than 4 m s^{-1} at a height of 1.0 m. In the study presented here, the wind speed as measured during the sampling periods at a height of 0.7 m remained below that value (**Fig. 4.21**). However, the low number of utilizable sampling series obtained in this study did not allow for a deeper understanding and evaluation of the differences between the applied micrometeorological methods and for a detailed discussion on the effect of environmental conditions on volatilization.

4.2.3 Model Approach: Volatilization from Plants

The process of calibration and testing of the new model approach using a laminar air-boundary layer concept (cf. 2.2.2.2) for predicting volatilization from plant surfaces is summarized as follows:

- A series of wind-tunnel experiments with the fungicide ^{14}C -fenpropimorph applied to different plants (Stork et al., 1998; Ophoff et al., 1999) were used for calibration of the new model approach. Model predictions were fitted to the experimental findings by adjusting the thickness of the laminar air boundary layer and the rate coefficients. A range of values for the coefficients under defined scenarios after application to different crops was obtained (cf. 4.2.3.1).
- Application of the model to the experimental findings obtained in the wind-tunnel study on winter wheat allowed for testing and evaluation of the model's ability to predict cumulative volatilization of three pesticides, including ^{14}C -labeled and non-labeled compounds, applied simultaneously under identical environmental conditions (cf. 4.2.3.2).
- Implementation and calibration of the novel approach in PELMO enabled the simultaneous calculation of volatilization from soil and plants (cf. 4.2.3.2).

4.2.3.1 Calibration of Rate Coefficients and Boundary-layer Thickness

Data of a series of wind-tunnel experiments after application of fenpropimorph under defined conditions, as described by Stork et al. (1998) and Ophoff et al. (1999), were used for calibration of the rate coefficients and the thickness of the air boundary layer implemented in the boundary-layer model for predicting plant volatilization (cf. 2.2.2.2).

The studies included application of ^{14}C -labeled fenpropimorph in EC formulation to dwarf beans (two studies) and radish plants (two studies), respectively. An additional study used for calibration was performed after spray-application of non-labeled fenpropimorph on sugar beets. Measurements of volatilization rates and mineralization rates and determination of plant and soil residues at the end of the experiments were performed as described in 3.1.2.

Most of the wind-tunnel experiments after application of ^{14}C -labeled fenpropimorph to dwarf beans and radish plants revealed volatilization to occur as a two stage process. Immediately after application (about 6 to 24 hours) high volatilization rates were measured, while during the following days volatilization rates decreased, reaching a minimum at the end of the experiments. This volatilization behavior was simulated with values for the equivalent thickness of the air boundary layer in the range of 0.7 to 1.0 mm assuming a well-exposed scenario (cf. 2.2.2.2), as exemplified in **Fig. 4.23A** for volatilization from radish plants. The highest values of the boundary layer were found in the sugar beet experiment in which the wind velocity was comparatively low during the first two days, indicating that calm periods cause an increase of the stagnant boundary layer.

The rate coefficients for the penetration of fenpropimorph into the plants were estimated to be 3.9 and 4.6 d^{-1} (radish), 2.2 d^{-1} (sugar beets), and 1.3 and 1.6 d^{-1} (dwarf beans). The number of replicates is too small to derive systematic differences in the penetration into the plant species.

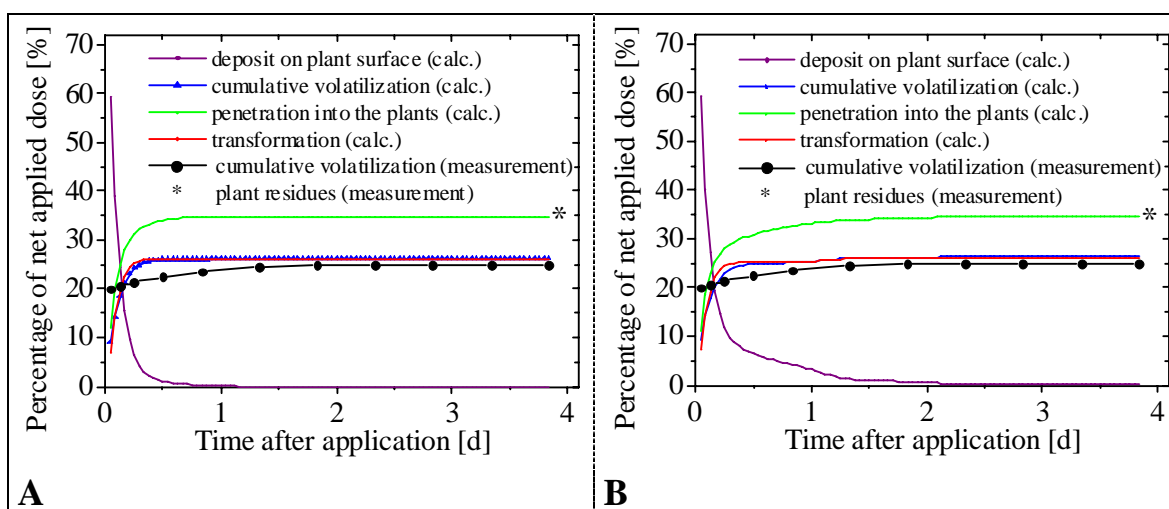


Figure 4.23 Measured (wind-tunnel study; cf. 4.2.1) and predicted (boundary-layer concept; cf. 2.2.2.2) cumulative volatilization of ^{14}C -fenpropimorph after application to radish plants. A diffusion coefficient in air of $0.36 \text{ m}^2 \text{ d}^{-1}$ and a vapor pressure of 2.30 mPa at 20°C were used. **A:** Plant deposit was assumed to be well-exposed. The following parameters were calibrated: $k_{\text{pen}} = 3.9 \text{ d}^{-1}$; $d_{\text{lam}} = 1.0 \text{ mm}$; $k_{\text{ph,ref}} = 3.1 \text{ d}^{-1}$. **B:** 20% of the actual plant deposit were assumed to be poorly-exposed (cf. 2.2.2.2). Rate coefficients of all decrease processes were set at 20% of the coefficients for the corresponding processes of the well-exposed deposit. The following parameters were calibrated: $k_{\text{pen}} = 4.6 \text{ d}^{-1}$; $d_{\text{lam}} = 0.8 \text{ mm}$; $k_{\text{ph,ref}} = 4.0 \text{ d}^{-1}$.

The rate coefficients for phototransformation of fenpropimorph at reference sunlight irradiation (sunny conditions) were estimated to be 0.9 d^{-1} when the inlet air was filtered (beans). The coefficients were estimated to be 3.1 and 4.0 d^{-1} (radish) and 2.4 d^{-1} (sugar beets) when the inlet air was not filtered. Ophoff et al. (1999) concluded that enhanced amounts of OH radicals formed from ozone in the non-filtered air contributed to an increase of indirect phototransformation of fenpropimorph.

On the basis of the systemic activity of fenpropimorph, a fast penetration into the plant leaves was assumed. Indeed, cumulative penetration was measured to be about 34% of the dose by the end of the study after application to radish plants (**Fig. 4.23A**). The high extent of penetration led to a decrease in deposit remaining on the plant surface, which resulted in decreasing volatilization rates. However, the computed disappearance of detectable residues on the leaves within the first day and the subsequent disrupting of volatilization did not correspond to experimental findings, which revealed slight volatilization to continue after the first day until the end of the study.

By replacing the assumption of all deposit on the leaves being well-exposed by a poorly-exposed scenario, a more realistic reflection of the course of volatilization at the later stages of the study was obtained (**Fig. 4.23B**). In order to approximate the measured results, the rate coefficients for penetration and phototransformation had to be increased to 4.6 and 4.0 d^{-1} , respectively, while the boundary-layer thickness was decreased to 0.8 mm. Rate coefficients for the poorly-exposed deposit were set at 20% of the corresponding values for the well-exposed deposit, leading to a slower disappearance of the plant deposit, accompanied by continued volatilization until the end of the simulated period. Even though this modification generally improved the correspondence between observed and simulated time course of the volatilization of fenpropimorph by the end of the study, the underestimation during the first hours increased. Thus, reducing the deposit being available for volatilization by introducing a poorly-exposed fraction causes a decrease of the volatilization rates at the beginning. The lower initial volatilization is compensated by higher rates at the end, finally leading to similar cumulative volatilization under well-exposed and poorly-exposed conditions over the experimental period.

The measurement of pesticide residues at the end of the study enabled the calibration of the final penetration computed for ^{14}C -labeled fenpropimorph. However, due to the lack of measurements on the time course of penetration, the course of the curve is uncertain. Generally, the problem of uncertainty also refers to the course of phototransformation. Thus, as part of the advanced calibration of the model approach a detailed experimental program is required to determine the kinetics of penetration and phototransformation. In addition, further testing of the model should include comparison with experimental scenarios in which combinations of pesticides are applied simultaneously to a crop to provide comparable environmental conditions (cf. 4.2.3.2). Application of the model to field situations requires independent estimations for the processes missed when using non-labeled compounds.

4.2.3.2 Advanced Testing: Wind-tunnel Study on Winter Wheat

Application of the new model approach to the experimental scenario after simultaneous application of ^{14}C -parathion-methyl, fenpropimorph, and quinoxifen to winter wheat

(cf. 4.2.1) allows for an evaluation of the model's ability to reflect the behavior of different pesticides under identical environmental conditions.

Adjusting the boundary-layer thickness and the rate coefficients for penetration and phototransformation to the experimental findings, as shown in **Fig. 4.24** under well-exposed conditions, revealed a reasonable agreement between experimental findings and predictions for parathion-methyl. However, the user is still left with the responsibility to choose an appropriate set of parameters to reflect the time course of the study. For instance, in **Fig. 4.24A** the initial volatilization rates during the first hours of the experiment were significantly underestimated by the model approach. Varying the parameters, especially decreasing the boundary-layer thickness from 0.5 to 0.3 mm, led to an enhanced volatilization and consequently resulted in a better agreement at the initial stage of the study (**Fig. 4.24B**), but over the further time course volatilization was overestimated. The simultaneously occurring fast decrease of the remaining deposit on the leaf surface counteracts the higher volatilization tendency under the conditions applied in **Fig. 4.24B**, consequently leading to approximately the same cumulative volatilization at the end of the study as observed under the conditions illustrated in **Fig. 4.24A**. The predicted disappearance of detectable residues on the leaves after 3.6 days (**Fig. 4.24A**) and 2.3 days (**Fig. 4.24B**), respectively, and the subsequent disrupting of volatilization is contrary to experimental findings, which revealed slight volatilization rates by the end of the study. In addition, measurements of the rinsability of the pesticides after finishing the experiment by using pesticides of increasing polarity revealed that about 1.2% of the net applied parathion-methyl were rinsable with water (cf. 4.2.1.4; **Fig. 4.18**), indicating that the prediction of a complete disappearance of parathion-methyl during the first two days of the study requires revision.

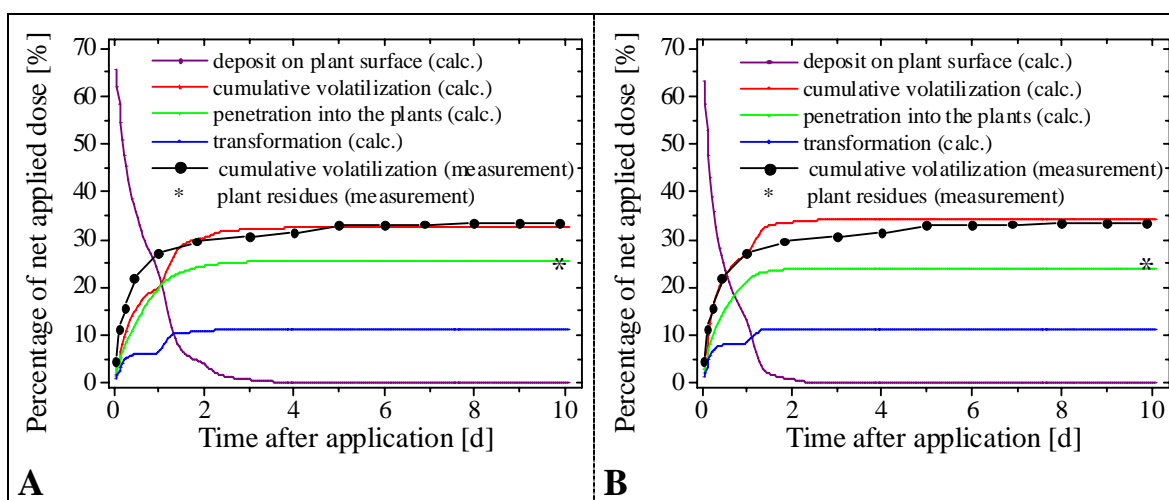


Figure 4.24 Measured (wind-tunnel study; cf. 4.2.1) and predicted cumulative volatilization of ^{14}C -parathion-methyl after application to winter wheat. Plant deposit was assumed to be well-exposed (cf. 2.2.2.2). **A:** $k_{\text{pen}} = 0.5 \text{ d}^{-1}$; $d_{\text{lam}} = 0.5 \text{ mm}$; $k_{\text{ph,ref}} = 1.2 \text{ d}^{-1}$. **B:** $k_{\text{pen}} = 0.7 \text{ d}^{-1}$; $d_{\text{lam}} = 0.3 \text{ mm}$; $k_{\text{ph,ref}} = 1.8 \text{ d}^{-1}$. For both scenarios, a diffusion coefficient in air of $0.5 \text{ m}^2 \text{ d}^{-1}$ and vapor pressure of 1.3 mPa at 20°C were used.

Replacing the well-exposed scenario by a poorly-exposed scenario as described in 4.2.3.1 led to a more realistic reflection of the time course of the disappearance of the plant deposit at the later stage of the study (**Fig. 4.25**).

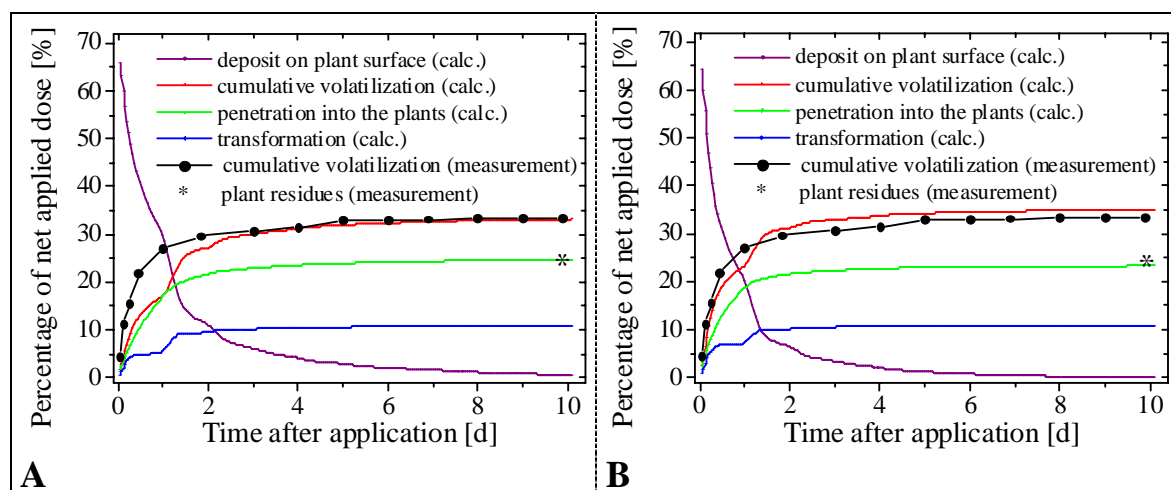


Figure 4.25 Measured (wind-tunnel study; cf. 4.2.1) and predicted cumulative volatilization of ^{14}C -parathion-methyl after application to winter wheat. 20% of the actual plant deposit were assumed to be poorly-exposed (cf. 2.2.2.2). Rate coefficients of all decrease processes were set at 20% of the coefficients for the corresponding processes of the well-exposed deposit. **A:** $k_{\text{pen}} = 0.5 \text{ d}^{-1}$; $d_{\text{lam}} = 0.5 \text{ mm}$; $k_{\text{ph,ref}} = 1.2 \text{ d}^{-1}$. **B:** $k_{\text{pen}} = 0.7 \text{ d}^{-1}$; $d_{\text{lam}} = 0.3 \text{ mm}$; $k_{\text{ph,ref}} = 1.8 \text{ d}^{-1}$. For both scenarios, a diffusion coefficient in air of $0.5 \text{ m}^2 \text{ d}^{-1}$ and a vapor pressure of 1.3 mPa at 20°C were used.

Even though this modification generally improved the agreement of observed and simulated volatilization of parathion-methyl at the end of the study, the underestimation of volatilization during the first day increased. Reducing the deposit being available for volatilization by introducing a class of plant deposits being poorly-exposed causes a decrease in volatilization rates at the beginning. Obviously, the lower volatilization at the beginning is compensated by higher rates at the end, finally leading to comparable cumulative volatilization under well-exposed and poorly-exposed conditions over the total experimental period.

As mentioned above, the determination of pesticide residues at the end of the study enabled a calibration of the penetration curves for ^{14}C -labeled parathion-methyl, even though the time course of penetration is afflicted with uncertainty (cf. 4.2.1.4).

The use of activated charcoal filters during the wind-tunnel study on winter wheat reduced the amount of OH radicals and ozone in the inlet air (cf. 4.2.3.1), thus limiting the expected degree of cumulative photodegradation (approx. 11% of the net applied dose) to occur. However, experimental data on the kinetics of phototransformation will be of prime importance for future improvements of the model approach.

For fenpropimorph, two simulations were performed, reflecting the well-exposed scenario (**Fig. 4.26A**) and the poorly-exposed scenario (**Fig. 4.26B**). The lack of complete radioactivity and mass balances after application of non-labeled fenpropimorph (cf. 4.2.1.2) complicated the calibration of rate coefficients for penetration and phototransformation. In comparison with the calibration studies using ^{14}C -labeled fenpropimorph, a much higher penetration of fenpropimorph was predicted, that is, about 60% of the net applied dose were expected to penetrate over the course of the study. As mentioned above (cf. 4.2.3.1), experimental findings revealed that both penetration and metabolism might have contributed to the low volatilization of fenpropimorph measured in the wind-tunnel study. Due to penetration counteracting the volatilization process, volatilization rates of non-labeled fenpropimorph (about 6%) were significantly lower than the volatilization rates determined previously (Ophoff et al., 1999; **Fig. 4.23**).

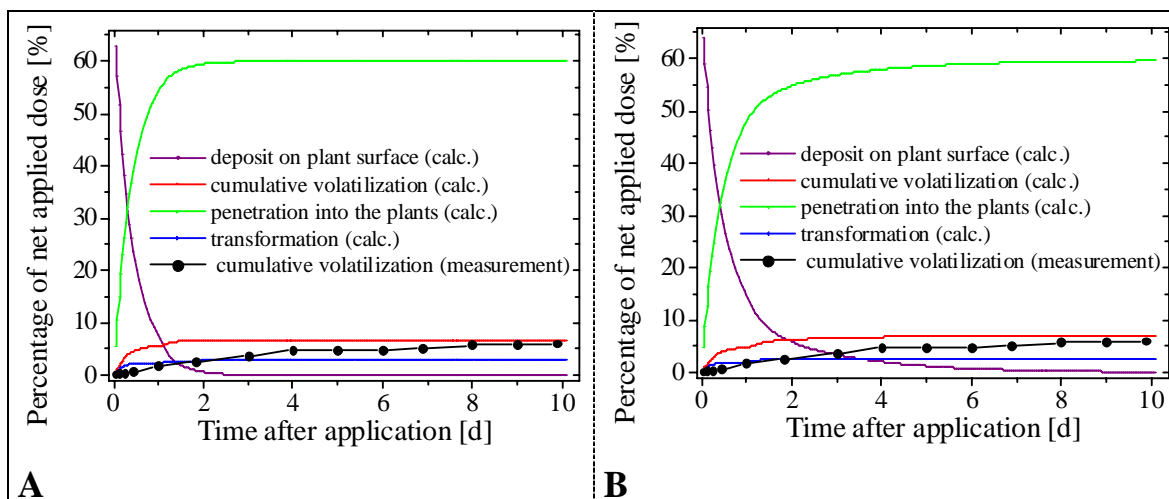


Figure 4.26 Measured (wind-tunnel study; cf. 4.2.1) and predicted cumulative volatilization of fenpropimorph after application to winter wheat. **A:** Well-exposed scenario. **B:** Poorly-exposed scenario (20% of the actual plant deposit were assumed to be poorly-exposed (cf. 2.2.2.2). Rate coefficients of all decrease processes were set at 20% of the coefficients for the corresponding processes of the well-exposed deposit). For both scenarios, a diffusion coefficient in air of $0.5 \text{ m}^2 \text{ d}^{-1}$ and a vapor pressure of 2.3 mPa at 20 °C were used and the following values for the parameters to be calibrated were obtained: $k_{\text{pen}} = 2.0 \text{ d}^{-1}$; $d_{\text{lam}} = 2.0 \text{ mm}$; $k_{\text{ph,ref}} = 0.5 \text{ d}^{-1}$.

Aside from the fact that the studies were performed at differing environmental conditions, the differences in penetration might be attributed to different properties of the chosen pesticide formulations. The studies with ^{14}C -labeled fenpropimorph were performed using the commercial product CORBEL (emulsified concentrate; Ophoff et al., 1999), whereas the combination product FORTRESS TOP (suspension concentrate, **Table 3.3**), containing fenpropimorph and quinoxifen, was applied to winter wheat. The impact of formulation additives on volatilization is a well-known effect, but a comprehensive investigation to quantitate the effect of the commercially available formulations on pesticide emission is still missing. Particularly, little is known on the effect of the formulation type on the waxy layer, which may be partially destroyed when using a specific formulation (Van den Berg et al., 1999).

Both, the well-exposed (**Fig. 4.26A**) and the poorly-exposed (**Fig. 4.26B**) scenario revealed a slight overestimation of volatilization of fenpropimorph, even though the counteracting penetration was assumed to be the dominant process over the course of the study. The calibrated boundary layer thickness ($d_{\text{lam}} = 2 \text{ mm}$) and the predicted volatilization (about 6% of the net applied dose) in comparison to the corresponding values of Ophoff's study ($d_{\text{lam}} = 1 \text{ mm}$; cumulative volatilization of about 50% AR; **Fig. 4.23**) pointed to this parameter exerting a disproportionate influence. Taking into consideration that the rate coefficient for penetration was lower after application to winter wheat ($k_{\text{pen}} = 2.0 \text{ d}^{-1}$) than in Ophoff's study ($k_{\text{pen}} = 3.1 \text{ d}^{-1}$), while the penetration on winter wheat was predicted to be much higher, indicated the boundary layer thickness to be the most crucial parameter affecting the predicted pesticide distribution.

Calculation of volatilization, penetration and transformation of quinoxifen applied as non-labeled compound in the wind-tunnel study to winter wheat, was performed under a well-exposed and a poorly-exposed scenario (**Fig. 4.27**).

In comparison to fenpropimorph, a lower penetration over the course of the study (about 38% of the net applied dose) was predicted for quinoxifen, which is in full agreement with

the classification of quinoxifen as a surface-mobile fungicide (cf. 3.4.5). As quinoxifen is known to be photodegraded on the wheat leaf surface (cf. 4.2.1.4), its comparatively high predicted transformation of approx. 14% of the applied dose appears realistic. In both scenarios, measured volatilization rates were overestimated by the model approach, but the calculated cumulative volatilization at the end of the simulated period showed reasonably good agreement with experimental findings. This agreement is caused by the low volatilization rates calculated for the final period of the experiment, which is attributed to the disappearance of plant deposit after Day 3 (well-exposed scenario; **Fig. 4.27A**) and Day 8 (poorly-exposed scenario; **Fig. 4.27B**), respectively.

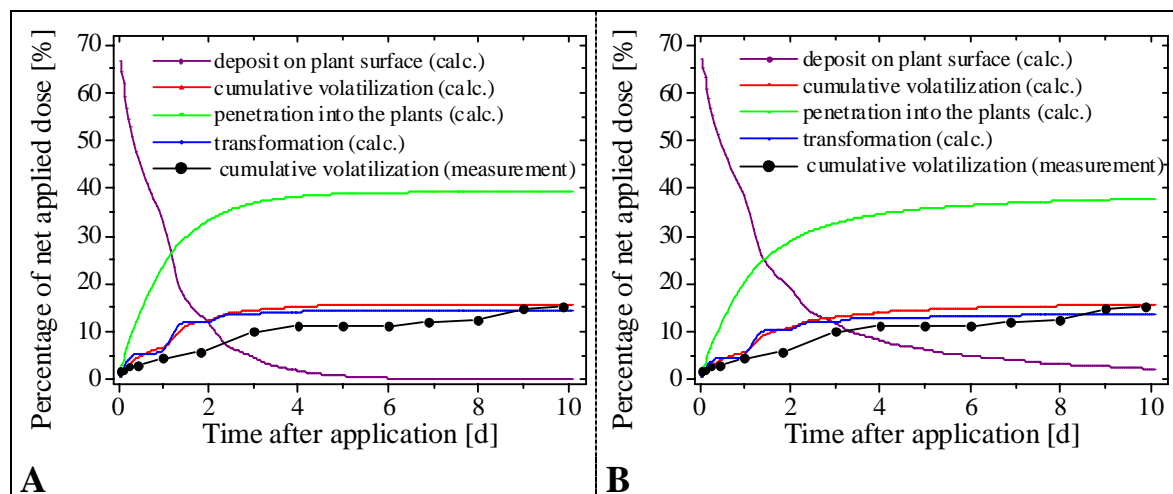


Figure 4.27 Measured (wind-tunnel study; cf. 4.2.1) and predicted cumulative volatilization of quinoxifen after application to winter wheat. **A:** well-exposed scenario. **B:** poorly-exposed scenario (20% of the actual plant deposit were assumed to be poorly-exposed (cf. 2.2.2.2). Rate coefficients of all decrease processes were set at 20% of the coefficients for the corresponding processes of the well-exposed deposit). For both scenarios, a diffusion coefficient in air of $0.5 \text{ m}^2 \text{ d}^{-1}$ and a vapor pressure of 0.3 mPa at 20°C were used and the following values for the parameters to be calibrated were obtained: $k_{\text{pen}} = 0.5 \text{ d}^{-1}$; $d_{\text{lam}} = 0.4 \text{ mm}$; $k_{\text{ph,ref}} = 1.0 \text{ d}^{-1}$.

Even though the adjustment of the parameters to experimental findings allows for a good agreement between predicted and measured volatilization rates for the applied pesticides, the applicability of the new model approach is limited by a lack of experimental data on rate coefficients for penetration, photodegradation and wash-off. Furthermore, the boundary-layer thickness was shown to be a crucial parameter affecting calculated volatilization rates. Due to the simultaneous application of parathion-methyl, fenpropimorph, and quinoxifen the boundary-layer thickness was expected to be equal for the applied compounds. Therefore, the calibrated values of the boundary-layer thickness covering a broad range of values for the applied compounds between 0.2 mm (quinoxifen) and 2.0 mm (fenpropimorph) illustrate this parameter to be afflicted with a high degree of uncertainty.

Vapor pressure is a critically important pesticide property in emission models because vapor pressure is the primary driving force for moving pesticides from a consolidated state to the vapor. Due to the vapor concentration of pesticides in the air at the plant-air interface being strongly affected by the vapor pressure (cf. 2.2.2.2; eq. 15), a sensitivity analysis on the influence of varying vapor pressure on model predictions was performed. Vapor pressure of parathion-methyl and fenpropimorph were varied in the range of the values given in the literature. For parathion-methyl, Spencer et al. (1979) obtained a vapor

pressure of 2.3 mPa at 25 °C, corresponding to 1.2 mPa at 20 °C. A comparable value (1.3 mPa at 20 °C) was given by Kidd & James (1991). Predictions for both values were in good agreement with experimental findings (**Fig. 4.28A**), as indicated by cumulative volatilization of 32.8% and 34.1% for a vapor pressure of 1.2 mPa and 1.3 mPa, respectively. Using a vapor pressure of 0.2 mPa, as given by Tomlin (2000), led to a strong deviation from the measurements (**Fig. 4.28A**), indicating that the selection of reliable values for vapor pressure is of particular importance.

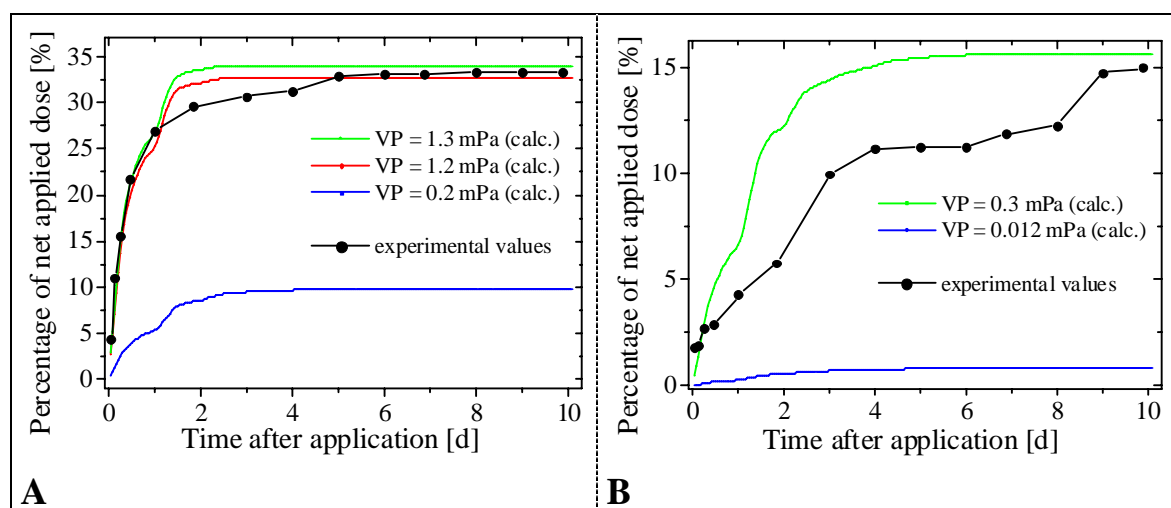


Figure 4.28 Influence of varying vapor pressure on predicted cumulative volatilization of pesticides after application to winter wheat. **A:** Parathion-methyl ($k_{\text{pen}} = 0.7 \text{ d}^{-1}$; $d_{\text{lam}} = 0.3 \text{ mm}$; $k_{\text{ph,ref}} = 1.8 \text{ d}^{-1}$). **B:** Quinoxifen ($k_{\text{pen}} = 0.5 \text{ d}^{-1}$; $d_{\text{lam}} = 0.4 \text{ mm}$; $k_{\text{ph,ref}} = 1.0 \text{ d}^{-1}$). For both compounds, plant deposit was assumed to be well-exposed (cf. 2.2.2.2).

For quinoxifen, this problem was even enhanced by major differences in vapor pressure. The vapor pressure of 0.012 mPa at 20 °C reported by Tomlin (2000) deviates markedly from the calculated value (0.3 mPa at 20 °C) given by Grain (1982). The corresponding cumulative volatilization ranged between 0.8% (0.012 mPa) and 15.7% (0.3 mPa). The comparison with experimental findings (**Fig. 4.28B**) suggested the latter value to be closer to the actual vapor pressure. However, with regard to the predictive use of the model approach the broad range of literature values increases the uncertainty of calculations. Therefore, it becomes important to select the “best” vapor pressure values from the literature or to estimate them in a consistent and reliable manner (Woodrow et al., 2001).

As an advanced model, a volatilization approach based on atmospheric transport resistances is currently under construction (Leistra, personal communication, 2003). In accordance with the module to be implemented for the estimation of volatilization from soil (cf. 4.1.3.3), the concept of a stagnant boundary layer will be replaced by the description of aerodynamic resistances and boundary-layer resistances (Van den Berg et al., 2003). For field conditions, this approach should describe the effects of soil surface conditions, nature of the vegetation and meteorological conditions in a more mechanistic way. The transport resistance approach is expected to be applied in a future version of the PEARL model, thus enabling a better reflection of field conditions.

4.2.3.3 Implementation of the Boundary-layer Concept in PELMO

The implementation of the boundary-layer concept in PELMO enables the simultaneous estimation of volatilization of pesticides from plant and soil surfaces. Application of the improved PELMO version to the environmental scenario of the wind-tunnel study after application of fenpropimorph to winter wheat (cf. 4.2.3.2) allows for the prediction of the relevant plant and soil processes summarized in **Fig. 4.29**.

Plant processes, including volatilization from crops, penetration into the leaves and photodegradation, were computed by adjustment of the boundary-layer thickness and the rate coefficients used for the well-exposed scenario given in **Fig. 4.26A**. For the calculation of the soil processes including volatilization, degradation and root-uptake, the advanced volatilization module included in PELMO (cf. 2.1.2.3.2) was applied to the soil deposit. The scenario for the PELMO simulation included default values for the top soil layer thickness of 1 mm and for the fraction of the applied dose intercepted by the crops of 69.4%.

Computations of the plant processes were in agreement with the predictions given in **Fig. 4.23B**, illustrated by a cumulative volatilization from the plants of approximately 3.5% of the net applied dose. The predicted cumulative volatilization from soil was about 2.6% of the net applied dose, corresponding to 8.5% of the estimated soil deposit. Calculations indicated that degradation in soil ($\approx 0.9\%$) and root-uptake ($< 0.1\%$) were negligible. In agreement with the PELMO predictions for volatilization from bare soil (cf. 4.1.3.2), an increase in soil volatilization was calculated after irrigation was given on Day 7 and 8. In addition, a slight wash-off of the remaining plant deposit ($\approx 0.2\%$) was calculated after Day 7. The experimental set-up used in the wind-tunnel study did not allow to distinguish between volatilization arising from soil and plant deposits. A comparison with the wind-tunnel study after application of ^{14}C -fenpropimorph to gleyic cambisol (cf. 4.1.2.2) revealed the predicted volatilization of fenpropimorph from soil lying in the range of experimental findings. This was exemplified by a cumulative volatilization of 6.4% of the applied radioactivity measured during 13 days after application (**Table 4.5**).

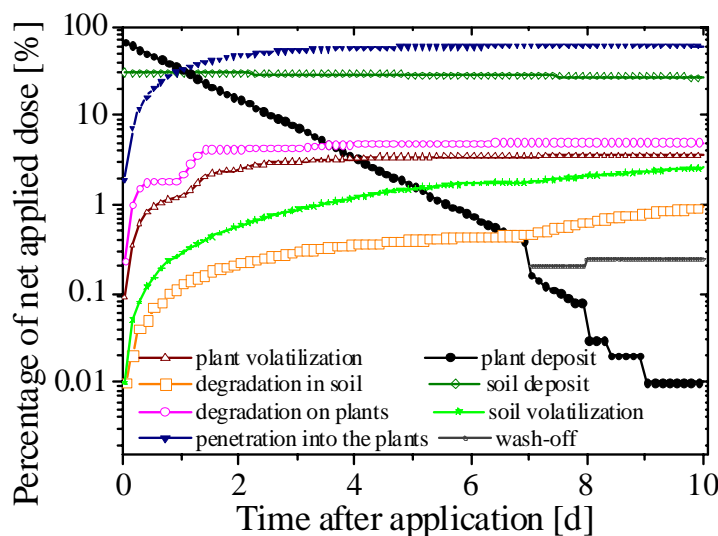


Figure 4.29 PELMO calculation for application of ^{14}C -labeled fenpropimorph to winter wheat (semi-logarithmic plot). For the plant processes, the well-exposed scenario as given in Fig. 4.26A was adjusted. For the computation of the soil processes, a compartment size of the top soil layer of 1 mm and an air boundary layer thickness of 1.73 cm were assumed. The fraction of the applied dose intercepted by the crops was estimated to be 69.4%.

At this early stage of model development, both, the soil volatilization module and the boundary-layer concept for computation of plant volatilization implemented in PELMO need further testing. Further research should reveal the contribution of volatilization from soil after application to the soil-crop system, especially under field conditions providing a soil coverage > 80%. For a final evaluation of the relevance of soil volatilization after pesticide application to plants, calibration of the PELMO predictions under field conditions including various plants and soil types is required.

4.3 Phase Partitioning Studies

The equilibrium distribution of a pesticide between the different phases of the soil and the soil air, can be characterized by the use of partitioning coefficients, which are affected by environmental variables such as temperature and soil moisture. As follows, studies for the determination of phase partitioning are summarized, including the construction and application of a novel chamber system for measurement of soil-air partitioning (cf. 4.3.1) and soil-water partitioning studies in accordance with the OECD Guideline (cf. 4.3.2).

4.3.1 Soil-Air Partitioning: Development of a Novel Chamber

Measurements of soil-air exchange carried out to date utilized flow through systems (Hippelein & McLachlan, 1998; Cousins et al., 1998; Ayris & Harrad, 1999; Morrissey & Grismer, 1999). One of the major limitations in using flow-through chambers is that it remains unclear whether such systems actually allow for compounds having very high soil-air-partitioning coefficients to come into equilibrium with the air. Even at slower air flow rates, the contact time between air and soil may be insufficient to allow for equilibration.

A main advantage of the pseudo-static system (cf. 3.2.1.1) for measuring soil-air partitioning is that sufficient time can be factored into the experiment to ensure the system achieving equilibrium. To optimize the air-soil exchange, so as to reach as fast as possible an equilibrium, the soil was spread in a layer of approx. 5 mm on the metal tray occupying the length of the chamber.

4.3.1.1 Validation and Preliminary Studies

The development of a cleanup method (cf. 3.2.1.3) for the spiked soil samples used in the partitioning chamber was deemed necessary to allow for the determination of the soil concentrations to be used in the soil-air partitioning calculations. Recoveries of the cleanup procedure were calculated by subtracting the blank levels from the levels found in the spiked samples, as shown in **Table 4.12** for orthic luvisol (cf. 3.5.2) spiked with various pesticides.

Recoveries covered an acceptable range of values between 85% (terbuthylazine) and 112% (fenpropimorph). In addition, the homogeneity of the soil concentrations was documented by low standard deviations between 4 and 8%.

The soil-air partitioning coefficient pertains to the gaseous concentration in the air. Possibly, ultra fine particles could have been suspended from the soil surface during the running of the experiment. Thus, inclusion of a particle fraction in the air concentration

measurements would lead to incorrect estimations of the soil-air partitioning coefficient, and in particular to its relationship with environmental variables like temperature or relative humidity. Although soil resuspension should not have been an issue, given the very low mixing of the air in the chamber (cf. 3.2.1.2), this artifact was tested for by employing a glass fiber filter prior to the gaseous adsorbent. This potential artifact was discounted as it was found to be negligible.

Table 4.12 Soil-air partitioning chamber: Pesticide recoveries for orthic luvisol.

Pesticide	Spiked amount [μg]	Recovery [%]	RSD \dagger
Chlorpyrifos	10	105	6
Fenpropimorph	2	112	8
Parathion-methyl	10	85	5
Terbuthylazine	10	85	4

\dagger RSD: relative standard deviation of three replicates

Preliminary studies and calculations allowed for an estimation of the flow rate and the running time required for sampling sufficient amounts of pesticide to exceed analytical detection limits. The running time was expected to have consequences for the feasibility of the chamber to perform the required measurements, the significance of potential artifacts and the logistics of the study as a whole. Referring to the application of fenpropimorph, a running time of 5 hours and a flow rate of approximately 0.2 L min^{-1} was shown to ensure reliable detection.

The volumes of soil used in the chamber studies ought to contain a sufficient mass of compounds to avoid depletion during the running of the experiment. Another confounding factor to consider is the nature of the compound reservoir in the soil involved in the equilibration process. There exists evidence from a number of studies of a rapidly desorbing fraction of pesticide in soil, and a more inaccessible slow desorbing fraction (e.g. Cornelissen et al., 1997). For the purpose of this exercise, a conservative estimate of the fast responding surface compartment was preferable. This was set at 10% of the total mass of contaminant in the soil. For fenpropimorph, a soil concentration of $2 \mu\text{g kg}^{-1}$ applied in the chamber was shown to avoid depletion.

The fundamental assumption in measuring the soil-air partitioning coefficient is that the system attained equilibrium. The big advantage of the used pseudo-static system (cf. 3.2.1.1) is that the small air flow (0.2 L min^{-1}) maximized the contact time between air and soil. Conditions close to equilibrium could be verified by sequential measurements of the air concentrations. As the air and soil approached equilibrium the air concentrations reached a plateau. Equilibrium conditions were attained more rapidly by stirring the air in the chamber using a glass axis provided with propellers (Annex 2C) to reduce any boundary layer above the soil surface. This results in a large surface area / volume ratio of soil available for exchange with the air.

4.3.1.2 Temperature Dependence of Soil-Air Partitioning of Fenpropimorph

Studies on the soil-air partitioning of fenpropimorph were performed at ambient temperatures of 10 and 40 °C (cf. 3.2.1.3). The fraction in the gas phase was calculated as the ratio of the pesticide amount in the gaseous phase of the chamber to the amount remaining on the soil (**Table 4.13**). An increase of approximately 20% of the fraction in the gas phase was determined when temperature was increased from 10 to 40 °C, thus indicating that rises in temperature are accompanied by an increasing tendency towards volatilization (cf. 2.1.1).

Table 4.13 Soil-air partitioning chamber: Fraction of fenpropimorph in the gas phase.

Temperature [°C]	Measured fraction in the gas phase [-]	Calculated fraction in the gas phase [-] †
10	$2.0454 \cdot 10^{-5}$	$2.5180 \cdot 10^{-7}$ (1.2% of measured fraction)
40	$2.4826 \cdot 10^{-5}$	$3.6235 \cdot 10^{-6}$ (14.6% of measured fraction)

† according to Smit et al. (1997)

Measurements were compared to the calculated fraction in the gas phase using the estimation method by Smit et al. (1997). The formulation of the post-application pesticide distribution over the gas, liquid and solid phases (cf. 2.1.2.1.1) resulted in a calculated pesticide fraction in the gas phase of $2.5180 \cdot 10^{-7}$ at 10 °C, thus underestimating the measured value by 2 orders of magnitude. Deviations between measurements and calculations might be attributed to the underlying assumptions for the calculations, e.g. linear adsorption isotherms, which are supposed to be idealized. Model predictions on the basis of calculated values would lead to an underprediction of volatilization. Consequently, the introduction of experimentally determined soil-air partitioning data instead of calculated values will contribute to a clear improvement of model approaches.

The increase of the calculated pesticide amount in the gas phase due to the rise in temperature was higher than the corresponding increase of the measured values (**Table 4.13**), even though wash bottles were used for achieving water-saturated air and to prevent soil drying (**Fig. 3.12**). These findings suggest a slight drying of the soil due to the temperature increase leading to enhanced sorption. Due to the enhanced pesticide sorption, the increase of pesticide transfer in the gaseous phase was apparently lower than the increase predicted by the idealized model approach. However, further studies using various pesticides under a broad range of environmental conditions are required to substantiate knowledge on the temperature dependence of soil-air partitioning. In addition, detailed investigations to elucidate the soil moisture effect on soil-air partitioning ought to be performed.

Regarding the behavior of pesticides in the soil, a number of important questions remain unresolved. It is not clear whether the total amount measured in the soil using conventional analytical techniques is in fact available for exchange with the atmosphere. The fraction that is available for soil-air partitioning may decrease over time as the pesticide becomes

more tightly bound to the soil matrix. The question arises whether this association is reversible or not, e.g. when the organic matter component of the soil which acts as the main sorbing compartment undergoes degradation. A detailed understanding will form an important part of the risk assessment process for such chemicals.

4.3.2 Temperature Dependence of Soil-Water Partitioning

Attempts to analyze the pesticide sorption in soil as a combination of interactions with separated soil constituents have had only limited success (Wauchope et al., 2002). Approaches to determine exactly (within a few per cent) the degree of sorption of a pesticide in a specific soil under specific temperature conditions, are still empirical. The batch experiment used within this thesis to determine the temperature dependence of soil-water partitioning has become the standard method of sorption testing required by regulatory agencies as part of the risk assessment of toxic chemicals. Efforts to harmonize the details of the procedure between European, Canadian and US regulators are currently under way.

For both pesticides studied (parathion-methyl, terbuthylazine), preliminary experiments were performed to confirm a radioactivity and mass balance. Measurements of radioactivity in solution and in soil samples (cf. 3.3.2) resulted in constant ^{14}C -recoveries exceeding 90%. Due to the almost complete mass balance, the following studies on temperature dependence of parathion-methyl and terbuthylazine were done without subsequent soil analysis.

4.3.2.1 Adsorption Isotherms of Parathion-methyl

Studies on the adsorption of ^{14}C -labeled parathion-methyl on gleyic cambisol and orthic luvisol at temperatures ranging from 7 to 30 °C revealed that in all cases the adsorption isotherms could be described by Freundlich equations (**Fig. 4.30**), illustrated by coefficients of determination $R^2 = 0.999$ (**Table 4.14**). Due to the comparatively high water solubility of parathion-methyl (60 mg L⁻¹), concentrations ranging from 0.1 to 12 mg L⁻¹ were chosen to ensure complete solubility within the experimental temperature range. The observed deviation from linearity was a gradual decrease in soil water partitioning with increasing apparent pesticide equilibrium concentration, resulting in a non-linear isotherm with a negative curvature. This deviation was characterized by $1/n$ lying between 0.71 and 1.02, thus representing the most commonly observed range of $1/n$ values for pesticides (Wauchope et al., 2002). In general, non-linearity is observed, especially with pesticides which are not extremely hydrophobic and therefore not limited by solubility to extremely low concentrations (Chiou et al., 1983). Thus, the water solubility of parathion-methyl and the applied concentrations within the studies obviously permitted non-linear deviations.

The most important consequence of isothermic non-linearity of the Freundlich type with $1/n < 1$ is that mobilities for compounds at very high concentrations will be underestimated by K_D or K_{OC} values measured at lower concentrations, and vice versa. This effect may be amplified under field conditions where several solutes are present at higher concentrations. It is a common agricultural practice to apply several pesticides simultaneously. Thus, immediately after spray application and subsequent soil-drying of the uppermost millimeters (cf. 4.1.1.3), a highly concentrated solution of different pesticides and

formulation additives is located on the soil top layer, which finally may lead to an increase of the above mentioned effect of underestimation of mobility.

Table 4.14 Freundlich coefficients (K_F , n) and coefficients of determination (R^2) for adsorption isotherms of parathion-methyl on gleyic cambisol and orthic luvisol at different temperatures.

GLEYIC CAMBISOL				ORTHIC LUVISOL		
Temp.	K_F [$\mu\text{g}^{1-1/n}$ g $^{-1}$ mL $^{1/n}$]	1/n	R^2	K_F [$\mu\text{g}^{1-1/n}$ g $^{-1}$ mL $^{1/n}$]	1/n	R^2
7 °C	10.2	0.84	0.999	10.6	0.71	0.999
10 °C	9.3	1.02	0.999	5.2	0.85	0.999
21 °C	7.8	0.97	0.999	4.4	0.79	0.999
30 °C	5.5	0.98	0.999	3.3	0.71	0.999

With regard to volatilization and its description in models, the use of overestimated soil sorption partition coefficients will generally result in underestimated volatilization rates, regardless whether a simple screening approach or a more sophisticated model is used. In addition, the assumption of linear adsorption isotherms in the models in use at present requires the pesticide concentrations to be regarded as of little environmental relevance, e.g. mostly below the maximum solubility of the pesticide in water. Considering the above mentioned high concentrations at the soil surface, this assumption obviously ought to be revised to take into account non-linear sorption. Some researchers have also highlighted the fact that equilibrium sorption may not be attained under field conditions due to rapid transport (Stangroom et al., 2000). Thus, both equilibrium and non-equilibrium sorption need to be studied to improve the accuracy of predicted partitioning behavior.

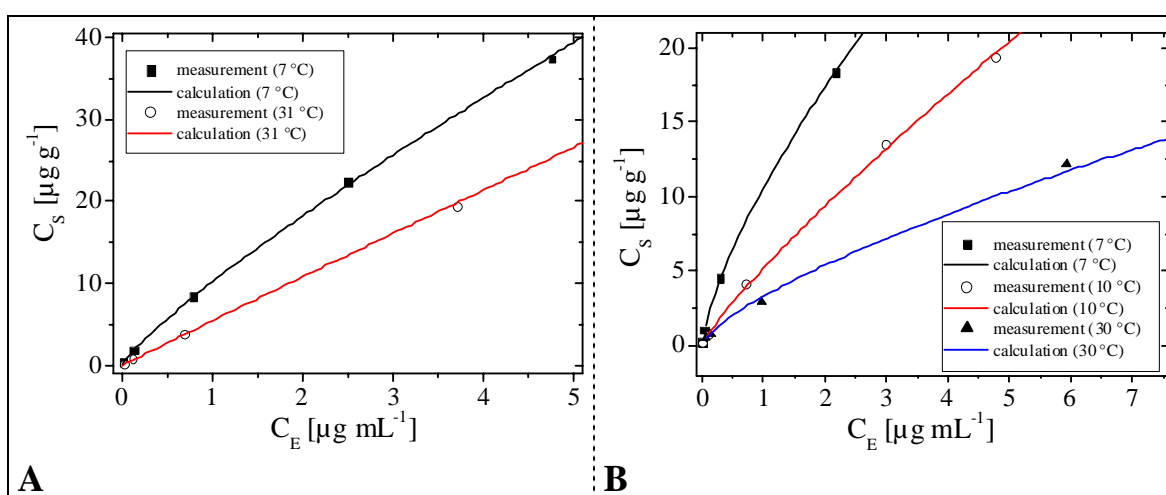


Figure 4.30 Adsorption isotherms of parathion-methyl measured at different temperatures. **A:** Gleyic cambisol (cf. 3.5.1). **B:** Orthic luvisol (cf. 3.5.2) Each measurement point is the mean value of three replicates. Calculations were performed according to the Freundlich equation (cf. 3.2.2.2). C_E : equilibrium concentration remaining in solution [$\mu\text{g mL}^{-1}$]. C_s : concentration bound to the soil [$\mu\text{g g}^{-1}$].

A clear correlation between the sorption behavior of parathion-methyl and the ambient temperature was detected in both soils. Temperature raising from 7 to 30 °C decreased K_F values by a factor of approx. 2 and 3 for gleyic cambisol and orthic luvisol, respectively (Table 4.14).

Decreasing sorption coefficients of parathion-methyl can be attributed to the well-known effect of temperature raising on water solubility. Increasing temperature results in rising water solubility and consequently shifts the equilibrium distribution towards the solute amount. Koskinen & Cheng (1983) have done the most thorough investigation of the effects of experimental variables on slurry experiments, their studies revealed that a temperature change from 5 to 35 °C changed K_D by about 25%. Soil water partitioning coefficients of pesticides can change significantly within the environmental range of temperatures, and the sensitivity is dependent on the solute (Brucher & Bergstrom, 1997). Beyond that, the studies on the sorption of parathion-methyl clearly illustrate an influence of the soil type on K_F and an influence on the magnitude of the temperature effect. Obviously, the temptation to regard K_{OC} calculated from Freundlich coefficients as a universal constant, which applies to a given pesticide in all soils, is inexact. In spite of much accumulated evidence that K_{OC} is variable, the assumption of K_{OC} being a “universal parameter” is still used in pesticide fate simulation models and ought to be revised. Details on the much more complex interaction between soil organic matter and pesticides are beyond the scope of this thesis and can be taken from a review by Wauchope et al. (2002).

4.3.2.2 Adsorption Isotherms of Terbutylazine

In all studies on the sorption of terbutylazine (Table 4.15), the isotherms obtained followed the Freundlich equation with a good approximation ($R^2 > 0.97$). The slopes ($1/n < 1$) of the isotherms indicated that as the initial concentrations of terbutylazine increased, the percentage adsorbed by the soil decreased. This might be explained by an increasingly difficult access to the adsorption sites when pesticide concentrations rose. For both gleyic cambisol and orthic luvisol studied at 30 °C, the fits were poorer when the initial concentration increased because of the fact that the Freundlich calculation overestimated the concentration bound to soil at equilibrium. The constant ($1/n$), which is supposed to express this saturation, was not sufficiently lower than 1 (0.89 and 0.77 for gleyic cambisol and orthic luvisol, respectively) to describe correctly the adsorption of the highest initial terbutylazine concentration in solution (Fig. 4.31).

Table 4.15 Freundlich coefficients (K_F , n) and coefficients of determination (R^2) for adsorption isotherms of terbutylazine on gleyic cambisol and orthic luvisol at different temperatures.

Temp.	GLEYIC CAMBISOL				ORTHIC LUVISOL		
	K_F [$\mu\text{g}^{1-1/n} \text{g}^{-1} \text{mL}^{1/n}$]	$1/n$	R^2		K_F [$\mu\text{g}^{1-1/n} \text{g}^{-1} \text{mL}^{1/n}$]	$1/n$	R^2
10 °C	2.9	0.92	0.999		1.5	0.86	0.999
20 °C	3.0	0.94	0.990		1.7	0.89	0.990
30 °C	1.9	0.89	0.970		0.9	0.77	0.970

Although the Freundlich-type equation is empirical and not based on physicochemical mechanisms, it is often considered to be the most suitable model for the description of adsorption isotherms. However, the $1/n$ value failed to describe the terbuthylazine adsorption at 30 °C.

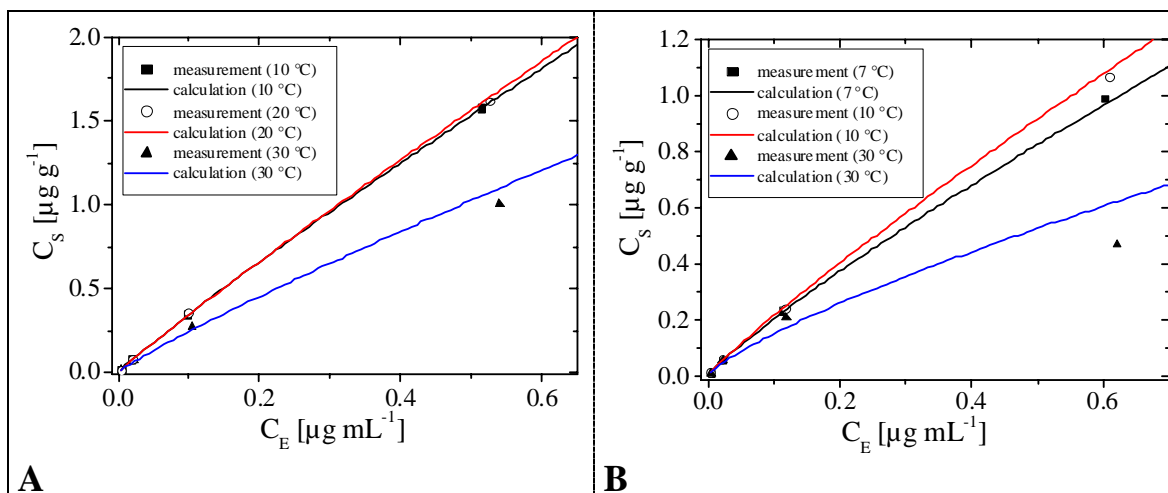


Figure 4.31 Adsorption isotherms of terbuthylazine measured at different temperatures. **A:** Gleyic cambisol (cf. 3.5.1). **B:** Orthic luvisol (cf. 3.5.2) Each measurement point is the mean value of three replicates. Calculations were performed according to the Freundlich equation (cf. 3.2.2.2). C_E : equilibrium concentration remaining in solution [$\mu\text{g mL}^{-1}$]. C_s : concentration bound to the soil [$\mu\text{g g}^{-1}$].

Absolute values of K_F were found to be in agreement with the range of values as observed in previous studies (e.g. Dousset et al., 1994). Though, sorption behavior did not correlate as definitely with temperature as illustrated in the experiments on parathion-methyl (**Fig. 4.30**), especially the studies performed at 10 and 20 °C did not reflect the decrease of partitioning coefficients. Sorption processes are generally exothermic, thus soil water partitioning coefficients were expected to decrease with increasing temperature. This effect is inversely related to water solubility which, on the contrary, increases with temperature for most organic compounds. Therefore, decrease of sorption coefficients with temperature as observed in most studies is a result of the contribution of sorption effect and solubility effect (Delle Site, 2001). The slight aberrations determined in the experiments may be attributed to the general variability of sorption coefficients. Even single, well-mixed soil samples might have great confidence limits of sorption coefficients (Wauchope et al., 2002). Due to K_F being a primary parameter in models designed for risk assessment, these variations might significantly influence the predicted environmental concentrations. Currently, studies to achieve empirical data on the temperature dependence of sorption, as performed within this study, are the only way to take into consideration this effect as closely as possible.

5 CONCLUSIONS AND SUGGESTIONS FOR FURTHER WORK

Volatilization experiments in a photovolatility chamber were performed to apply field-like but well-defined environmental conditions. Essential preconditions for process studies on the influence of varying environmental conditions on volatilization were met: First, the flow profile in the glass dome of the photovolatility chamber illustrates that the wind velocity in the chamber can be adjusted to fulfill the requirements of guidelines on volatilization studies for registration purposes. Second, the use of polyurethane foam plugs for adsorption of pesticides and metabolites was proved to be suitable for increased flow rates within volatilization studies. Third, defined water content in the top layer of the soil and prevention of drying-out during volatilization studies was shown to be achievable by water saturation of the air.

Experimental studies after soil surface application of ^{14}C -parathion-methyl under dry and moist conditions revealed enhanced volatilization rates after increasing the water content of the top soil layer. These findings were the first photovolatility chamber studies to confirm quantitatively the influence of drying and remoistening on volatilization from surface soils, as was requested by Taylor & Spencer (1990). The established functionality of the chamber and thorough controlling of environmental conditions within experiments will permit detailed characterization of volatilization processes.

In addition to these process studies on soil volatilization, the set-up of the chamber enables the extension of detailed studies to volatilization from plants. Special attention will have to be given to photodegradation occurring on the leaf surfaces. Studies on photodegradation, including pesticide application to various plants and soil types under defined conditions will enable a characterization of the processes at the leaf-atmosphere interface.

The wind-tunnel study after soil surface application to gleyic cambisol revealed a comprehensive picture concerning the fate of the applied pesticides, illustrated by ^{14}C -recoveries ranging from 94.4 to 103.9%. The observed order of cumulative volatilization of ^{14}C -labeled compounds (parathion-methyl > terbuthylazine > fenpropimorph) deviated markedly from previous studies on orthic luvisol. These findings documented that comparisons of volatilization studies are to be handled with care due to the strong influence of micro-climatic conditions and soil conditions.

To overcome limitations of measurements and to enable full comparability of atmospheric emission of low-volatile compounds, chemical movement and distribution in the soil should be simultaneously monitored with volatilization. Future experimentation should combine the study of pesticide movement in gas and liquid phases of the soil profile with real-time concentration measurement in air. A promising approach would be to modify a dynamic sequential volatilization flux chamber attached to the top of a two-dimensional rectangular soil column for investigating volatile organic compounds (VOC) movement, as constructed by Allaire et al. (2002), for studies on pesticides. At present, an automated experimental set-up which overcomes the detection limits of low-volatile compounds, e.g. pesticides, is not available. The measurement of pesticide volatilization at high temporal resolution would facilitate an easier validation of model computations to be performed on an hourly basis (cf. 2.1.2.3.2), especially with respect to the processes affecting volatilization during the first hours after application.

Extension of experiments as described above should moreover improve the knowledge on phototransformation on leaf and soil surfaces. Therefore, an up-scaling of the above-

mentioned photovolatility chamber studies by installing an additional ozone analyzer for monitoring ozone concentrations inside the wind tunnel is of prime importance.

Application of the previous versions of the PEC models PEARL and PELMO to the wind-tunnel results revealed that both models did not allow for an adequate prediction of soil volatilization rates. Significant differences between measurements and predictions were determined at the initial stage of the experiment. These results illustrate a general limitation of available models that were not able to handle the non-equilibrium state regarding phase partitioning in a concentrated pesticide mixture at the top layer. Moreover, adsorption and its dependence on soil moisture was not reflected by PEARL and PELMO. Consequently, the models did not describe the soil moisture dependence of film volatilization. The thickness of the upper computation layer in soil was found to influence the predicted volatilization rates significantly. Thus, a reliable estimation of the compartment layer thickness is an essential precondition for the prediction of pesticide volatilization, especially after soil surface application.

The implementation of soil-moisture dependent soil-water partitioning coefficients and temperature-dependent Henry's law constants in an improved PELMO version resulted in a much better agreement between computations and measurements, especially at the initial stages of the studies. In accordance with experimental findings, enhanced volatilization fluxes were predicted for increasing water content. Starting from the findings of this work, further refinements are required, e.g. the increase of sorption coefficients by a factor of 100 below water content corresponding to that at the wilting point is to be replaced by an experimentally-determined correction factor. For this purpose, measurements of the soil-air partitioning under various water conditions using the phase partitioning chamber are to be performed.

Based on the results of this thesis, an advanced PEARL version, which is currently under construction, will also take into consideration the soil-moisture effect on sorption. Furthermore, the simplified concept of stagnant boundary layers will be supplemented with a dynamic description of aerodynamic resistances, that is, in a next version of PEARL there will be two options available to describe the volatilization process: one is based on the stagnant air boundary-layer concept and the second is based on the concept of transport resistances (aerodynamic plus boundary resistance). An official PEARL version including these improved volatilization modules will probably be released in the course of the year 2004 (Van den Berg, personal communication, 2003).

For the computation of pesticide volatilization from plant surfaces, an approach based on a boundary-layer concept, including volatilization from the leaves, wash-off and phototransformation, was applied to the results obtained in wind-tunnel studies. Model predictions were markedly influenced by the selected values for boundary layer thickness and rate coefficients, thus indicating that the reliability of the default values limits the predictive use of the model. Therefore, future improvements of this approach will require a deeper understanding of the underlying processes, e.g. phototransformation and penetration.

The boundary-layer volatilization module was calibrated and included in PELMO, enabling the simultaneous calculation of soil and plant volatilization. Application of PELMO to experimental wind-tunnel scenarios were the first comprehensive PEC model calculations to imply all relevant processes affecting the post-application fate of pesticides. First calculations indicated the amount of soil volatilization being negligible after

application to plants, though an enlarged experimental program including various crops and soil types is to be performed for a final evaluation of the relevance of soil volatilization.

In accordance with the above-mentioned development of an advanced soil volatilization module to be included in PEARL, a comparable approach based on a dynamic description of atmospheric transport resistances will be included for the consideration of volatilization from plants in the course of the next year.

Limitations of recent model predictions supported the need to establish generalized methods to gauge critical factors, especially phase partitioning coefficients, impacting volatilization immediately after application. Batch studies on the temperature dependence of soil-water partitioning of parathion-methyl and terbuthylazine reflected the general tendency of pesticides towards enhanced soil sorption after reducing the temperature. However, the quantification revealed marked deviations from an idealized correlation between temperature and sorption, indicating that experimental sorption studies will still be an indispensable tool for gaining reliable sorption coefficients to be used as default values in models.

The set-up of a novel chamber system and subsequent validation enabled the determination of equilibrium gas-phase concentrations of low-volatile pesticides over the soil surface for the first time. Future studies will contribute to a detailed understanding of the influence of temperature and water content on soil-air partitioning. By now, the broad application spectrum of the chamber has not been utilized fully, especially measurements of Henry's law constants requiring reconstructing the chamber by using a water reservoir and a modified glass axis (Annex 2C) instead of a metal tray (Annex 2D) are expected to deliver substantial progress in elucidating phase partitioning.

6 REFERENCES

- Abo-El-Seoud, M.A.**, and M. Frost. 1994. Metabolism and degradation of ^{14}C -parathion-methyl applied to leaves of soybean and wheat plants grown under sterile conditions. *Nachrichtenbl. Deut. Pflanzenschutz* 46:195-198.
- Adamson, J.**, and T.D. Inch. 1973. Possible relationships between structure and mechanism of degradation of organophosphorous insecticides in the soil environment. p. 65-72. *In* Proceedings of the 7th British Insecticide and Fungicide Conference, Vol. 1, Brighton, UK.
- Addison, R.F.**, and T.G. Smith. 1974. Organochlorine residue levels in arctic ringed seals: Variation with age and sex. *Oikos* 25:335-377.
- Allaire, S.E.**, S.R. Yates, F.F. Ernst, and J. Gan. 2002. A dynamic two-dimensional system for measuring volatile organic compound volatilization and movement in soils. *J. Environ. Qual.* 31:1079-1087.
- Anderssen, R.S.**, F.R. de Hoog, and B.R. Markey. 1997. Modelling the volatilization of organic soil contaminants: Extension of the Jury, Spencer and Farmer Behaviour Assessment Model and solution. *Appl. Math. Lett.* 10:31-34.
- Anonymous.** 2000. Bekanntmachungen über die Abtrifteckwerte, die bei der Prüfung und Zulassung von Pflanzenschutzmitteln herangezogen werden vom 08. Mai 2000. p. 9879–9880. *Bundesanzeiger* Nr. 100.
- Asman, W.A.H.** 2001. Modelling atmospheric transport and deposition of pesticides up to 2 km from a source. *In* W.A.H. Asman, G. Felding, P. Kudsk, J. Larsen, S. Mathiassen, N.H. Spliid (eds.) *Pesticides in air and in precipitation and effects on plant communities. Report Pesticides Research 57*, Danish Environmental Protection Agency, Copenhagen, Denmark.
- Asman, W.A.H.**, M.O. Andreae, R. Conrad, O.T. Denmead, L.N. Ganzeveld, W. Helder, T. Kaminski, M.A. Sofiev, and S. Trumbore. 1999. How can fluxes of trace gases be validated between different scales? p. 85-97. *In* A.F. Bouwman (ed.) *Approaches to scaling of trace gas fluxes in ecosystems*. Elsevier Science B.V., Amsterdam, the Netherlands.
- Aspelin, A.L.** 1994. Pesticides industry sales and usage; 1992 and 1993 market estimates. 733-K-92-001, USEPA, Washington, D.C., USA.
- Ayris, S.**, and S. Harrad. The fate and persistence of polychlorinated biphenyls in soil. *J. Environ. Monit.* 1:395-401.
- Baker, J.M.**, W.C. Koskinen, and R.H. Dowdy. 1996. Volatilization of EPTC: Simulation and Measurement. *J. Environ. Qual.* 25:169-177.
- Barrie, L.A.** 1986. Arctic air pollution – an overview of current knowledge. *Atmos. Environ.* 20:643-663.
- BBA.** 2002. EVA 1.1: Programm zur Abschätzung der abdrift- und verflüchtigungsbedingten Deposition von PSM-Wirkstoffen im Nichtzielbereich nach Freilandanwendungen. http://www.bba.de/ap/ap_psm/eva/eva.htm.

- BBA.** 1990. Prüfung des Verflüchtigungsverhaltens und des Verbleibs von Pflanzenschutzmitteln in der Luft. Richtlinien für die Prüfung von Pflanzenschutzmitteln im Zulassungsverfahren, Teil IV, 6-1, Biologische Bundesanstalt für Land- und Forstwirtschaft Abt. f. Pflanzenschutz und Anwendungstechnik, Braunschweig, Germany.
- Bedos, C.,** P. Cellier, R. Calvet, E. Barriuso, and B. Gabrielle. 2002. Mass transfer of pesticides into the atmosphere by volatilization from soils and plants: overview. *Agronomie* 22:21-33.
- Bentson, K.P.** 1990. Fate of xenobiotics in foliar pesticide deposits. *Rev. Environ. Contam. T.* 114:125-161.
- Bidleman, T.F.** 1988. Atmospheric processes – wet and dry deposition of organic compounds are controlled by their vapor-particle partitioning. *Environ. Sci. Technol.* 22:361-367.
- Bidleman, T.F.,** and E.J. Christensen. 1979. Atmospheric removal processes for high molecular weight organochlorines. *J. Geophys. Res.* 84:7857-7862.
- Boesten, J.J.T.I.** 2000. From laboratory to field: uses and limitations of pesticide behaviour models for the soil/plant system. *Weed Res.* 40:123-138.
- Breeze, V.G.,** J.C. Simmons, and M.O. Roberts. 1992. Evaporation and uptake of the herbicide 2,4-D-butyl applied to barley leaves. *Pestic. Sci.* 36:101-107.
- Brucher, J.,** and L. Bergstrom. 1997. Temperature dependence of linuron sorption to three different agricultural soils. *J. Environ. Qual.* 26:1327-1335.
- Brutsaert, W.** 1975. A theory for local evaporation (or heat transfer) from rough and smooth surfaces at ground level. *Water Resour. Res.* 11:543-550.
- Burkhard, N.,** and J.A. Guth. 1981. Rate of volatilisation of pesticides from soil surfaces, comparison of calculated results with those determined in a laboratory model system. *Pestic. Sci.* 12:37-44.
- Burrows, H.D.,** M. Canle L, J.A. Santaballa, and S. Steenken. 2002. Reaction pathways and mechanisms of photodegradation of pesticides. *J. Photochem. Photobiol. B* 67:71-108.
- Carsel, R.F.,** C.N. Smith, L.A. Mulkey, J.D. Dean, and P. Jowise. 1984. PRZM-1, a model for predicting pesticide and nitrogen fate in the crop root and unsaturated soil zones: User's manual for release 1. National Exposure Res. Lab., USEPA, Athens, GA, USA.
- Cherif, S.,** and H. Wortham. 1997. A new laboratory protocol to monitor the volatilization of pesticides from soils. *Intern. J. Environ. Anal. Chem.* 68:199-212.
- Chiou, C.T.,** P.E. Porter, and D.W. Schmedding. 1983. Partition equilibria of non-ionic compounds between soil organic matter and water. *Environ. Sci. Technol.* 17:227-231.
- Cornelissen, G.,** P.C.M. van Noort, J.R. Parsons, and H.A.J. Govers. 1997. Temperature dependence of slow adsorption and desorption kinetics of organic compounds in sediments. *Environ. Sci. Technol.* 31:454-460.
- Cotham, W.E.,** and T.F. Bidleman. 1991. Estimating the atmospheric deposition of organochlorine contaminants to the arctic. *Chemosphere* 22:165-188.

- Council Directive.** 1991. Council Directive 91/414/EEC of 15 July 1991 concerning the placing of plant protection products on the market. O.J. No L230.
- Cousins, I.T.,** A.J. Beck, and K.C. Jones. 1999. A review of the processes involved in the exchange of semi-volatile organic compounds (SVOC) across the air-soil interface. *Sci. Total Environ.* 228:5-24.
- Cousins, I.T.,** M.S. McLachlan, K.C. Jones. 1998. Lack of an aging effect on the soil – air partitioning of polychlorinated biphenyls. *Environ. Sci. Technol.* 32:2734-2740.
- Delle Site, A.** 2001. Factors affecting sorption of organic compounds in natural sorbent / water systems and sorption coefficients for selected pollutants. A review. *J. Phys. Chem. Ref. Data* 30:187-439.
- Dickerson, R.R.,** G.J. Huffman, W.T. Luke, L.J. Nunnermacker, K.E. Pickering, A.C.D. Leslie, C.G. Lindsey, W.G.N. Slinn, T.J. Kelly, P.H. Daum, A.C. Delany, J.P. Greenberg, P.R. Zimmerman, J.F. Boatman, J.D. Ray, and D.H. Stedman. 1987. Thunderstorms – An important mechanism in the transport of air-pollutants. *Science* 235:460-464.
- Domsch, K.H.** 1992. *Pestizide im Boden: Mikrobieller Abbau und Nebenwirkungen auf Mikroorganismen*, p. 65-66, 1st edition, VCH, Weinheim, Germany.
- Doull, J.** 1989. *Pesticide carcinogenicity, Carcinogenicity and Pesticides: Principles, Issues and Relationships*. Am. Chem. Soc., Washington, D.C., 246 pp, USA.
- Dousset, S.,** C. Mouvet, and M. Schiavon. 1994. Sorption of terbuthylazine and atrazine in relation to the physico-chemical properties of three soils. *Chemosphere* 28:467-476.
- Ebing, W.,** M. Frost, R. Kreuzig, and I. Schuphan. 1995. Investigations on degradation and leaching of fenpropimorph in a lysimeter experiment. *Nachrichtenbl. Deut. Pflanzenschutzd.* 47:5-9.
- Eisenreich, S.J.,** B.B. Looney, and J.D. Thornton. 1981. Airborne organic contaminants in the Great Lakes ecosystem. *Environ. Sci. Technol.* 15:30-38.
- FAO** (Food and Agriculture Organization of the United Nations). 2001. *FAO Statistical Databases*. <http://apps.fao.org/>.
- FAO** (Food and Agriculture Organization of the United Nations). 1990. *Guidelines for Soil Profile Description*. Soil Resources, Management and Conservation Service, Land and Water Development Division, FAO, Rome, Italy.
- Farmer, W.J.,** J.P. Martin, W.F. Spencer, and K. Igue. 1972. Volatility of organochlorine insecticides from soil: I. Effect of concentration, temperature, air flow rate, and vapor pressure. *Soil Sci. Soc. Am. Proc.* 36:443-447.
- Fowler, D.** 1999. Experimental designs appropriate for flux determination in terrestrial and aquatic ecosystems. p. 99-121. *In* A.F. Bouwman (ed.) *Approaches to scaling of trace gas fluxes in ecosystems*. Elsevier Science B.V., Amsterdam, the Netherlands.
- Führ, F.** 1987. Non-extractable pesticide residues in soil. p. 381-389. *In* R. Greenhalg, and T.R. Roberts (eds.) *Pesticide Science and Biotechnology. Proceedings, 6th Intern. Congr. Pestic. Chem.*, Ottawa, Canada. Blackwell Scientific Publications, Oxford, UK.

- Führ, F.,** P. Burauel, M. Dust, W. Mittelstaedt, T. Pütz, G. Reinken, and A. Stork. 1998. Comprehensive tracer on environmental behaviour of pesticides: The lysimeter concept. p. 1-20. *In* F. Führ, R.J. Hance, J.R. Plimmer, and J.O. Nelson (eds.) The lysimeter concept. ACS Symp. Ser. 699. Am. Chem. Soc., Washington, D.C., USA.
- Ganzelmeier, H.,** D. Rautmann, R. Spangenberg, M. Streloke, M. Herrmann, H.-J. Wenzelburger, and H.-F. Walter. 1995. Untersuchungen zur Abtrift von Pflanzenschutzmitteln – Ergebnisse eines bundesweiten Versuchsprogramms. Mitteilg. BBA, Heft 304, Berlin.
- George, J.L.,** and E.H. Frear. 1966. Pesticides in Antarctica: J. Applied Ecol. 3: 155-176.
- Gerstl, Z.,** and C.S. Helling. 1984. Influence of agronomic amendments on the fate of bound methyl parathion residues in soil. p. 7-16. *In* Radiotracer Studies of Bound Pesticides Residues in Soil, Plants and Food. IAEA, IAEA-Tecdod 306, Vienna, Austria.
- Gerstl, Z.,** C. Sluszný, A. Alayof, and E.R. Graber. 1997. The fate of terbuthylazine in test microcosms. Sci. Total Environ. 196:119-129.
- Gilbert, A.J.** 1999 Regulatory risk assessment of pesticide residues in air. Water Air Soil Pollut. 115:183-194.
- Glotfelty, D.E.,** and C.J. Schomburg. 1989. Volatilization of pesticides from soil. p. 181-207. *In* B.L. Sawhney, and K. Brown (eds.) Reactions and movement of organic chemicals in soils. SSSA, and ASA, Madison, WI, USA.
- Glotfelty, D.E.,** C.J. Schomburg, and M.M. McChesney. 1990. Preliminary studies of the distribution, drift, and volatilization of diazinon resulting from spray application to a dormant peach orchard. Abstr. Pap. Am. Chem. Soc. 199:135.
- Glotfelty, D.E.,** A.W. Taylor, B.C. Turner, and W.H. Zoller. 1984. Volatilization of surface-applied pesticides from fallow soil. J. Agric. Food Chem. 32:638-643.
- Grain, C.F.** 1982. Vapor pressure. p. 14/1-14/20. *In* W.J. Lyman (ed.) Handbook of chemical property estimation methods. Environmental behavior of organic compounds. McGraw-Hill Book Company, New York, USA.
- Harper, L.A.,** A.W. White Jr., R.R. Bruce, A.W. Thomas, and R.A. Leonard. 1976. Soil and microclimate effects on trifluralin volatilization. J. Environ. Qual. 5:236-242.
- Hippelein, M.,** and M.S. McLachlan. 1998. Soil-air partitioning of semivolatile organic compounds. 1. Method development and influence of physical-chemical properties. Environ. Sci. Technol. 32:310-316.
- Hornsby, G.H.,** R.D. Wauchope, and A.E. Herner. 1996. Pesticide properties in the environment. Springer Verlag, New York, USA.
- Hurle, K.** 1982. Untersuchungen zum Abbau von Herbiziden in Böden. Acta Phytomedica 8, Beihefte zur Phytopathologischen Zeitschrift. Verlag Paul Parey, Berlin u. Hamburg, Germany.
- Jury, W.A.** 1993. Volatilization of organic chemicals from soil. p. 105-126. *In* R. Schulín, A. Desaulés, R. Webster, and B. von Steiger (eds.) Soil monitoring methods for early detection and surveying of soil contamination and degradation. Birkhäuser Verlag, Basel, Switzerland.

- Jury, W.A.,** W.J Farmer, and W.F. Spencer. 1984A. Behavior assessment models for trace organics in soil: II. Chemical classification and parameter sensitivity. *J. Environ. Qual.* 13:567-572.
- Jury, W.A.,** W.F. Spencer, and W.J. Farmer. 1984B. Behavior assessment models for trace organics in soil: III. Application of screening model. *J. Environ. Qual.* 13:573-579.
- Jury, W.A.,** W.F. Spencer, and W.J. Farmer. 1984C. Behavior assessment models for trace organics in soil: IV. Review of experimental evidence. *J. Environ. Qual.* 13:580-586.
- Jury, W.A.,** W.F. Spencer, and W.J. Farmer. 1983. Behavior assessment models for trace organics in soil: I. Model description, *J. Environ. Qual.* 12:558-564.
- Kidd, H.,** and D.R. James (eds.). 1991. *The Agrochemicals Handbook*. The Royal Society of Chemistry, Cambridge, UK.
- Klein, M.** 1995. PELMO: Pesticide Leaching Model, User's Manual Version 2.01. Fraunhofer-Institute for Environmental Chemistry and Ecotoxicology, Schmallenberg, Germany.
- Klotz, I.M.,** and R.M. Rosenberg. 1974. *Chemical thermodynamics: Basic theory and methods*. 3rd ed. Benjamin/Cummings Publ. Co., Menlo Park, CA, USA.
- Koskinen, W.C,** and H.H. Cheng. 1983. Effects of experimental variables on 2,4,5-T adsorption-desorption in soil. *J. Environ. Qual.* 12:325-330.
- Kromer, T.** 2001. Photovolatility chamber for simultaneous measurement of photo-degradation and volatilization of environmental chemicals on surfaces using the insecticide parathion-methyl. PhD thesis, University of Bonn, Germany.
- Kromer, T.,** H. Ophoff, A. Stork, and F. Führ. 2003. Photodegradation and volatility of pesticides: Chamber experiments. *Environ. Sci. Pollut. Res.*, In press.
- Kromer, T.,** H. Ophoff, A. Stork, and F. Führ. 1999. Photodegradation and volatilization of parathion-methyl on glass and soil dust under laboratory conditions. p. 363-374. *In* A.A.M. Del Re, C. Brown, E. Capri, G. Errera, S.P. Evans, M. Trevisan (eds.) *Proc. XI Symp. Pestic. Chem. - Human and environmental exposure to xenobiotics*. La Goliardica Pavese, Pavia, Italy.
- Kubiak, R.,** T. Maurer, and K.W. Eichhorn. 1993. A new laboratory model for studying the volatilization of pesticides under controlled conditions. *Sci. Total Environ.* 132:115-123.
- Kurtz, D.A.,** and E.L. Atlas. 1990. Distribution of hexachlorocyclohexanes in the Pacific Ocean basin, air and water, 1987. p. 143-160. *In* D.A. Kurtz (ed.) *Long Range Transport of Pesticides*. Lewis Publishers Inc., Chelsea, MI, USA.
- Langenbach, T.,** R. Schroll, and I. Scheunert. 2001. Fate of the herbicide ¹⁴C-terbutylazine in Brazilian soils under various climatic conditions. *Chemosphere* 45:387-398.
- Leistra, M.,** A.M.A. Van der Linden, J. Boesten, A. Tiktak, and F. Van den Berg. 2001. PEARL model for pesticide behaviour and emissions in soil-plant systems; Descriptions of the processes in FOCUS PEARL v 1.1.1. Alterra-rapport 013, Alterra Green World Research, Wageningen, the Netherlands.
- Lembrich, D.,** F. Beese, and I. Scheunert. 1999. Microcosm studies on the volatility of pesticides from soil surfaces. *J. Environ. Qual.* 28:721-726.

- Linnemann, V.** 2002. Transport of volatile hydrocarbons through an undisturbed soil core into the atmosphere after contamination of the groundwater with the fuel additive methyl-tert-butyl ether (MTBE). PhD thesis, University of Bonn, Germany.
- Livingston, G.P.,** and G.L. Hutchinson. 1995. Enclosure-based measurement of trace gas exchange: applications and sources of error. p. 14-51. *In* P.A. Matson, and R.C. Harris (eds.) Biogenic trace gases: measuring emissions from soil and water. Blackwell Sci., Malden, MA, USA.
- Longhurts, C.,** K. Dixon, A. Mayr, U. Bernhard, K. Prince, J. Sellars, P. Prove, C. Richard, W. Arnold, B. Dreikorn, and C. Carson. 1996. Quinoxifen, a novel fungicide for the control of powdery mildew in cereals, grapes and vegetables. p. 27-32. *In* Proceedings, Brighton Crop Prot. Conf. – Pests and Diseases, Farnham, Surrey, UK.
- Majewski, M.S.** 1999. Micrometeorological methods for measuring the post-application volatilization of pesticides. *Water Air Soil Pollut.* 115:83-113.
- Majewski, M.S.,** and P.D. Capel. 1995. Pesticides in the atmosphere: distribution, trends, and governing factors. Ann Arbor Press, Inc., Chelsea, Michigan, USA.
- Majewski, M.S.,** D.E. Glotfelty, U. Paw, and J.N. Seiber. 1990. A field comparison of several methods for measuring pesticide evaporation rates from soil. *Environ. Sci. Technol.* 24:1490-1497.
- Majewski, M.S.,** D.E. Glotfelty, and J.N. Seiber. 1989. A comparison of the aerodynamic and the theoretical-profile shape methods for measuring pesticide evaporation from soil. *Atmos. Environ.* 23:929-938.
- Matson, P.A.,** P.M. Vitousek, and D.S. Schimmel. 1989. Regional extrapolation of trace gas flux based on soils and ecosystems. p. 97-108. *In* M.O. Andreae, and D.S. Schimmel (eds.) Exchange of trace gases between terrestrial ecosystems and the atmosphere. Wiley and Sons, Chichester, USA.
- McCall, P.J.,** L.E. Stafford, P.S. Zorner, and P.D. Gavit. 1986. Modeling the foliar behavior of atrazine with and without crop oil concentrate on Giant Foxtail and the effect of tridiphane on the model rate constants. *J. Agric. Food Chem.* 34:235-238.
- McConnell, L.L.,** E. Nelson, C.P. Rice, J.E. Baker, W.E. Johnson, J.A. Harman, and K. Bialek. 1997. Chlorpyrifos in the air and surface water of Chesapeake Bay: predictions of atmospheric deposition fluxes. *Environ. Sci. Technol.* 31:1390-1398.
- Misra, B.,** P.W. Graebing, J.S. Chib. 1997. Photodegradation of chloramben on a soil surface: a laboratory controlled study. *J. Agric. Food Chem.* 45:1464-1467.
- Monteith, J.L.** 1965. Evaporation and the environment. p. 205-234. *In* G.E. Fogg (ed.) The state and movement of water in living organisms. Cambridge University Press, UK.
- Morrissey, F.A.,** and M.E. Grismer. 1999. Kinetics of volatile organic compound sorption / desorption on clay minerals. *J. Contamin. Hydr.* 36:291-312.
- Müller, T.,** N. Staimer, and R. Kubiak. 1998. Influence of soil pH and contents of organic carbon and clay on the volatilization of [¹⁴C]fenpropimorph after application to bare soil. *Pestic. Sci.* 53:245-251.

- Nash, R.G.**, and T.J. Gish. 1989. Halogenated pesticide volatilization and dissipation from soil under controlled conditions. *Chemosphere* 18:2353-2362.
- Niehaus, R.**, B. Scheulen, and H.W. Dürbeck. 1990. Determination of airborne polycyclic aromatic hydrocarbons using a filter/adsorber combination. *Sci. Total Environ.* 9:163-172.
- OECD** (Organization for Economic Co-operation and Development). 2000. Guideline for the testing of chemicals. OECD Paris, France.
- Ophoff, H.** 1999. Volatilization and mineralization of fluoranthene, parathion-methyl and fenpropimorph under simulated field conditions. PhD thesis, University of Bonn, Germany.
- Ophoff, H.**, F. Führ, A. Stork, and J.H. Smelt, 1999. Volatilization of fenpropimorph under simulated field conditions after application onto different plants. p. 199-209 *In* A.A.M. Del Re, C. Brown, E. Capri, G. Errera, S.P. Evans, M. Trevisan (eds.) Human and environmental exposure to xenobiotics. Proc. XI Symposium Pesticide Chemistry. La Goliardica Pavese, Pavia, Italy.
- Ophoff, H.**, A. Stork, W. Veerkamp, and F. Führ. 1996. Volatilization and mineralization of [3-¹⁴C]fluoranthene after soil incorporation and soil surface application. *Intern. J. Environ. Anal. Chem.* 64:97-109.
- Orchard, B.J.**, W.J. Doucette, J.K. Chard, B. Bugbee. 2000. A novel laboratory system for determining fate of volatile organic compounds in planted systems. *Environ. Toxicol. Chem.* 19:888-894.
- Plimmer, J.R.** 1992. Dissipation of pesticides in the environment. p. 79-90. *In* J.L. Schnoor (ed.) Fate of pesticides and chemicals in the environment. John Wiley & Sons, New York, USA.
- Prandtl, L.** 1990. Führer durch die Strömungslehre, 9th edition. Vieweg Verlag, Braunschweig, Germany.
- Racke, K.D.** 1993. Environmental fate of chlorpyrifos. *Rev. Environ. Contam. Toxicol.* 131:1-154.
- Rawn, D.F.K.**, and D.C.G. Muir. 1999. Sources of chlorpyrifos and dacthal to a small canadian prairie watershed. *Environ. Sci. Technol.* 33:3317-3323.
- Reichman, R.**, and D.E. Rolston. 2002. Design and performance of a dynamic gas flux chamber. *J. Environ. Qual.* 31:1774-1781.
- Rice, C.P.**, C.B. Nochetto, and P. Zara. 2002. Volatilization of trifluralin, atrazine, metolachlor, chlorpyrifos, α -Endosulfan, and β -Endosulfan from freshly tilled soil. *J. Agric. Food Chem.* 50:4009-4017.
- Riederer, M.**, A. Daiß, N. Gilbert, and H. Köhle. 2002. Semi-volatile organic compounds at the leaf/atmosphere interface: numerical simulation of dispersal and foliar uptake. *J. Exp. Bot.* 53:1815-1823.
- Roberts, T.R.**, and D.H. Hutson. 1999. Metabolic pathways of agrochemicals. The Royal Society of Chemistry, Cambridge, UK.
- Rüdel, H.**, and B. Waymann. 1992. Volatility testing of pesticides in a wind tunnel. p. 841-846. *In* Proceedings, Brighton Crop Prot. Conf. – Pests and Diseases, Brighton, UK.

- Sanders, P.F.**, and J.N. Seiber. 1983. A chamber for measuring volatilization of pesticides from model soil and water disposal systems. *Chemosphere* 12:999-1012.
- Schönherr, J.**, and P. Baur. 1994. Modelling penetration of plant cuticles by crop protection agents and effects of adjuvants on their rates of penetration. *Pestic. Sci.* 42:185-208.
- Schroll, R.**, U. Dörfler, and I. Scheunert. 1999. Volatilization and mineralization of ^{14}C -labelled pesticides on lysimeter surfaces. *Chemosphere* 39:595-602.
- Schultz, M.**, M. Heitlinger, D. Mihelcic, and A. Volz-Thomas. 1995. Calibration source of peroxy radicals with built-in actinometry using H_2O and O_2 photolysis at 185 nm. *J. Geophys. Res.* 100:18811-18815.
- Seiber, J.N.**, B.W. Wilson, and M.M. McChesney. 1993. Air and fog deposition residues of four organophosphate insecticides used on dormant orchards in the San Joaquin Valley, California. *Environ. Sci. Technol.* 27:2236-2243.
- Simunek, J.**, and R. van Genuchten. 1994. The CHAIN_2D code for simulating the two-dimensional movement of water, heat, and multiple solutes in variably-saturated porous media. Version 1.1. Res. Rep. 136, US Salinity Lab., USDA-ARS, Riverside, CA, USA.
- Smelt, J.H.**, R.A. Smidt, F. van den Berg, A.M. Matser, A. Stork, and H. Ophoff. 1997. Volatilization of fenpropimorph and clopyralid after spraying onto a sugar beet crop, DLO Winand Staring Centre, Report 136, Wageningen, the Netherlands.
- Smit, A.A.M.F.R.**, M. Leistra, and F. van den Berg. 1998. Estimation method for the volatilization of pesticides from plants, DLO Winand Staring Centre, Environmental Planning Bureau series 4, Wageningen, the Netherlands.
- Smit, A.A.M.F.R.**, F. van den Berg, and M. Leistra. 1997. Estimation method for the volatilization of pesticides from fallow soil, DLO Winand Staring Centre, Environmental Planning Bureau series 2, Wageningen, the Netherlands.
- Smith, F.B.**, and R.D. Hunt. 1978. Meteorological aspects of transport of pollution over long distances. *Atmos. Environ.* 12:461-477.
- Spencer, W.F.** 1970. Distribution of pesticides between soil, water and air. p. 120-128. *In* Proc. Intern. Symp. On Pesticides in the soil. East Lansing, Michigan State Univ., USA.
- Spencer, W.F.**, and M.M. Cliath. 1990. Movement of pesticides from soil to the atmosphere. p. 1-16. *In* D.A. Kurtz (ed.) Long Range Transport of Pesticides. Lewis Publishers Inc., Chelsea, MI, USA.
- Spencer, W.F.**, and M.M. Cliath. 1974. Factor affecting vapor loss of trifluralin from soil. *J. Agric. Food Chem.* 20:987-991.
- Spencer, W.F.**, M.M. Cliath, and S.R. Yates. 1995. Soil-pesticide interactions and their impact on the volatilization process. p. 371-382. *In* Environmental impact of soil component interactions, Volume I, Natural and anthropogenic organics, CRC Press, Lewis Publishers Inc., Chelsea, MI, USA.
- Spencer, W.F.**, and M.M. Cliath. 1973. Pesticide volatilization as related to water loss from soil. *J. Environ. Qual.* 2:284-289.
- Spencer, W.F.**, W.J. Farmer, and M.M. Cliath. 1973. Pesticide volatilization. *Residue Reviews* 49:1-47.

- Spencer, W.F.,** T.D. Shoup, M.M. Cliath, W.J. Farmer, and R. Haque. 1979. Vapor pressures and relative volatility of ethyl and methyl parathion. *J. Agric. Food Chem.* 27:273-278.
- Staimer, N.,** T. Müller, and R. Kubiak. 1996. Volatilization of ^{14}C -labelled fenpropimorph after application to plants and soil under simulated outdoor conditions. *Intern. J. Environ. Anal. Chem.* 65:183-191.
- Stangroom, S.J.,** J.N. Lester, and C.D. Collins. 2000. Abiotic behaviour of organic micropollutants in soils and the aquatic environment. A review: I. Partitioning. *Environ. Technol.* 21:845-863.
- Stockmaier, M.** 1996. Untersuchungen zum Verhalten der Morpholinfungizide Aldimorph und Fenpropimorph im Boden unter besonderer Berücksichtigung korrespondierender Metaboliten. PhD thesis, University of Technology Braunschweig, Germany.
- Stork, A..** 1995. Wind tunnel for the measurement of gaseous losses of environmental chemicals from the soil-/plant system under practice-like conditions with direct air analytics using ^{14}C -labelled chemicals. PhD thesis, University of Bonn, Germany.
- Stork, A.,** H. Ophoff, J.H. Smelt, and F. Führ. 1998. Volatilization of pesticides: measurements under simulated field conditions. p. 21-39. *In* F. Führ, R.J. Hance, J.R. Plimmer, and J.O. Nelson (eds.) *The lysimeter concept*. ACS Symp. Ser. 699. Am. Chem. Soc., Washington, D.C., USA.
- Stork, A.,** R. Witte, and F. Führ. 1997. $^{14}\text{CO}_2$ measurement in air: Literature review and a new sensitive method. *Environ. Sci. Technol.* 31:949-955.
- Stork, A.,** R. Witte, and F. Führ. 1994. A wind tunnel for measuring the gaseous losses of environmental chemicals from the soil/plant system under field-like conditions. *Environ. Sci. Pollut. Res.* 1:234-245.
- Symons, P.E.K.** 1977. Dispersal and toxicology of the insecticide fenitrothion; predicting hazards of forest spraying. *Residue Rev.* 68:1-36.
- Taylor, A.W.,** and W.F. Spencer. 1990. Volatilization and vapor transport processes. p. 213-269. *In* H.H. Cheng (ed.) *Pesticides in the soil environment: Processes, impacts, and modeling*. SSSA, Madison, WI, USA.
- Tiktak, A.,** F. van den Berg, J.J.T.I. Boesten, D. van Kraalingen, M. Leistra, and A.M.A. van der Linden. 2000. Manual of FOCUS PEARL version 1.1.1. RIVM Report 711401008, Alterra Report 28. National Institute of Public Health and the Environment, Bilthoven, the Netherlands.
- Tilman, D.,** K.G. Cassman, P.A. Matson, R. Naylor, S. Polasky. 2002 Agricultural sustainability and intensive production practices. *Nature* 418:671-677.
- Tinsley, I.J.** 1979. *Chemical concepts in pollutant behaviour*. John Wiley & Sons, New York, USA.
- Tomlin, C.** (ed.). 2000. *The pesticide manual*, 12th edition. British Crop Protection Council and The Royal Soc. of Chem., Cambridge, UK.
- Tomlin, C.** (ed.). 1994. *The pesticide manual*, 10th edition. British Crop Protection Council and The Royal Soc. of Chem., Cambridge, UK.

- Tucker, W.A.**, and L.H. Nelken. 1982. Diffusion coefficients in air and water. p. 17/1-17/25. *In* W.J. Lyman (ed.) Handbook of chemical property estimation methods. Environmental behavior of organic compounds. McGraw-Hill Book Company, New York, USA.
- USEPA** (U.S. Environmental Protection Agency). 2001. Water Models; EPA 738-R-00-022. <http://www.epa.gov/oppefed1/models/water/index.html>.
- VDI** (Verein Deutscher Ingenieure). 1981. VDI-Handbuch Reinhaltung der Luft. VDI-Richtlinie 2066, Blatt 1 und 2.
- Van Dam, J.C.**, J. Huygen, J.G. Wesseling, R.A. Feddes, P. Kabat, P.E.V. Van Walsum, P. Groenendijk, and C.A. Van Diepen. 1997. SWAP version 2.0, Theory. Rep. 71, Dep. Water Resources, Agriculture Univ., Wageningen, the Netherlands.
- Van den Berg, F.**, G. Bor, R.A. Smidt, A.E. van de Peppel-Groen, J.H. Smelt, T. Müller, and T. Maurer. 1995. Volatilization of parathion and chlorothalonil after spraying onto a potato crop, DLO Winand Staring Centre, Report 102, Wageningen, the Netherlands.
- Van den Berg, F.**, R. Kubiak, W.G. Benjey, M.S. Majewski, S.R. Yates, G.L. Reeves, J.H. Smelt, and A.M.A. Van der Linden. 1999. Emission of pesticides into the air. *Water Air Soil Pollut.* 115:195-218.
- Van den Berg, F.**, A. Wolters, N. Jarvis, M. Klein, J.J.T.I. Boesten, M. Leistra, V. Linne-mann, J.H. Smelt, and H. Vereecken. 2003. Improvement of concepts for pesticide volatilisation from bare soil in PEARL, PELMO, and MACRO models. p. 973-983. *In* A.A.M. Del Re, E. Capri, L. Padovani, M. Trevisan (eds.) Proc. XII Symp. Pestic. Chem. – Pesticide in air, plant, soil & water system, La Goliardica Pavese, Pavia, Italy.
- Vanclooster, M.**, J. Boesten, M. Trevisan, C.D. Brown, E. Capri, O.M. Eklo, B. Gottesbüren, V. Gouy, and A.M.A. Van der Linden. 2000. A European test of pesticide-leaching models: methodology and major recommendations. *Agric. Water Manag.* 44:1-19.
- Vanclooster, M.**, A. Armstrong, F. Baouroui, G. Bidoglio, J.J.T.I. Boesten, P. Burauel, E. Capri, D. de Nie, E. Fernandez, N. Jarvis, A. Jones, M. Klein, M. Leistra, V. Linnemann, J.D. Pineros-Garcet, J.H. Smelt, A. Tiktak, M. Trevisan, F. van den Berg, A.M.A. van der Linden, H. Vereecken, and A. Wolters. 2003. Effective approaches for predicting environmental concentrations of pesticides: The APECOP project. p. 923-931. *In* A.A.M. Del Re, E. Capri, L. Padovani, M. Trevisan (eds.) Proc. XII Symp. Pestic. Chem. – Pesticide in air, plant, soil & water system, La Goliardica Pavese, Pavia, Italy.
- Walter, U.** 1998. Pesticide volatilization: a comparison of methods for measuring and approaches to fuzzy logic modeling. Ph.D. thesis, Humboldt-Univ., Berlin, Germany.
- Walter, U.**, M. Frost, G. Krasel, and W. Pestemer. 1996. Assessing volatilization of pesticides: A comparison of 18 laboratory methods and a field method. *Berichte aus der BBA 16*, Federal Research Centre for Agriculture and Forestry (BBA), Braunschweig, Germany.
- Wang, D.**, S.R. Yates, and J. Gan. 1997. Organic chemicals in the environment: Temperature effect on methyl bromide volatilization in soil fumigation. *J. Environ. Qual.* 26:1072-1079.
- Wauchope, D.R.**, S. Yeh, J.B.H.J. Linders, R. Kloskowski, K. Tanaka, B. Rubin, A. Katayama, W. Kördel, Z. Gerstl, M. Lane, and J.B. Unsworth. 2002. Pesticide soil sorption

parameters: theory, measurement, uses, limitations and reliability. *Pest. Manag. Sci.* 58:419-445.

Waymann, B. 1994. Überprüfung eines Systems zur Bestimmung der Verflüchtigung von Pflanzenschutzmitteln. PhD thesis, University of Duisburg, Germany.

Whang, J.M., C.J. Schomburg, D.E. Glotfelty and A.W. Taylor. 1993. Volatilization of fonofos, chlorpyrifos, and atrazine from conventional and no-till surface soils in the field. *J. Environ. Qual.* 22:173-180.

Whitney, W.K. 1967. Laboratory tests with Dursban and other insecticides in soil. *J. Econ. Entomol.* 60:68-74.

WHO (World Health Organization). 1998. Guidelines for drinking-water quality, Addendum to Vol. 2. Health criteria and other supporting information. p. 245-253. WHO, Geneva, Switzerland.

Winberry, W.T., L. Forehand, N.T. Murphy, A. Ceroli, B. Phinney, and A. Evans. 1990. Compendium of methods for the determination of air pollutants in indoor air. Chapter IP-10. *In* Determination of respirable particulate matter in indoor air. USEPA, EPA/600/4-90/010, Research Triangle Park, New York, USA.

Wolters, A., T. Kromer, V. Linnemann, H. Ophoff, A. Stork, and H. Vereecken. 2002. Volatilization of [¹⁴C]fluoranthene and [¹⁴C]diflufenican after soil surface application under field-like conditions: measurement and comparison with different model approaches. *Agronomie* 22:337-350.

Woodrow J.E., M.M. McChesney, and J.N. Seiber. 1990. Modeling the volatilization of pesticides and their distribution in the atmosphere. p. 61-81. *In* D.A. Kurtz (ed.) Long Range Transport of Pesticides. Lewis Publishers Inc., Chelsea, Michigan, USA.

Woodrow, J.E., J.E. Oodrow, T. Mast, and J.N. Seiber. 1977. Rates of photochemical conversion of pesticides in atmosphere. *Abstr. Pap. Am. Chem. Soc.* 173:3.

Woodrow, J.E., and J.N. Seiber. 1997. Correlation techniques for estimating pesticide volatilization flux and downwind concentrations. *Environ. Sci. Technol.* 31:523-529.

Woodrow J.E., J.N. Seiber, and C. Dary. 2001. Predicting pesticide emissions and downwind concentrations using correlations with estimated vapor pressures. *J. Agric. Food Chem.* 49:3841-3846.

Wyngaard, J.C. 1990. Scalar fluxes in the planetary boundary-layer – Theory, modeling, and measurement. *Bound.-Lay. Meteorol.* 50:49-75.

Yates, S.R. 1993. Determining off-site concentrations of volatile pesticides using the trajectory-simulation model. *J. Environ. Qual.* 22:481-486.

Yates, S.R., D. Wang, F.F. Ernst, and J. Gan. 1997. Methyl bromide emissions from agricultural fields: bare-soil, deep injection. *Environ. Sci. Technol.* 31:1136-1143.

Yates, S.R., D. Wang, S.K. Papiernik, and J. Gan. 2002. Predicting pesticide volatilization from soils. *Environmetrics* 13:569-578.

Zadoks, J.C., T.T. Chang, and C.F. Konzak. 1974. A decimal code for the growth stages of cereals. *Weed Res.* 14:415-421.

Field Study: Data for Calculation of Pesticide Volatilization Fluxes

Annex 1.A Moisture content of surface soil (0-8 cm depth) as percentage of dry weight and bulk density.

Day after application	Moisture content		Bulk density	
	Av. [%]	RSD †	Av. [kg soil dm ⁻³]	RSD †
1	21.413	0.348	1.381	0.041
2	20.668	0.484	1.307	0.049
4	19.264	0.412	1.361	0.027
7	16.835	0.690	1.323	0.031

† RSD: relative standard deviation of four replicates

Annex 1.B Data needed for the calculation of the soil heat flux density at the surface and for calculation of the Bowen ratio coefficient as used for the Bowen ratio method.

Time after application [d]	Soil heat flux density at a depth of 0.08 m [W m ⁻²]	Δ soil temperature [°C]	Δ air temperature [°C]	Bowen ratio coefficient difference [-]	Soil heat flux density [W m ⁻²]
0.104	2.54	-0.034	0.002	0.012	-2.72
0.145	2.68	-0.063	-0.104	-0.738	-7.22

Annex 1.C Energy balance for the field and the dispersion coefficient for sensible heat.

Time after application [d]	Net radiation [W m ⁻²]	Soil heat flux density [W m ⁻²]	Sensible heat flux density [W m ⁻²]	Latent heat flux density [W m ⁻²]	Dispersion coefficient [m ² h ⁻¹]
0.104	88.3	-2.72	1.1	90.0	945
0.145	32.6	-7.22	-112.1	152.0	1596

Annex 1.D Difference in concentration of the pesticides in air between 1.0 and 1.5 m above the soil surface. Values were estimated from the measured concentrations at three sampling heights.

Time after application [d]	Concentration difference of fenpropimorph [$\mu\text{g m}^{-3}$]
0.104	0.866
0.145	0.112

Annex 1.E Richardson number and the correction coefficients used for the aerodynamic method.

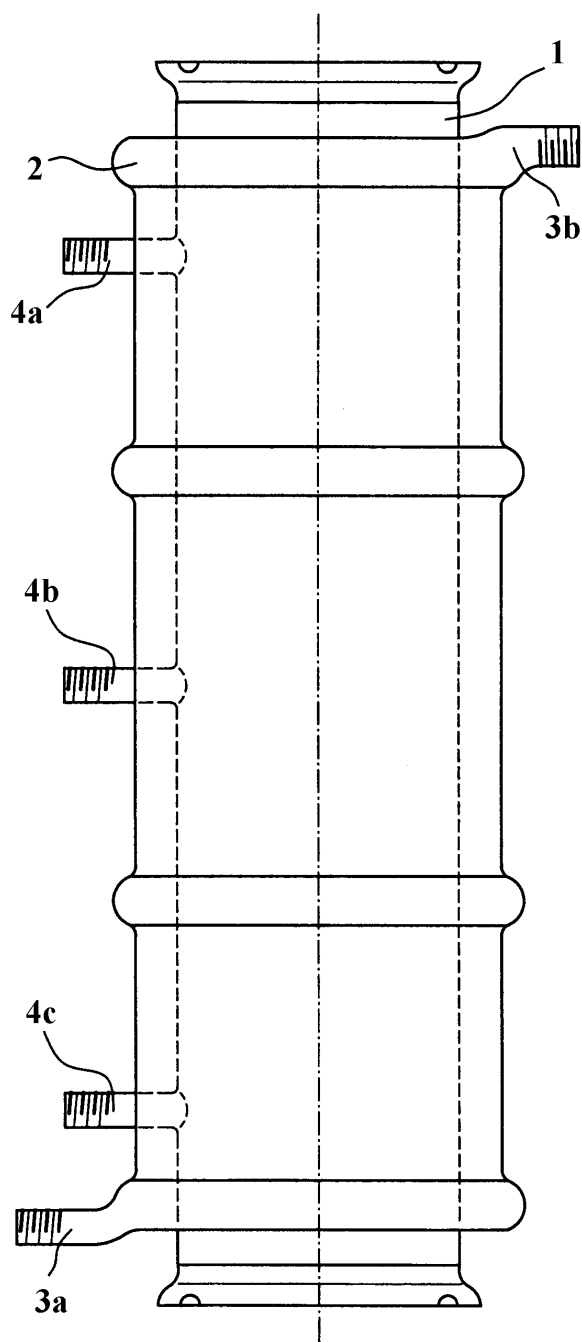
Time after application [d]	Richardson number [-]	Correction factor momentum [-]	Correction factor pesticide [-]
0.104	-0.0001	0.999	0.884
0.145	0.0059	1.031	0.952

Annex 1.F Wind speed and air temperature used for the aerodynamic method.

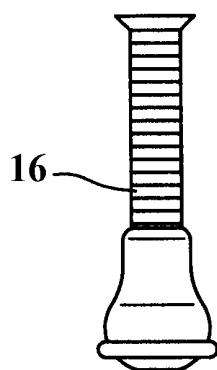
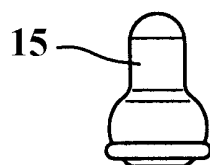
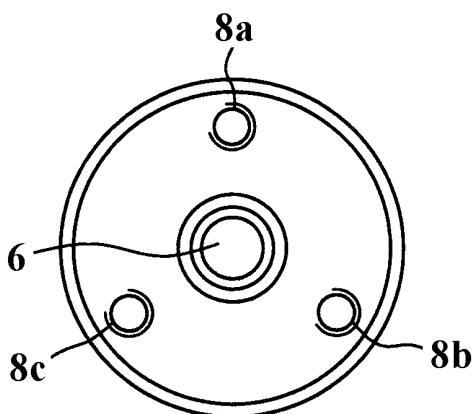
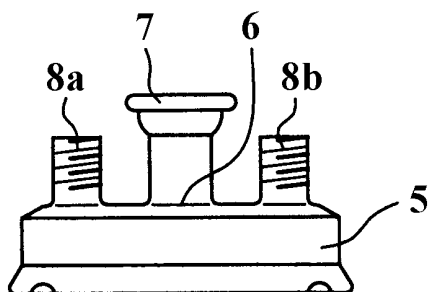
Time after application [d]	Wind speed [m s^{-1}]		Δ wind speed [m s^{-1}]	Air temperature at 1.0 m [$^{\circ}\text{C}$]	Δ air temperature [$^{\circ}\text{C}$]
	1.0 m	1.5 m			
0.104	2.164	2.701	0.537	13.06	0.002
0.145	2.145	2.694	0.549	13.42	-0.104

Phase Partitioning Chamber: Main Elements

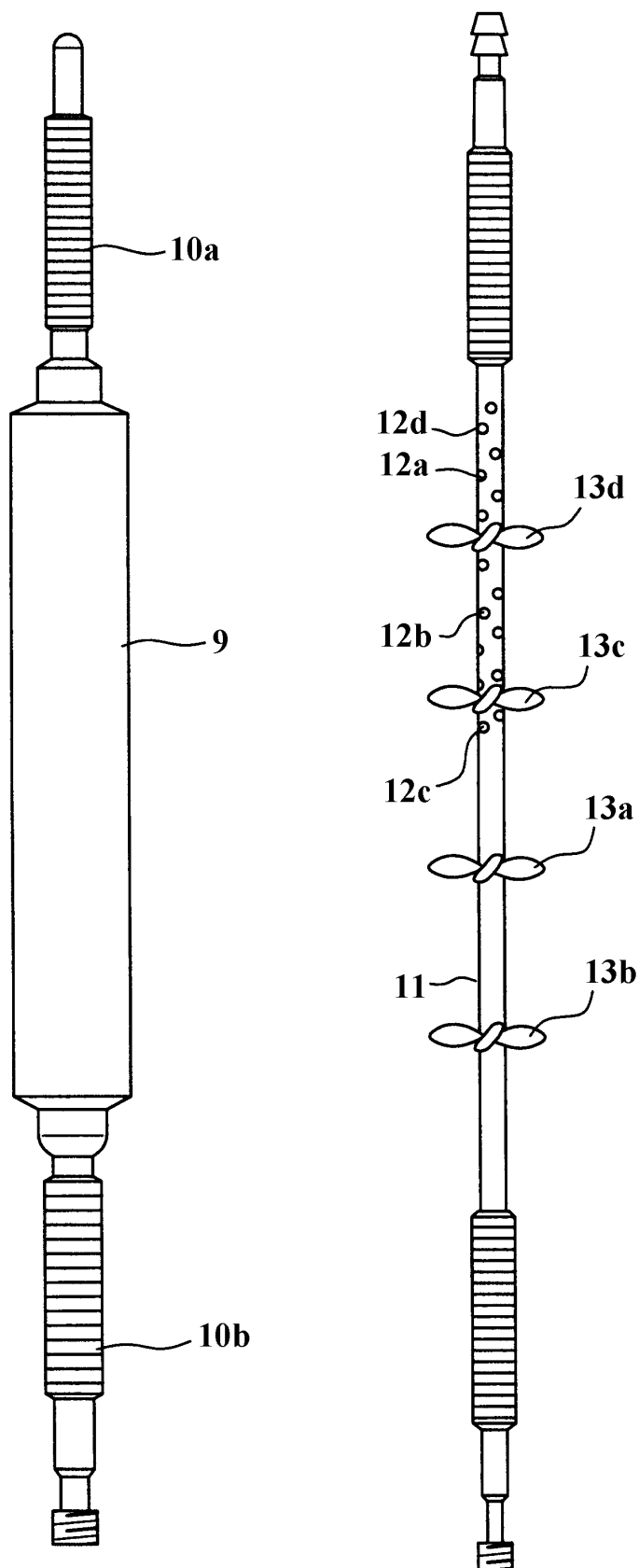
Annex 2.A Double-walled glass tube equipped with sampling ports and glass threads. **1** = double-walled glass cylinder (total length: 116 cm, 15 cm i.d.), **2** = cooling jacket, **3a,b** = glass threads for connection with cooling inlet/outlet, **4a,b,c** = sealable ports for sampling and measuring device.



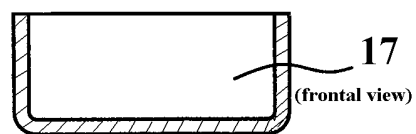
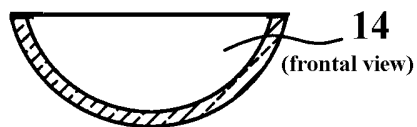
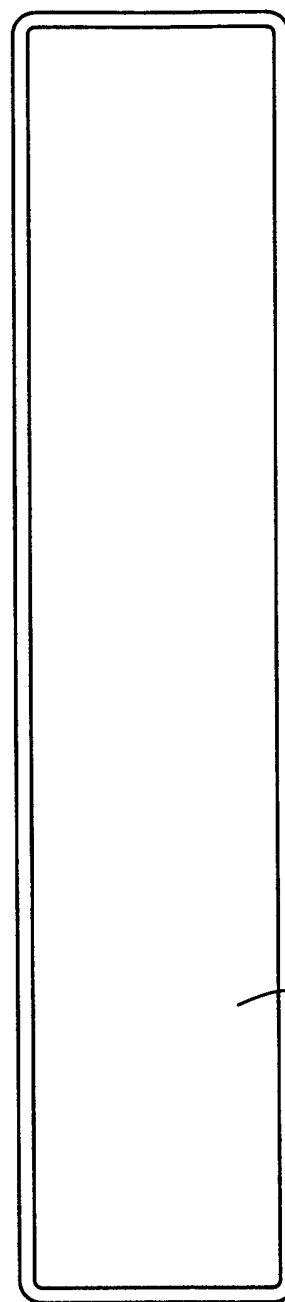
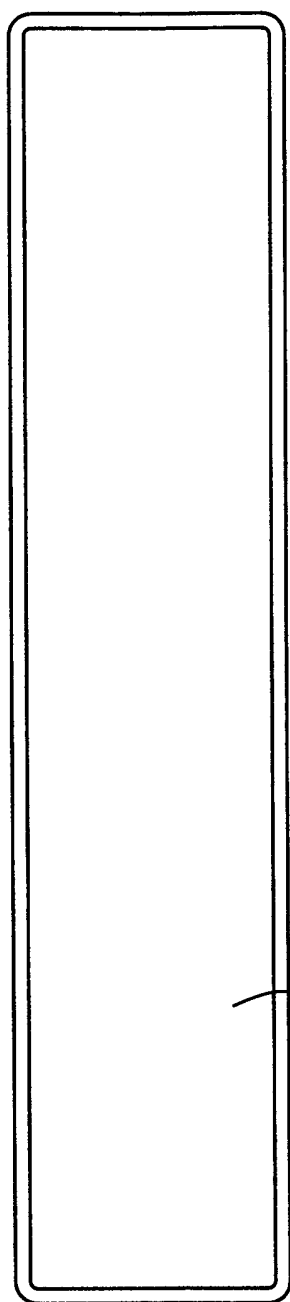
Annex 2.B Sealing rings and quick-release caps for gas-tight sealing of the phase partitioning chamber. **5** = quick-release cap for gas-tight sealing of the chamber, **6** = central opening, **7** = adaptor fitting (ball-and-socket joint), **8a,bc** = glass threads for installation of measuring device, **15** = plug for ball-and-socket joint, **16** = guide bush for glass axis.



Annex 2.C Glass axes to be used for studies on Henry's law constants and soil-air partitioning. **9** = sand-blasted glass cylinder to be used for studies on Henry's law constants (total length: 181 cm, 9.5 cm o.d.), **10a,b** = part of the cylinder to stick out through the central opening (6), **11** = glass axis to be used for studies on soil-air partitioning (total length: 184 cm, 1.4 cm i.d.), **12a,b,c,d** = ingress of air, **13a,b,c,d** = propellers for mixing air.



Annex 2.D Reservoir for soil/water to be spiked with defined pesticide amounts. **14** = glass tray (total length: 90 cm, width: 19.6 cm, depth: 4 cm) for studies on soil-water partitioning, **17** = metal tray (total length: 90 cm, width: 10.0 cm, depth: 4 cm) for studies on soil-air partitioning.



Parts of this work have already been published:

Peer-reviewed Publications

Wolters, A., V. Linnemann, M. Herbst, M. Klein, A. Schäffer, and H. Vereecken. 2003. Pesticide volatilization from soil: Lysimeter measurements versus predictions of European registration models. *J. Environ. Qual.* 32:1183-1193.

Wolters, A., T. Kromer, V. Linnemann, A. Schäffer, and H. Vereecken. 2003. A new tool for laboratory studies on volatilization: Extension of applicability of the photovolatility chamber. *Environ. Toxicol. Chem.* 22:791-797.

Wolters, A., T. Kromer, V. Linnemann, H. Ophoff, A. Stork, and H. Vereecken. 2002. Volatilization of [¹⁴C]fluoranthene and [¹⁴C]diflufenican after soil surface application under field-like conditions: Measurement and comparison with different model approaches. *Agronomie* 22:337-350.

Patent Application

Wolters, A., V. Linnemann, K.E.C. Smith, J.H. Smelt, G. D'Orsaneo. Verfahren zur Bestimmung von Phasenverteilungskoeffizienten sowie eine für das Verfahren geeignete Vorrichtung. Deutsche Patentanmeldung Nr. 101 62 852.8 (20.12.2001).

Conference Proceedings

Wolters, A., M. Leistra, V. Linnemann, J.H. Smelt, F. van den Berg, M. Klein, N. Jarvis, J.J.T.I. Boesten, and H. Vereecken. 2003. Pesticide volatilisation from plants: Improvement of the PEARL, PELMO, and MACRO models. p. 985-994. *In* A.A.M. Del Re, E. Capri, L. Padovani, M. Trevisan (eds.) Proc. XII Symp. Pestic. Chem. – Pesticide in air, plant, soil & water system, La Goliardica Pavese, Pavia, Italy.

Van den Berg, F., A. Wolters, N. Jarvis, M. Klein, J.J.T.I. Boesten, M. Leistra, V. Linnemann, J.H. Smelt, H. Vereecken. 2003. Improvement of concepts for pesticide volatilisation from bare soil in PEARL, PELMO, and MACRO models. p. 973-983. *In* A.A.M. Del Re, E. Capri, L. Padovani, M. Trevisan (eds.) Proc. XII Symp. Pestic. Chem. – Pesticide in air, plant, soil & water system, La Goliardica Pavese, Pavia, Italy.

Vanclooster, M., A. Armstrong, F. Baouroui, G. Bidoglio, J.J.T.I. Boesten, P. Burauel, E. Capri, D. de Nie, E. Fernandez, N. Jarvis, A. Jones, M. Klein, M. Leistra, V. Linnemann, J.D. Pineros-Garcet, J.H. Smelt, A. Tiktak, M. Trevisan, F. van den Berg, A.M.A. van der Linden, H. Vereecken, and A. Wolters. 2003. Effective approaches for predicting environmental concentrations of pesticides: The APECOP project. p. 923-931. *In* A.A.M. Del Re, E. Capri, L. Padovani, M. Trevisan (eds.) Proc. XII Symp. Pestic. Chem. – Pesticide in air, plant, soil & water system, La Goliardica Pavese, Pavia, Italy.

Prof. Dr. A. Schäffer danke ich für die wissenschaftliche Betreuung dieser Arbeit und für seine Bereitschaft, sich in Ergänzung zu seinen Forschungsaktivitäten im Bereich Boden-Pflanze-Wasser auf ein „aus der Luft gegriffenes“ Thema einzulassen.

Prof. Dr. H. Vereecken danke ich für die Überlassung des Themas, für die jederzeit gewährte Unterstützung und für die Erkenntnis, dass Experiment und Modell in der Umweltforschung nicht zwangsläufig im Widerspruch stehen müssen.

Ein besonderer Dank gebührt Dr. V. Linnemann für die hervorragende Zusammenarbeit und seinen angenehmen Führungsstil in der Arbeitsgruppe „Verflüchtigung“. Ohne seine Hilfe wäre diese Arbeit nicht zustande gekommen.

Dr. T. Kromer danke ich für sein Engagement beim Umbau der Photovolatilitätskammer und für den Optimismus, den er in der schwierigen Anfangsphase des Projektes verbreitet hat.

Funding was provided by the European Commission within the framework of the APECOP project (Effective Approaches for Assessing the Predicted Environmental Concentrations of Pesticides). I am very grateful to the colleagues involved in this project for their support and encouragement. Above all I am indebted to the team of *Alterra Green World Research* (Wageningen, NL), especially to Dr. M. Leistra who provided invaluable help by modeling volatilization from plants. J.H. Smelt is specially acknowledged for his support in the experimental parts of this work. Thanks are also due to Dr. F. van den Berg for fruitful discussions on volatilization from soil.

I owe gratitude to Dr. K. Smith for initiating the subproject “phase partitioning chamber”. I also extend my appreciation to B.-J. Park and E. Klingelmann for their contributions to the further development of the chamber.

Dr. M. Klein danke ich für die Durchführung zahlreicher PELMO-Berechnungen und die Zusammenarbeit bei der Bewertung der Resultate. Für die Unterstützung bei meinen ersten Versuchen der PEARL-Anwendung danke ich Dr. M. Herbst.

Die intensive und angenehme Zusammenarbeit mit meinen Kollegen im ICG-IV des Forschungszentrums Jülich hat wesentlich zum Gelingen dieser Arbeit beigetragen. Besonders dankbar bin ich M. Krause, deren Unterstützung bei Probenvorbereitung und Analytik die Durchführung des umfangreichen experimentellen Teils dieser Arbeit erst ermöglicht hat. Für die kompetente, oft kurzfristige Durchführung der HPLC-Analysen bedanke ich mich bei S. Köppchen. Für die Hilfe bei der GC-MS-Analytik gilt mein Dank R. Niehaus.

Ich danke den Mitarbeitern der Zentralabteilung Technologie des Forschungszentrums Jülich für die Unterstützung bei Umbau und Optimierung der experimentellen Vorrichtungen. Für die schnelle und unkomplizierte Hilfe bei glastechnischen Problemen bedanke ich mich bei G. D’Orsaneo.

Mein größter Dank gilt Dr. S. Althausen für unbarmherziges Korrekturlesen und zahlreiche Verbesserungsvorschläge, in erster Linie aber bedanke ich mich für ihre unerschöpfliche Geduld.

Forschungszentrum Jülich
in der Helmholtz-Gemeinschaft



Jül-4073
Juli 2003
ISSN 0944-2952